A journey into the total synthesis of Aspochalasins.From a two-phase strategy to peroxide rearrangements.

Oscar Gayraud

INSTITUT POLYTECHNIQUE DE PARIS

NNT : 2020IPPAX071

Thèse de doctorat

A Journey into the Total Synthesis of Aspochalasins. From a Two-phase Strategy to Peroxide Rearrangements.

Thèse de doctorat de l'Institut Polytechnique de Paris
préparée à Ecole Polytechnique

École doctorale n°ED 626 École Doctorale de l'Institut Polytechnique de Paris (ED IP Paris)
Spécialité de doctorat : Biologie et chimie

Thèse présentée et soutenue à Palaiseau, le 10/12/2020, par

OSCAR GAYRAUD

Composition du Jury :

Amandine Guérinot Professeur assistant, ESPCI (UMR7167)	Rapportrice
Guillaume Vincent Directeur de recherche, Université Paris Saclay (UMR 8182)	Rapporteur
Delphine Joseph Professeur, Université Paris Saclay (UMR 8076)	Présidente du jury
Gilles Frison Chargé de recherche, Sorbonne université (UMR 7616)	Examinateur
Bastien Nay Directeur de recherche, Ecole Polytechnique (UMR 7652)	Directeur de thèse

Une plongée dans la synthèse totale des aspochalasines. D'une stratégie en deux phases aux réarrangements de peroxydes.

Oscar Gayraud

Directeur de thèse: Bastien Nay

Résumé

Pendant près de deux siècles, les chimistes de synthèse se sont intéressé·e·s à la reproduction des molécules issues du monde du vivant. Les produits naturels présentent une importante diversité structurale combinés avec leur complexité ils représentent une source presque infinie de défis synthétiques. Les chimistes de synthèse ont utilisé diverses approches pour accéder à un grand nombre d'entre eux. De la synthèse totale ciblée s'intéressant à un unique produit naturel à la synthèse totale diversifiée, composée d'une phase de construction et d'une phase de diversification, se focalisant sur une famille de molécules, les stratégies de synthèse des produits naturels ont évolué pour produire divers composés à partir d'intermédiaires communs en un court nombre d'étapes. Lors de la phase de diversification, des procédés d'oxydoréductions peuvent être utilisés pour synthétiser plusieurs produits naturels d'une même famille. On parle dans ce cas d'approche en deux phases, une phase de construction et une phase d'oxydation, s'inspirant de l'approche de la Nature que l'on retrouve par exemple dans la biosynthèse des terpènes ou des polycétides. De plus, les calculs DFT ont parfois été utilisés pour aider les chimistes de synthèse à résoudre les problèmes rencontrés lors des synthèses totales. Ces derniers peuvent être prédictifs, visant à prévoir en amont la meilleure stratégie, ou explicatifs, visant à comprendre les résultats expérimentaux observés. Le but de cette thèse était de réaliser la synthèse totale de substances naturelles de la famille des cytochalasines, tout en développant des méthodes de synthèse appropriées, en s'aidant fortement des calculs DFT. Une approche en deux phases pour produire des produits naturels de la famille des aspochalasines, tels que la trichoder-

mone et la trichodérone A, sera présentée. La construction du noyau principal utilisera une réaction de couplage croisé de Suzuki-Miyaura, une dihydroxylation asymétrique de Sharpless, un réarrangement d'Ireland-Claisen et une réaction intramoléculaire de Diels-Alder. La synthèse du noyau isoindolone sera améliorée par des calculs DFT utilisant l'aspect prédictif et explicatif. Ensuite, une deuxième phase utilisant divers procédés d'oxydoréduction sera employée pour oxyder sélectivement un intermédiaire tétracyclique afin d'atteindre diverses aspochalasines. Lors de cette phase, une approche biomimétique s'inspirant de l'oxydation des lipides par l'oxygène singulet, réaction de Schenck-ène, suivi d'un clivage de Hock sera envisagée.

Les réarrangements de peroxydes organiques peuvent produire une grande variété de fonctions oxygénées telles que des cétones, des lactones, des alcools ou encore des acides carboxyliques. Le procédé au cumène, utilisant le réarrangement de Hock, reste le plus connu et représente en 2018 plus de 99% de la production mondiale de phénol. Lors des réarrangements de Criegee et de Hock, les peroxydes allyliques et benzyliques se réarrangent pour former des oxocarbéniums qui sont ensuite piégés par de l'eau, générée lors du réarrangement, pour former des dérivés carbonylés, des aldéhydes et des cétones. L'approche développée dans cette partie s'intéresse à l'interruption de ces deux réarrangements en utilisant des nucléophiles internes ou externes. Dans un premier temps, la génération de l'hydroperoxyde allylique sera réalisée in-situ utilisant une réaction de Schenck-ène et l'interruption du réarrangement de Hock sera intramoléculaire. Cette approche permet d'accèder aux squelettes des produits naturels issus de la famille des lignanes. Dans un second temps, l'utilisation d'hydroperoxydes et de peroxydes benzyliques sera envisagée lors d'interruption du réarrangement de Hock ou de Criegee avec une approche intermoléculaire. Ces méthodes permettent d'accéder à des éthers cycliques par exemple l'alpha-tocophérol qui est une forme de la vitamine E. Finalement une dernière partie sera consacrée à une approche de la synthèse totale de l'isolaurepan utilisant les méthodes d'interruption du réarrangement de Criegee précédemment développées.

A Journey into the Total Synthesis of Aspochalasins. From a Two-phase Strategy to Peroxide Rearrangements.

Oscar Gayraud

Thesis Advisor: Bastien Nay

Abstract

Natural products are an almost infinite source of synthetic challenges by their complex structural diversity. Chemists have employed diverse approaches to access a vast number of them. In our era, interdisciplinary is a powerful tool to synthesize efficiently complicated targets. The purpose of this thesis was to develop synthetic methods to reach different natural products using DFT calculations.

■ **Chapter 1.** Over almost two centuries, synthetic chemists have been interested in reproducing molecules found in Nature. From target-oriented synthesis to diverted total synthesis, strategies in natural product synthesis have evolved to produce diverse compounds from common intermediates in a short number of steps. Furthermore, the use of DFT calculations has been used to assist chemists to solve problems encountered during total syntheses. This chapter aims to present a brief overview of different strategies in natural product synthesis and to link them with the work done in this thesis.

■ **Chapter 2.** A two phase approach to produce aspochalasine natural products, such as trichodermone **2** and trichoderone A **3**, will be presented. The construction of the main core **1** will use cross coupling reaction, asymmetric dihydroxylation, rearrangement and cycloaddition. The synthesis of the isoindolone core will be enhanced by DFT calculations. Then, a second phase using diverse redox processes will be employed to selectively oxidized tetracyclic intermediate **1** to reach diverse aspochalasines.

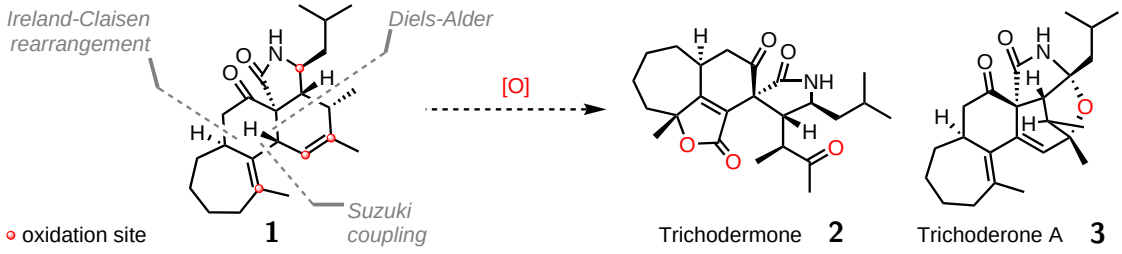

■ **Chapter 3.** Organic peroxide rearrangements can produce a diverse variety of oxygenated functions. During the Criegee and Hock rearrangement, allylic and benzylic peroxides (**4**) rearrange to form oxocarbenium species (**5**) which are then trapped by water to form acetals. In this chapter, new methods will be presented where diverse nucleophiles will be used to trap oxocarbeniums (**5**) and generate cyclic ethers (**6**).

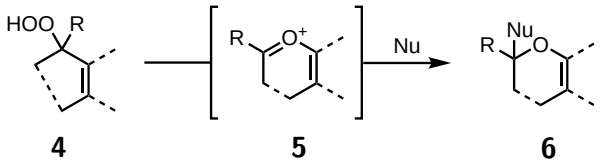

Contents

Acknowledgements

First of all, I would like to express my deepest gratitude to my research director, Dr. Bastien Nay, for accepting me as a PhD candidate in his team. Thank you for training me with the perfect rigor necessary in the field of total synthesis of natural products, always taking the time to talk about chemistry; thanks to these discussions, I have learned a lot.

I want to thank Dr. Gilles Frison for teaching me the art of DFT calculations. I really enjoyed working on this project.

I would like to thank all the members of the jury committee, Prof. Amandine Guérinot, Dr. Guillaume Vincent, Prof. Delphine Joseph and Dr. Gilles Frison for taking the time to evaluate my research and creating a very interesting discussion during the defense.

Dr Alexis Archambeau, thank you for helping me set up my first distillation and for the discussions on chemistry. I would like to thank all the members of the LSO group for their help during my PhD.

Dr. Wei Zang, thank you for your warm welcome when I started working in the laboratory. Dr. Vincent Revil-Baudard, thank you for your interesting discussions and your different musical tastes. Jean Michalland, thank you for accepting PBB in laboratory 2. Antoine Escola, thank you for the culinary discussions. Anaïs Scuiller, thank you for your good humour. Dr Alexandra Bosnidou, Dr Mansour Kerim Dolé, Valentin Dorokhov, Benjamin Joyeux, Quentin Ronzon, Dr Bruce Walters, Xianzhu Zeng, Antoine Roblin, thank you for creating this special atmosphere in the laboratory.

Big thanks to Laurent El Kaim, Julien Morain, Sébastien Prévost, Yvan Six, Samir Zard

and any other members in LSO that I haven't mentioned.

I would like to express my gratitude to my mother and father for your support and for all these Sunday dinners. Special thanks to my brother and I wish you good luck with your doctorate!

Finally, I would like to thank all my srabs. Without you, I don't think I could have completed this journey. In a totally random order, thanks to Theo for his close friendship, Ismail for the running, falafel and Thursday beers, Alix for the time spent cooking, Odile for always being there, Florence for the lockdown team, Clément, Yacine for being the best cycling partner I could imagine, Speaker Louis for his massive release, Dr. Taz don't forget to subscribe to his channel, Ann, Tinj for Lyon and more, Christine for Lille and the rum, Penelope for too many things, Hugo for introducing me to yoga, Raph for the beers, Victor for the cold ravioli, Alexandre, Mélie for introducing me to bikepacking, Noé, Clara, Kevin for your non-climbing, Robinson for the festival, Renaud, Pierre for our exploration of Parisian gastronomy, Sixtine, Jean and Leah for being perfect roommates, Nicolas, Jeremy for Grenoble, Arthur, Eva, Sandra and Hermann for our not that frequent beers, Marie and Juan.

List of Abbreviations

$[\alpha]$	specific rotation
Å	angstrom
Ac	acetyl
acac	acetylacetonyl
ACF	addition/cyclization/fragmentation
ACP	acyl carrier protein
AIBN	2,2'-azobis(2-methylpropionitrile)
AQN	anthraquinone-1,4-diyl diether
Ar	aryl (substituted aromatic ring)
AT	acyl transferase
BHT	2,6-di-tert-butyl-4-methylphenol
Bn	benzyl
Boc	*tert*-butoxycarbonyl
bpy	2,2'-bipyridine
br	broad (NMR)
Bu	butyl
Bz	benzoyl
CDI	1,1'-carbonyldiimidazole
CoA	coenzyme A
conv	conversion
Cy	cyclohexyl
d	day(s); doublet (NMR)

dba	dibenzylideneacetone
DCE	dichloroethane
DCM	dichloromethane
dd	doublet of doublets (NMR)
ddd	doublet of doublet of doublets (NMR)
dF(CF_3)ppy	2-(2,4-difluorophenyl)-5-trifluorometylpyridine
DFT	density functional theory
DH	dehydratase
DHQ	hydroquinine
DHQD	hydroquinidine
DMAP	4-dimethylaminopyridine
DMAPP	dimethylallyldiphosphate
DMDO	dimethyldioxirane
DMF	*N*,*N*-dimethylformamide
DMI	1,3-dimethyl-2-imidazolidinone
DMPU	*N,N'*-dimethylpropyleneurea
DMSO	dimethylsulfoxide
dp	doublet of pentets (NMR)
DPEPhos	Bis[(2-diphenylphosphino)phenyl] ether
DPP	2,3-diphenylpyrazino[2,3-d]pyridazine
dppe	1,2-bis(diphenylphosphino)ethane
dppf	1,1'-ferrocenediyl-bis(diphenylphosphine)
dppp	1,3-bis(diphenylphosphino)propane
dq	doublet of quartets (NMR)

dr	diastereomeric ratio
dtbbpy	4,4'-di-*tert*-butyl-2,2'-dipyridyl
DTS	diverted total synthesis
EDC	*N*-(3-dimethylaminopropyl)-*N'*-ethylcarbodiimide
EI+	electronic ionisation (positive ion mode)
equiv.	equivalent(s)
er	enantiomeric ratio
ER	enoyl reductase
ESI+	electrospray ionization (positive ion mode)
Et	ethyl
g	grams(s)
GC	gas chromatography
Hex	hexyl
HFIP	hexafluoroisopropanol
HOMO	highest occupied molecular orbital
h	hour(s)
HF	Hartree-Fock
HMDS	hexamethyldisilazane
HMPA	hexamethylphosphoramide
HRMS	high resolution mass spectrometry
HWE	Horner–Wadsworth–Emmons
i-Pr	isopropyl
IBX	2-iodoxybenzoic acid
IMDA	intramolecular Diels-Alder reaction

IND	9-*O*-indolinylcarbamoate
IPP	isopentenyldiphosphate
IR	infrared spectroscopy
IRC	intrinsic reaction coordinate
J	coupling constant in Hz (NMR)
kcal	kilocalorie
KR	keto reductase
KS	keto synthetase
L	liter(s)
LED	light emitting diode
LDA	lithium diisopropylamide
LUMO	lowest unoccupied molecular orbital
M	molarity (mol / L); molecular formula (HRMS)
m	*meta*
m	milli; multiplet (NMR)
MB	methylene blue
m-CPBA	*meta*-chloroperbenzoic acid
Me	methyl
men	menthol
MHz	megahertz
min	minute(s)
MMPP	magnesium monoperoxyphthalate hexahydrate
mol	mole(s)
Ms	mesyl

MS	molecular sieves
MT	methyl transferase
n	normal (unbranched alkyl chain)
ND	not determined
NMO	4-methylmorpholine *N*-oxide
NMR	nuclear magnetic resonanace
NR	no reaction
NRPS	nonribosomal peptide-synthetases
Nu	nucleophile
o	*ortho*
Oct	octyl
p	*para*
p	pentet (NMR)
Pent	pentyl
PG	protecting group
Ph	phenyl
pin	pinacol
PHAL	1,4-phthalazinediyl diether
Phth	phthalimides
PKS	polyketide synthases
Pr	propyl
PYR	2,5-diphenyl-4,6-pyrimidinediyl diether
q	quartet (NMR)
qq	quartet of quartets (NMR)

quant.	quantitative
rt	room temperature
RuPhos	2-dicyclohexylphosphino-2',6'-diisopropoxybiphenyl
s	singlet (NMR)
SAM	*S*-adenosyl methionine
SG	Stewart-Grubbs catalyst
SPhos	2-dicyclohexylphosphino-2',6'-dimethoxybiphenyl
t	tertiary alkyl chain
t	triplet (NMR)
TBAF	tetrabutylammonium fluoride
TBS	*tert*-butyldimethylsilyl
^{t}Bu	*tert*-butyl
Tc	thiophene-2-carboxylate
td	triplet of doublets (NMR)
Tf	trifluoromethanesulfonyl
TFA	trifluoroacetic acid
TFAA	Trifluoroacetic anhydride
TFP	tri(2-furyl)phosphine
THF	tetrahydrofuran
TLC	thin layer chromatography
TMEDA	*N,N,N',N'*-Tetramethylethylenediamine
TMP	tetramethylpiperidide
TMS	trimethylsilyl
TOS	target-oriented synthesis

TPP	tetraphenylporphyrin
TPPA	tris(N,N-tetramethylene)phosphoric acid triamide
TS	transition state
Ts	*para*-toluenesulfonyl
Xantphos	4,5-bis(diphenylphosphino)-9,9-dimethylxanthene
XPhos	2-dicyclohexylphosphino-2',4',6'-triisopropylbiphenyl

Chapter 1

General Introduction

1.1 Introduction

In Nature, organisms produce molecules called natural products using diverse strategies. Among them, the mevalonate and non-mevalonate pathways are used to synthesize dimethylallyldiphosphate (DMAPP) **7** and isopentenyldiphosphate (IPP) **8**, key precursors of terpenoids and steroids, more than half of natural products known.[1] Using these two fragments, Nature uses a two phases approach composed of a main skeleton construction and an oxidative phase, where redox processes take place to reach natural products. For example, DMAPP **7** and IPP **8** are condensed using geranyl diphosphate synthase to form geranyl diphosphate **9**, precursor of limonene **10** which can be transform to menthol **11** after selective C-H oxidation. Another IPP **8** can be condensed with geranyldiphosphate **9** by farnesyl pyrophosphate synthase to reach farnesyl diphosphate **12**. This intermediate can give birth to amorphadiene **13** which can lead to artemisinin **14** after multiple redox processes (Figure 1.1).[2]

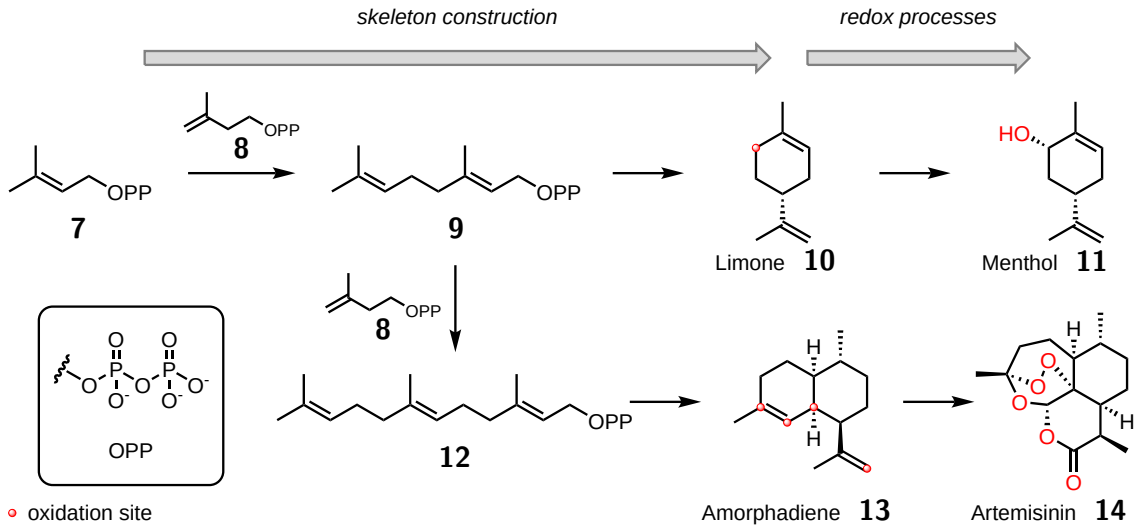

Figure 1.1: Biosynthesis of terpenoid natural products.

Natural products have attracted synthetic chemists attention for almost two centuries

[1] R. Firn, *Nature's Chemicals*, Oxford University Press, Oxford, USA, **2011**.
[2] P. M. Dewick, *Nat. Prod. Rep.* **2002**, *19*, 181-222.

(Figure 1.2). Starting in 1828, Friedrich Wöhler reported what is nowadays described as the first total synthesis by heating the inorganic salt ammonium cyanate to generate urea **15**.[3]

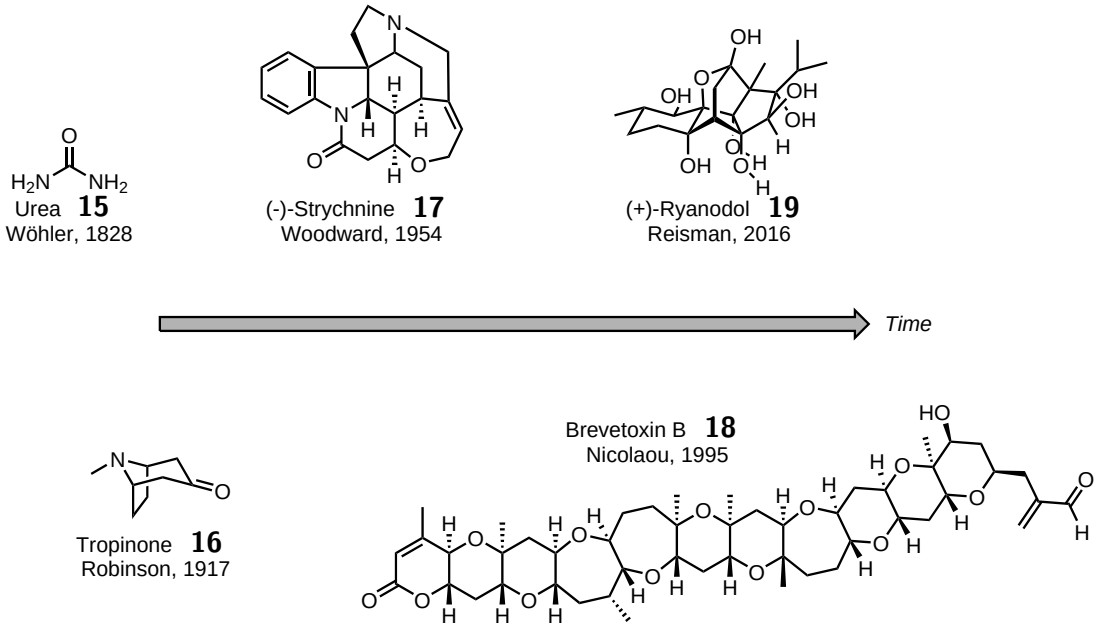

Figure 1.2: Timeline in total synthesis.

In the Twentieth Century, diverse motivations such as confirming structures of natural products, developing new synthetic methods or accessing pharmaceutical valuable compounds has led to a rapid development of the field. From small molecules, such as tropinone **16** with Robinson's impressive one-step synthesis starting from succinaldehyde and acetonedicarboxylic acid,[4] to larger one, such as strychnine **17**,[5] or brevetoxin B **18**,[6] two flagships of the multistep total synthesis with 29 and 123 steps, almost all targets seemed reachable.

In our era, the field evolved with new goals, such as the reduction of the number of steps,

[3] F. Wöhler, *Ann. Phys. Chem.* **1828**, *12*, 253-256.
[4] R. Robinson, *J. Chem. Soc., Trans.* **1917**,*111*, 762-768.
[5] R. B. Woodward, M. P. Cava, W. D. Ollis, A. Hunger, H. U. Daeniker, K. Schenker, *J. Am. Chem. Soc.* **1954**, *76*, 4749-4751.
[6] K. C. Nicolaou, F. P. J. T. Rutjes, E. A. Theodorakis, J. Tiebes, M. Sato, E. Untersteller, *J. Am. Chem. Soc.* **1995**, *117*, 10252-10263.

the development of scalable syntheses or better atom economy.[7] For example, Reisman and co-workers developed a 15 steps synthesis for ryanodol **19** using efficient redox processes.[8]

With the continuous discovery of new natural products, the generation of new synthetic challenges seems infinite. Chemists thus need to develop new strategies, efficient methods and use new tools such as DFT calculations to shorten the total syntheses and access more complicated scaffolds.

In this context, the aim of this introduction is to provide a brief overview of the objectives of this thesis, and the tools that can help us and synthetic chemists to design effective strategies to unlock complex natural product.

[7] T. Newhouse, P. S. Baran, R. W. Hoffmann, *Chem. Soc. Rev.* **2009**, *38*, 3010-3021.
[8] K. V. Chuang, C. Xu, S. E. Reisman, *Science*, **2016**, *353*, 912-915.

1.2 Targets and objectives of this thesis

Total synthesis of aspochalasines

A first part of this thesis will aim to develop the total syntheses of aspochalasines and derivatives. The strategy is inspired by Nature's two phases approach and can be considered as biomimetic. In a first time, a synthesis of biomimetic intermediate **1** with a low level of oxidation will be elaborated. The following steps will be to selectively oxidize different positions to produce a large variety of oxygenated compounds. For example, trichodermone **2** and trichoderone A **3**, two natural products extracted from the same endophytic fungus *Trichoderma gamsii* found in the Chinese plant *Panax notoginseng*, might be accessed using this strategy.[9] Furthermore, DFT calculations will be used to have a better understanding and enhance the intramolecular Diels-Alder reaction used to form the isoindolone core of intermediate **1** (Figure 1.3).

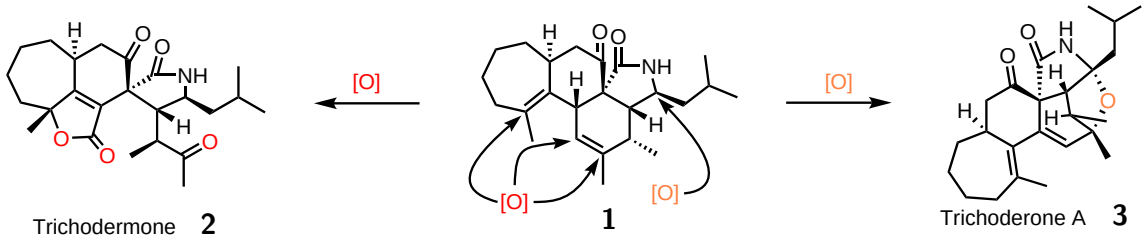

Figure 1.3: Trichoderone A **3** and trichodermone **2**.

A new method to cyclic and acyclic ethers

The second part will aim to have a better understanding of the Hock cleavage, a reaction that might be used on biomimetic intermediate **1** to deliver trichodermone **2**. The focus will be on the development of a method to access cyclic and acyclic ethers (**22**) from allylic

[9] (a) G. Ding, H. Wang, L. Li, B. Song, H. Chen, H. Zhang, X. Liu, Z. Zou, *J. Nat. Prod.* **2014**, *77*, 164-167. (b) G. Ding, H. Wang, L. Li, A. J. Chen, L. Chen, H. Chen, H. Zhang, X. Liu, Z. Zou, *Eur. J. Org. Chem.* **2012**, *13*, 2516-2519.

and benzylic hydroperoxides (**20**) through interrupted Hock cleavage by trapping oxocarbenium reactive intermediate (**21**) with different nucleophiles (Figure 1.4, top). Cyclic ethers are well spread among natural products and especially in marine metabolites where they generally appears as polycyclic ethers such as brevotoxin B **18** (Figure 1.2).[10] Other compounds can adopt diverse structural conformations such as salinomycin **23**, an antibiotic which shows promising anticancer properties and also antibacterial, antifungal, antiviral and antiparasitic activities,[11] radulanine A **24**, recently studied in our laboratory have also demonstrated a particular interest as herbicide natural product,[12] and stellatumolides A **25**[13] (Figure 1.4, bottom).

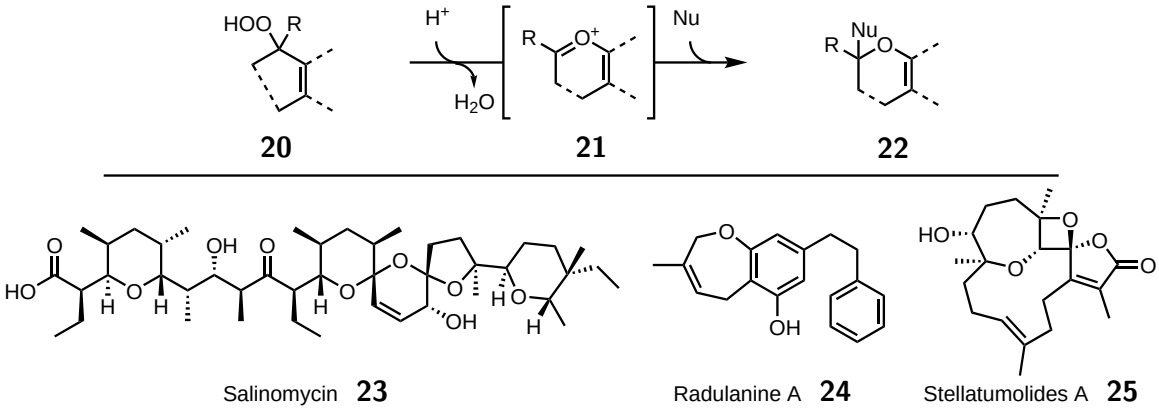

Figure 1.4: Top, Interrupted Hock cleavage; bottom, Natural products containing cyclic ethers.

[10] M. Sasaki, H. Fuwa, *Nat. Prod. Rep.* **2008**, *25*, 401-426.
[11] (a) M. Antoszczak, A. Huczyński, *Eur. J. Med. Chem.* **2019**, *176*, 208-227. (b) A. Markowska, J. Kaysiewicz, J. Markowska, A. Huczyński, *Bioorg. Med. Chem. Lett.* **2019**, *29*, 1549-1554.
[12] W. Zhang, E. Baudouin, M. Cordier, G. Frison, B. Nay, *Chem. Eur. J.* **2019**, *25*, 8643-8648.
[13] A. F. Ahmed, Y. W. Chen, C. Y. Huang, Y. J. Tseng, C. C. Lin, C. F. Dai, Y. C. Wu, J. H. Sheu, *Mar. Drugs*, **2018**, *16*, 210-215.

1.3 Old and new tricks in Total Synthesis

1.3.1 *Diverted Total Synthesis*

The target compounds presented in the first section show that chemists can mostly reach any level of complexity through target-oriented synthesis (TOS). However, this approach needs to design a new route for any new natural product, whereas in nature, secondary metabolite biosynthetic pathways can produce hundreds different products from common advanced intermediates.[14] Taking inspiration from this observation, can chemists use this type of strategy to access a collection of natural products from a common intermediate? This approach, known as diverted total synthesis (DTS), was first proposed by Boger and Brotherton back in 1984 with their total synthesis of rufescine and imeluteine.[15] In 2018, Sarpong and co-workers successfully applied this strategy to construct from a common intermediate **26** six phomactin terpenoids for example **27**-**29** (Figure 1.5).[16]

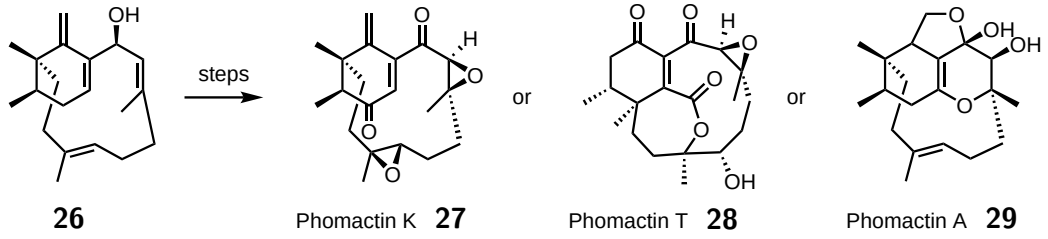

Figure 1.5: Sarpong's total synthesis of phomactin terpenoids.

In order to plan an efficient DTS approach, four different strategies (redox processes, reorganisation, stereochemistry and appendage) have been considered:[17]

[14] M. A. Fischbach, J. Clardy, *Nat. Chem. Biol.* **2007**, *3*, 353-355.
[15] D. L. Boger, C. E. Brotherton, *J. Org. Chem.* **1984**, *49*, 4050-4055.
[16] Y. Kuroda, K. J. Nicacio, I. A. da Silva-Jr, P. R. Leger, S. Chang, J. R. Gubiani, V. M. Deflon, N. Nagashima, A. Rode, K. Blackford, A. G. Ferreira, L. D. Sette, D. E. Williams, R. J. Andersen, S. Jancar, R. G. S. Berlinck, R. Sarpong, *Nat. Chem.* **2018**, *10*, 938-945.
[17] (a) L. Li, Z. Chen, X. Zhang, Y. Jia *Chem. Rev.* **2018**, *118*, 3752-3832. (b) J. Shimokawa, *Tetrahedron*, **2014**, *55*, 6156-6162.

Redox processes in DTS

Within a family of natural products, many differ from others only in their oxidation state. By manipulating a common intermediate through the redox process, a variety of natural compounds can be obtained. This concept has been described by Baran in 2009 as a two phase approach in the generation of complex terpenes.[18] Inspired by Nature, a first stage refers to the "cyclase phase" where the common intermediate is built, with its full natural product skeleton.[19] Then, a second stage called "oxidase phase" takes place where alkenes and the C-H bonds are oxidized to access a variety of natural products. The recent total synthesis of Taxol® **35** by Baran and co-workers is an example of this two phases approach. During the cyclase phase, a nortaxane core **34** is forged with a low level of oxidation starting from commercially available materials.[20] The oxidase phase allowed the oxidation of the diverse sites required to access Taxol® **35** (red dots on **34**, Figure 1.6).[21]

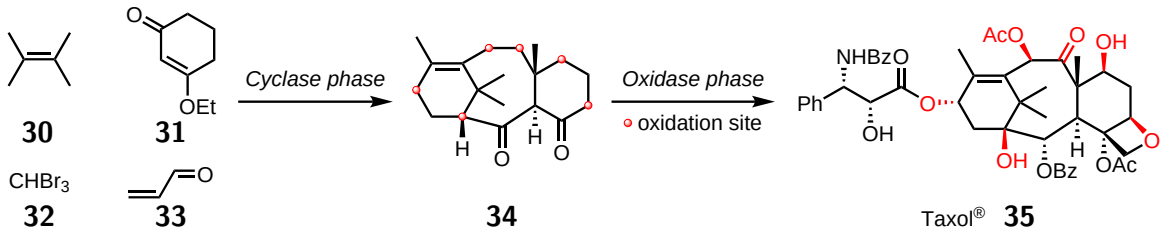

Figure 1.6: Two phase total synthesis of Taxol®.

Maimone and co-workers used this strategy to access different members of the pseudoanisatin family. From a common terpene intermediate **36** by manipulating the alkene through various oxidative reactions, they succeeded to reach (-)-3-deoxypseudoanisatin **37**, (+)-pseudoanisatin **38** and (-)-3-oxo-pseudoanisatin **39** (Figure 1.7).[22] The total synthesis

[18] K. Chen, P. S. Baran, *Nature*, **2009**, *459*, 824-828.
[19] E. M. Davis, R. Croteau, *Top. Curr. Chem.* **2000**, *209*, 53-95.
[20] A. Mendoza, Y. Ishihara, P. S. Baran, *Nat. Chem.* **2012**, *4*, 21-25.
[21] Y. Kanda, H. Nakamura, S. Umemiya, R. K. Puthukanoori, V. R. M. Appala, G. K. Gaddamanugu, B. R. Paraselli, P. S. Baran, *J. Am. Chem. Soc.* **2020**, *142*, 10526-10533.
[22] K. Hung, M. L. Condakes, L. F. T. Novaes, S. J. Harwood, T. Morikawa, Z. Yang, T. J. Maimone, *J. Am. Chem. Soc.* **2019**, *141*, 3083-3099.

of phomactin terpenoids developed by Sarpong's group used the same strategy (Figure 1.5).[16]

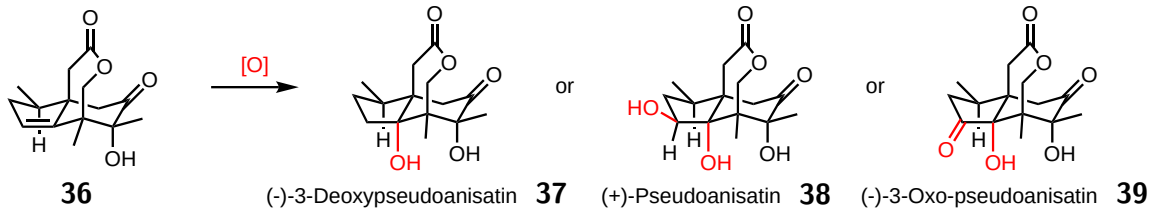

Figure 1.7: Pseudoanisatin natural products from common platform **36**.

Reorganisation in DTS

Diversification can also be achieved by playing with the different functional groups present in a common core and with the reactivity of key-intermediates. By reacting them in a different order, large families of natural compounds can be created. Reisman's group used this type of approach to develop a total synthesis of (-)-trichorabdal A **41**, (-)-longikaurin E **42** and (-)-maoecrystal Z **43** from common intermediate **40** thanks to a highly diastereoselective Sm^{II}-mediated reductive cyclizations and a Pd^{II}-mediated oxidative cyclization (Figure 1.8).[23]

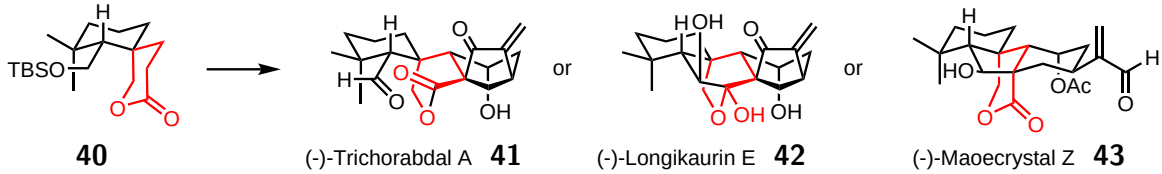

Figure 1.8: Reisman and co-workers reorganisation strategy from intermediate **40**.

Stereochemistry in DTS

In a natural product family, some compounds only diverge by their stereochemistry. The control of different centres through the use of highly stereospecific reactions can result in a diversity of natural products. For example, the Chen group successfully managed

[23] (a) J. Y. Cha, J. T. S. Yeoman, S. E. Reisman, *J. Am. Chem. Soc.* **2011**, *133*, 14964-14967. (b) J. T. S. Yeoman, V. W. Mak, S. E. Reisman, *J. Am. Chem. Soc.* **2013**, *135*, 11764-11767. (c) J. T. S. Yeoman, J. Y. Cha, V. W. Mak, S. E. Reisman, *Tetrahedron*, **2014**, *70*, 4070-4088.

to access members of the gabosine natural products by a selective reduction of enone **44** (Figure 1.9).[24]

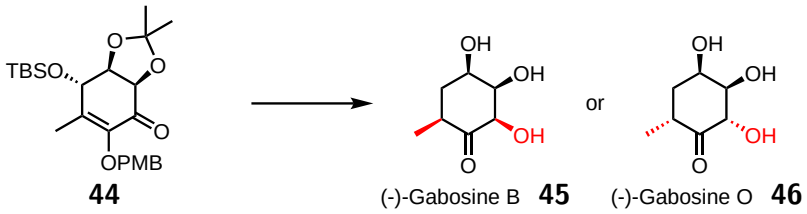

Figure 1.9: Selective reduction in (-)-gabosine B **45** and O **46** total synthesis.

Appendage in DTS

Diversity can also arise from the assembly of different moieties on a common precursor. In this way, a collection of natural products containing the same sub-structure can be rapidly generated. Jiang and co-workers accomplished the synthesis of fourteen *Aspidosperma* alkaloids. Three of them were achieved thanks to a Fischer indolization on the common ketone **47** with different phenylhydrazines (Figure 1.10).[25]

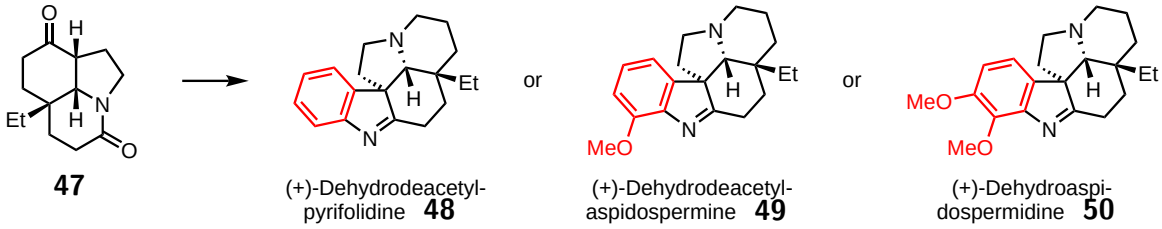

Figure 1.10: Collection of alkaloids obtained by different appendage from common core **44**.

The application of redox processes to the total of our two targets, trichodermone **2** and trichoderone A **3**, is envisaged from the common tetracyclic intermediate **1**. For example, the γ position of γ-lactam **53** was previously oxidized by Yoshihiro and co-workers to γ-hydroxy-γ-lactam **54** using RuO_4 and $NaIO_4$.[26] Similar conditions might give rise in our

[24] X. Yang, P. Yuan, F. Shui, Y. Zhou, X. Chen, *Org. Biomol. Chem.* **2019**, *17*, 4061-4072.
[25] N. Wang, S. Du, D. Li, X. Jiang, *Org. Lett.* **2017**, *19*, 3167-3170.
[26] Y. Shigeyuki, A. Yukimi, N. Yoshihiro, *Chem. Pharm. Bull.* **1985**, *33*, 5042-5047.

project to various possible products due to the presence of alkenes (Figure 1.11). These alkenes might be desymmetrized using their different chemical nature. For example conjugated dienol **52** was obtained by epoxidation of tetracyclic compound **51** using peroxyacetic acid followed by syn elimination using LDA,[27] tetrasubstituted alkene **55** was selectively transformed into epoxide **56** using *m*-CPBA,[28] and diol **58** was selectively synthesized from trisubstituted alkene **57** using OsO_4 and NMO. [29]

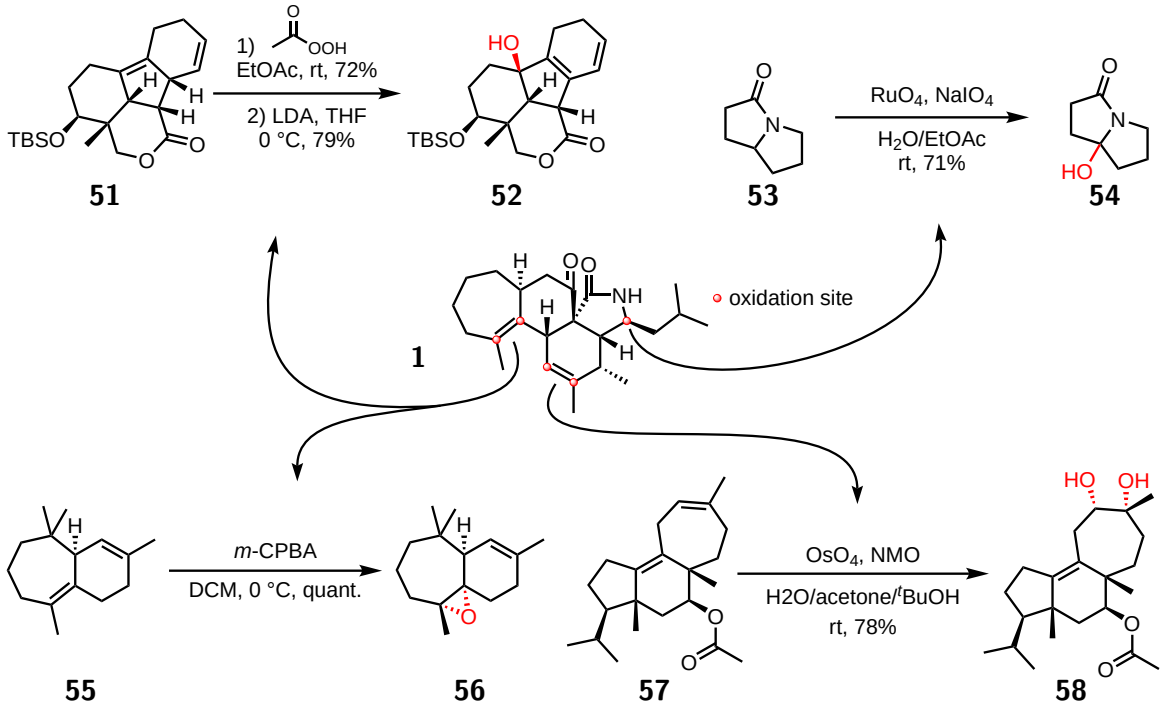

Figure 1.11: Examples of redox processes on similar substrates of tetracylic intermediate **1**.

DTS applied to the synthesis of natural products can be a powerful tool for delivering highly complex scaffolds in an optimal way. In addition to these approaches, the interface with other fields of science can be used to assist natural product chemists in their search for simplicity and efficiency. Computational chemistry is one of them.

[27] E. J. Corey, A. G. Myers, *J. Am. Chem. Soc.* **1985**, *107*, 5574-5576.
[28] A. Auhmani, E. Kossareva, H. El Jamili, M. Réglier, M. Pierrot, A. Benharref, *J. Chem. Crystallogr.* **2000**, *30*, 525-530.
[29] G. M. Molina-Salinas, J. Borquez, A. Ardiles, S. Said-Fernandez, L. A. Loyola, A. San-Martin, I. Gonzalez-Collado, L. M. Pena-Rodriguez, *Fitoterapia*, **2010**, *81*, 50-54.

1.3.2 *Computational chemistry*

Computational chemistry is based on the use of theoretical chemistry and powerful computing capabilities to help chemists simulate and solve their chemical problems. The interface with organic chemistry led to significant improvements of the field, being able to interpret the different properties observed experimentally.[30] In the field of natural product synthesis, the collaboration between these two domains allowed interesting predictions, such as the selectivity of a reaction, the choice and design of a substrate or a new synthetic approach.[31]

In this subsection, the only method presented will be the density functional theory (DFT).[32] This computational quantum chemistry method relies on the study of the electron density to calculate all the properties of a chemical system. Compared to Hartree-Fock (HF) and post Hartee Fock methods, DFT provides an exact Hamiltonian of the system, an operator representing the system studied, with an approximate solution, the energy of the system. This approach is less time- and memory-consuming because the electron density is only dependant of three space variables compared to three variables for each atom in HF and post HF methods. Furthermore, energies, geometries and reaction pathways provided by DFT are effectively accurate. To approach the best solution for a system, researchers have developed a broad range of functionals.[33] Among them hybrid functionals are the most used in computational organic chemistry, especially B3LYP and M06 functionals.[34] In addition a basis set is needed, this set of functions will describe the atomic orbitals. The larger the size, the more accurate the result will be, but the cost of the calculation will be higher. The Pople basis set composed of split valence functions, such as 6-31G and 6-311G,

[30] (a) S. Niu, M. B. Hall, *Chem. Rev.* **2000**, *100*, 353-405. (b) N. Fey, *Dalton Trans.* **2010**, *39*, 296-310.
[31] (a) Q. N. N. Nguyen, D. J. Tantillo, *Chem. Asian J.* **2014**, *9*, 674-680. (b) M. Elkin, T. R. Newhouse, *Chem. Soc. Rev.* **2018**, *47*, 7830-7844. (c) D. J. Tantillo, *Chem. Soc. Rev.* **2018**, *47*, 7845-7850.
[32] W. Kohn, M. C. Holthausen, *A Chemist's Guide to Density Functional Theory*, Wiley-VCH, Weinheim, **2000**.
[33] N. Mardirossian, M. Head-Gordon, *Mol. Phys.* **2017**, *115*, 2315-2372.
[34] (a) A. D. Becke, *Phys. Rev. A*, **1988**, *38*, 3098-3100. (b) A. D. Becke, *J. Chem. Phys.* **1988**, *109*, 2092-2098. (c) C. Lee, W. Yang, and R. Parr, *Phys. Rev. B*, **1988**, *37*, 785-789. (d) Y. Zhao, D.G. Truhlar, *Theor. Chem. Acc.* **2006**, *120*, 215-241.

polarization functions, such as d orbitals for heavy atoms and p orbitals for hydrogen, and diffuse functions, "+" on heavy atoms and "++" on heavy and hydrogen atoms will be used in this thesis.[35] For example, 6-311+G(2df,2p), 6-31+G(d,p) and 6-31G(d) are high, medium and low level basis set, respectively. The choice of the basis set and functional will be driven by the system and what the chemist want to model (geometry, transition states...).

DFT as a tool to substrate design

DFT calculations can be used to rationalize the observed chemical reactivity by modelling reaction pathways. Once found, a comparison with the experimental results can validate the model and an optimisation of the reaction is possible by for example adding diverse substitutions on one substrate.

In 2018, Overman and co-workers published the total synthesis of (-)-chromodorolide B **66**.[36] In their article, they described two different generations of synthesis. The first one used only the classical approach of organic synthesis (Figure 1.12). Starting from ketone **59** and acetal **60**, they quickly built intermediate **61**. Compounds **61** and **62** were subjected to a radical addition/cyclization/fragmentation (ACF) cascade in order to obtain the desired diastereomer **65**. This audacious reaction created in a single step 4 contiguous stereocenters and two C-C bonds. Unfortunately for them, radical **63** led to 2 diastereomers **65** and **64** at C-8 position, through the 5-*exo* cyclization. Only the minor one (**65**) got all the stereocenters required for delivering (-)-chromodorolide B **66**. In order to develop a more efficient total synthesis, Overman's group decided to use computational methods to design a better substrate for the ACF cascade.

To achieve such a goal, they turned to DFT methods for energy minimization (TPSS/def2-

[35] R. Ditchfield, W. J. Hehre, J. A. Pople, *J. Chem. Phys.* **1971**, *54*, 724-728.
[36] D. J. Tao, Y. Slutskyy, M. Muuronen, A. Le, P. Kohler, L. E. Overman, *J. Am. Chem. Soc.* **2018**, *140*, 3091-3102.

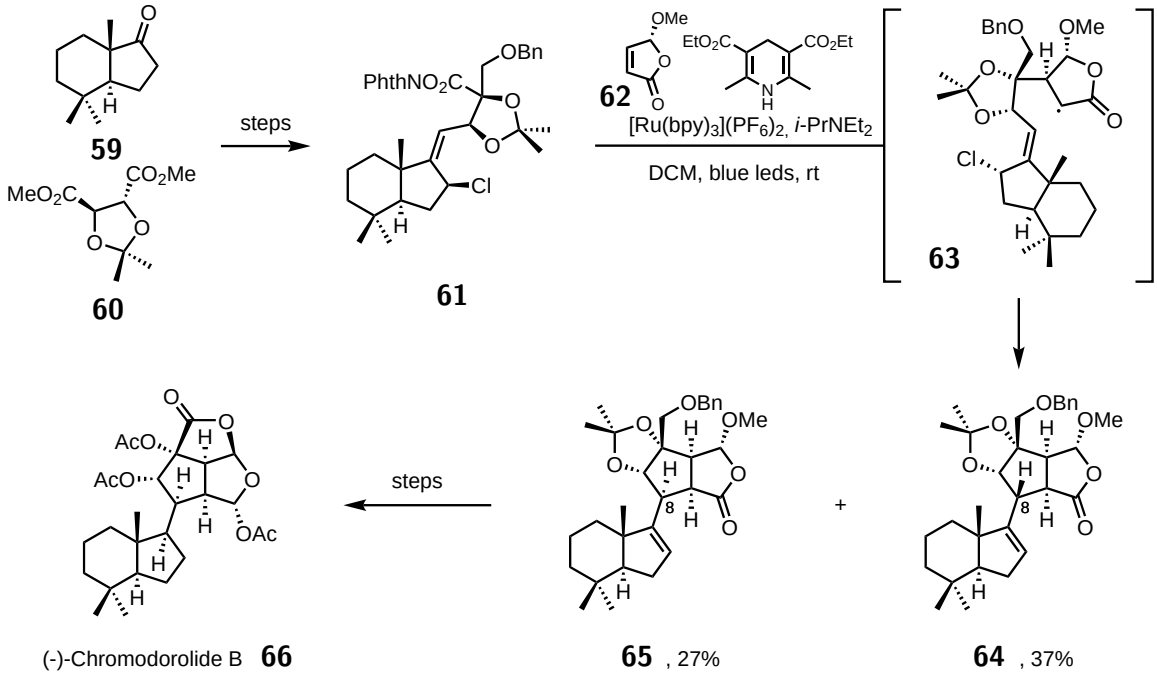

Figure 1.12: Overman first approach to (-)-chromodorolide B **66**.

TZVP with BJ-damped D3-dispersion) [37] and single point calculation (TPPSh/def2-TZVP) to get a better understanding of the reaction mechanism and therefore proposed a second-generation substrate design. They first considered two possible pathways, with either **69** and **70** reacting through a radical mechanism by a direct *5-exo* cyclization, or the radical being reduced to an enolate to be engaged in an intramolecular S_N2' reaction with the corresponding allyl chloride. After modelling both systems, they found that they were both thermodynamically and kinetically feasible. To choose one of them, they compared the outcome of the first approach with the results they obtained from calculation. The radical pathway was found to have the lowest energy for the transition state **68**, leading to the undesired diastereomer, by 1.0 kcal/mol in DCM or 0.5 kcal/mol in MeCN compared to TS **67**, leading to the desired diastereomer. This can be translated by a theoretical ratio **64**:**65** of 2.5:1 in MeCN, which is comparable to the experimentally obtained 1.4:1. When the

[37] (a) H. Kruse, L. Goerigk, S. Grimme, *J. Org. Chem.* **2012**, *77*, 10824-10834. (b) J. P. Wagner, P. R. Schreiner, *Angew. Chem., Int. Ed.* **2015**, *54*, 12274-12296.

enolate pathway was examined, calculations revealed an inverse trend favourably leading to a theoretical ratio **64**:**65** of 1:3.4. They assumed that the most possible mechanism was the radical pathway due to closest modelled ratio of diastereoisomers compared to the one obtained experimentally. Based on that discovery, they pursued their optimization by trying to favour the *cis* transition state. By closely studying the two transition states when X = H, they observed that TS **68** has a longer forming bond with 2.38 Å compared to 2.25 Å for TS **67**. They then postulated that having a larger atom at the α-position of the lactone will result in a destabilizing steric interaction for the *trans*-transition state. The introduction of a chlorine atom stabilized TS **71** compared to TS **72** by 2.0 kcal/mol, leading to the desired diastereomer.

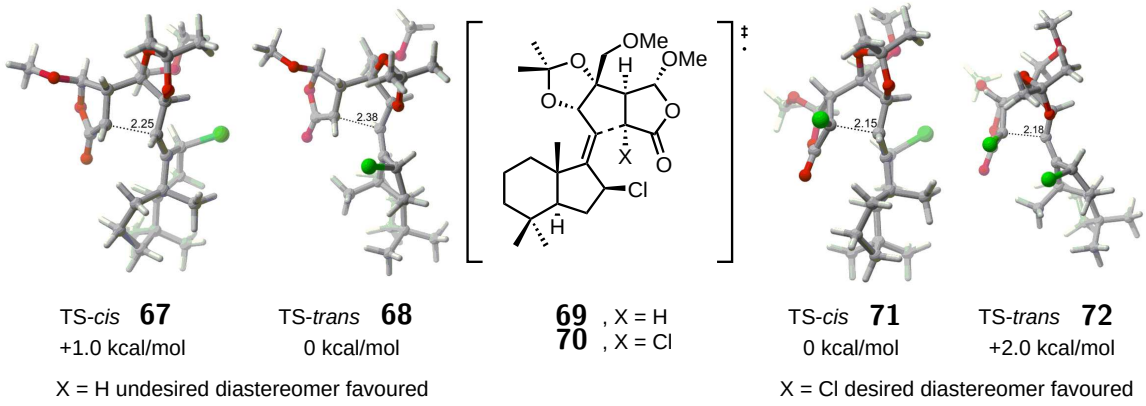

Figure 1.13: Radical pathway calculation in the key ACF cascade.

These calculated results were then subjected to an experimental second approach of the total synthesis of (-)-chromodorolide B **66**. They found that the reaction of alkene **61** and lactone **73** proceeded smoothly and afforded only the desired diastereomer **74** with a yield of 57%.

This example illustrates the power of computational methods to design a new substrate in order to develop a more robust total synthesis. However these calculations occur after encountering a problem. Thus, the use of quantum chemistry calculations to provide a possible retron before conducting an experiment might be a useful tool in natural product

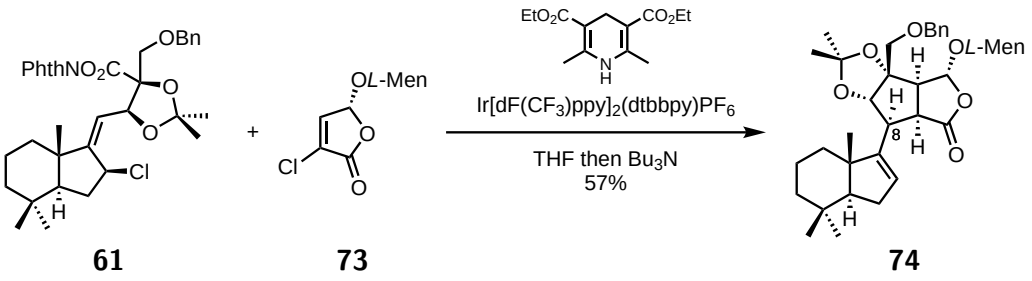

Figure 1.14: Overman second approach to (-)-chromodorolide B **66**.

synthesis.

DFT calculations as a predictive tool for retrosynthesis analysis

In order to achieve an efficient total synthesis, Newhouse and co-workers developed in 2019 a new approach using DFT.[38] They used this tool to select, before any experimental work, the most appropriate retrosynthetic pathway to reach paspaline A **75**,[39] and emindole PB **76**,[40] two complex indole diterpenoid natural products (Figure 1.15). When this article was published, the authors stated that this was the first time that DFT calculations had been used to improve and assist retron selection by modelling the viability of a key reaction.

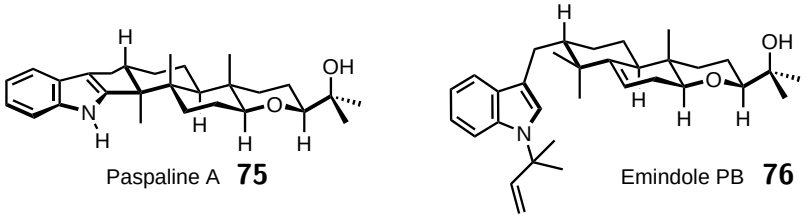

Figure 1.15: Paspaline A **75** and emindole PB **76**.

To do this, they considered using a common intermediate cation to reach both natural products. They decided to assess the feasibility of the reaction by looking at three different retrons: **79**, **80** and **81** (Figure 1.16). They differ only by a structural variation of the

[38] D. E. Kim, J. E. Zweig, T. R. Newhouse, *J. Am. Chem. Soc.* **2019**, *141*, 1479-1483.
[39] J. P. Springer, J. Clardy, *Tetrahedron Lett.* **1980**, *21*, 231-234.
[40] (a) K. Kawai, K. Nozawa, S. Nakajima, *J. Chem. Soc., Perkin Trans. 1*, **1994**, *0*, 1673-1674. (b) T. Hosoe, T. Itabashi, N. Kobayashi, S. Udagawa, K. Kawai, *Chem. Pharm. Bull.* **2006**, *54*, 185-187.

last ring, **79** being acyclic, **80** being monocyclic and **81** being bridged, implying a different flexibility. Using DFT calculations, they hoped to choose the perfect substrate capable of performing a Friedel-Crafts reaction leading to paspaline A **75** and a 1,2 methyl shift migration leading to emindole PB **76**. To reduce the number of possible reaction pathways, they assumed that the 1,2 methyl shift would be either a concerted or stepwise mechanism and that the cyclization to form the quaternary center would only be carbocationic.[41] Their goal was to predict the best substrate that would promote cyclization rather than the 1,2 methyl shift, e.g. the highest $\Delta\Delta G^{\ddagger}$ between transition states **82** and **78**. To do this, they compared different pathways from the three starting carbocationic substrates using mPW1PW91/6-31+G(d,p)//B3LYP/6-31G* level of theory. They found that carbocation **81** was the most prone to cyclization, via a stepwise pathway, with $\Delta\Delta G^{\ddagger}$ of 4.5 kcal/mol.[42] The next challenge was to confirm that the *trans*-cyclization would be preferred over the *cis* one. In general, the formation of a 5-membered ring generates a *cis*-fused system.[43] In the indole terpenoid natural product family, both mechanism have been observed.[44] In the course of their investigation, they found that the *trans*-cyclization was favoured over the *cis* with a $\Delta\Delta G^{\ddagger}$ of 1.3 kcal/mol for carbocation **81**.

[41] M. Elkin, A. C. Scruse, A. Turlik, T. R. Newhouse, *Angew. Chem. Int. Ed.* **2019**, *58*, 1025-1029.
[42] S. P. T. Matsuda, W. K. Wilson, Q. Xiong, *Org. Biomol. Chem.* **2006**, *4*, 530-543.
[43] A. L. J. Beckwith, G. Phillipou, A. K. Serelis, *Tetrahedron Lett.* **1981**, *22*, 2811-2814.
[44] (a) X. Xiong, D. Zhang, J. Li, Y. Sun, S. Zhou, M. Yang, H. Shao, A. Li, *Chem. Asian J.* **2015**, *10*, 869-872. (b) D. H. Dethe, S. K. Sau, S. Mahapatra, *Org. Lett.* **2016**, *18*, 6392-6395.

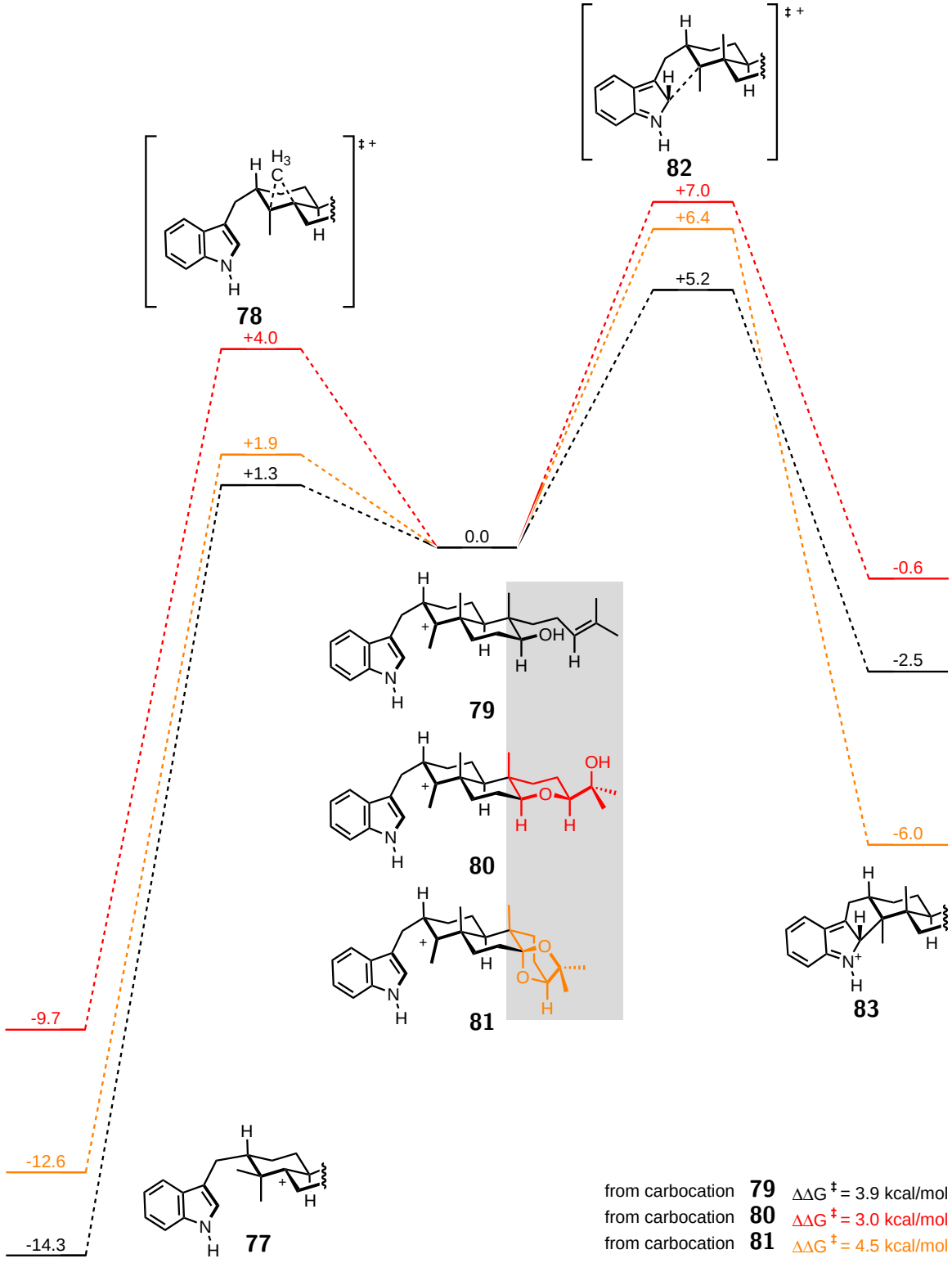

Figure 1.16: Computed enthalpies energies for the Friedel-Crafts reaction and the 1,2 methyl shift of three different carbocation candidates. Energies relative to the starting materials are given in kcal.mol^{-1}. On the bottom right corner, $\Delta\Delta G^{\ddagger}$ between the two transition states.

With these results in hand, they synthesized key intermediate **87** starting from a Wieland-Miescher ketone derivative **84**, isoprenyl derivative **85** and 3-iodomethyl indole **86**. They subjected tetracyclic intermediate **87** to a Lewis acid-catalyzed reaction to generate predicted carbocation **81**. This one underwent the two calculated pathways leading to products **88** and **89** in a 1:3 ratio without any *cis*-cyclization product observed (Figure 1.17).

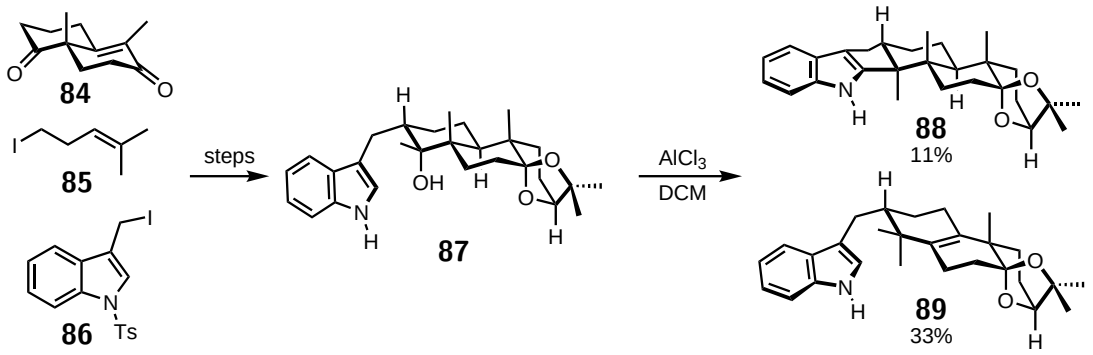

Figure 1.17: Newhouse and co-workers key reaction in the total synthesis of paspaline A **75** and emindole PB **76**.

This example illustrates the power of DFT calculations applied to natural product synthesis as a predictive tool. The drawback of this approach is that the obtained model cannot be compared to experimental data but a main advantage is the bench time saving for the synthetic chemist. The authors were able to synthesize paspaline A **75** in only nine steps, whereas the total syntheses previously reported required more than 25 steps,[45] and emindole PB **76**.

Desired use of DFT calculations in our project

In the previous subsections, two applications of DFT calculations were developed; one use to explain and improve a reaction and the other to predict an outcome. The same type of modelling is envisaged for our total synthesis of aspochalasines. In fact, during previous cytochalasins total syntheses, the IMDA reaction was the method of choice to form the

[45](a) A. B. Smith, R. Mewshaw, *J. Am. Chem. Soc.* **1985**, *107*, 1769-1771. (b) A. B. Smith, T. L. Leenay, *J. Am. Chem. Soc.* **1989**, *111*, 5761-5768.

isoindolone core **91** (red part, Figure 1.18). A more detailed presentation will be made in the dedicated chapter. Some of these reactions were efficiently catalysed, while others were not and in a particular cases, the protecting group on the γ-lactam played a crucial role. We aim to answer with DFT calculations to two questions:

- Can DFT calculations rationalize previously observed catalyst effects on this reaction and allow to improve conditions for effective use of catalyst?
- Can DFT calculations help us to predict the most appropriate protecting group for a more efficient IMDA reaction?

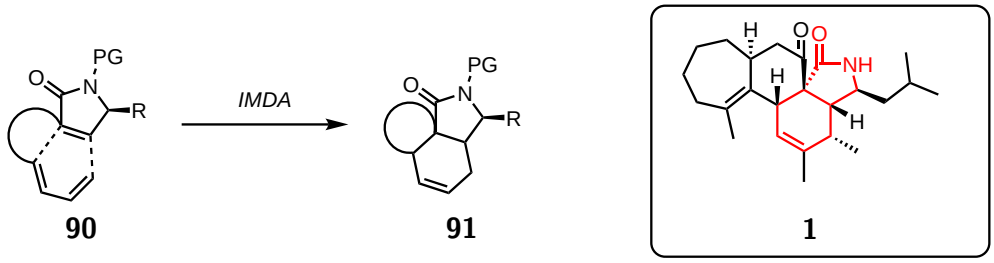

Figure 1.18: IMDA reaction used to forge isoindolone core **91** in the cytochalasins total synthesis.

Chapter 2

A Journey into the Total Synthesis of Cytochalasins

2.1 Introduction

2.1.1 *Origin and structure of cytochalasins*

Cytochalasins are a family of polyketide natural products of fungal origin. The first members, named cytochalasin A **92** and cyctochalasin B **93**, were extracted from a culture of *Phoma S298*,[1] and *Helminthosporium dematioideum*,[2] and characterized in 1966 and 1967. Today, hundreds of different cytochalasins have been discovered.[3] The majority of cytochalasins consists of an isoindolone core (red part) derived from an amino-acid (bold part), with different oxidation states at the C5-C7 region, for example alkene in phomopsichalasin **95**,[4] allylic alcohol in cytochalasin A **92** or epoxide in armochaetoglobins A **94**.[5] This amino-acid will determine the nomenclature of the cytochalasins:

- Cytochalasins will come from L-phenylalanine, e.g. cytochalasin A **92** or B **93**.
- Pyrichalasins will arise from L-tyrosin, e.g. pyrichalasin H **98**.[6]
- Alachalasins will be derived from L-alanine, e.g. alachalasin C **96**.[7]
- Chaetoglobosins will come from L-tryptophan, e.g. armochaetoglobins A **94**.
- Aspochalasines, monomer, and asperchalasines, dimer, will be derived from L-leucine, e.g. aspochalasine D **99**,[8] and asperchalasine A **97**.[9]

[1] W. Rothweiler, C. Tamm, *Experientia* **1966**, *22*, 750-752.
[2] D. C. Aldridge, J. J. Armstrong, R. N. Speake, W. B. Turner, *Chem. Commun. (London)*, **1967**, 26-27.
[3] (a) E. Skellam, *Nat. Prod. Rep.* **2017**, *34*, 1252-1253. (b) K. Scherlach, D. Boetteger, N. Remme, C. Hertweck, *Nat. Prod. Rep.* **2010**, *27*, 869-886.
[4] W. S. Horn, M. S. J. Simmonds, R. E. Schwartz, W. M. Blaney, *Tetrahedron*, **1995**, *51*, 3969-3978.
[5] C. Chen, J. Wang, J. Liu, H. Zhu, B. Sun, J. Wang, J. Zhang, Z. Luo, G. Yao, Y. Xue, Y. Zhang, *J. Nat. Prod.* **2015**, *78*, 1193-1201.
[6] M. Nukina, *Agric. Biol. Chem.* **1987**, *51*, 2625-2628.
[7] Y. Zhang, R. Tian, S. Liu, X. Chen, X. Liu, Y. Che, *Bioorg. Med. Chem.* **2008**, *16*, 2627-2634.
[8] W. Keller-Schierlein, E. Kupfer, *Helv. Chim. Acta*, **1979**, *62*, 1501-1523.
[9] H. Zhu, C. Chen, Y. Xue, Q. Tong, X.-N. Li, X. Chen, J. Wang, G. Yao, Z. Luo, Y. Zhang, *Angew. Chem. Int. Ed.* **2015**, *54*, 13374-13378.

To the isoindolone core, a macrocycle, up to 14, is generally fused but some exceptions can be observed such as a long chain in armochaetoglobins A **94**, or a polycyclics moeity in phomopsichalasin **95** (Figure 2.1).

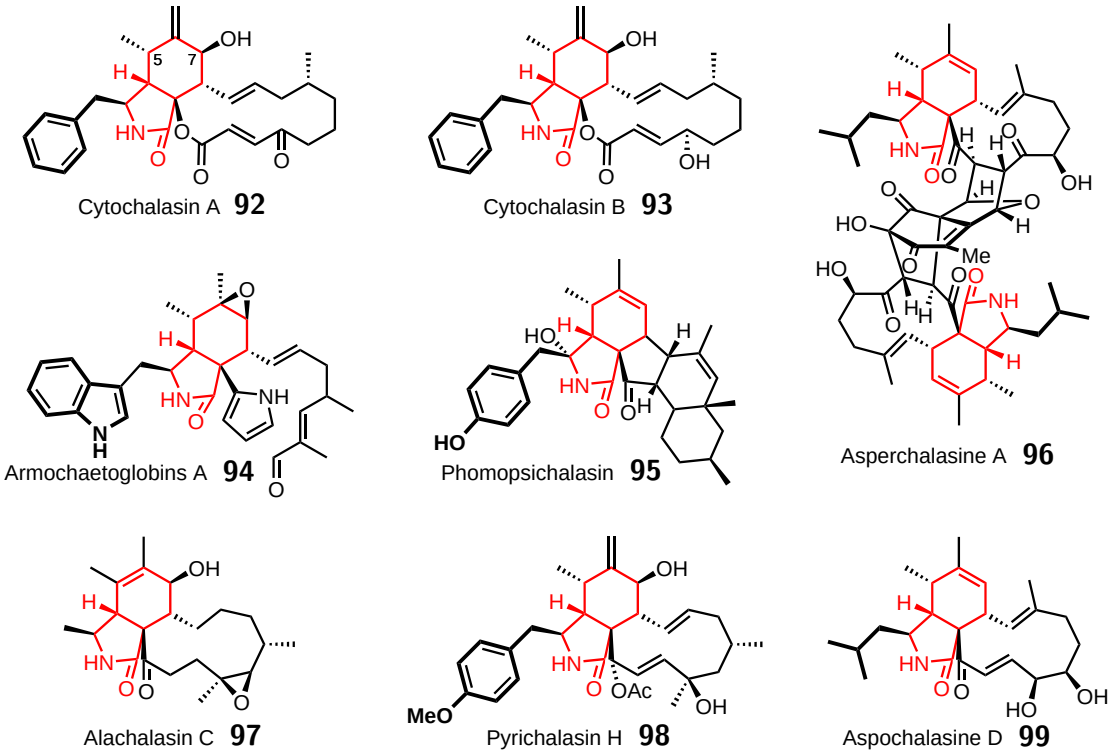

Figure 2.1: Diversity in the cytochalasins family.

Their biosynthetic pathway can be divided in two parts.[10] The first one, controlled by the polyketide synthases, PKS, and the nonribosomal peptide-synthetases, NRPS, will form a linear precursor. This starts with an acetyl fragment linked to an acyl carrier protein, ACP, **100**. The elongation is then achieved by bringing malonyl CoA **101** to the ACP via the acyl transferase, AT, and catalysed by the keto synthetase, KS, through a decarboxylative Claisen condensation leading to a β-keto acyl group. The newly formed carbonyl function can be reduced to the alcohol function by the keto reductase, KR. The dehydratase, DH, is able to transform the alcohol to an alkene and the enoyl reductase,

[10] J. Schemann, C. Hertweck, *J. Am. Chem. Soc.* **2007**, *129*, 9564-9565.

ER, can then reduced it into a saturated acyl chain which can start a new elongation cycle. Thus, this cycle adds two more carbons to the acyl chain and can be stop at different stages to produce diverse functions: ketone, alcohol, alkene or saturation. After the KS enzyme, a methyl transferase, MT, can add a methyl group to the chain between the two carbonyls via *S*-adenosyl methionine, SAM, **104**. Once the linear chain is constructed, the activated amino acid **102** linked to the NRPS module reacts with the linear thioester linked to the ACP to form the final linear precursor **105** (Figure 2.2).

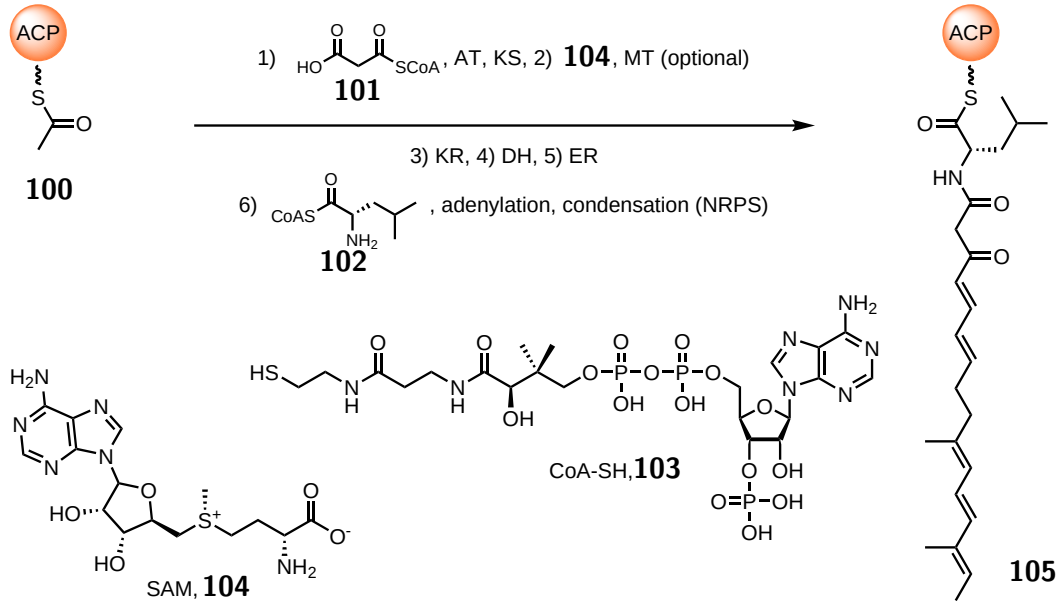

Figure 2.2: Elongation during a hypothetic aspocytochalasine biosynthesis.

The second part of the biosynthesis will form the isoindolone core of the cytochalasins. Polyketide **106** is first released via a reduction of the thioester into an aldehyde.[11] The aldehyde might be trapped through a Knoevenagel condensation to form the α,β unsaturated γ-lactam **107** which can then react through an intramolecular Diels-alder reaction

[11] (a) U. Oppermann, C. Filling, M. Hult, N. Shafqat, X. Wu, M. Lindh, J. Shafqat, E. Nordling, Y. Kallberg, B. Persson, H. Jörnvall, *Chem-Biol. Interact.* **2003**, *143-144*, 247-253. (b) J. W. Sims, E. W. Schmidt, *J. Am. Chem. Soc.* **2008**, *130*, 11149-11155. (c) L. M. Halo, J. W. Marshall, A. A. Yakasai, Z. Song, C. P. Butts, M. P. Crump, M. Heneghan, A. M. Bailey, T. J. Simpson, C. M. Lazarus, R. J. Cox, *ChemBioChem*, **2008**, *9*, 585-594.

(IMDA) to form tricyclic intermediate **108** (Figure 2.3). For example, dihydroxylation of the γ,δ position of the carbonyl might produce aspochalasine D **99**.

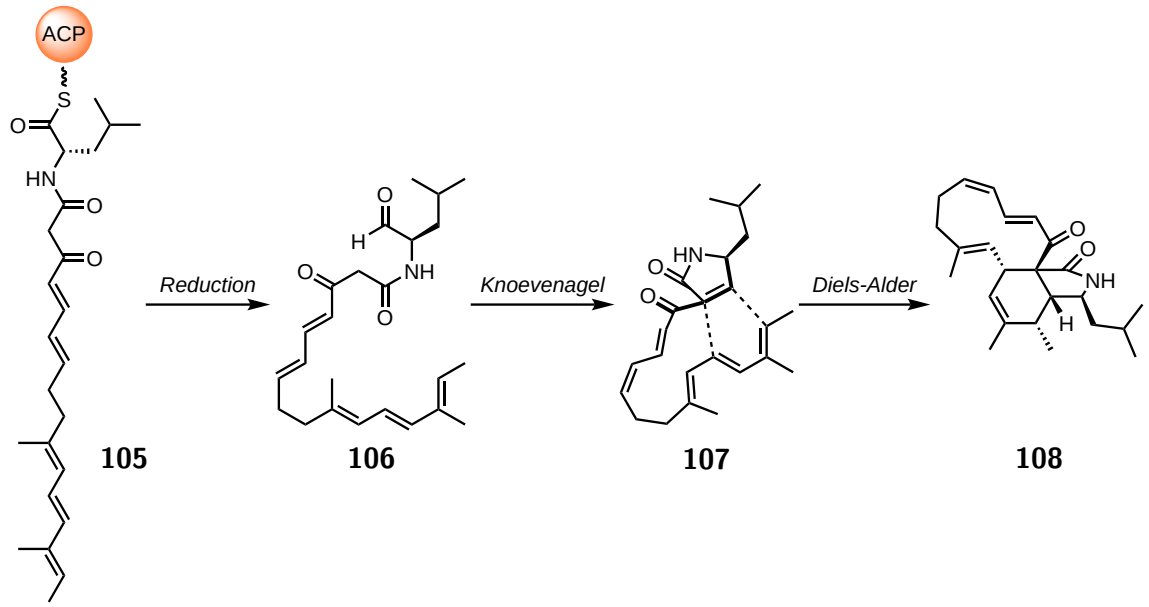

Figure 2.3: Construction of the isoindolone core during a hypothetic aspochalasine biosynthesis.

2.1.2 *Biological interest of cytochalasins*

The main known biological feature of cytochalasins is suggested in their names, from Greek *kytos* meaning cell and *chalasis* meaning relaxation, in reference to the property of some of these molecules (cytochalasin B **93** and D **122**) to destructure the actin filament.[12] The microfilaments called actin-F, a helical structure forming the cell cytoskeleton (Figure 2.4), consist of the assembly of a globular subunit called actin-G (green sphere, Figure 2.4). Their field of action is vast; it includes inhibition of cellular processes such as cell motility, cytokinesis, muscle contraction or exo- and endocytosis.[13] Actin-F is a dynamic structure

[12] (a) S. MacLean-Fletcher, T. D. Pollard, *Cell*, **1980**, *20*, 329-341. (b) M. Schliwa, *J. Cell Biol.* **1982**, *92*, 79-91.

[13] (a) I. Foissner, G. O. Wasteneys, *Plant. Cell. Physiol.* **2007**, *48*, 585-597. (b) W. Berger, M. Mickske, L. Elbling, *Exp. Cell Res.* **1997**, *237*, 307-317. (c) T. Hirose, Y. Izawa, K. Koyama, S. Natori, K. Lida, I. Yahara, S. Shimaoka, K. Maruyama, *Chem. Pharm. Bull.* **1990**, *38*, 971-974. (d) J. R. Peterson, T. J. Mitchison, *Chem. Biol.* **2002**, *9*, 1275-1285.

where acting-G binds at the barbed end or (+)-end, and dissociates at the pointed end or (-)-end. Cytochalasins B **93** and D **122** can block polymerization of the actin filament by binding at the (+)-end.[14]

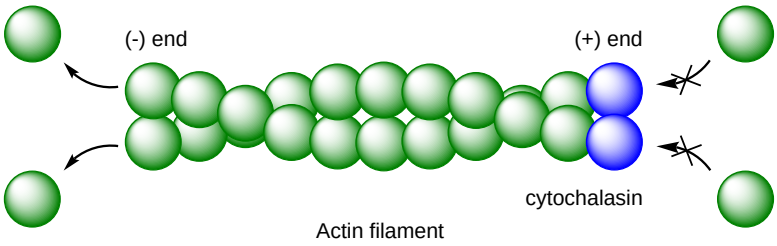

Figure 2.4: Simplified cytochalasins activity on the actin filament (green).

These and other cytochalasin compounds exhibit other biological activities, such as cytotoxic and possibly antitumour properties, and can also inhibit glucose transport across the cell membrane.[15] In addition, some antimicrobial and antifungal activities have been observed, for example by cytochalasin A **92** against the bacteria *Bacillus subtilis* and *Escherichia coli* and the fungus *Botrytis cinerea*.[16]

2.1.3 *Common strategies in cytochalasins total synthesis*

Despite their structural diversity, a common strategy has been employed in the different total synthesis reported to date. The core isoindolone moiety is built by a Diels-Alder reaction between a α,β unsaturated γ-lactam, derived from the corresponding amino acid, and a diene bearing the functionnalized chain percursor of the macrocycle. This Diels-Alder reaction can be inter- or intramolecular (Table 2.1). To date, 12 cytochalasins have been synthetized using an IMDA approach and 11 using an intermolecular strategy. The main

[14] D. W. Goddette, C. Frieden, *J. Biol. Chem.* **1986**, *261*, 15974-15980.
[15] (a) S. B. Carter, *Nature* **1967**, *213*, 261-264. (b) S. Sekita, K. Yoshihira, S. Natora, S. Udagawa, F. Sakabe, H. Kurata, M. Umeda, *Chem. Pharm. Bull.* **1982**, *30*, 1609-1617. (c) H. Oikawa, Y. Murakami, A. Ichihara, *Tetrahedron Lett.* **1991**, *32*, 4533-4536. (d) W. Jiao, Y. Feng, J. W. Blunt, A. L. Cole, M. H. Munro, *J. Nat. Prod.* **2004**, *67*, 1722-1725. (e) K. A. Alvi, B. Nair, H. Pu, R. Ursino, C. Gallo, U. Mocek, *J. Org. Chem.* **1997**, *62*, 2148-2151. (f) T. Udagawa, J. Yuan, D. Panigrahy, Y. H. Chang, J. Shah, R. J. D'Amato, *J. Pharmacol. Exp. Ther.* **2000**, *294*, 421-427.
[16] V. Betina, D. Micekova, P. Nemec, *J. Gen. Microbiol.* **1972**, *71*, 343-349.

advantage of the IMDA strategy is an easier construction of the macrocycle or polycyclics core, but the disadvantage is the linear precursor that is more complex to synthesize. For the intermolecular approach, dienes and dienophiles are generally easier to prepare and the main disadvantage is the construction of the macrocycle once the isoindolone core is formed.

Table 2.1: Total syntheses of cytochalasins.

Intermolecular Diels-Alder cyclization			Intramolecular Diels-Alder cyclization (IMDA)		
Stork[17]	Cytochalasin B **93**	1978	Stork[18]	Cytochalasin B **93**	1983
Vedejs[19]	Zygosporin E **110**	1988	Thomas[20]	Cytochalasin G **120**	1986
Trost[21]	Aspochalasin B **111**	1989	Thomas[22]	Cytochalasin H **121**	1986
Myers[23]	L-696,474 **112**	2004	Thomas[24]	Cytochalasin D **122**	1990
	Cytochalasin B **93**		Thomas[25]	Cytochalasin O **123**	1999
Tang[26]	Asperchalasines A-E **113-117**	2018	Overman[27]	Aspergillin PZ **119**	2011
Deng[28]	Asperchalasines A **113**, D **116**	2018	Tang[29]	Periconiasins A-E **124-128**	2016
	E **117** and H **118**		Nay[30]	Periconiasin G **129**	2016
Trauner[31]	Aspergillin PZ **119**	2018	Zhang[32]	Periconiasins A **124**	2018

[17] G. Stork, Y. Nakahara, Y. Nakahara, W. J. Greenlee, *J. Am. Chem. Soc.* **1978**, *100*, 7775-7777.
[18] G. Stork, E. Nakamura, *J. Am. Chem. Soc.* **1983**, *105*, 5510-5512.
[19] E. Vedejs, J. D. Rodgers, S. J. Wittenberger, *J. Am. Chem. Soc.* **1988**, *110*, 4822-4823.
[20] H. Dyke, R. Sauter, P. Steel, E. J. Thomas, *J. Chem. Soc., Chem. Commun.* **1986**, 1447-1449.
[21] B. M. Trost, M. Ohmori, S. A. Boyd, H. Okawara, S. J. Brickner, *J. Am. Chem. Soc.* **1989**, *111*, 8281-8284.
[22] E. J. Thomas, J. W. F. Whitehead, *J. Chem. Soc., Chem. Commun.* **1986**, 727-728.
[23] A. M. Haidle, A. G. Myers, *PNAS*, **2004**, *101*, 12048-12053.
[24] E. Merifield, E. J. Thomas, *J. Chem. Soc., Chem. Commun.* **1990**, 464-466.
[25] E. Merifield, E. J. Thomas, *J. Chem. Soc. Perkin. Trans. 1* **1999**, 3269-3283.
[26] R. Bao, C. Tian, H. Zhang, Z. Wang, Z. Dong, Y. Li, M. Gao, H. Zhang, G. Liu, Y. Tang, *Angew. Chem. Int. Ed.* **2018**, *57*, 14216-14220.
[27] S. M. Canham, L. E. Overman, P. S. Tanis, *Tetrahedron*, **2011**, *67*, 9837-9843.
[28] X. Long, Y. Ding, J. Deng, *Angew. Chem. Int. Ed.* **2018**, *57*, 14221-14224.
[29] C. Tian, X. Lei, Y. Wang, Z. Dong, G. Liu, Y. Tang, *Angew. Chem. Int. Ed.* **2016**, *55*, 6992-6996.
[30] M. Zaghouani, C. Kunz, L. Guédon, F. Blanchard, B. Nay, *Chem. Eur. J.* **2016**, *22*, 15257-15260.
[31] J. R. Reyes, N. Winter, L. Spessert, D. Trauner, *Angew. Chem. Int. Ed.* **2018**, *57*, 15587-15591.
[32] Z. Zeng, C. Chen, Y. Zhang, *Org. Chem. Front.* **2018**, *5*, 838-840.

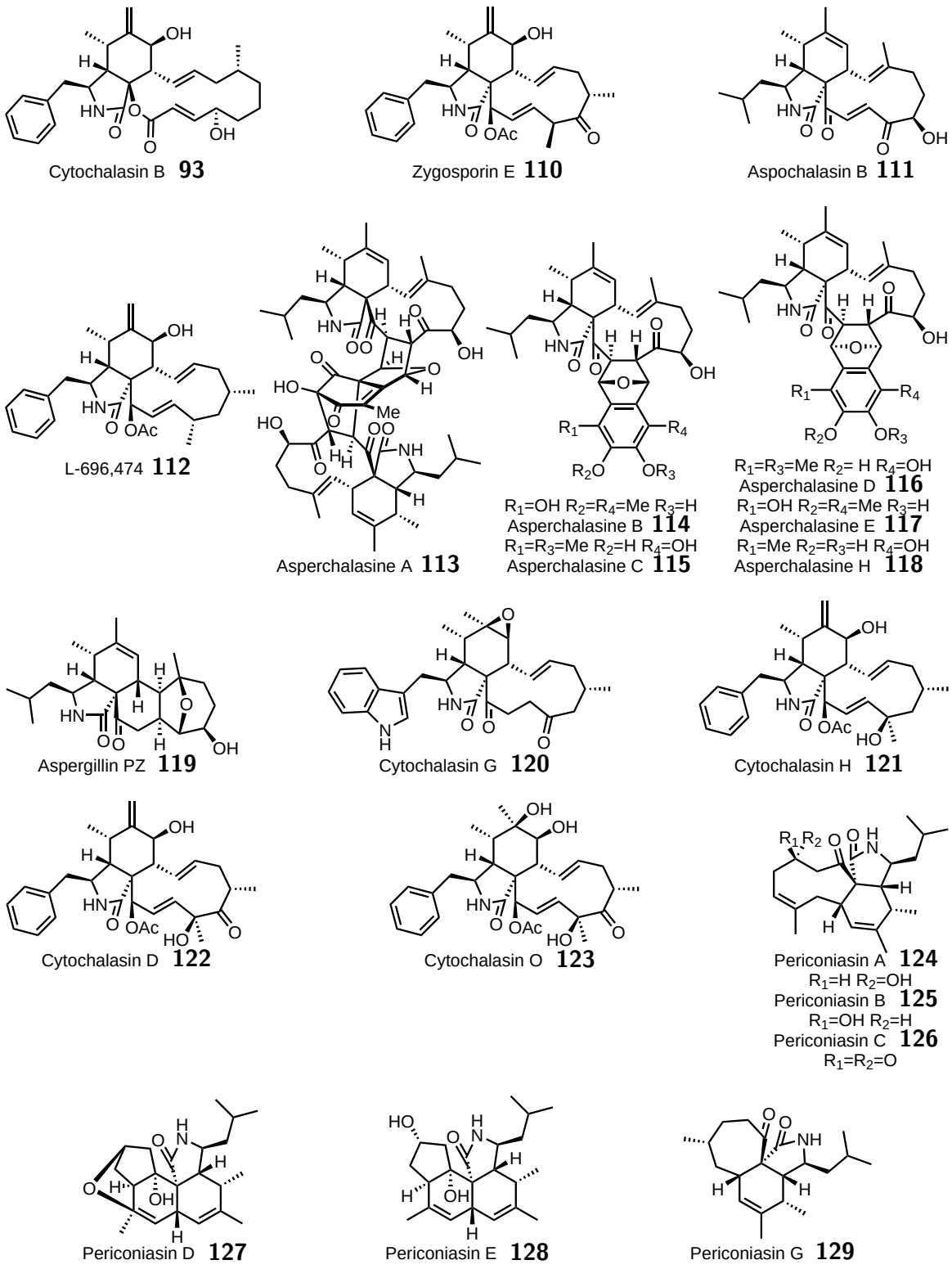

Figure 2.5: Cytochalasins synthesised to date.

For example, Stork and co-workers developed in 1978 the first total synthesis of cytochalasin B **93** via an intermolecular Diels-Alder reaction,[17] and in 1983 through an IMDA reaction (Figure 2.6).[18] They found that the intermolecular Diels-Alder reaction between γ-lactam **130** and linear chain **131** gave bicyclic product **132** with a better yield than tricyclic compound **134** formed with the IMDA reaction of triene **133**, 40% versus 30%, with the same ratio of 4:1 *endo*/*exo* adduct. However, the IMDA approach was preferred because its avoids the inefficient macrolactonization, 36%, required in the intermolecular approach.[33]

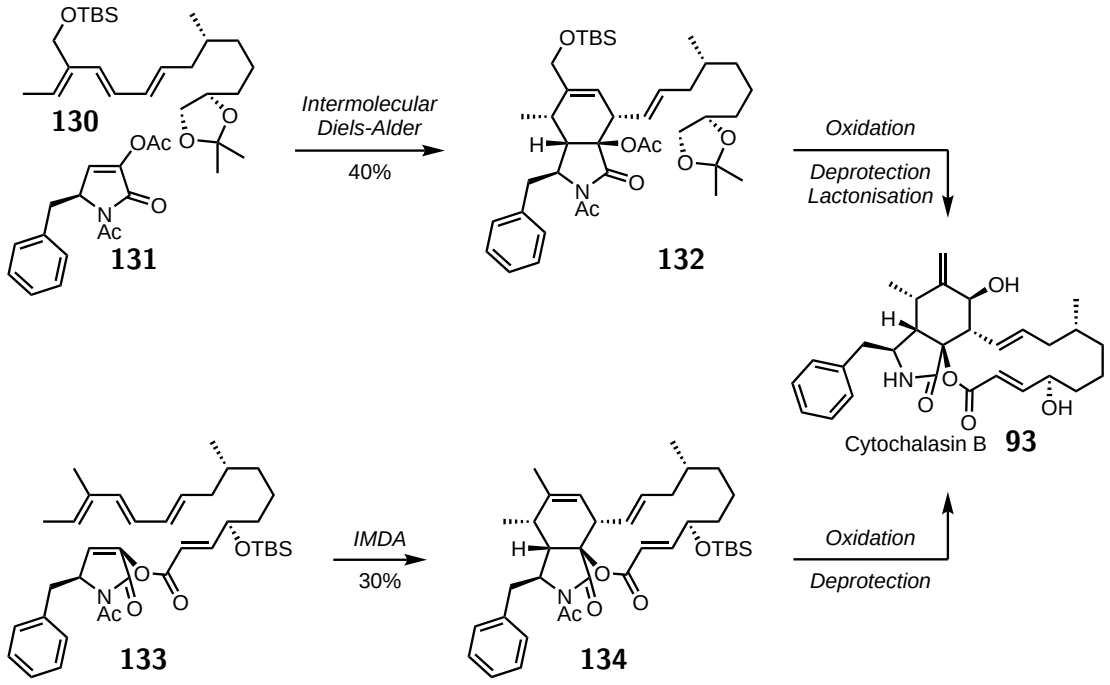

Figure 2.6: Stork and co-workers intra- and intermolecular approaches for the total synthesis of cytochalasin B **93**.

Another comparison can be made for the total synthesis of aspergillin PZ where Overman's group developed an IMDA approach,[27] and more recently Trauner and co-workers published an intermolecular Diels-Alder strategy.[31] The total synthesis proposed by Overman and co-workers started with the decoration of dihydropyran **135** to glycoside **136**.

[33] S. Masamune, Y. Hayase, W. Schilling, W. K. Chan, G. S. Bates, *J. Am. Chem. Soc.* **1977**, *99*, 6756-6758.

This acetal was subjected to $SnCl_4$ in DCM at 0 °C to release oxocarbenium **137**. This can react though a 2-oxonia[3,3]sigmatropic rearrangement to deliver oxocarbenium **138** that can be trapped by the enol silyl ether to form bicyclic product **139**. Unfortunately, this transformation delivered the *trans*-aldehyde and 8 additional steps were needed to access the *cis*-aldehyde, which could further be functionalized to Diels-Alder substrate **140**. The IMDA reaction furnished selectively the *endo*-adduct in 56% yield, and further deprotection finally delivered the natural product. Overall, aspergillin PZ **119** was reached in 27 steps and a yield of 0.3% (Figure 2.7).

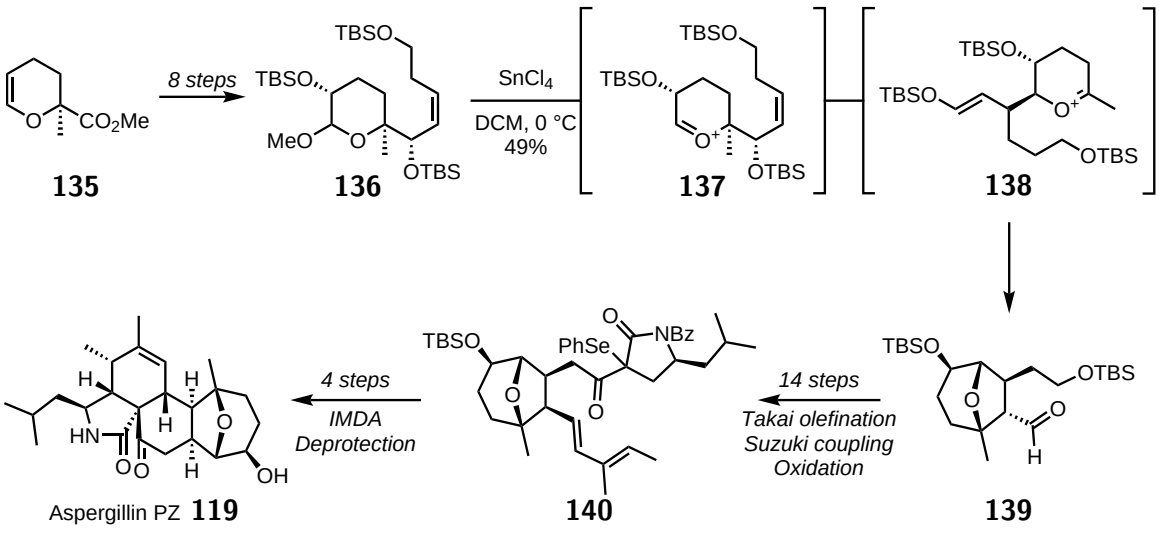

Figure 2.7: Overman's group total synthesis of (+)-aspergillin PZ **119**.

In 2018, Trauner and co-workers published a biomimetic synthesis of (+)-aspergillin PZ **119**. Starting from known fragments comprising chiral epoxy alcohol **141** and tiglic aldehyde **142**, they synthetized triene **145** by a set of reactions including a Suzuki cross coupling, an ozonolysis and a Grignard reaction. Dienophile **144** was assembled from protected amino acid **143**. The core isoindolone moiety was then accessed by an intermolecular Diels-Alder reaction between α,β unsaturated γ-lactam **144** and triene **145** to generate *endo* adduct **146** in a 13:1 *endo*/*exo* ratio. The remaining macrocycle was obtained, after a few functional group interconversions, through a Horner-Wadsworth-Emmons reaction leading

to **147**. Finally, the pentacyclic skeleton of aspergilin PZ **119** was unlocked by the use of hydrofluoric acid in acetonitrile. The Brønsted acid allowed an equilibrium between two conformers of **148**. The one forming the *cis*-fused aspergilin PZ **119** have been found to be more stable by 35 kJ.mol^{-1} using DFT calculations at DSD-PBEP86/def2-QZVPP level of theory. This led to a stereoselective and high yielding reaction with concomittant deprotection in 89% (Figure 2.8).

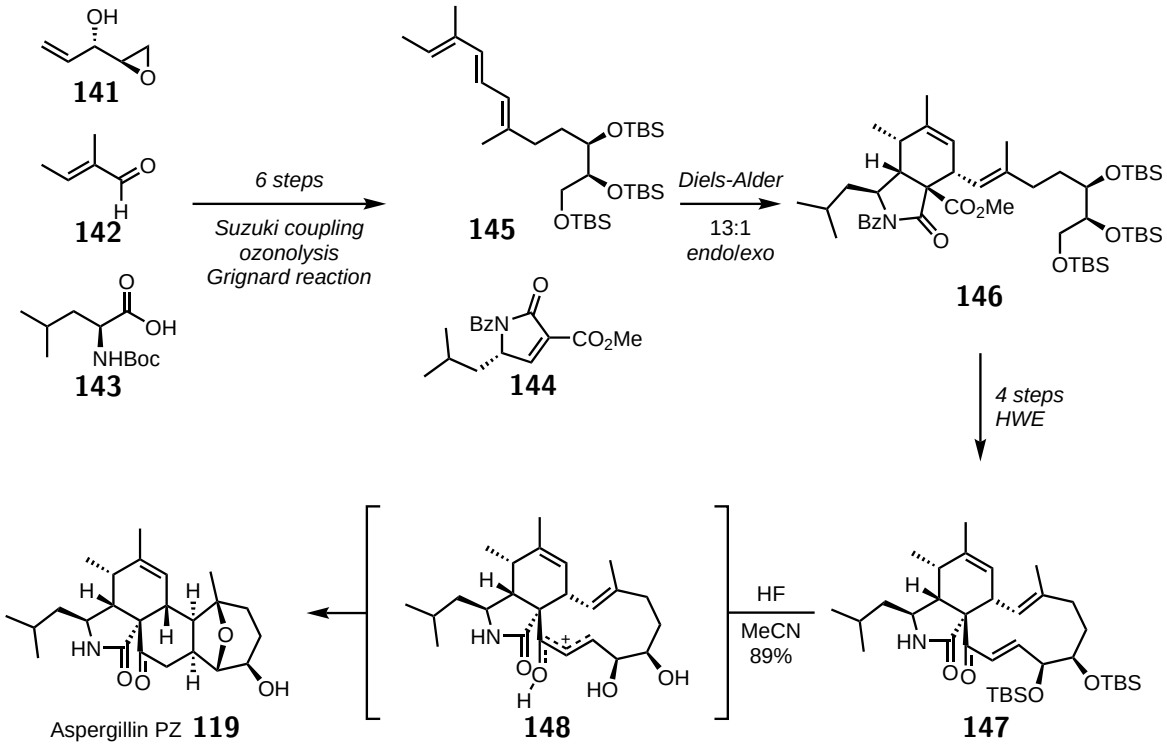

Figure 2.8: Trauner's group total synthesis of (+)-aspergillin PZ **119**.

The total synthesis developed by Trauner and co-workers is more efficient, with 12 steps for the longest linear sequence, due to the last step involving multiple transformations and the reduced number of protecting groups used. Regarding the Diels-Alder reaction, the IMDA strategy proved to allow the unique formation of the *endo*-adduct with a yield of 56% where the intermolecular approach furnished a 13:1 *endo*/*exo* mixture with a yield of 41%. The example of cytochalasin B **93** and aspergillin PZ **119** cannot furnish any

preferences between the inter- and intramolecular Diels-Alder strategy.

In 2017, Nay's group published the total synthesis of the smallest cytochalasin known to date, called periconiasin G **129**.[30] They assembled commercially available (*R*)-(+)-citronellal **149**, boronic acid **150** and *N*-Boc-leucine **143**, through alkene oxidative cleavage and Suzuki cross coupling to deliver key Diels-Alder substrate **151**. Heating at 100 °C promoted the IMDA reaction that furnished a 3:1 *endo*/*exo* mixture with a yield of 44%. After deprotection of the tricyclic intermediate, periconiasin G **129** was obtained in 14 steps (Figure 2.9). During this work, the stereochemistry of the natural product was revised.

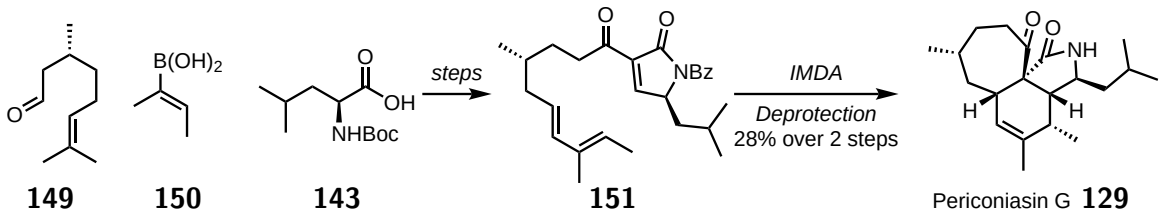

Figure 2.9: Nay and co-workers total synthesis of periconiasin G **129**.

2.1.4 *Targets, previous work and strategy*

Trichodermone 2 and trichoderone A 3

Isolated in 2012 and 2014 from the same endophytic fungus *Trichoderma gamsii* found in the Chinese plant *Panax notoginseng*, trichodermone **2** and trichoderone A **3** are two polycyclic aspochalasines.[34] Trichodermone **2** is the first "spiro-chalasin" isolated to date with a tetracyclic 7/5/6/5 skeleton. Trichoderone A **3** is a pentacyclic 7/6/6/5/5 system bearing an oxygen bridge. Their interesting and unique structure combined with their biological activity against cancerous cell HeLa, IC_{50} of 5.72 μM for **2** and IC_{50} of 40 μM for **3**, their poor extractive yield, 0.004% for **2** and 0.003% for **3**, their biosynthetic origin and the fact that no total synthesis of these molecules is reported to date, make them perfect

[34](a) G. Ding, H. Wang, L. Li, B. Song, H. Chen, H. Zhang, X. Liu, Z. Zou, *J. Nat. Prod.* **2014**, *77*, 164-167. (b) G. Ding, H. Wang, L. Li, A. J. Chen, L. Chen, H. Chen, H. Zhang, X. Liu, Z. Zou, *Eur. J. Org. Chem.* **2012**, *13*, 2516-2519.

choice for total synthesis.

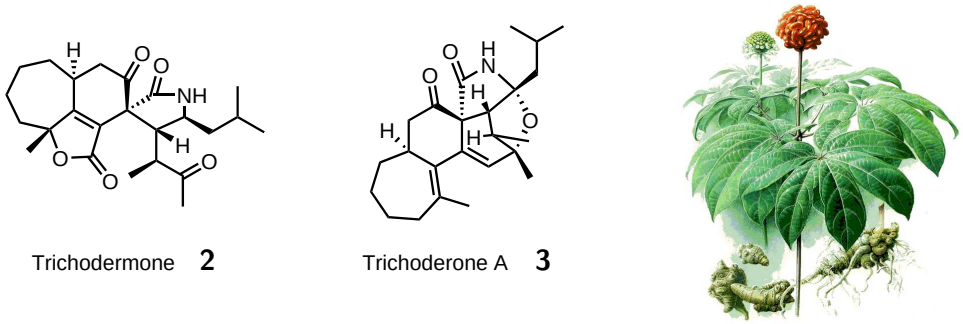

Figure 2.10: Trichodermone **2**, trichoderone A **3** and *Panax notoginseng*.

General strategy

To reach these molecules, a divergent total synthesis approach was planned combined with late-stage oxidations. The possible biosynthetic pathway might start from tricyclic aspochalasine ??, which comes from the oxidation of tricyclic aspochalasine **108** from the PKS-NRPS sequence. Selective dihydroxylation at the γ,δ position of the carbonyl might produce aspochalasine D **99** which has been isolated with trichodermone **2** and trichoderone A **3**. Transannular cyclization and reduction of the disubstituted alkene might form key tetracyclic intermediate **1**. Selective oxidation of tetrasubstituted alkene might allow the formation of 1,3 s-*trans*-diene **152**. This might rearrange to 1,3 s-*cis*-diene **153** which might lead to trichoderone A **3** through cyclization at the γ position of the lactam. 1,3 s-*Trans*-diene **152** might also react through a selective oxidative cleavage of the trisubstituted alkene to form aldehyde **154**. This might be oxidized to carboxylic acid **155**. Finally, a lactonisation might allow the synthesis of trichodermone **2** (Figure 2.11).

Based on these observations, the total synthesis of key biomimetic intermediate **1** is envisaged and, from this platform, a series of various oxidations to trichoderone A **3** and trichodermone **2** will be attempted.

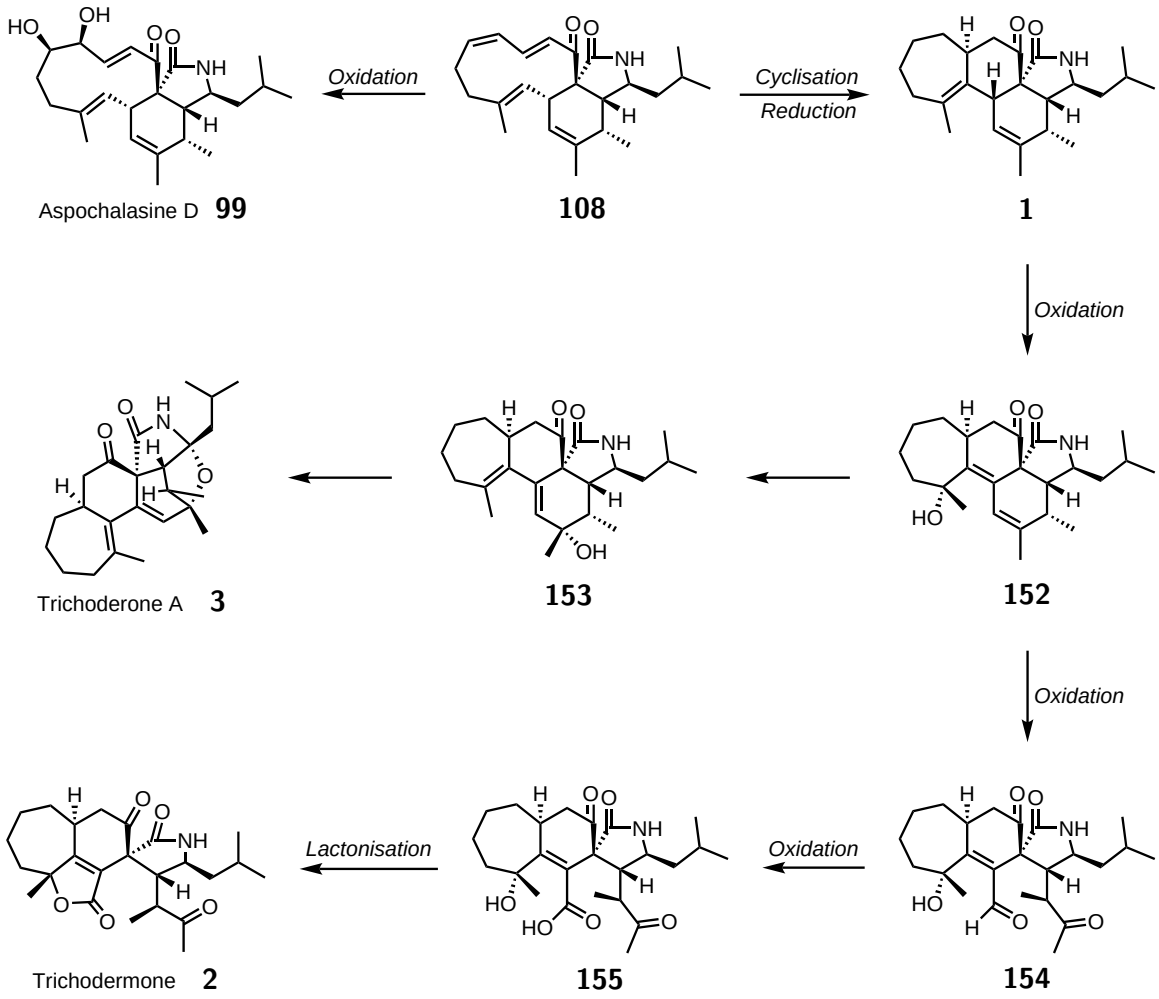

Figure 2.11: Possible biosynthetic pathway for trichodermone **2** and trichoderone A **3** from a common intermediate **1**.

Initial strategy: Benjamin Laroche's previous work

The team has already tried to access these two molecules. Benjamin Laroche, a former PhD student, worked on the total synthesis of **1** with the aim of performing some late-stage biomimetic oxidations.[35] During his PhD, he synthesized tetracyclic compound **161** in 12 steps starting from commercially available aldehyde **156**. To do this, a tertiary propargylic

[35] B. Laroche, Synthèse totale d'un précurseur biomimétique des chalasines polycyliques et développement d'une méthodologie de photooxygénation bioinspirée, Doctoral dissertation, Université Paris 6, **2016**.

acetate was installed on aldehyde **156** leading to enyne **157**. Enyne metathesis was then performed to forge seven membered ring **158**. An Ireland-Claisen rearrangement allowed the migration of the acetyl fragment to form carboxylic acid **159** which can then be decorated with a diene and a pre-dienophile as a selenide to form intermediate **160** in 8 additional steps. By subjecting selenium derivative **160** to oxidative condition, the dienophile was released and was subjected to the IMDA reaction at 100 °C to access protected biomimetic intermediate **161** (Figure 2.12).

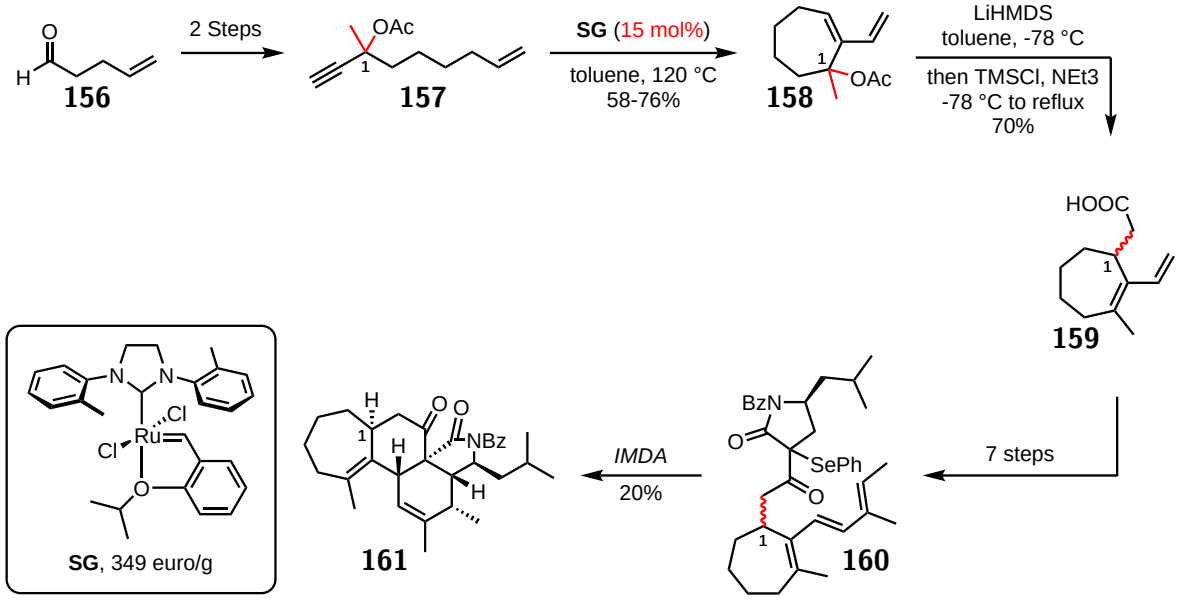

Figure 2.12: Laroche's total synthesis of protected key intermedate **161** highlighting the drawbacks of this strategy (red).

Unfortunately, two major problems arose from this total synthesis. The first was economical. The price of starting aldehyde **156** is expensive, 35.6 euro/g.[36]. In addition, the early use of the Stewart-Grubbs catalyst (SG, the only one working in this reaction) in this multi-step synthesis with a price of 349 euro/g,[37] and the high catalyst loading (15%, despite important optimization attempts[38]) were a problem in the development of a scal-

[36] https://www.alfa.com/en/catalog/L13351/
[37] https://www.sigmaaldrich.com/catalog/product/aldrich/682373?lang=fr&region=FR
[38] B. Laroche, M. Detraz, A. Blond, L. Dubost, P. Mailliet, B. Nay, *J. Org. Chem.* **2015**, *80*, 5359-5363

able total synthesis. The second was the racemic synthesis of enyne **157**. Without any control of the enantioselectivity at C-1 during the acetylide addition reaction on a ketone, two enantiomers are formed at the beginning of the synthesis. Any attempts to control the enantioselectivity failed. This limits the yield of the IMDA reaction to a maximum of 50% in the best case. These points were sufficient to redesign a new enantioselective route to tetracyclic compound **161** in order to reach trichodermone **2** and trichoderone A **3**. However, the successful Ireland-Claisen reaction was expected to be conserved, as a key step in this strategy.

2.2 Total synthesis of tetracyclic key intermediate **1**

2.2.1 *Retrosynthesis*

Access to unprotected tetracyclic intermediate **1** was envisaged through an IMDA reaction from compound **162**. This molecule might be obtained by a coupling reaction between γ-lactam **163** and carboxylic acid **164**. γ-Lactam can be synthesized from *N*-Boc-leucine as previously reported in the literature.[39] The carboxylic function might be generated by an Ireland-Claisen rearrangement of triene acetate **165**. This triene might be synthesized by a Suzuki sp^2-sp^2 cross-coupling between a possible dienylboron reagent **166** and enol triflate **167**. Coupling partner **167** might be obtained by oxidation and triflation on diol **168** available in an enantioselective manner through the robust Sharpless asymmetric dihydroxylation reaction. This reaction might be applied to 1-methylcycloheptene **171** generated from commercially available cycloheptanone **169** (Figure 2.13).

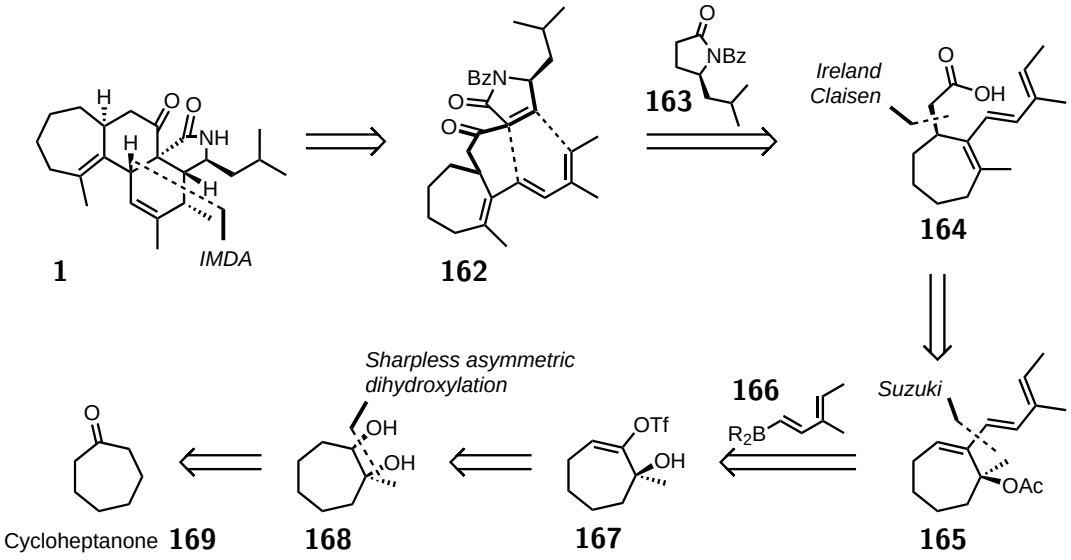

Figure 2.13: Retrosynthesis of biomimetic key intermediate **1**.

[39] M. Smrcina, P. Majer, E. Majerová, T. A. Guerassina, M. A. Eissenstat, *Tetrahedron*, **1997**, *53*, 12867-12874.

2.2.2 *Introduction of chirality in the synthesis*

The first steps of the total synthesis start with a Grignard reaction of the in situ generated methylmagnesium iodide and the commercially available and cheap cycloheptanone **169**, 0.46 euro/g,[40] in diethyl ether at rt, followed by a dehydration of alcohol **170** in the presence of potassium bisulfate under reflux. After distillation of the crude mixture, 1-methylcycloheptene **171** was obtained in 70% over 2 steps on a multi decagram scale (Figure 2.14).[41]

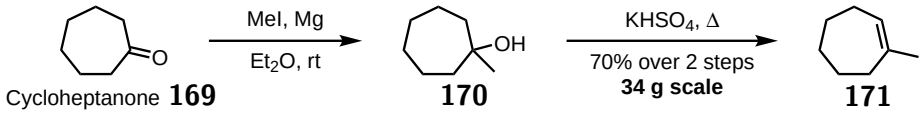

Figure 2.14: Alkene **171** synthesis from cycloheptanone

Sharpless and co-workers developed in 1988 the first catalytic system capable of asymmetric dihydroxylation of alkenes.[42] Four years later, two major discoveries were made by using a phthalazine class of ligands and methanesulfonamide as an additive. A universal set of conditions was able to produce a diverse library of highly enantioenriched and high-yielding diols.[43] The methanesulfonamide additive has an effect on the species formed during the catalytic cycle. Two catalytic cycles can be found for the Sharpless asymmetric dihydroxylation, but only one gives high *ee*. The first starts with the reaction between alkene and alkaloid Os^{VIII} complex **172** to give Os^{VI} species **173**. This cyclic intermediate is then oxidized to form Os^{VIII} complex **174**. The methanesulfonamide additive will play a key role in accelerating the hydrolysis of previous complex **174** and releasing chiral diol. If the hydrolysis has not occured, a second non-stereoselective catalytic cycle may begin with the addition of another alkene to Os^{VIII} complex **174** to allow formation of bicyclic Os^{VI}

[40] `https://www.sigmaaldrich.com/catalog/product/aldrich/c99000?lang=fr&region=FR`
[41] M. Barbier, M. F. Hugel, *Bull. Soc. Chem. Fr.* **1961**, 951.
[42] E. N. Jacobsen, I. Marko, W. S. Mungall, G. Schroeder, K. B. Sharpless, *J. Am. Chem. Soc.* **1988**, *110*, 1968-1970.
[43] K. B. Sharpless, W. Amberg, Y. L. Bennani, G. A. Crispino, J. Hartung, K.-S. Jeong, H.-L. Kwong, K. Morikawa, Z.-M. Wang, D. Xu, X.-L. Zhang, *J. Org. Chem.* **1992**, *57*, 2768-2771.

complex **175**. This one can be oxidized into Os^{VIII} complex **176** and hydrolysis will release a racemic diol (Figure 2.15).[44]

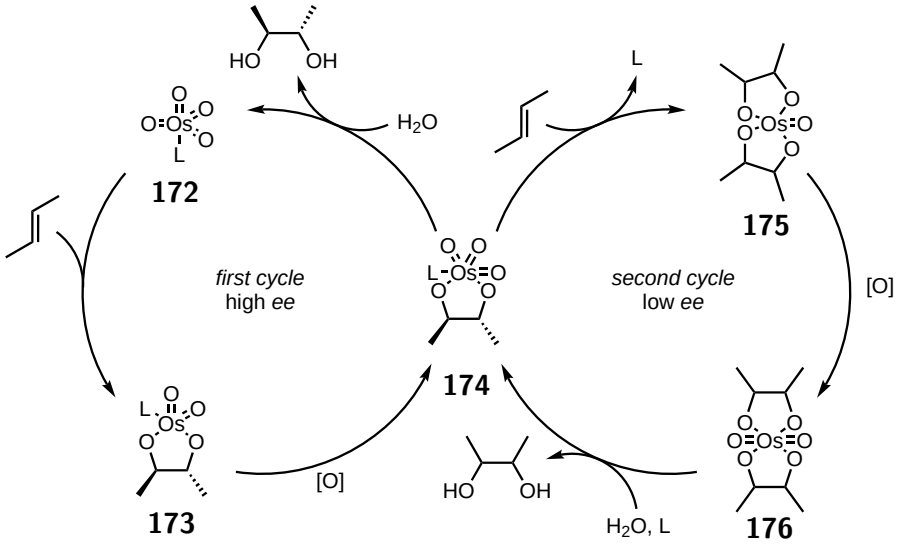

Figure 2.15: Mechanism of the Sharpless asymmetric dihydroxylation of alkene.

The optimization of the reaction conditions was made simple. Only three parameters were left to guide the chemist's choice: chiral alkaloid ligand, composed of a platform where one or two cinchona alkaloids are linked, catalyst loading and temperature. Sharpless and Kolb were able to propose a guide to choose the most suitable ligand for the alkene dihydroxylation (Figure 2.16).[45] Five types of platforms, PHAL **177**, PYR **178**, IND **179**, AQN **180** and DPP **181**, were developed. By swapping the chiral alkaloid part, DHQD **182** or DHQ **183**, on these platforms both enantiomers can be accessed.

Looking at precedents in the literature, alkene **171** has never been subjected to the Sharpless asymmetric dihydroxylation. The closest structures are either 1-methylcyclohexene with an *er* of 76:24 using PHAL ligand at 0 °C or 1-phenylcycloheptene with an *er* of 97.5:2.5

[44] J. S. M. Wai, I. Markó, J. S. Svendsen, M. G. Finn, E. N. Jacobsen, K. B. Sharpless, *J .Am. Chem. Soc.* **1989**, *111*, 1123-1125.

[45] H. C. Kolb, K. B. Sharpless In *Transition Metals for Organic Synthesis*, Vol. 2; M. Beller, C. Bolm, Eds.; Wiley-VCH: Weinheim, **2004**, 275-307.

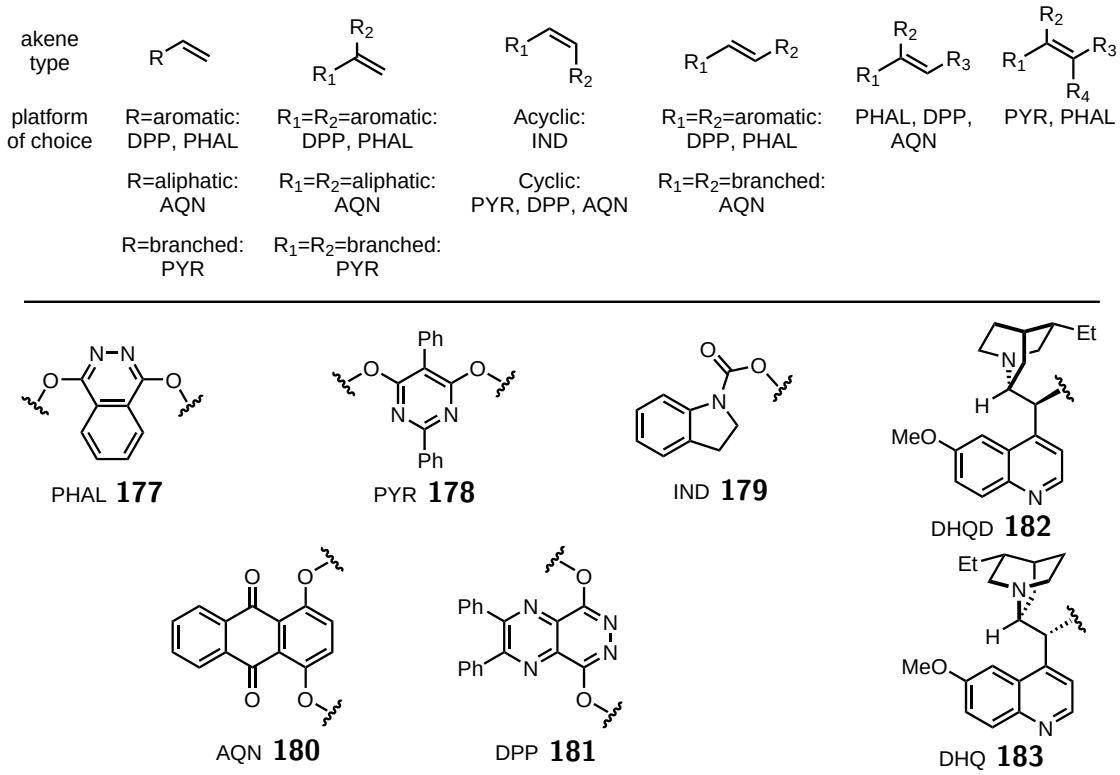

Figure 2.16: Sharpless and Kolb ligand guide for asymmetric dihydroxylation.

using PHAL ligand and 93:7 using PYR ligand both at 0 °C.[46] When optimizing our reaction conditions on **171**, three parameters were modified: ligands, catalytic loading and temperature. Under conventional conditions, using commercially available AD-mix-β,[47] composed of 3 equivalents of K_2CO_3, 3 equivalents of $K_3Fe(CN)_6$, 0.01 equivalent of $(DHQD)_2PHAL$ and 0.004 equivalent of K_2OsO_4, combined with 1 equivalent of methanesulfonamide in a 1:1 ^{t}BuOH/H_2O at room temperature, promising results were obtained, giving 65% yield and 84:16 *er*.[48] By lowering the temperature to 0 °C, the *er* was improved to 90:10. As proposed in Sharpless's guide, the AQN ligand was evaluated, the yield was better than in the previous attempt, but an erosion of the *er* prevented the use of this ligand. Finally

[46] H. C. Kolb, M. S. VanNieuwenhze, K. B. Sharpless *Chem. Rev.* **1994**, *94*, 2483-2547.

[47] `https://www.sigmaaldrich.com/catalog/product/aldrich/392766?lang=fr&region=FR`

[48] *er* were measured by reaction of crude diol **168** with BzCl and then subjected to chiral HPLC using column Cosmosil CHiRAL 3B.

increasing the catalyst loading from 0.4% to 0.7% and the ligand loading from 1% to 1.75% resulted in good yield, 81%, and good *er*, 89.5:10.5. More importantly, the reaction was reproducible, in terms of reaction time, yield and *ee*, and scalable. Due to glassware limitations, only the 5-gram scale of this reaction was achieved, but with a suitable reactor, a higher scale may be possible.

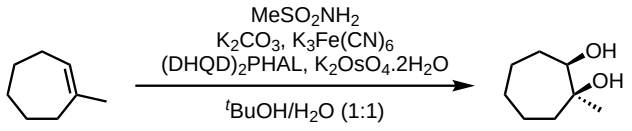

171 **168**

L (mol%)	$K_2OsO_4.2H_2O$ (mol%)	T (°C)	t (d)	Yield (%)	*er*
$(DHQD)_2PHAL$ (1)	0,4	rt	3	65	84:16
$(DHQD)_2PHAL$ (1)	0,4	0	7	69	90:10
$(DHQD)_2AQN$ (1)	0,4	0	6	88[b]	86.5:13.5
$(DHQD)_2PHAL$ (1.75)	0,7	0	4	81	89.5:10.5

[a] Using commercially AD-mix β mixture [b] NMR Yield

Figure 2.17: Sharpless asymmetric dihydroxylation optimisation.

After successfully obtaining the desired enantionenriched diol **168**, the next target was the synthesis of the coupling partner, triflate **167**.

2.2.3 *Dead-ends*[49]

The approach to enol triflate **167** began with the oxidation of diol **184** by an in-situ generation of IBX from a catalytic amount of 2-iodobenzoic acid and oxone as oxidant, in a mixture of water and acetonitrile at 70 °C.[50] The installation of the acetyl fragment required for the Ireland-Claisen rearrangement was carried out in a non classical solvent for this type

[49] In this subsection, reactions were only perform on racemic compounds.
[50] A. P. Thottumkara, M. S. Bowsher, T. K. Vinod, *Org. Lett.* **2005**, *7*, 2933-2936.

of transformation. When trying DCM, a more conventional solvent, the NMR yield was lower, 73%, and the reaction time higher. Switching to pentane, a reproducible and efficient pathway to acetoxy ketone **186** was forged (Figure 2.18).[51]

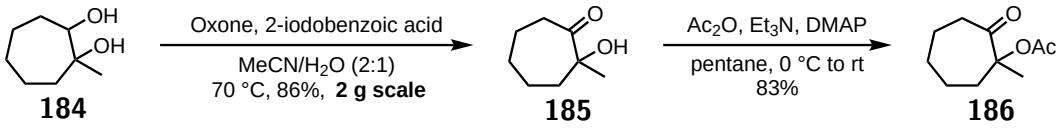

Figure 2.18: Synthesis of ketone **186**.

Enol triflation of acetoxy ketone **186** by deprotonation with LiHMDS and quenching of the remaining enolate with the Comins' reagent,[52] only yielded to bicyclic compound **188**. In the literature, one similar transformation have been attempted on a cyclic acetoxy ketone resuting in the formation of an enol triflate with a low yield of 29%.[53] This can be explained by the *in-situ* formation of lithiated species **187** due to the fact that the proton of the acetyl moiety is more sterically accessible. Other bases such as NaH, KHMDS, NaHMDS or bulky pyridine did not afford any desired product.

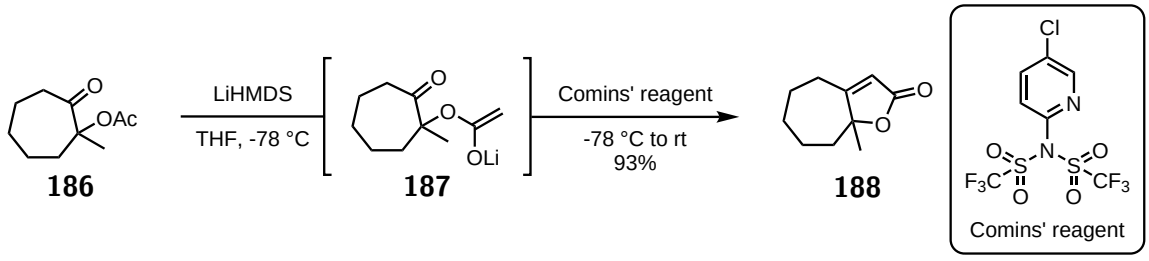

Figure 2.19: Impasse during the synthesis of enol triflate **167**.

No acidic condition or triflation using trifluoromethanesulfonic anhydride were tested on acetoxy ketone **186**.

[51] A. Sakakura, K. Kawajiri, T. Ohkubo, Y. Kosugi, K. Ishihara, *J. Am. Chem. Soc.* **2007**,*129* , 14775-14779.
[52] D. L. Comins, A. Dehghani, *Tetrahedron Lett.* **1992**, *33*, 6299-6302.
[53] M. Shen, M. Kretschmer, Z. G. Brill, S. A. Snyder, *Org. Lett.* **2016**, *18*, 5018-5021.

2.2.4 *Synthesis of coupling partners*

Synthesis of enol triflate 191

Returning to the enantiomeric pathway, the oxidation into hydroxy ketone **189** from diol **168** was achieved thanks to the classical and robust Swern oxidation reaction. This was preferred to the previous oxidation using *in-situ* IBX generation due to an easier scalable process. Finally, the protection of the remaining alcohol was made possible by the use of 1-(trimethylsilyl)imidazole, which was more efficient (quantitative) compared to the combination of triethylamine and trimethylsilyl trifluoromethanesulfonate (84% yield on 0.2 mmol scale). This sequence was run on an eleven gram scale from diol **168** affording hydroxy protected ketone **190** in 84% over 2 steps (Figure 2.20).

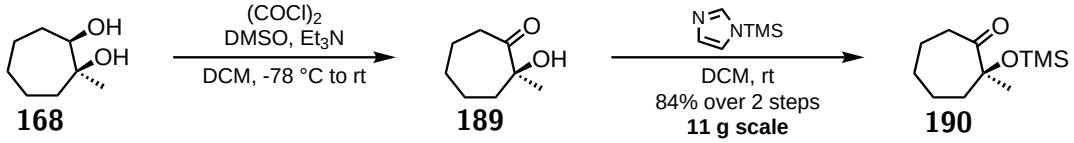

Figure 2.20: Synthesis of protected ketone **190**.

After protecting the alcohol, optimisation of the synthesis of enol triflate **167** was undertaken in presence of the Comins' reagent. The first set of reactions was designed to afford the TMS-protected enol triflate, but the addition of a 2 M solution of hydrochloric acid at the end of the reaction allowed the direct access to enol triflate **167** (Figure 2.21). The base was the first parameter evaluated. Different counter-cations of the commercially available bis(trimethylsilyl)amide base solution were assessed. LiHMDS was the most attractive candidate due to a higher yield than NaHMDS, 52% compared to 43%, and as a less expensive alternative to KHMDS (0.18 euro/mL compared to 1.3 euro/mL for a 1.0 M solution in THF).[54] Next, the amount of base and triflating reagent was tested. The decrease to 1.1 equivalents of both base and Comins' reagent induced a poorer yield of 43%. Increasing

[54] https://www.sigmaaldrich.com/catalog/product/aldrich/225770?lang=fr&region=FR
https://www.sigmaaldrich.com/catalog/product/aldrich/702722?lang=fr&region=FR

the amount of both base and Comins' reagent to 2 equivalents resulted in a better yield of 74%. Finally, it was found that only the base was needed to be increased to 2 equivalents and that the reduction of the amount of triflate reagent to 1.5 equivalents to give the same efficiency, i.e. 74%. However, if the amount of the base was reduced to 1.5 equivalents and the amount of Comins' reagent maintained at 2 equivalents, the yield dropped to 52%.

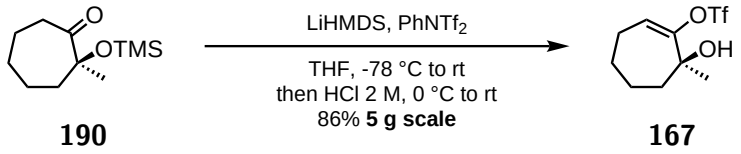

190 **167**

Base (eq)	Triflate reagent (eq)	NMR Yield (%)
LiHMDS (1.5)	Comins' (1.5)	52
KHMDS (1.5)	Comins' (1.5)	53
NaHMDS (1.5)	Comins' (1.5)	43
LiHMDS (1.1)	Comins' (1.1)	43

Base (eq)	Triflate reagent (eq)	NMR Yield (%)
LiHMDS (2)	Comins' (2)	73
LiHMDS (2)	Comins' (2)	52[a]
LiHMDS (2)	Comins' (1.5)	74
LiHMDS (1,5)	Comins' (2)	52

[a] Comins' reagent was added before LiHMDS

Figure 2.21: Synthesis of enol triflate **167**.

Unfortunately, these optimized conditions were not scalable and an erosion of the yield was observed when the five gram scale was attempted. The solution to afford scalable and reproducible results for this reaction was to swap the Comins' reagent to the more affordable bis(trifluoromethanesulfonyl)aniline (0.24 compared to 0.89 euro per mmol)[55]. In addition, a crucial practical detail was to add the triflate reagent before the base, which was not efficient with the Comins' reagent. By doing so, an even better yield of 86% was finally achieved on the 5-gram scale reaction.

The acetylation of enol triflate **167** was not an easy reaction to optimize. In fact, a classical set of conditions including acetic anhydride, an amine base and DMAP in DCM

[55] http://www.fluorochem.co.uk/Products/Search?searchType=C&searchText=%2037595-74-7
http://www.fluorochem.co.uk/Products/Search?searchType=C&searchText=%20145100-51-2

did not achieve full conversion, even when warming up to reflux for several days. Switching to pentane, as previously to synthesize acetoxy ketone **186** (Figure 2.18), or removing the solvent did not improve the conversion. A set of stronger bases, *n*BuLi, NaH or LiHMDS, was evaluated but only afforded complex mixtures. Moving to less common condition, iodine was assessed to catalyse the reaction in acetic anhydride as a solvent.[56] On a small scale (0.2 mmol) promising results were obtained; unfortunately these conditions were not scalable. A different approach using acid catalysis was then tried, using *p*-toluenesulfonic acid; two sources of acetyl were evaluated in DCM. Acetic acid did not furnished any conversion but when using isoprenyl acetate, a full conversion with an excellent isolated yield of 96% on a 0.5 mmol scale was obtained.

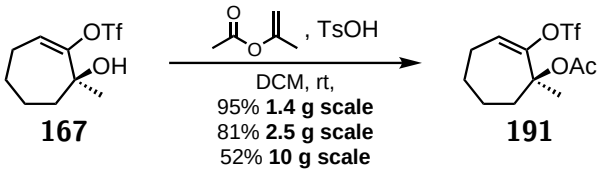

Acetyl source	Base	Catalyst	Solvent	Temperature	NMR Yield (%)
Ac_2O	NEt_3 or pyr or *i*PrNEt_2	DMAP	DCM or heptane or neat	rt to reflux	no total conversion
Ac_2O	*n*BuLi or NaH or LiHMDS	-	THF or hexane	0 °C to rt	complex mixture
Ac_2O	-	I_2	-	rt	63%[a], not scalable
AcOH	-	TsOH	DCM	rt	no conversion
Isopropenyl acetate	-	TsOH	DCM	rt	98%[a] (96%[b])

[a] On 0.2 mmol scale [b] Isolated yield on 0.5 mmol scale

Figure 2.22: Synthesis of coupling partner **191**.

During the scale-up of this acetylation, an erosion of the yield was observed. At 1.4 g scale the yield remained excellent, 95%, but going at 2.5 g scale the yield dropped by 14% and when trying a larger scale, 10 g, only 52% of desired product **191** was obtained. The

[56] P. Phukan, *Tetrahedron Lett.* **2004**, *45*, 4785-4787.

side-reaction observed during the scale-up was the regeneration of the ketone through the loss of the enol triflate. To solve this problem, the reaction was only run on a 1.4 g scale in multiple flasks, up to 5 at a time.

Approaches to other coupling partners[57]

A direct approach to a suitable vinyl bromide **192** was tested. Starting with either hydroxy ketone **185**, acetoxy ketone **186** or O-TMS protected hydroxy ketone **190**, different reaction conditions were applied. The first set of conditions was inspired from a previous report where triphenyl phosphite was used in synergy with bromine to convert ketones into vinyl bromides.[58] Unfortunately, only complex mixtures without any trace of the desired products (**192**) were observed. A second set using phosphorus tribromide with acetic acid was evaluated but no reaction was observed with the different starting materials (Figure 2.23).

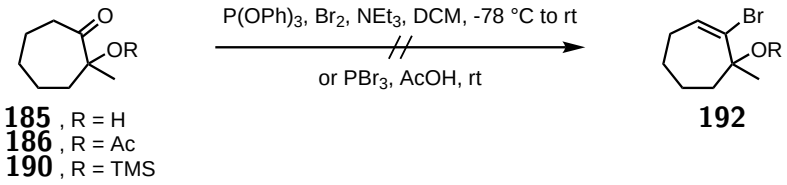

Figure 2.23: Impasse during the synthesis of the bromo vinyl **192**.

A different approach was then attempted to find a suitable coupling partner for the Suzuki-cross coupling reaction. Using hydrazone chemistry, an attempt was made to synthesised an iodine derivative **196** or boronic ester derivative **194** from hydroxy ketone **185** or acetate derivative **186**. The reaction between tosyl hydrazine and ketone **185** in ethanol afforded tosyl hydrazone **193** in quantitative yield. This compound was then subjected to various conditions to perform a Shapiro reaction to deliver a coupling partner **194**.[59] Unfortunately, no desired products were observed. Another approach was then tested, using hydrazine to generate *in-situ* hydrazone **195** from hydroxy ketone **185**. Various amine bases

[57] In this subsection, reactions were only perform on racemic compounds.
[58] A. Spaggiari, D. Vaccari, P. Davoli, G. Torre, F. Prati, *J. Org. Chem.*, **2007**, *72*, 2216-2219.
[59] R. H. Shapiro, M. J. Heath, *J. Am. Chem. Soc.* **1967**, *89*, 5734-5735.

and sources of iodine were evaluated to perform a Barton vinyl iodine synthesis.[60] Again, only complex mixtures were obtained with no traces of desired product **196** (Figure 2.24).

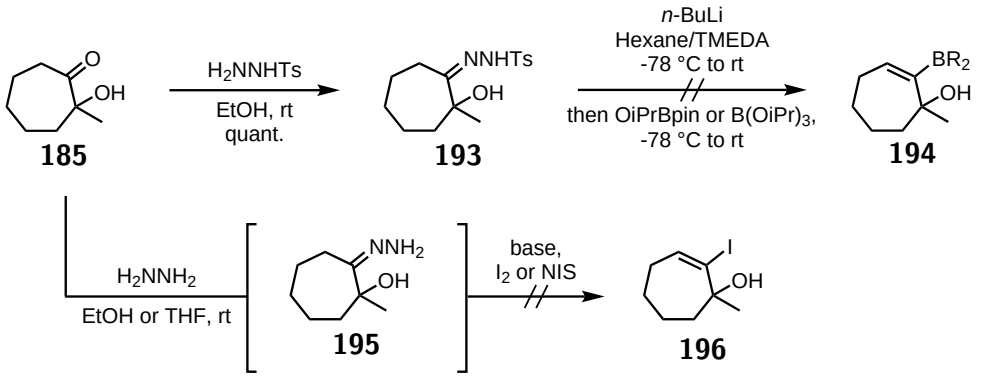

Figure 2.24: Impasse during the synthesis of coupling partners **194** and **196**.

Finally, the reaction between tosyl hydrazine or hydrazine and acetoxy ketone **186** did not afford any conversion, probably due to steric hindrance.

Knowing that enol phosphates are suitable coupling partners for cross coupling reactions, an approach to this type of compound was also tried.[61] From O-TMS protected hydroxy ketone **190**, various conditions were applied to synthesize different enol phosphates **197**. Unfortunately, none of them were successful and no traces of the desired enol phosphates were ever observed (Figure 2.25).

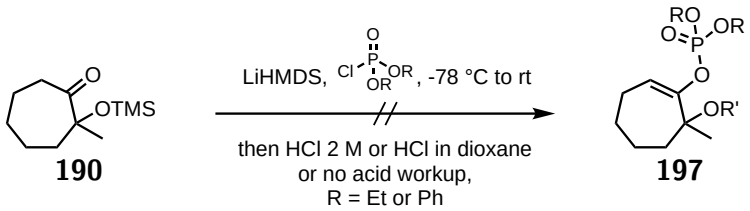

Figure 2.25: Impasse during the synthesis of different enol phosphates **197**.

[60] D. H. R. Barton, R. E. O'Brien, S. Sternhell, *J. Chem. Soc.* **1962**, 470-476.
[61] J. D. Sellars, P. G. Steel, *Chem. Soc. Rev.* **2011**, *40*, 5170-5180.

Synthesis of boron partners

Thanks to the work carried out by Lallemand and co-workers, a route to catechol boronic ester **201** was already known.[62] Based on a Sonogashira cross coupling reaction between a mixture of *cis* and *trans* 2-bromo-2-butene **198** and trimethylsilylacetylene, only the formation of desired *E* isomer **199** was observed in excellent yield of 91%. Deprotection of alkyne **199** was achieved with potassium carbonate in methanol. After a work-up, the crude solution containing highly volatile alkyne **200** was directly engaged in the following step. Treatment of the previous solution with catecholborane afforded boronic catechol ester **201**. From this coupling partner, boronic pinacol ester **202** was accessed by ligand exchange using pinacol in pentane. Potassium trifluoroborate **203** can also be prepared from the previous boronic ester using potassium bifluoride in a mixture of water and acetonitrile (Figure 2.26).

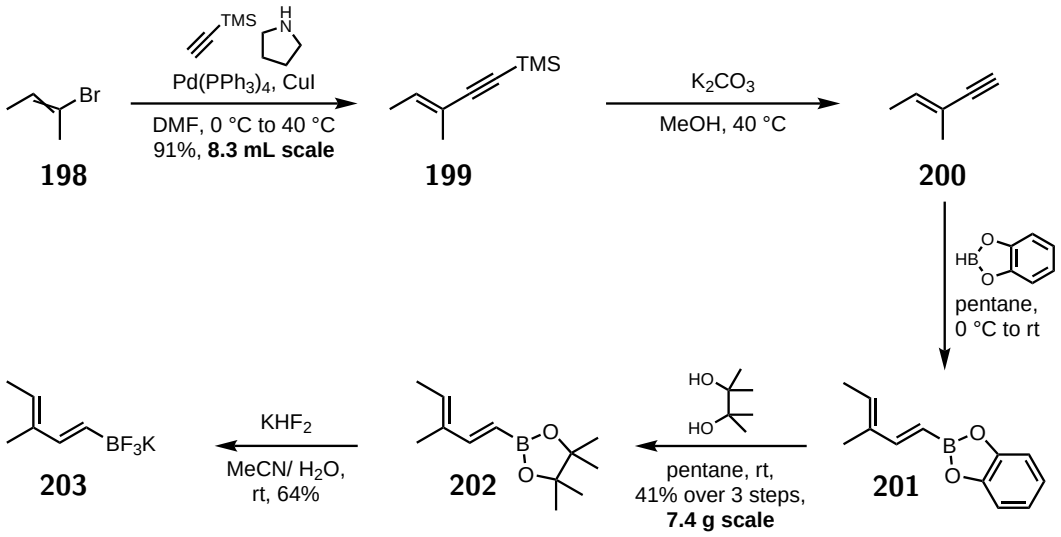

Figure 2.26: Synthesis of boron partners **202** and **203**.

Sadly, after months of reproducible results, the first step of the process, the Sonogashira reaction, no longer provided the single *E* isomer. The yield of the reaction dropped from

[62] G. Ohanessian, Y. Six, J.-Y. Lallemand, *Bull. Soc. Chim. Fr.* **1996**, *133*, 1143-1148.

91% to 30% and the desired isomer was obtained in a 1:1.1 E/Z ratio (Figure 2.27). Even after screening a lot of different $Pd(PPh_3)_4$ sources, commercially available and home made, and different batches of reagents and solvents, no improvement of the reaction was ever observed.

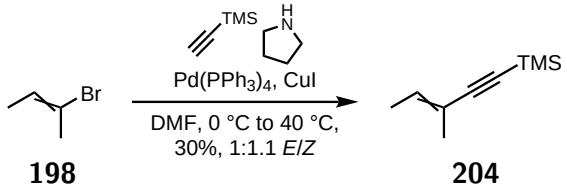

Figure 2.27: Non reproducible cross coupling reaction.

Fortunately, another route was reported in the literature. Morken and co-workers published in 2017 a more direct route to desired boronic pinacol ester **202** using a boron-Wittig reaction.[63] Starting from dibromomethane **205**, a large quantity of bis pinacol boron derivative **206** was obtained through a modified reported procedure.[64] The use of tiglic aldehyde **207** for the boron-Wittig reaction afforded desired boronic pinacol ester **202** in good yield. This reaction was scalable and reproducible.

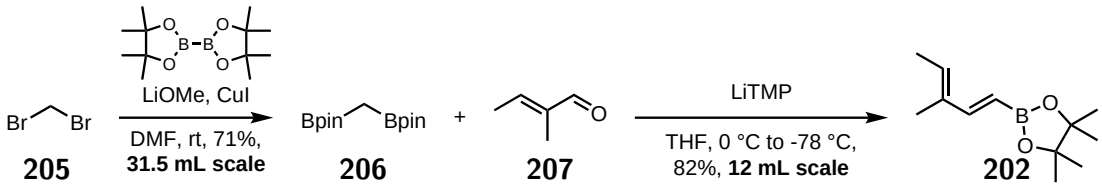

Figure 2.28: Second route to desired coupling partner **202**.

2.2.5 *Suzuki cross coupling*

Discovered in 1979, the Suzuki-Miyaura cross coupling is a reaction that allows the formation of a C-C bound by the reaction between an organoboron and a halide catalysed by a Pd^0

[63] J. R. Coombs, L. Zhang, J. P. Morken, *Org. Lett.* **2015**, *17*, 1708-1711.
[64] X. Liu, T. M. Deaton, F. Haeffner, J. P. Morken, *Angew. Chem. Int. Ed.* **2017**, *56*, 11485-11489.

complex.[65] The catalytic cycle begins with the oxidative addition of the Pd^0 complex onto the organo halide or pseudo halide, such as an enol triflate, silicate or phosphate, to generate Pd^{II}) complex **208**.[66] Ligand exchange then occurs to form complex **209** which can react via transmetalation with boronate **210** to generate borate **211** and Pd^{II} complex **212**. Finally, reductive elimination will release the desired product and regenerate the Pd^0 complex (Figure 2.29).

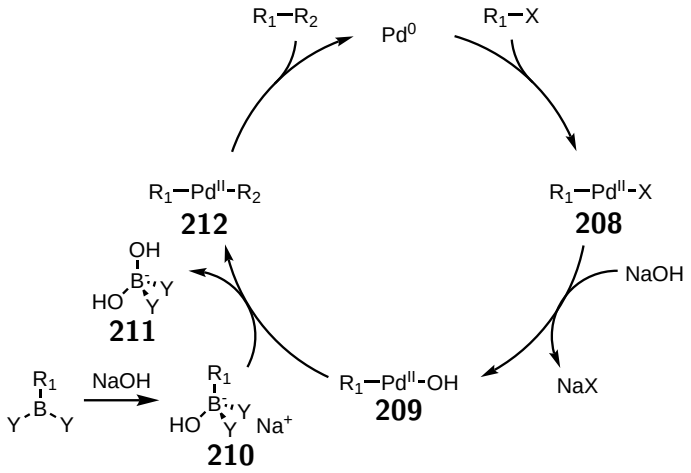

Figure 2.29: Suzuki-Miyaura cross coupling reaction mechanism (ligand on palladium have been omitted for more clarity).

During the optimization of this reaction, various parameters, such as bases, palladium sources, ligands, solvents and temperatures, were explored in order to deliver a reproducible and scalable cross coupling reaction. In the presence of $Pd(OAc)_2$, PCy_3, in a 7:3 solvent mixture of dioxane and water at room temperature, the first parameter to be assessed were the bases. By affecting the pKa of the solution, bases influence the concentration of the boronate species in the medium and therefore the ligand exchange step (Figure 2.30). If the base is too strong, like KO^tBu, it might degrade the starting material or the product. If the base has a smaller counter cation, like Na^+, which is less solvated, it might result in a

[65] N. Miyaura, K. Y. A. Suzuki, *Tetrahedron Lett.* **1979**, *20*, 3437-3440.
[66] N. Miyaura, A. Suzuki, *Chem. Rev.* **1995**, *95*, 2457-2483.

less nucleophilic anion and the yield of the reaction will be reduced.[67] Finally K_3PO_4 was chosen for the rest of the investigation.

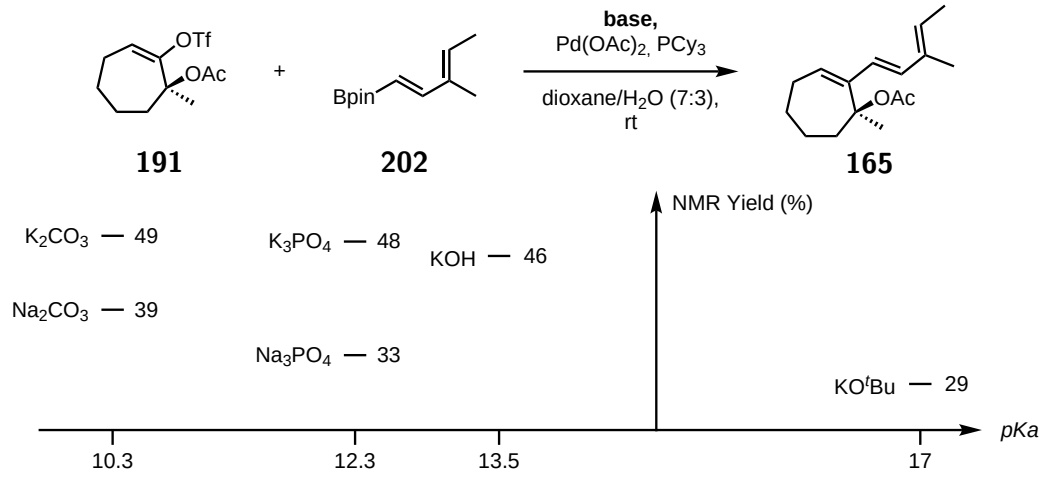

Figure 2.30: Influence of the base on the Suzuki-Miyaura cross coupling (0.2 mmol of **191**, 0.3 mmol of **202**, 0.6 mmol of base, 0.012 mmol of $Pd(OAc)_2$, 0.024 mmol of PCy_3 at 0.1 M); NMR yields are given in the graph as a function of pKa of the base used.

The evaluation of highly used ligands for the Suzuki-Miyaura coupling revealed that SPhos **214** and RuPhos **216** were not able to afford any desired products compared to XPhos **215** which was less efficient than PCy_3 **213** (Figure 2.31). This might be due to the size of the ligand which has an effect on the concentration of LPd^0 complex in the media.[68]

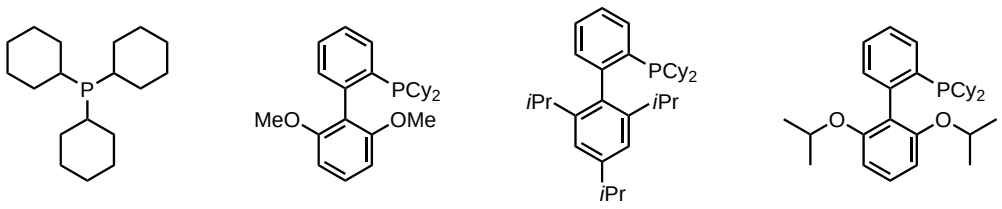

Figure 2.31: Influence of the ligand on the Suzuki-Miyaura cross coupling (0.2 mmol of **191**, 0.3 mmol of **202**, 0.6 mmol of K_3PO_4, 0.012 mmol of $Pd(OAc)_2$, 0.024 mmol of ligand at 0.1 M).

Testing more conventional solvents, THF, toluene and DMF only afforded lower yields.

[67] H. Zhang, F. Y. Kwong, Y. Tian, S. Chan, *J. Org. Chem.* **1998**, *63*, 6886-6890.
[68] R. Martin, S. L. Buchwald, *Acc. Chem. Res.* **2008**, *41*, 1461-1473.

However, the reaction temperature gave interesting results (Figure 2.32). While heating the media to 60 °C resulted in greater degradation, a reduction to 0 °C yielded 75% of desired product **165**. Since the reaction on this scale is very fast (even at 0 °C, the reaction time was only 2 min) lowering the temperature might prevent decomposition of the product, especially by a competing Tsuji-Trost reaction due to the presence of the allyl acetate part. $Pd_2(dba)_3$ was found less efficient than $Pd(OAc)_2$ at 0 °C (Figure 2.32).

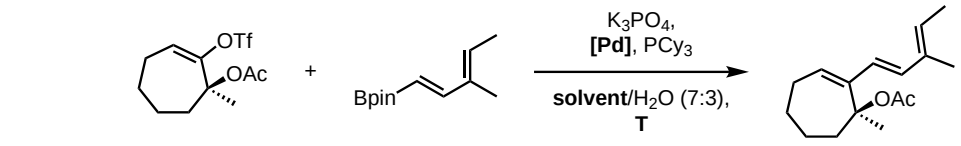

191 **202** **165**

[Pd]	solvent	T (°C)	Yield (%)
$Pd(OAc)_2$	toluene	rt	22
$Pd(OAc)_2$	THF	rt	19
$Pd(OAc)_2$	DMF	rt	15

[Pd]	solvent	T (°C)	Yield (%)
$Pd(OAc)_2$	dioxane	60	33
$Pd(OAc)_2$	dioxane	0	75
$Pd_2(dba)_3$	dioxane	0	40

Figure 2.32: Influence of the palladium source, solvent and temperature on the Suzuki-Miyaura cross coupling (0.2 mmol of **191**, 0.3 mmol of **202**, 0.6 mmol of K_3PO_4, 0.012 mmol of Pd source, 0.024 mmol of PCy_3 at 0.1 M).

Other coupling partners were also evaluated. Alcohol enol triflate **167** did not afford any desired product. Regarding dienyl trifluoroborate salt **203** and dienylboron catechol ester **201**, only a low yield, less than 10%, was obtained under the best conditions found previously (Figure 2.33).

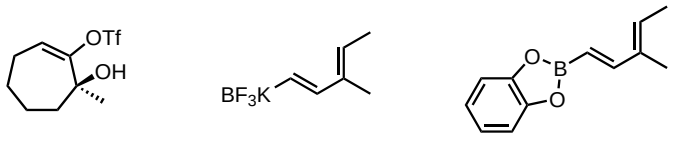

167 **203** **201**

Figure 2.33: Other coupling partners tested during the optimization.

The attempt to scale-up the reaction to gram-scale only provided non reproducible results. The yield was fluctuating between 40% and 81% with a reaction time between

2 minutes and more than 3 hours. The investigation of the different reaction parameters revealed that the phosphine ligand was in fact partially oxidized, but even after doing the reaction with a new batch of PCy_3, no improvement was observed. New ligands were then again evaluated in order to provide a reproducible and scalable reaction. Interesting results were obtained with tri(2-furyl)phosphine **217**, dppf **219** and DPEPhos **220**. Only tri(2-furyl)phosphine **217** was able to furnish the desired product at 0 °C. Unfortunately the reaction was not scalable.

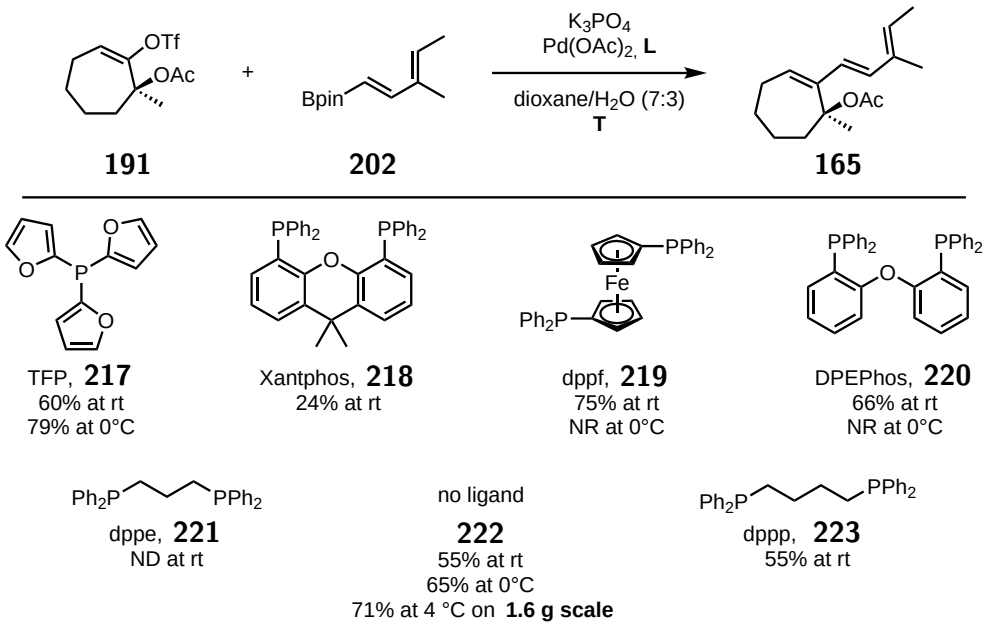

Figure 2.34: Influence of the ligand on the Suzuki-Miyaura cross coupling (0.2 mmol of **191**, 0.22 mmol of **202**, 1.8 mmol of K_3PO_4, 0.02 mmol of Pd source, 0.04 mmol of PCy_3 at 0.1 M).

Trying the reaction without any phosphine ligands was finally the trick to achieve the desired transformation. Not only the reaction was scalable, on a 1.6 gram scale, but also reproducible in term of yield and reaction time (around 1 h) when performed at 4 °C. The removal of O_2 from the solvent by bubbling argon while sonicating was not necessary in these conditions.[69] The enantiomeric excess was determined and no erosion was observed (Figure 2.35).

[69] L. A. Adrio, B. N. Nguyen, G. Guilera, A. G. Livingston, K. K. Hii, *Catal. Sci. Technol.* **2012**, *2*, 316-323.

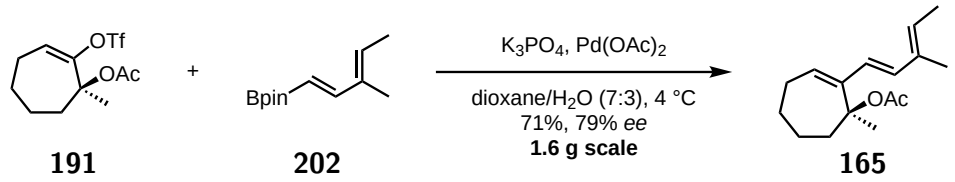

Figure 2.35: Optimized reaction condition for the Suzuki-Miyaura cross coupling between enol triflate **191** and boronic pinacol ester **202**.

2.2.6 *Claisen rearrangement*

First disclosed in 1912, the Claisen rearrangement is a [3,3]-sigmatropic rearrangement involving an allyl vinyl ether (**224**) that reacts under heating through a cyclic transition state (**225**), to form a γ,δ unsaturated ketone (**226**) (Figure 2.36).[70] This reaction became widespread in the second half of the 20th century with the discovery of numerous variations of this rearrangement.[71] Among them, the Ireland-Claisen rearrangement, discovered and used to synthesize dihydrojasmone **227** in 1972, takes as input an allyl ester (**228**) and a base to generate a silyl enol ester (**229**) that can rearrange to allow the formation of γ,δ unsaturated silyl ester **230**.[72] The Johnson-Claisen variation, discovered and used to synthesize squalene **231** in 1970, provides access to γ,δ unsaturated ester **234** through the reaction of an allylic alcohol (**232**) and a trialkyl orthoacetate that will generate *in-situ* allyl ketene acetal **233**.[73]

To the best of my knowledge, no report of an Ireland-Claisen or Johnson-Claisen rearrangement has been published so far on a triene substrate like ours.

[70] L. Claisen, *Chem. Ber.* **1912**, *45*, 3157-3166.
[71] G. B. Bennett, *Synthesis*, **1977**, *09*, 589-606.
[72] R. E. Ireland, R. H. Mueller, *J. Am. Chem. Soc.* **1972**, *94*, 5897-5898.
[73] W. S. Johnson, L. Werthemann, W. R. Bartlett, T. J. Brocksom, T.-T. Li, D. J. Faulkner, M. R. Petersen, *J. Am. Chem. Soc.* **1970**, *92*, 741-743.

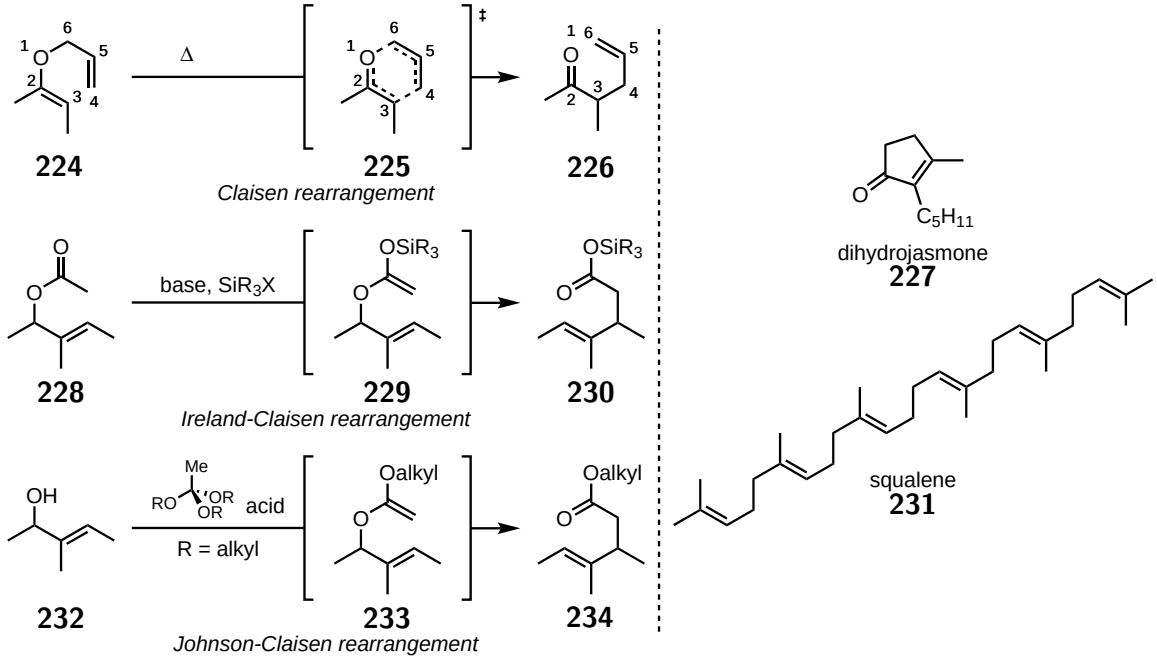

Figure 2.36: Claisen rearrangement and variations.

Johnson-Claisen rearrangement

The Johnson-Claisen rearrangement was the first to be evaluated. The reaction was only attempted on enol triflate **167** as the Suzuki coupling with this compound did not afford the desired triene. Combination of either triethyl or trimethyl orthoacetate with different acids, from mild to strong, using thermal or microwave heating did not afford any desired product. The reaction resulted only in complex mixtures (Figure 2.37).

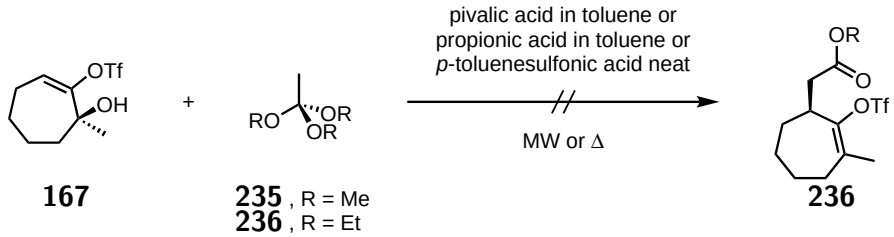

Figure 2.37: Johnson-Claisen attempt on enol triflate **167**.

Ireland-Claisen rearrangement

The Ireland-Claisen rearrangement was first attempted on enol triflate **191**. The different conditions attempted on this reaction only yielded an unknown product which could not be identified even through extensive NMR analysis (Figure 2.38).

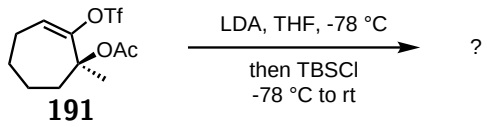

Figure 2.38: Attempt of Ireland-Claisen rearrangement on enol triflate **191**.

The optimization of the Ireland-Claisen rearrangement of triene **165** started with the evaluation of classical conditions, e.g. strong bases LiHMDS or LDA with TMSCl or TBSCl, but did not afford any conversion of the starting material. The stronger base LiTMP was the only one able to access Ireland-Claisen product **164**, without any additive. Unfortunately the yield was low, 32%. The improvement of the reaction came from the use of polar additives. The non-carcinogenic DMI and DMPU combined with LDA resulted in moderate yields for the transformation, in 47% and 54% respectively. The highly carcinogenic HMPA was the key parameter to achieve excellent NMR yield of 90%. The use of non carcinogenic TPPA as an aternative to HMPA by removing the methyl groups, a possible source of toxicity, was able to deliver a high yield, 84%, and allow a safer reaction condition to scale-up (Figure 2.39).[74]

[74] J. Coste, D. Le-Nguyen, B. Castro, *Tetrahedron Lett.* **1990**, *31*, 205-208.

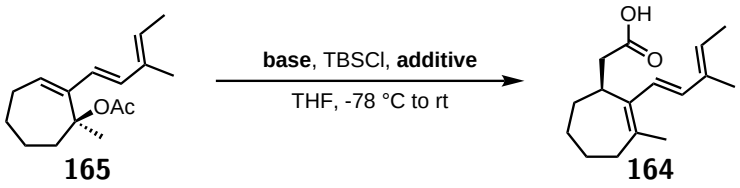

	-	-	DMI	DMPU	HMPA	TPPA
Additive	-	-	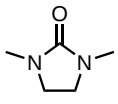	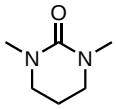	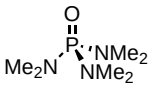	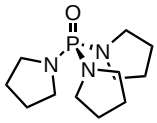
Base	LDA	LiTMP	LDA	LDA	LDA	LDA
NMR Y	0	32	47	54	90	84

Figure 2.39: Optimization of the Ireland-Claisen rearrangement on triene **165** (0.2 mmol of **165**, 0.4 mmol of base, 0.4 mmol of TBSCl, 0.4 mmol of additive at 0.1 M).

During the scale-up of the reaction, the Ireland-Claisen rearrangement did no longer yield carboxylic acid **164** but TBS ester **238**. The solution to obtain the desired product **164** was to quench the reaction with TBAF to generate the carboxylate and then make it precipitate by pouring the reaction mixture into pentane. A conventional workup of the precipitate using NH_4Cl and diethyl ether allowed the isolation of the carboxylic acid **164**. With this reproducible procedure, the carboxylic acid was isolated almost pure to be engaged in the following steps (Figure 2.40).

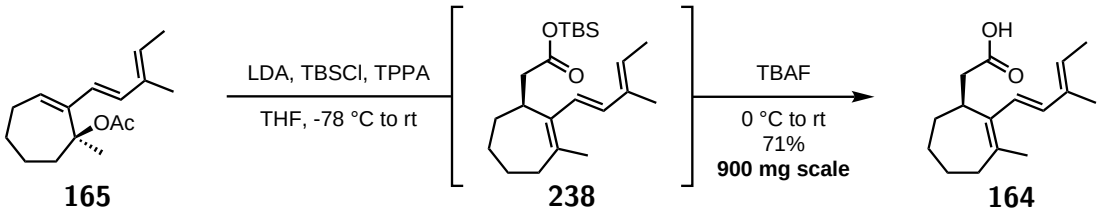

Figure 2.40: Scalable and reproducible conditions for the Ireland-Claisen rearrangement of triene **165**.

2.2.7 *Introduction of the dienophile fragment*

The synthesis of the last lactam fragment has already been described by Eissenstat and co-workers (Figure 2.41).[75] The first step consisted in the coupling of *N*-Boc-leucine **143** with Meldrum's acid **239** in presence of EDC.HCl and a catalytic quantity of DMAP to afford acyl Meldrum's acid derivative **240**. This compound was directly engaged in the complete reduction of ketone by the action of $NaBH_4$ in acidic media to generate alkyl Meldrum's acid derivative **241** in 83% over two steps. Heating this molecule in toluene generated ketene **242** which was intramolecularly trapped by the amino group, to form N-Boc protected γ-lactam **243** in quantitative yield. Stirring this compound in a mixture of DCM and TFA resulted in the synthesis of γ-lactam **244**. Finally protection of γ-lactam **244** into desired *N*-benzoylated compound **163** was performed in the presence of the benzoyl chloride in pyridine. γ-Lactam **163** was obtained in 5 steps with an overall yield of 52% from commercially available *N*-Boc-leucine **143**.

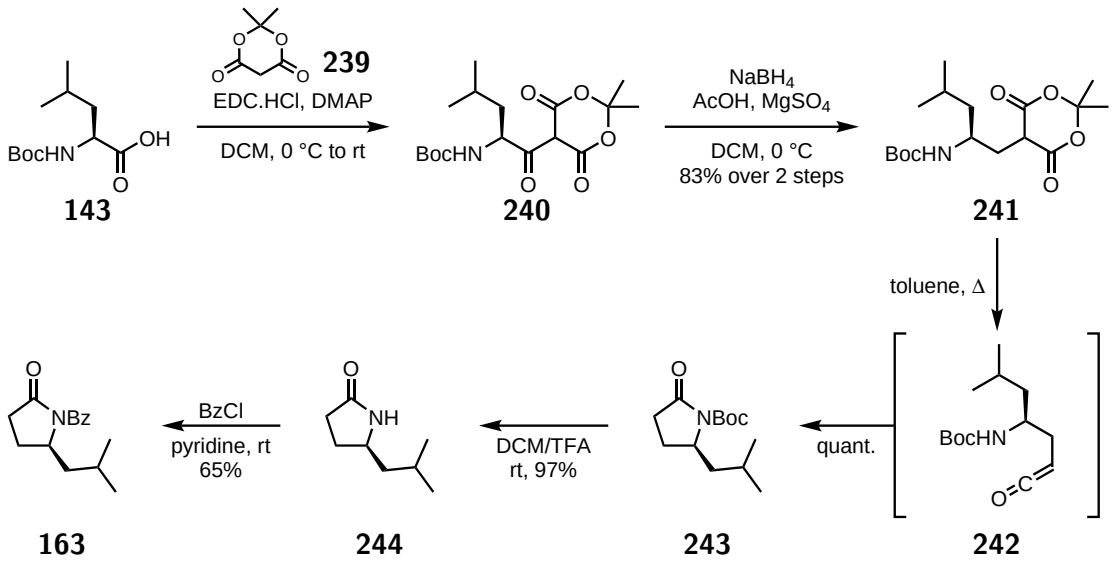

Figure 2.41: Synthesis of γ-lactam **163**.

[75] M. Smrcina, P. Majer, E. Majerova, T. A. Guerassina, M. A. Eissenstat, *Tetrahedron*, **1997**, *38*, 12867-12874.

With lactam **163** in hand, the coupling with carboxylic acid **164** was envisaged. It started with the activation of carboxylic acid **164** by CDI in the presence of the triethylamine in DCM to synthesize *N*-acyl imidazole **245**. This molecule could then react with γ-lactam **163** after deprotonation by the strong base LiHMDS in THF, to access α-acetylated γ-lactam **246**, in 40% over 2 steps. This sequence was not efficient due to the instability of acyl imidazole **245** which might regenerate carboxylic acid **164**. So a more efficient way had to be found (Figure 2.42).

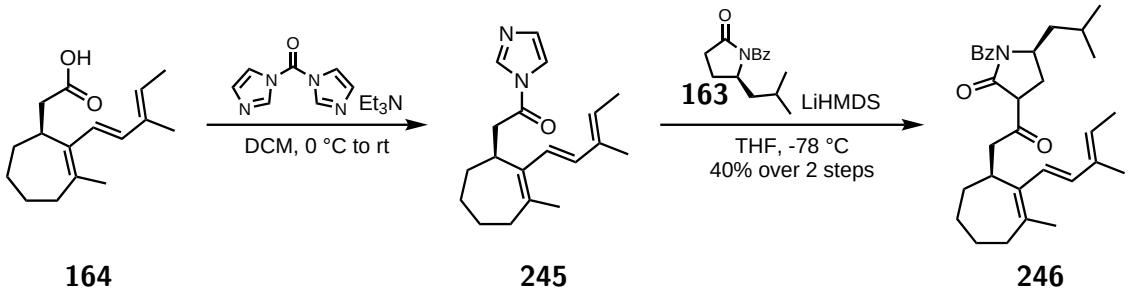

Figure 2.42: First pathway to γ-lactam **246**.

Another similar strategy uses pivaloyl chloride to generate a different activation of carboxylic acid **164**. Mixing the carboxylic acid, pivaloyl chloride and triethylamine at low temperature in DCM allowed the formation of mixed anhydride **247**. This molecule was more stable than previous acyl imidazole **245**. Using the same set of conditions with a longer reaction time, anhydride **247** was transformed into desired triene **246** with a yield of 58% over 2 steps (Figure 2.43).

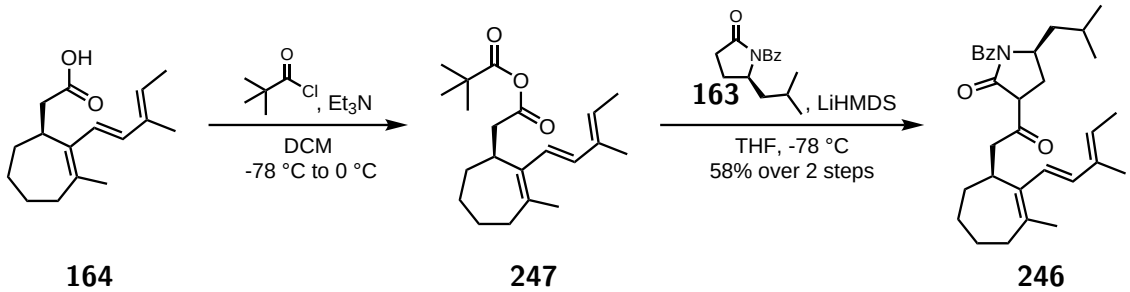

Figure 2.43: Second pathway to γ-lactam **246**.

Finally, the last step in the synthesis of the "pre-dienophile" **248** was the installation of the phenyl selenium fragment between the two carbonyl groups. Using LiHMDS and PhSeBr in THF at -78 °C, keto lactam **246** could be converted into selenide **248** (Figure 2.44).

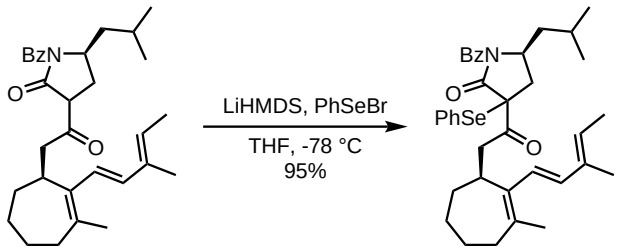

246 **248**

Figure 2.44: Synthesis of pre dienophile **248**.

2.3 Intramolecular Diels-Alder reaction

First reported by Otto Diels and Kurt Alder in 1928, the Diels-Alder reaction is a [4+2] cycloaddition between a s-*cis*-diene and a dienophile resulting in a cyclohexene product formation.[76] This pericyclic reaction creates in one step two new σ bounds and up to four stereogenic centers. The normal-electron demand Diels-Alder reaction, using an electron-rich diene and an electron-deficient dienophile, is favoured when the gap between the HOMO of the diene and the LUMO of the dienophile is small. The reaction is stereospecific and the outcome is generally the *endo* adduct due to the secondary orbital interaction between the carbonyl orbitals and the internal diene orbitals (red dashed cross, Figure 2.45). During the reaction between cyclopentadiene **250** and maleic anhydride **251**, no *exo* product **252** is formed and only the *endo* adduct **249** is observed.

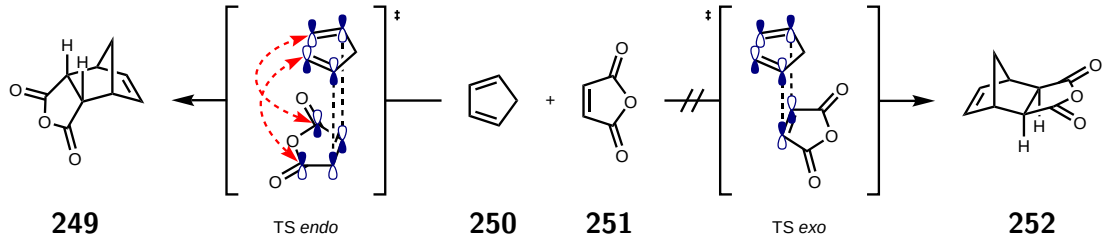

Figure 2.45: Different TS possible during a Diels-Alder reaction.

The intramolecular Diels-Alder (IMDA) reaction can be divided in two classes, type I when the diene is connected on its position 1 and type II when the diene is connected on its position 2 (Figure 2.46).[77] In these cases, the outcome of the reaction does not only follow the previously described intermolecular stereoelectronic effects but can be highly influenced by the structure of the substrate.

[76] O. Diels, K. Alder, *Liebigs Ann. Chem.* **1928**, *460*, 99-122.
[77] M. Juhl, D. Tanner, *Chem. Soc. Rev.* **2009**, *38*, 2983-2992.

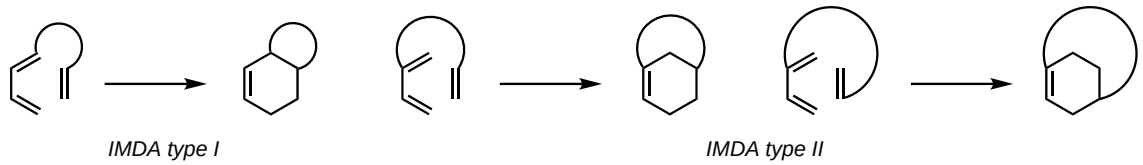

Figure 2.46: Type I and type II IMDA reactions.

During the total synthesis of cytochalasins, the Diels-Alder reaction is the general strategy used to generate the core isoindolone moiety (subsection 2.1.3). Overman and coworkers developed in 2011 the total synthesis of aspergillin PZ **119**, which is structurally related to our synthetic target.[27] The IMDA reaction, which was used to form the main core of the natural product, might thus be the closest model to our substrate. They oxidized selenium derivative **140** using hydrogen peroxide and *m*-CPBA in $CDCl_3$ to release the dienophile part of compound **253** that could be engaged in an IMDA reaction to only form *endo* adduct **254** in 56% over two steps (Figure 2.47).

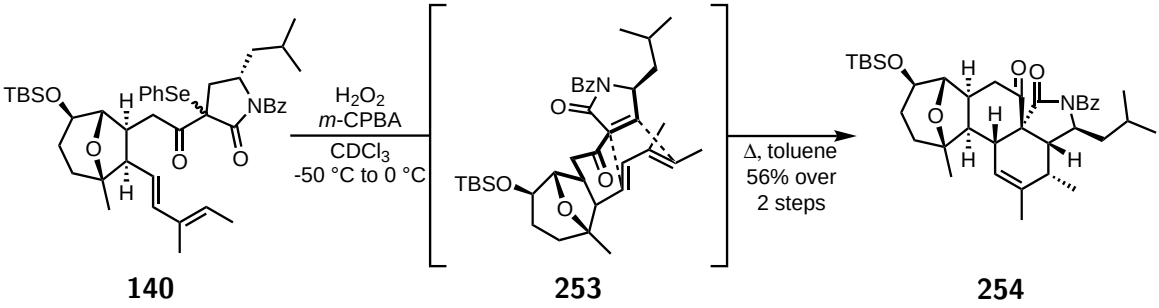

Figure 2.47: Key IMDA reaction during the total synthesis of aspergillin PZ **119**.

In this section, the work will be focused on a better understanding of this IMDA reaction in the total synthesis of cytochalasins. DFT calculations will be used to answer two questions:

Can we explain the anchoring and the effect of a catalyst observed in the IMDA reaction toward the cytochalasin core?

Can we predict the best protecting group for this IMDA reaction?

Finally, experimental results of the IMDA reaction starting from previously synthesized

pre-dienophile **248** will be presented.

2.3.1 *Can we catalyze the IMDA reaction to make (all) cytochalasins?*[78]

In this subsection, a study on the effect of Schreiner's thiourea catalyst **256** on a model Diels-Alder reaction will try to find prerequisites for an efficient catalysis in cytochalasin synthesis.

During the total synthesis attempt of periconiasins A-C **124-126**, Mehdi Zaghouani, a previous PhD student of the Nay group, revealed an acceleration of the IMDA reaction using Schreiner's thiourea catalyst **256** (Figure 2.48). By carrying out the IMDA reaction without any catalyst in chloroform at 140 °C, he observed a long reaction time, 4 days, and a low yield, 28%. Using thiourea catalyst **256** on substrate **255**, he observed a significant acceleration of the reaction, 1 day, and a better yield, 49%. Other catalysts such as Brønsted or Lewis acids did not afford any product, leading either to a complex mixture or no reaction in chloroform. The possible effect of the Schreiner's catalyst might be its ability to bind to multiple carbonyl functions through hydrogen bondings and London-type interactions.[79]

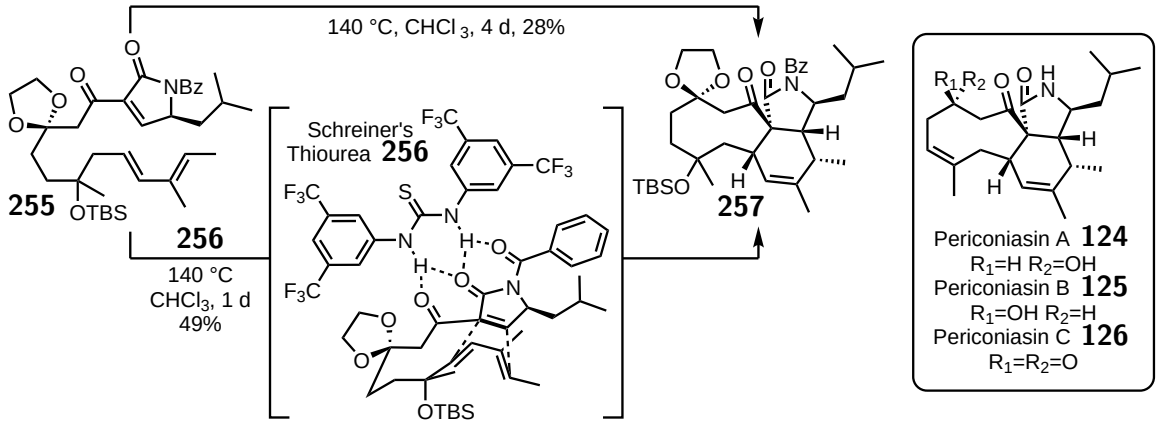

Figure 2.48: Effect of Schreiner's thiourea catalyst **256** on the IMDA reaction for the total synthesis of periconiasin A-C **124-126**.

[78] M. Zaghouani, O. Gayraud, V. Jactel, S Prévost, A. Dezaire, M. Sabbah, A. Escargueil, T.-L. Lai, C. Le Clainche, N. Rocques, S. Romero, A. Gautreau, F. Blanchard, G. Frison, B. Nay, *Chem. Eur. J.* **2018**, *24*, 16686-16691.

[79] A. Wittkopp, P. R. Schreiner, *Chem. Eur. J.* **2003**, *9*, 407-414.

Although DFT calculations were performed by Schreiner with this catalyst, on substrates bearing one or two adjacent carbonyl moieties, no results were reported with a molecule having a 1,3,5 carbonyl sequence like ours.[80] The objective of the following modelisation will be to have a better insight on the interaction of catalyst **256** with the dienophile part of compound **255**. To perform the calculations a simplified model was employed (Figure 2.49). Only the 1,3,5-carbonyl sequence was retained on dienophile fragment **258** and the diene was represented by compound **250**. Two Diels-Alder reactions, one catalysed by Schreiner's thiourea **256** and the other uncatalysed, were modeled using these substrates.

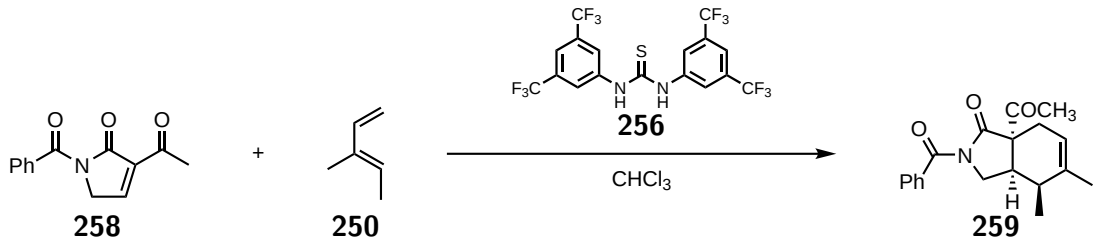

Figure 2.49: Model reaction for the Diels-Alder reaction of compound **255**.

The two pathways, catalyzed and uncatalyzed, were calculated using M06/6-31G(d,p) level of theory previously used to optimised such system.[81] The result of the calculations shows that dienophile **258** is stablized by its interaction with catalyst **256** by 14.2 kcal.mol^{-1} (Figure 2.50). The uncatalyzed pathway leading to isoindolone **259** is higher in energy by 4.9 kcal.mol^{-1}. Finally, it was found that the π^* orbital of dienophile **258** is lowered by 0.91 eV in the presence of catalyst **256**. These results are in good agreement with those obtained experimentally. By examining the calculated transition state in the catalyzed pathway, two usual hydrogen bondings can be observed between the oxygen O_1 and O_2 of the carbonyl and the hydrogen H_2 and H_3 of the thiourea, the distances found are consistent with those previously reported for such fragment (1.8-2.2 Å).[82] Non-usual hydrogen bondings are also

[80] (a) P. R. Schreiner, A. Wittkopp, *Org. Lett.* **2002**, *4*, 217-220. (b) K. M. Lippert, K. Hof, D. Gerbig, D. Ley, H. Hausmann, S. Guenther, P. R. Schreiner, *Eur. J. Org. Chem.* **2012**, 5919-5927.
[81] J. Wåhlander, M. Amedjkouh, D. Balcells, *Eur. J. Org. Chem.* **2019**, 442-450.
[82] P. R. Schreiner, *Chem. Soc. Rev.* **2003**, *32*, 289-296.

disclosed between the oxygen O_1 and O_3 of dienophile **258** and the hydrogen H_1 and H_4. These interactions have been previously reported and can be supported by the elongation of the C-H bound.[80] In our case, the distances between C_1-H_1 and C_2-H_4 are 1.089 Å and 1.092 Å respectively versus 1.086 Å for the C_3-H_5 bound.

The results obtained with the DFT calculations matched with the experimental observations. However, there are limitations to this modelling. The Diels-Alder model reaction might only work with substrates having enough liberty to align the 1,3,5-carbonyl sequence, as in this intermolecular cycloaddition. During the synthesis of periconiasin G **129**, Mehdi Zaghouani evaluated the Schreiner's thiourea catalyst **256** without any improvement.[83] In this case, the seven-membered ring formed might be too small to allow a good conformation of the carbonyl sequence. To confirm this hypothesis, more reactions need to be done with substrates forming different size of macrocycle. The modelling of the IMDA reaction starting from the previously synthesized pre-dienophile **248** might help us to predict a potential effect of Schreiner's thiourea catalyst **256**.

[83] Unpublished results

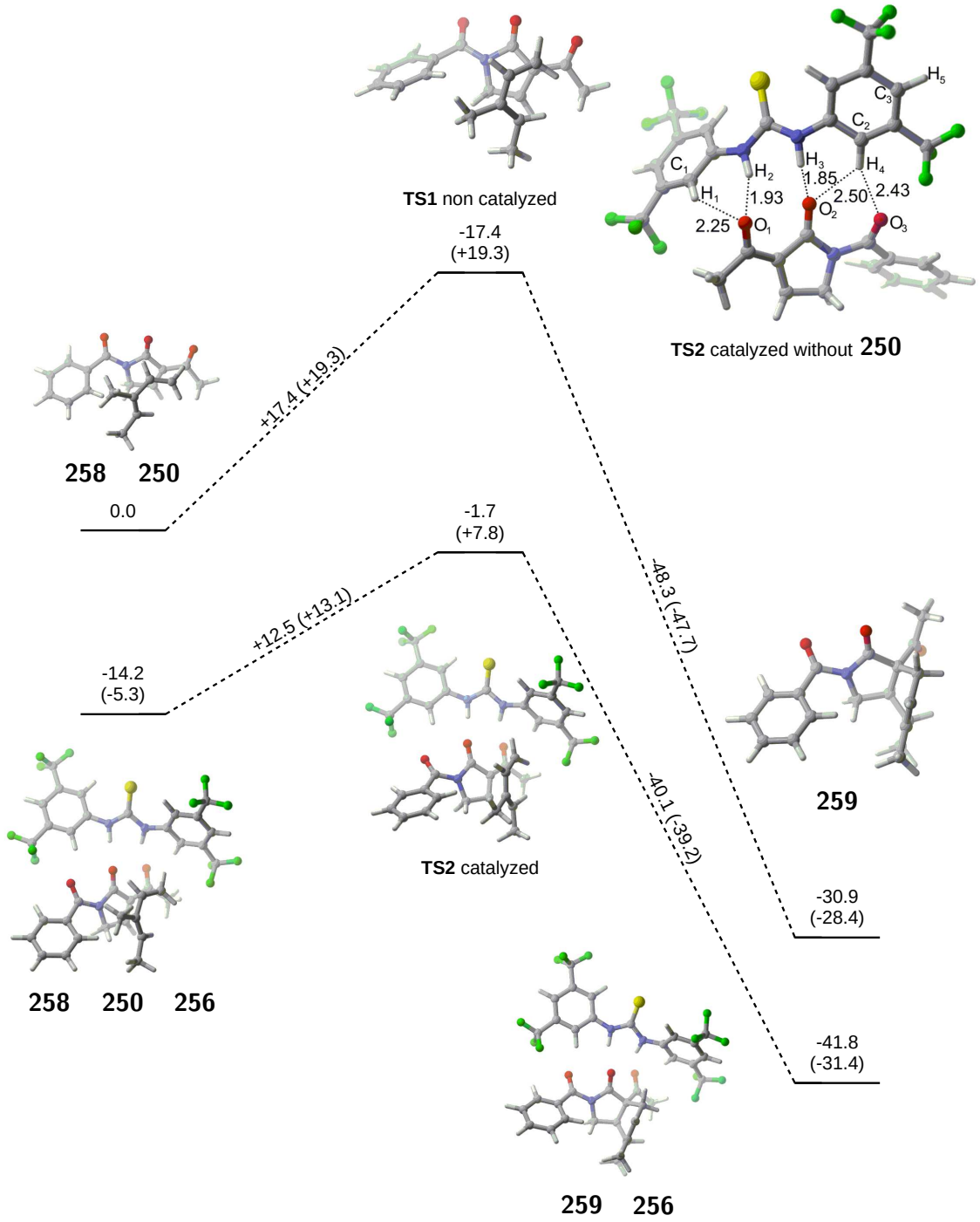

Figure 2.50: Computed enthalpies and Gibbs free energies, in parentheses, for the catalyzed and non catalyzed Diels-Alder model reaction between dienophile **258** and diene **250**. Energies relative to the starting materials are given in kcal.mol^{-1}. On the top right corner, calculated transition state without diene **250** for more clarity. Distances are given in Å .

2.3.2 *Can the protecting group be optimized to improve the IMDA reaction?*

In 2016, Tang and co-workers described the total synthesis of periconiasin A-E **124**-**128**.[29] They observed an increase of the IMDA yield by modifying the protecting group on the γ-lactam. During the synthesis of the precursor for the IMDA reaction, they synthesized two different pre-dienophiles **260** with the usual benzoyl fragment and **261** with the *ortho*-methyl-benzoyl group. These selenium derivatives were oxidized with hydrogen peroxide in DCM at 0 °C to give dienophiles **262** and **263**. These intermediates were directly engaged in the IMDA reaction. The benzoyl protected molecule yielded 20% of the desired *endo* adduct and 7% of the *exo* product. In the case of the *ortho*-methyl-benzoyl protecting group, the yield was increased to 38% for the *endo* compound and 12% for the *exo* molecule. The authors explained this effect by a probable stabilizing effect of this group on the 3-acylpyrrol-2($5H$)-one fragment of dienophile **263** compared to **262**.[84]

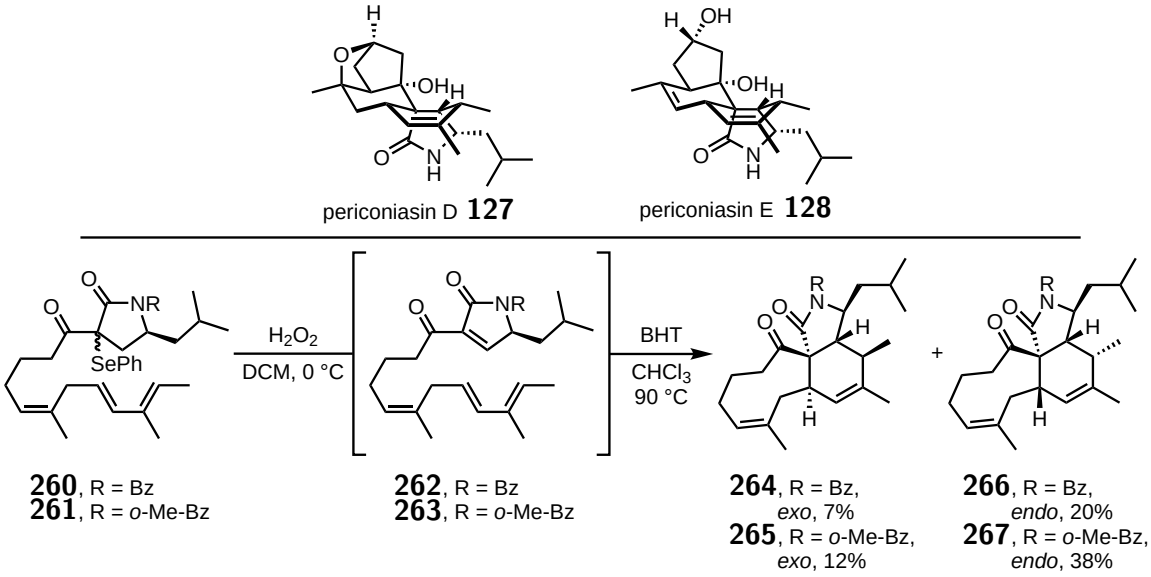

Figure 2.51: Effect of the γ-lactam protecting group on the IMDA reaction for the total synthesis of periconiasin A-E **124**-**128**.

[84] (a) E. J. Thomas, *Acc. Chem. Res.* **1991**, *24*, 229. (b) T. Schmidlin, C. Tamm, *Helv. Chim. Acta*, **1980**, *63*, 121-131.(c) S. A. Harkin, O. Singh, E. J. Thomas, *J. Chem. Soc., Perkin Trans. 1*, **1984**, 1489-1499.

By looking at these results, would it be possible to use DFT calculations to find the best protecting group for our IMDA reaction?

In order to make such predictions, a computed pathway for the IMDA reaction of substrate **272** was needed. Transition states for the cycloaddition were found using the M06-2X/6-31G(d,p) level of theory, previously used to optimize some IMDA reactions.[85] The carbonyl 1 needed to be in *trans*-configuration relatively to the carbonyl 3 in order to make this reaction possible, while the carbonyl 5 could adopt both *cis*- and *trans*-configuration. This led to 4 different transition states **268**-**271** (Figure 2.52). The lowest in energy was found to be transition states **268** with all carbonyls in *trans* geometry.

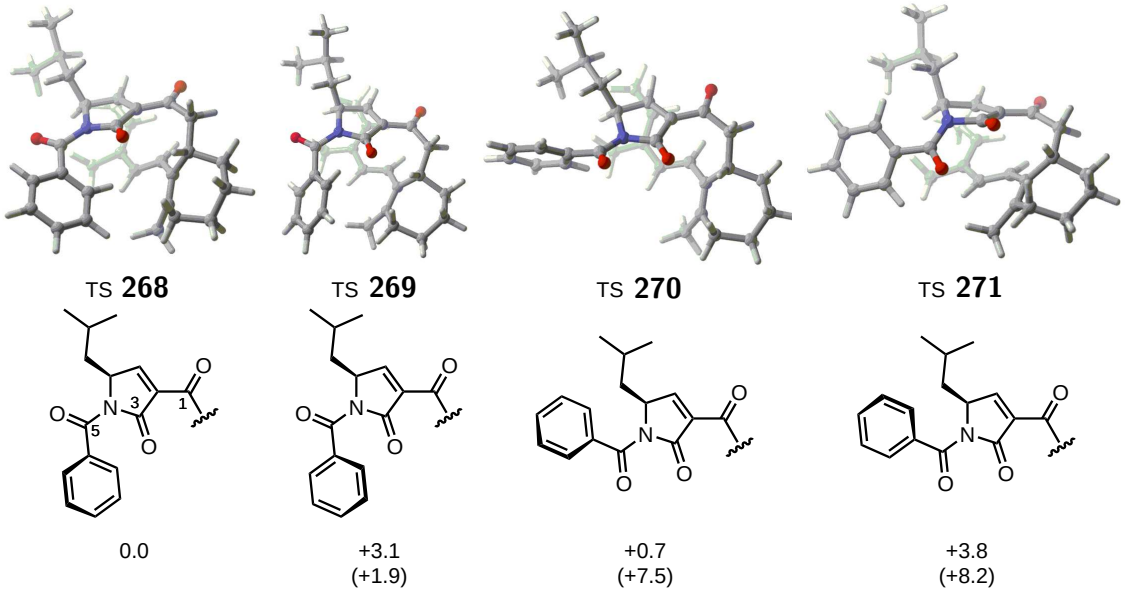

Figure 2.52: Computed enthalpies and Gibbs free energies, in parentheses, for the different transition states of the IMDA reaction of compound **272**. Energies relative to the lowest transition state are given in kcal.mol^{-1}.

It was then confirmed that transition state **268** found was connected to starting material **272** and *endo* product **273** through IRC calculations (Figure 2.53).

[85] (a) B. Maiga-Wandiam, A. Corbu, G. Massiot, F. Sautel, P. Yu, B. W.-Y. Lin, K. N. Houk, J. Cossy, *J. Org. Chem.* **2018**, *83*, 5975-5985. (b) V. Le Fouler, Y. Chen, V. Gandon, V. Bizet, C. Salomé, T. Fessard, F. Liu, K. N. Houk, N. Blanchard, *J. Am. Chem. Soc.* **2019**, *141*, 15901-15909.

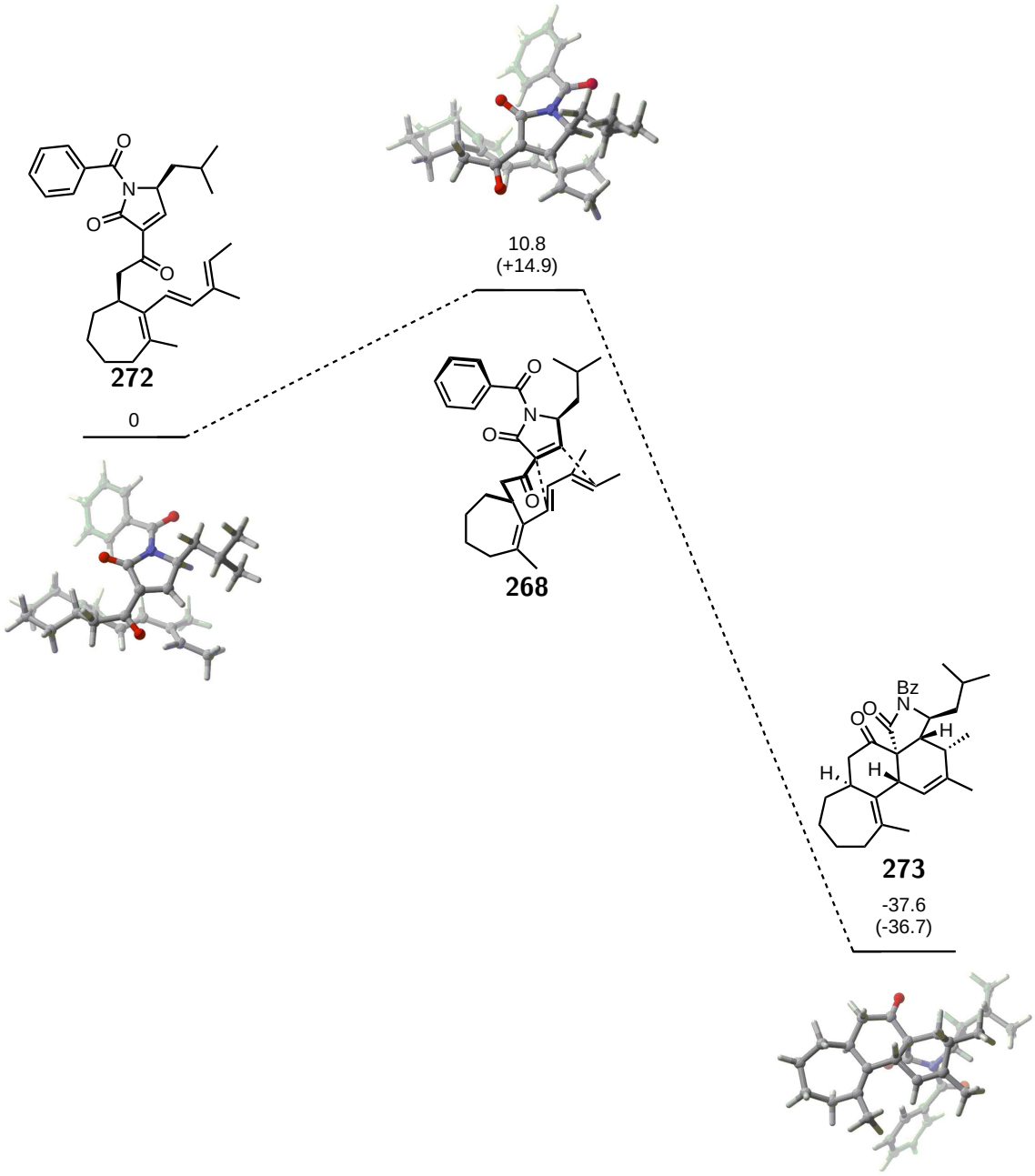

Figure 2.53: Computed enthalpies and Gibbs free energies, in parentheses, for the intramolecular Diels-Alder reaction of compound **272**. Energies relative to the starting material are given in kcal.mol^{-1}.

Starting from transition state **268**, different substitutions on the benzoyl protecting group were modelled. When it was possible to have the same substitution on two different positions (1 and 5 or 2 and 4), both transition states were computed and only the lowest in energy was kept. As in the total synthesis of periconiasin A-E **124-128** developed by Tang and co-workers, the *ortho*-methyl-benzoyl group was modelled but the relative energy between starting material and transition state **274** was found to be higher by 2.8 kcal.mol^{-1}. The same conclusion was found with other substitution at the *ortho* position of the benzoyl, CF_3 **275** and OMe **276**, and with the 1,3,5-trimethyl derivative **277**. Electron donating group (OMe) at *para* position **278** did not afford any significant change (+0.1 kcal.mol^{-1}). The same observation was made with an electron withdrawing group (CF_3) at the *meta* position **278** (-0.1 kcal.mol^{-1}). If a second trifluoromethyl was added at the other *meta* position **280** a stabilisation by 0.4 kcal.mol^{-1} was observed (Figure 2.54).

Unfortunately, no protecting group seemed to have a significant positive impact on the stabilisation of the transition state based on the DFT calculations. The benzoyl protecting group was used during the optimization of the IMDA reaction of substrate **272**.

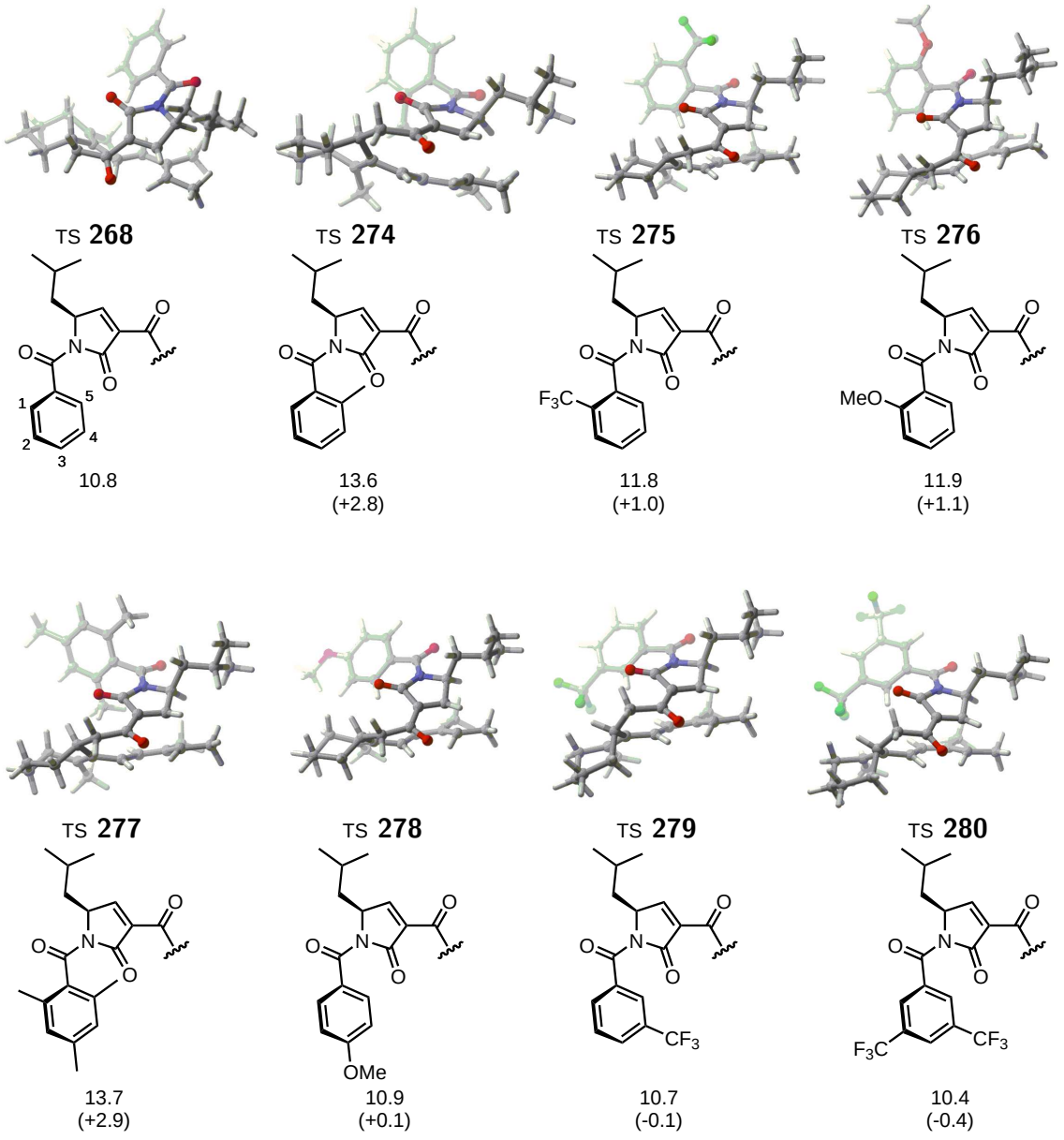

Figure 2.54: Computed enthalpies for the transition states of the IMDA reaction of dienophile bearing different protecting groups. Differences of relative energies with transition state **268** are given in parentheses. Energies relative to the starting materials are given in kcal.mol^{-1}.

2.3.3 *IMDA reaction of substrate* **272**

Returning to the experimental IMDA reaction, four different products can be synthesized from two starting diastereoisomers **272** and **281**. Minor compound **281** (present at maximum 10.5%) might form *endo* and *exo* transitions states, **283** and **284**, resulting in two undesired diastereoisomers **286** and **287**. Desired tetracyclic diastereoisomer **273** might be obtain through *endo* transition state **162** coming from major starting diastereoisomer **272**. An *exo* transition state **282** might produce another diastereoisomer **285**.

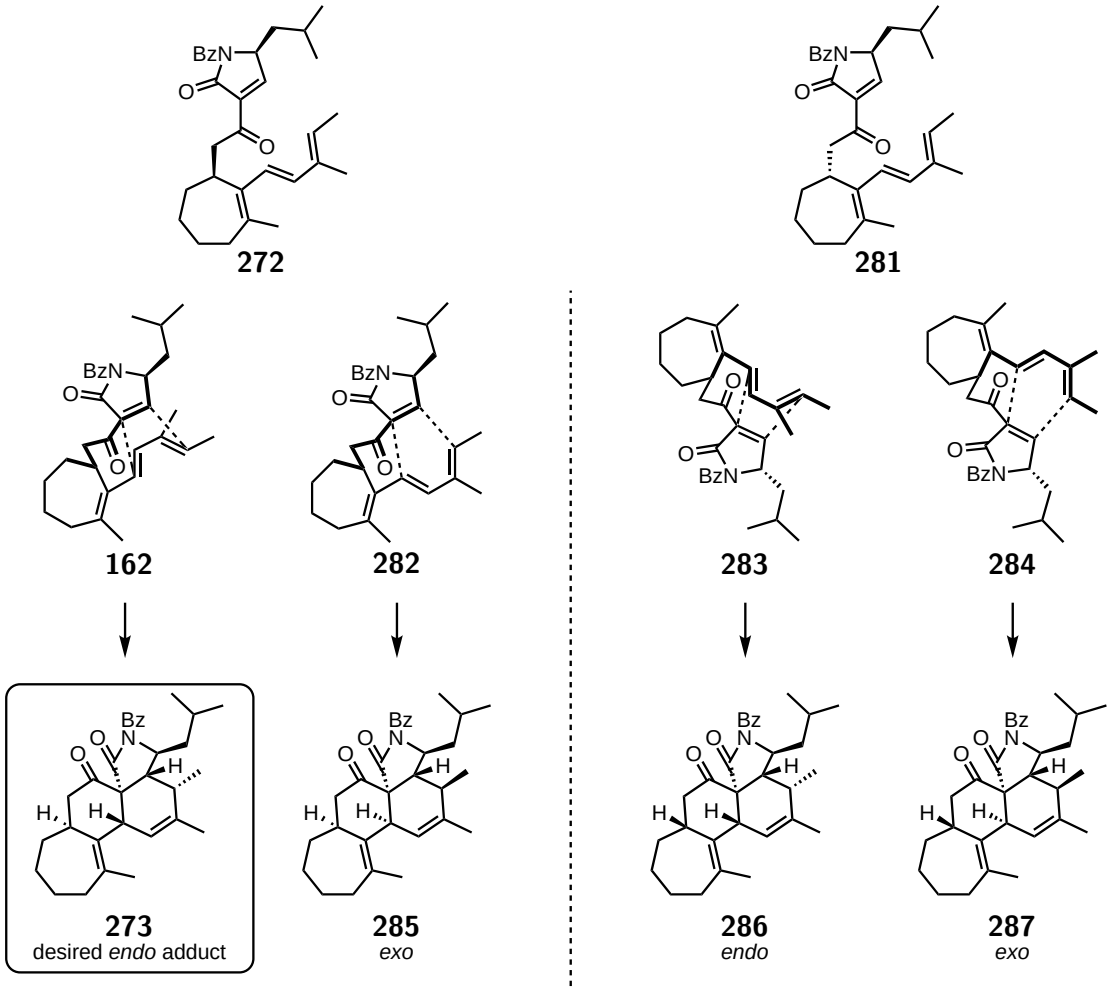

Figure 2.55: Possible diastereoisomers formed during the IMDA reaction of two dienophiles **272** and **281**.

The use of *m*-CPBA as an oxidant of selenide **248** and sodium hydrogen carbonate as a buffer at -78 °C in DCM revealed desired dienophile **272** through oxidative elimination. After reductive workup, this compound was directly engaged in the IMDA reaction by heating the organic DCM phase to 100 °C in the presence of a catalytic amount of BHT in a sealed tube. These conditions, previously optimized by Benjamin Laroche on selenium derivative **248**, furnished desired *endo* adduct **273** with a yield of 38% and *exo* product **285** with a yield of 27% (Figure 2.56). Some traces of possible other diastereoisomers, probably **286** and **287**, might have been seen on the NMR spectra of the crude mixture but were not isolated due to the small scale of the reaction. Other conditions were assessed for the IMDA reaction using Lewis acids, such as $BF_3.OEt_2$ or $AlMe_2Cl$, or the lithium salt, $LiClO_4$, did not afford any interesting results. The Schreiner's thiourea catalyst was not evaluated because with this substrate the 1,3,5 carbonyl functions are in *trans* position relative to each other according to DFT calculations, thus offering no possibility of multiple hydrogen bondings. Moreover, Benjamin Laroche tried this catalyst with no improvement of the yield.

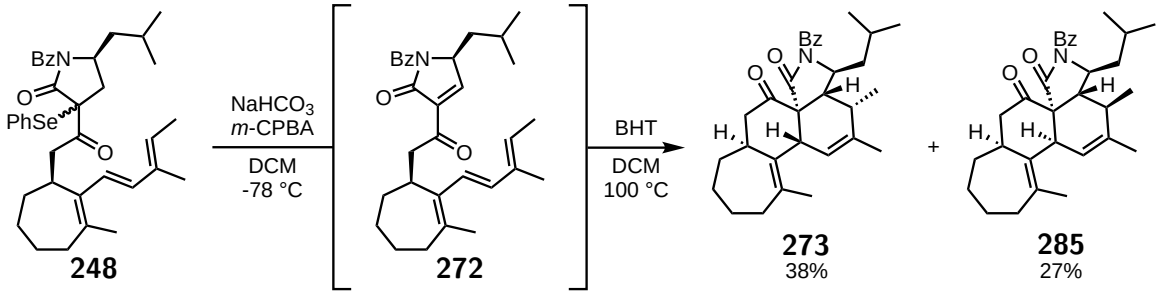

Figure 2.56: Oxidative elimination and IMDA reaction on selenium derivative **248**.

Other attempts were made to directly oxidized γ-lactam **246** to reveal dienophile **272**. The first set of conditions, developed by Mukaiyama and co-workers, involved the use of the oxidative reagent *N*-tert-butyl phenylsulfinimidoyl chloride **288** and a strong base to promote the formation of unstable species **289** that would directly evolved to reveal desired

dienophile **272**.[86] This direct one pot dehydrogenation method did not afford any conversion with the different bases, LiHMDS or LDA with TPPA as an additive, and solvents, toluene or THF, tested (Figure 2.57). The most possible explanation of this failure might be the steric hindrance of triene **246**.

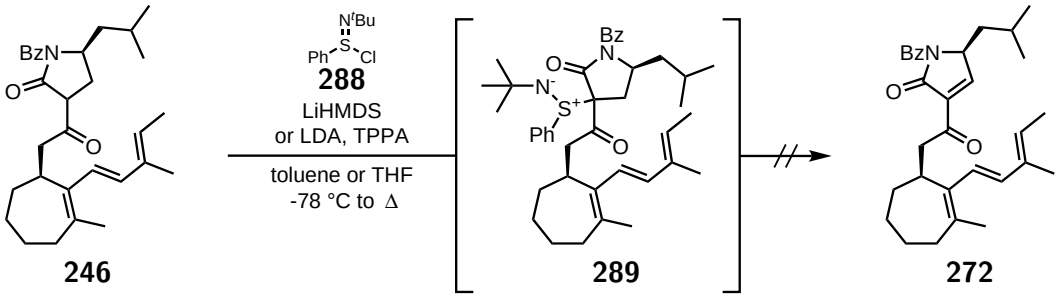

Figure 2.57: Attempt of direct dehydrogenation of γ-lactam **246** with oxidative agent **288**.

Recently, Chen and Dong published a new method to promote the one-pot dehydrogenation of cyclic ketones, lactams and lactones using *in-situ* generated copper(III) species.[87] Applying this condition to γ-lactam **246** did not afford any conversation to desired α-β unsaturated γ-lactam **272** even after long reaction time (Figure 2.58). This result might be due to the ability of the 1,3,5 carbonyl functions to chelate copper species thereby inhibiting the catalytic cycle.

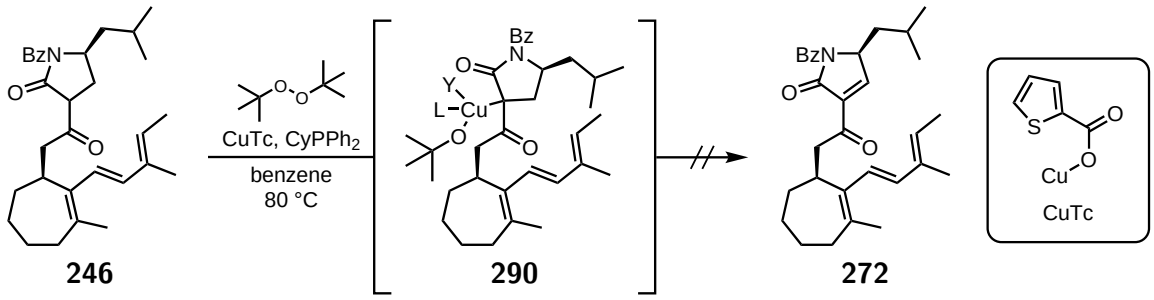

Figure 2.58: Attempt of direct dehydrogenation of γ-lactam **246** with an *in-situ* generated copper(III) species **290**.

Other recent methods known for the direct dehydrogenation of amide or ketone generally

[86] T. Mukaiyama, J. Matsuo, H. Kitagawa, *Chemistry Lett.* **2000**, *29*, 1250-1251.
[87] M. Chen, G. Dong, *J. Am. Chem. Soc.* **2019**, *141*, 14889-14897.

use transition metals and/or strong Lewis acids.[88] These methods have not been assessed due to the use of reagents which might not be compatible with the triene moiety present in our substrate **246**.

2.3.4 *Conclusion*

In summary, key protected biomimetic intermediate **273** has been reached in a stereoselective manner in 12 steps with an overall yield of 5.9% from known fragments 1-methylcycloheptene **171**, γ-lactam **163** and dienylboron pinacol ester **202**. Key transformations were the Sharpless asymmetric dihydroxylation, the Suzuki cross coupling, the Ireland-Claisen rearrangement and the intramolecular Diels-Alder reaction.

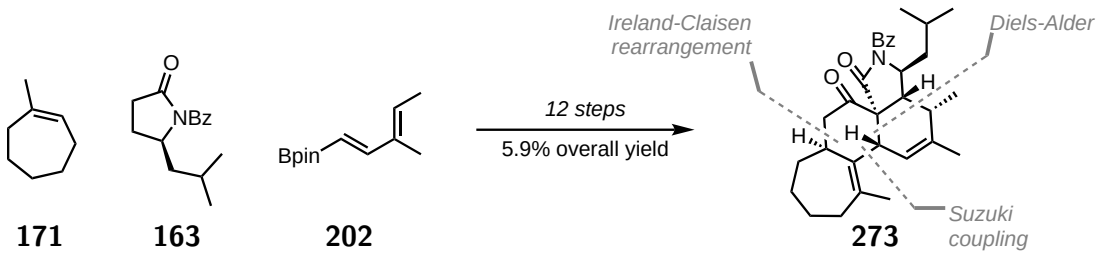

Figure 2.59: Total synthesis of key biomimetic intermediate **273**.

[88] (a) Y. Chen, A. Turlik, T. R. Newhouse, *J. Am. Chem. Soc.* **2016**, *138*, 1166-1169. (b) D. Huang, Y. Zhao, T. R. Newhouse, *Org. Lett.* **2018**, *20*, 684-687. (c) M. Chen, G. Dong, *J. Am. Chem. Soc.* **2017**, *139*, 7757-7760. (d) M. Chen, A. Rago, G. Dong, *Angew. Chem. Int. Ed.* **2018**, *57*, 16205-16209.

2.4 Late-stage functionalization

In this section, most of the reactions have been done on a very small scale, 10 μmol or less. In some cases, even if a product was isolated, it was not possible to fully characterize it due to the sensitivity of our NMR spectrometer. Further analyses by high-resolution NMR will be planned in the near future.

2.4.1 *Approach to trichodermone* **2**

Biomimetic pathway

The first pathway tested was inspired by the possible biosynthetic route developed in the introduction of this chapter. The strategy was to use oxygen to functionalize our tetracyclic biomimetic intermediate **273**. Starting from debenzoylated intermediate **1**, it was hypothesized that a Schenk-ene reaction might selectively occur at the trisubstituted alkene to generate allylic hydroperoxide **291** (Figure 2.60). Under acidic conditions, this compound might rearrange itself through the Hock cleavage reaction to form acetal **292** revealing a diene fragment. Furthermore, the use of tripet oxygen might allow a [4+2] cycloaddition leading to highly oxygenated product **293**. Finally, a basic treatment might be able to perform a Kornblum-DeLaMare rearrangement on the *endo* peroxide moiety, releasing carboxylic acid **294**. This compound might evolve spontaneously to desired trichodermone **2** through a lactonisation reaction.

Precedent attempts of such transformation were made by Benjamin Laroche during his PhD.[35] He tried different conditions for the Schenk-ene reaction. Unfortunately, he worked on a very small scale, which allowed him to only use mass spectroscopy to identify the products. One of his attempts resulted in a total conversion of tetracyclic compound **273** to a product of $m/z = 520$ [M+H$^+$] which is isobaric to the protected trichodermone. Reproducing these conditions, we used tetraphenylporphyrine **295** as a photosensitiser to generate *in-situ* singlet oxygen for the Schenk-ene reaction, and silica to act as a mild

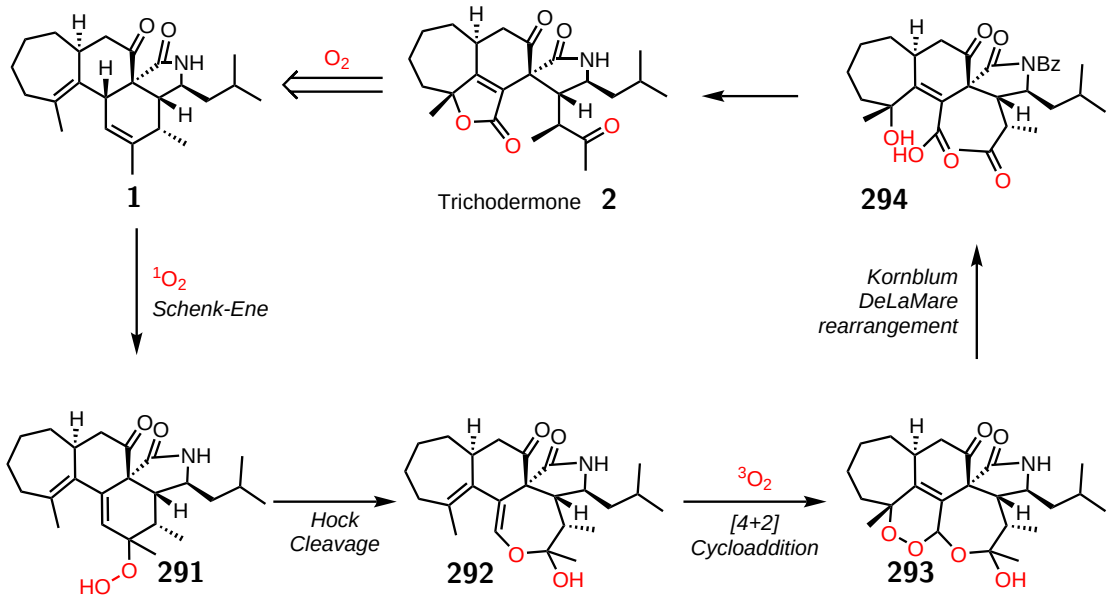

Figure 2.60: Possible biomimetic pathway to trichodermone starting from unprotected tetracyclic compound **1**.

acid for the Hock cleavage in DCM at room temperature. This led to the formation of acetal **296** in a yield of 31%. Sadly, the wrong regioselectivity was observed. Using DFT calculations to produce a realistic structure of **273** showed that the trisubstituted alkene is hindered by the methyl of the tetrasubstituted alkene (C_1) and by H_2 and H_1 (Figure 2.61). Since the singlet oxygen reactivity is highly influenced by steric hindrance, a Schenk-ene reaction on the trisubstituted alkene might not occur.[89] In addition, the DFT structure of **273** highlighted the accessibility of the Si face of the tetrasubstituted olefin. The structure of **296** was deduced from two-dimensional NMR data. Especially, beside the 1,3-diene, a hemiketal carbon was observed at 88.5 ppm. The regioselectivity was confirmed by the correlation of C_2 and H_3.

[89] M. Prein, W. Adam, *Angew. Chem. Int. Ed. Engl.* **1996**, *35*, 471-494.

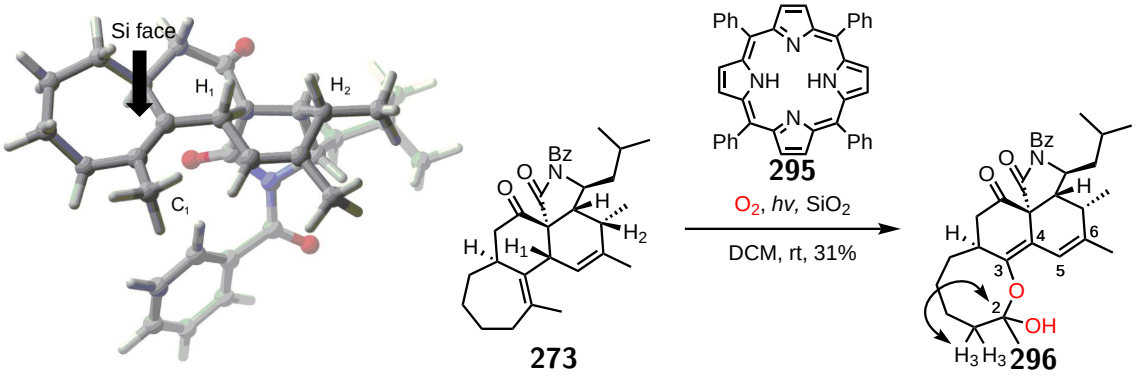

Figure 2.61: On the left, optimized structure of **273** at the M06-2X/6-31G(d,p) level of theory. On the right, Schenk-ene reaction followed by the Hock cleavage on protected biomimetic tetracyclic intermediate **273**.

Oxidative approach to unprotected tetracyclic compound 1

To escape some problems anticipated with the late stage deprotection of the γ-lactam, an approach was developed by removing first the benzoyl protection and then focusing on the late-stage oxidation. By adding a 15 M solution of sodium hydroxide in water to a solution of tetracyclic compound **273** in methanol at 0 °C and letting warm up to rt, clean deprotection occurred, leading to biomimetic intermediate **1** with a yield of 87%. A first set of conditions using osmium tetroxide, oxone and sodium hydrogen carbonate to promote the oxidative cleavage of the trisubstituted alkene in DMF at room temperature resulted in a complex mixture. The same result was obtained using osmium tetroxide in combination with sodium periodate in a mixture of acetone and water at room temperature (Figure 2.62). A possible explanation might come from the presence of two different alkenes and an unprotected lactam on compound **1** which might interfere during the reaction.

A pathway had to be found to discriminate the two alkenes in order to cleave the trisubstituted one. Using the higher nucleophilicity of the tetrasubstituted alkene, an epoxidation using *m*-CPBA and sodium hydrogen carbonate in dichloromethane was carried out at 0 °C allowing the synthesis of two diastereoisomer **298** with a low yield of 24% which was not

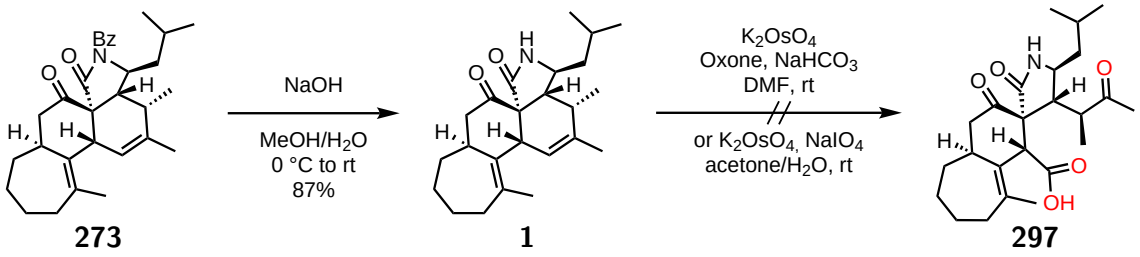

Figure 2.62: Oxidative cleavage attempt on the trisubstituted alkene of biomimetic intermediate **1**.

sufficient to fully characterize the compound. Due to the poor yield of the reaction, it was not possible to determine the major diastereoisomer. This compound was then engaged in an oxidative ozonolysis in THF at -78 ° C toward carboxylic acid **299**. A product was formed but it was not possible to fully characterize it due to the low yield of the epoxidation step (Figure 2.63). No characteristic peak of H_1 was observed on NMR spectra, neither traces of the natural product that may be formed upon epoxide opening. However, it would be worth to explore other conditions to perform this oxidative cleavage.

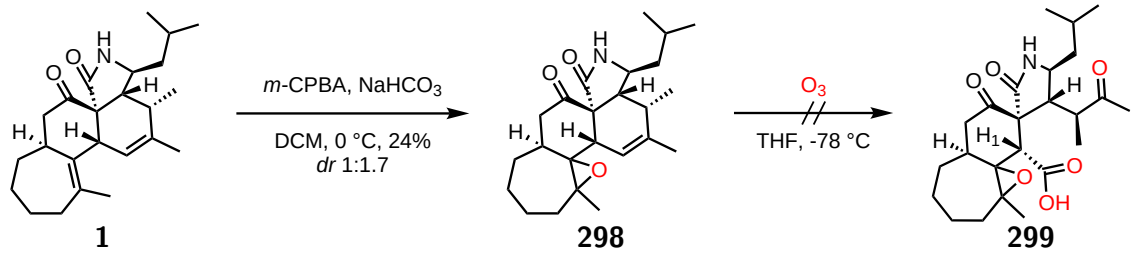

Figure 2.63: Oxidative cleavage attempt on the trisubstituted alkene of epoxide **298**.

Oxidative approach on protected tetracyclic compound 273

Due to the reactivity problem that might arise from the unprotected lactam, different pathways were tested on benzoyl protected tetracyclic compound **273**. Using osmium tetroxide with NMO as co-oxidant, a dihydroxylation of the trisubstituted alkene in different mixtures of solvent at room temperature was attempted without success (Figure 2.64). A possible explanation might come from the fact that the targeted alkene is hindered, as discussed

above, which cannot result in the formation of the desired diol **300**. No dihydroxylation was observed on the other double bond.

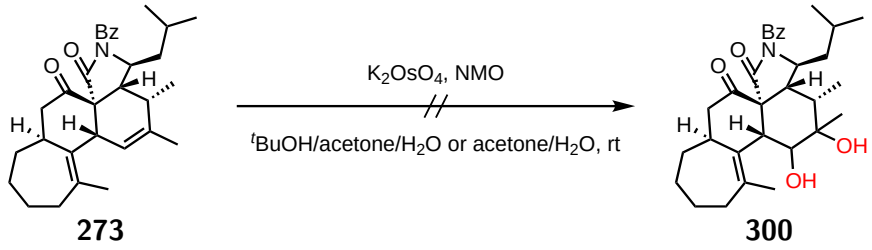

Figure 2.64: Dihydroxylation attempt on the trisubstituted alkene of protected tetracyclic compound **273**.

Previous epoxidation of unprotected tetracyclic compound **1** also allowed the discrimination of the alkenes; unfortunately, the yield was low. Interestingly, with protected compound **273**, the use of DMDO as an oxidant in acetone at 0 °C allowed selective oxidation of the trisubstituted alkene with a yield of 40%, surprisingly with a different regioselectivity. This selectivity is not usual and only furnished one, yet non identified diastereoisomer **301**. An attempt to cleave the epoxide using periodic acid in diethyl ether at room temperature did not afford any conversion to **302**, as starting material **301** remained untouched (Figure 2.65).

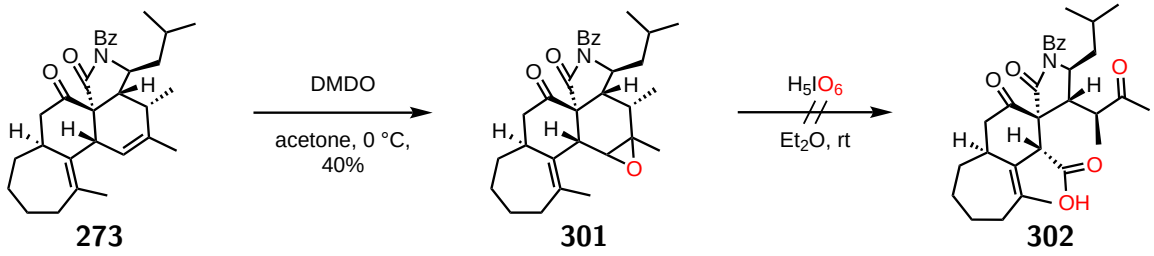

Figure 2.65: Oxidative cleavage attempt on the epoxide of protected tetracyclic compound **301**.

The use of *m*-CPBA as an oxidant and sodium hydrogen carbonate in dichloromethane finally allowed the formation of the epoxide on the tetrasubstituted alkene with a good yield of 75% and a *dr* of 1:2. Attempts to lower the reaction temperature to increase the *dr* did not afford any interesting results. This reaction needed only a basic workup to furnished clean

mixture of diastereoisomers **303**. As previously with unprotected compound **298**, exposure of the remaining alkene to oxidative ozonolysis conditions (O_3 generated in THF at -78 °C and then transfered to a solution of **303** in THF at -78 °C) did not afford any conversion of the starting material. Oxidative cleavage of the alkene was also tried under Lemieux-Johnson conditions, using osmium tetroxide and sodium periodate in a mixture of solvents at room temperature, only affording a complex mixture of compounds (Figure 2.66).

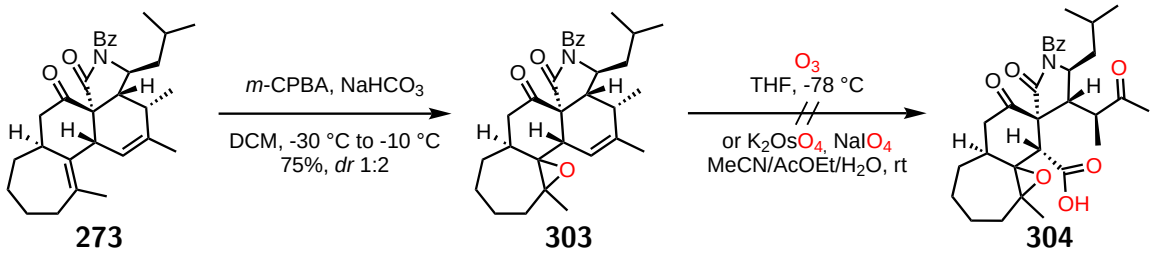

Figure 2.66: Oxidative cleavage attempt on the trisubstituted alkene of epoxide **303**.

In some cases, osmium tetroxide coupled with sodium periodate is not able to promote the dihydroxylation of alkenes and thus their oxidative cleavage.[90] For these reactions, the use of *in-situ* generated RuO_4 from ruthenium trichloride and sodium periodate might have an interesting effect. The application of ruthenium tetroxide in a mixture of solvents at rt did afford a product that showed on the crude NMR a doublet at 9.71 ppm corresponding to possible aldehyde **305**. The same coupling constant was found with the proton H_1, which supports the idea of a successful oxidative cleavage. Due to the instability of this compound, an opening of the epoxide thanks to the acidity of H_1, with a predicted pKa of 8 in THF,[??] and a possible deprotection of the lactam was tried by adding a solution of lithium hydroxide in methanol to a solution of crude aldehyde **305** in THF. Unfortunately, these conditions might have been strong for the substrate and no traces of desired acetal **306** was observed (Figure 2.67).

[90] (a) J. A. P. Pal, P. Gupta, Y. S. Reddy, Y. D. Vankar, *Eur. J. Org. Chem.* **2010**, 6957-6966. (b) H. Takamura, K. Tsuda, Y. Kawakubo, I. Kadota, D. Uemura, *Tetrahedron Lett.* **2012**, *53*, 4317-4319. (c) A. Furstner, M. Wuchrer, *Chem. Eur. J. Chem.* **2006**, *12*, 76-89. (d) H. Kawamoto, Y. Ohmori, M. Maekawa, M. Shimada, N. Mano, T. Iida, *Chem. Phys. Lipids*, **2013**, *175-176*, 73-78.

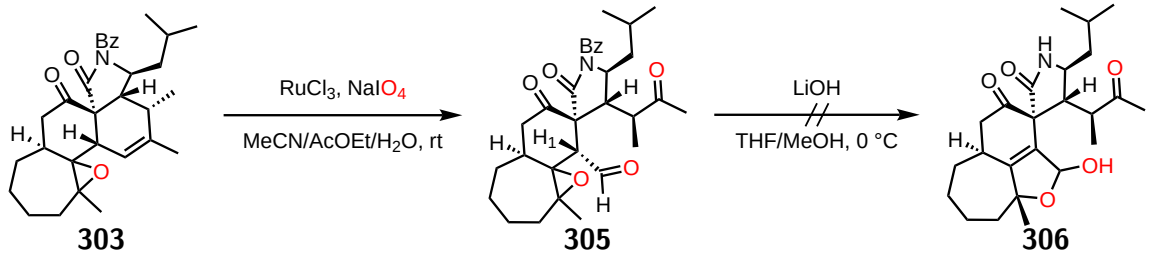

Figure 2.67: Hope with the oxidative cleavage attempt on the trisubstituted alkene of epoxide **303**.

Oxidative approach on protected *exo* diastereoisomer 285

The IMDA reaction provided the *exo* adduct in good proportion. The development of a pathway to reach trichodermone from **285** is desirable for a more efficient total synthesis. Using a set of oxidative conditions, *exo* tetracyclic compound **285** might be transformed into spiro product **307**. This compound has only one inverted stereocenter from reported natural trichodermone **2**. By chance, this chiral carbon, red sphere, is in α position of a ketone that might be epimerized using appropriate reaction conditions (Figure 2.68).

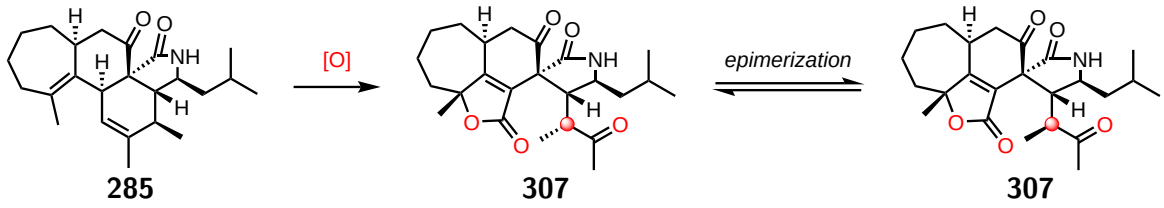

Figure 2.68: Possible route to reach trichodermone **2** starting from *exo* adduct **285** of the IMDA reaction.

The geometry of *exo* adduct **285** differs from that of *endo* product **273**, rendering the trisubstituted alkene more accessible. The direct oxidative cleavage of the desired alkene might be possible in this case and has been evaluated. The first trial was an oxidative ozonolysis. Unfortunately, no reaction occurred with the repeated addition of ozone in the media, up to 5 equivalents. When the *exo* adduct was let to stir while ozone was generated directly *in-situ*, a complex mixture of products was obtained. The second test was the use of *in-situ* generated ruthenium tetroxide, but only a complex mixture was also obtained

(Figure 2.69).

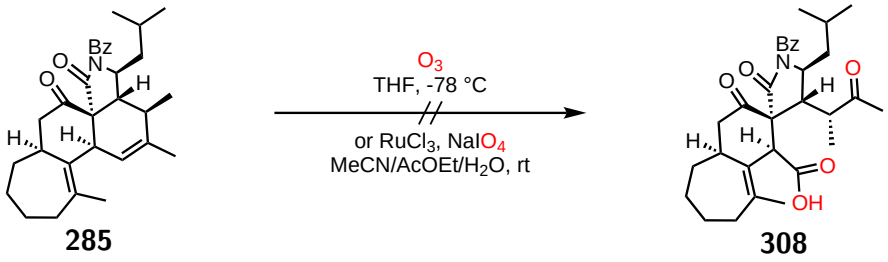

Figure 2.69: Direct oxidative cleavage attempt of the trisubstituted alkene of *exo* adduct **308**.

The same approach developed for the *endo* adduct was applied to the *exo* tetracyclic compound. The use of *m*-CPBA and sodium hydrogen carbonate in dichloromethane at -10 °C afforded only one diastereoisomer of epoxide **309** with a yield of 40%. This compound was then subjected to the *in-situ* formed ruthenium tetroxide and possibly yielded desired carboxylic acid **310** as no NMR peak of the aldehyde was observed (Figure 2.70). Unfortunately, after purification, the quantity of the product formed was not sufficient to be characterized by NMR.

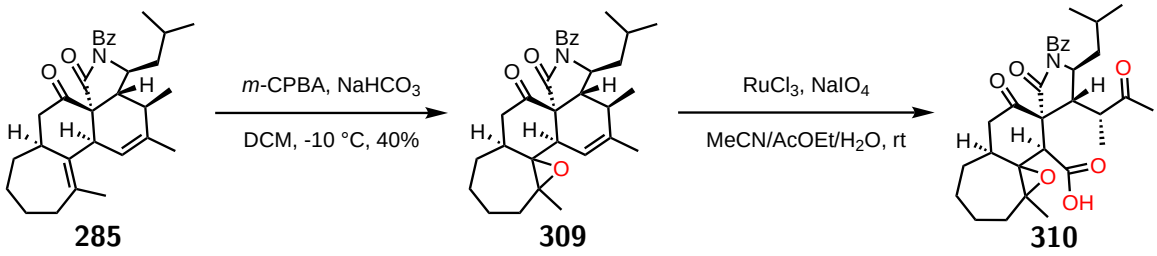

Figure 2.70: Oxidative cleavage attempt of the trisubstituted alkene of epoxide **309**.

2.4.2 *Approach to trichoderone A* **3**

In order to access trichoderone A **3**, an oxidation might take place at the γ position of the γ-lactam. This strategy might be attempted before the IMDA reaction. For example, γ-lactam **312** was first oxidized to α,β unsaturated γ-lactam **311** using hydrogen peroxide in ethyl acetate and secondly to hydroxylated γ-lactam **313** by letting the reaction warmed

up and stirred longer (Figure 2.71).[91] Makino and co-workers reported a double oxidation of selenide derivative **314** to oteromycin **315** using MMPP as an oxidant.[92]

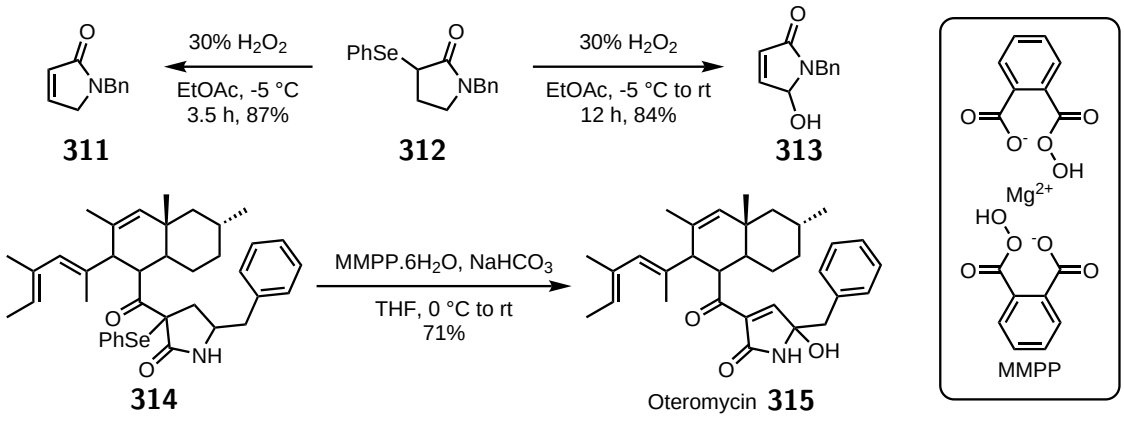

Figure 2.71: Two examples of double oxidation of γ-lactam into α,β unsaturated hydroxylated γ-lactam.

Access to the second natural product, trichoderone A **3**, might arise from a double oxidation of selenium derivative **248** to obtain a γ-hydroxy-γ-lactam intermediate **318**. Application of oxidative conditions to selenide **248** would release dienophile **272** as previously observed. Leaving this compound in a basic solution for a longer period of time might favour the formation of pyrrole **316**. This compound might react a second time with the oxidant to provide epoxide dienophile **317** which will rearrange to provide hydroxylated dienophile **318**. This can be engaged in the IMDA reaction to possibly formed hydroxylated tetracyclic compound **319**. Finally, an allylic oxidation and a deprotection reaction might allow access to desired trichoderone A **3** (Figure 2.72). During this hypothetical process, the stereochemistry of the γ-lactam might be lost but, as an aminal, this center might epimerise during the allylic oxidation reaction leading to a unique possible product **3**.

The first trial to promote a double oxidation of selenium derivative **248** was attempted using an excess of hydrogen peroxide in ethyl acetate. This reaction only afforded the release of dienophile **272** with no observed over-oxidation leading to desired hydroxylated product

[91] J. Mun, M. B. Smith, *Synth. Commun.* **2007**, *37*, 813-819.
[92] H. Uchiro, N. Shionozaki, R. Tanaka, H. Kitano, N. Iwamura, K. Makino, *Tetrahedron Lett.* **2013**, *54*, 506-511.

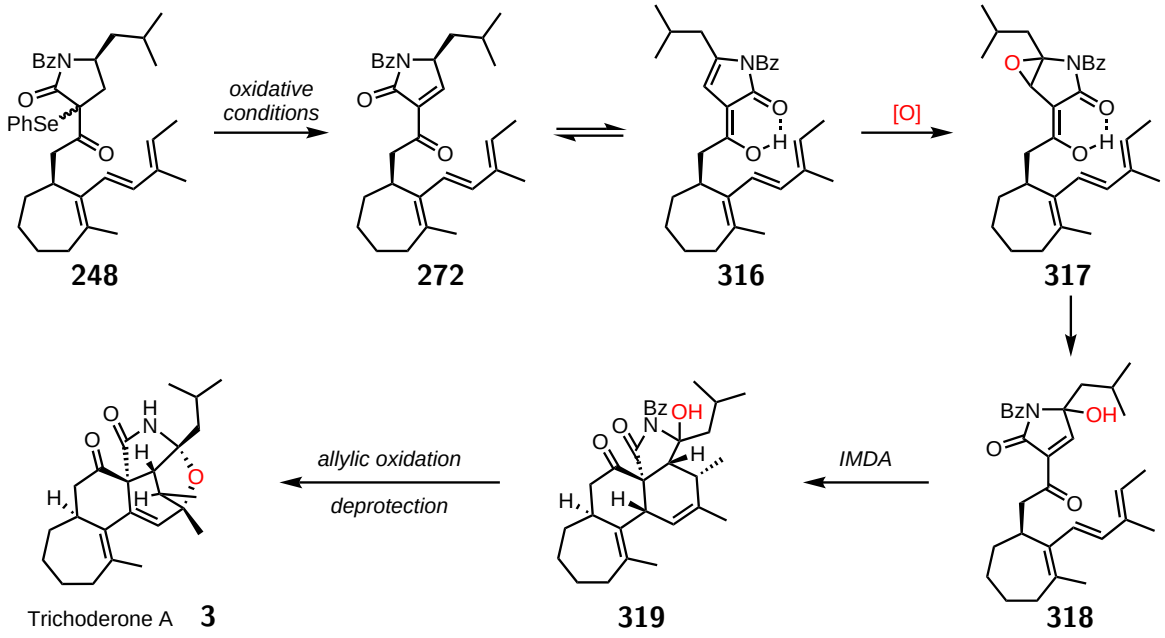

Figure 2.72: Possible pathway to trichoderone A **3** involving an oxidation of γ-lactam **248**.

317. Selenium derivative **248** was also subjected to magnesium monoperoxyphthalate and sodium carbonate in THF. The formation of α,β-unsaturated lactam **272** was seen by TLC; unfortunately, a longer reaction time did not allow the formation of desired hydroxylated product **318** and only a complex mixture of products was obtained, possibly arising from the oxidation of the triene.

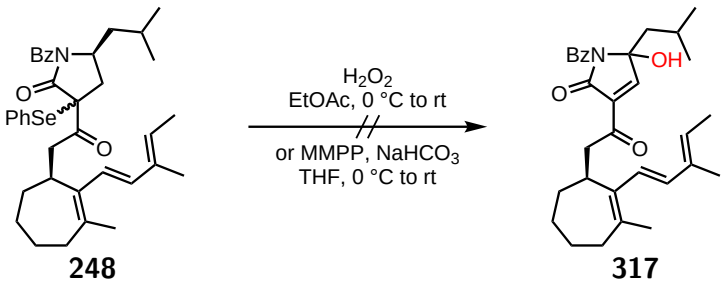

Figure 2.73: Oxidative attempt of the γ position of γ-lactam **163**

2.5 Conclusion and perspectives

2.5.1 *Conclusion*

The total synthesis of trichodermone **2** and trichoderone A **3** was envisaged as a two phases approach from a common precursor. The first phase consisted in the construction of protected biomimetic intermediate **273** in 12 steps with an overall yield of 5.9% from known starting materials 1-methylcycloheptene **171**, γ-lactam **163** and dienylboron pinacol ester **202**. The major challenges were the reproducibility and scalability of the reactions, such as the Suzuki cross coupling between triene **165** and boron pinacol ester **202** or the acetylation of hydroxy enol triflate **167**. The steps from the installation of γ-lactam **163** to the IMDA reaction have not been yet done on gram-scale and attempts are currently done to find scalable and reproducible conditions. The second phase was mainly focused on the oxidation of tetracyclic intermediate **273** to access natural products and analogues. Diverse oxidative conditions have been evaluated and some promising results have been obtained for the total synthesis of trichodermone **2** using first an epoxidation followed by an oxidative cleavage using Ru_4O. Unfortunately, due to the small scale of the reactions attempted some products have not been fully characterized (Figure 2.74).

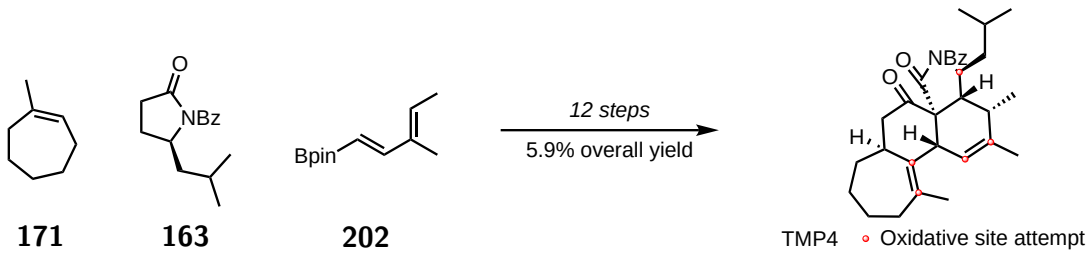

Figure 2.74: Route to tetracyclic intermediate **273** and oxidation attempts

2.5.2 *Perspectives*

A shorter path to tetracyclic intermediate 273

A shorter route to common intermediate **273** might be envisaged starting from known α-diazocycloheptanone.[93] Using a cross coupling reaction with dienylboron pinacol ester **202**, triene **321** might be accessed. The introduction of chirality might come from asymmetric methylation of enone **321** using organometallic chemistry.[94] Finally, the acetylation of alcohol **322** might reconnect this pathway to the one developed in this thesis. This hypothetical route will reduce the number of steps to access tetracyclic intermediate **273** from 12 to 9 (Figure 2.75).

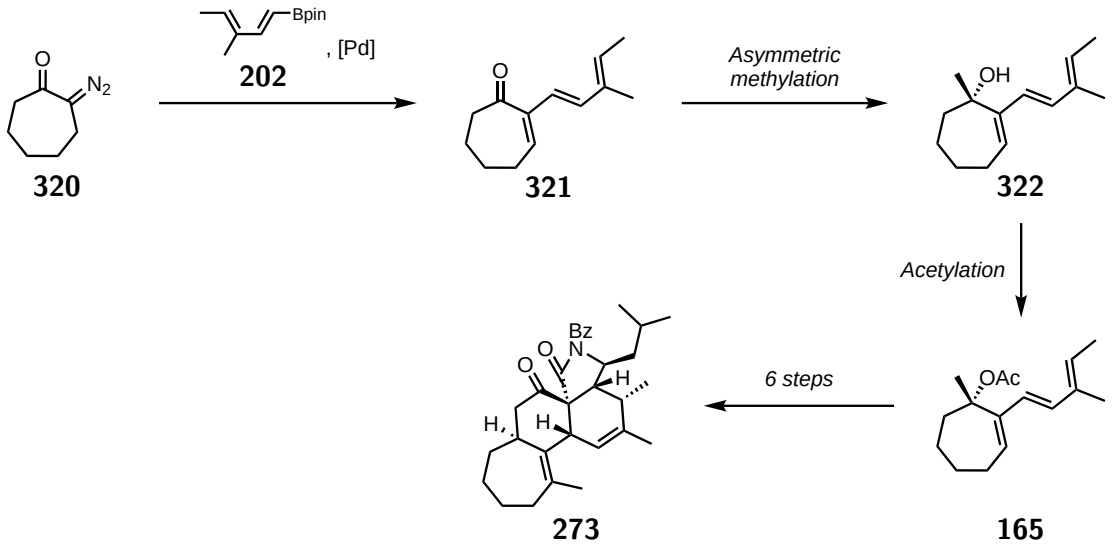

Figure 2.75: Possible shorter route to tetracyclic intermediate **273**

[93] (a) X. Yu, J. Hu, Z. Shen, H. Zhang, J.-M. Gao, W. Xie, *Angew. Chem. Int. Ed. 2017*, *56*, 350-353. (b) M. Regitz, F. Menz, J. Rüter, *Tetrahedron Lett.* **1967**, *8*, 739-742.

[94] For example: (a) J. Siewert, R. Sandmann, P. von Zezschwitz, *Angew. Chem. Int. Ed.* **2007**, *46*, 7122-7124. (b) S.-J. Jeon, H. Li, P. J. Walsh, *J. Am. Chem. Soc.* **2005**, *127*, 16416-16425.

Possible pathway to trichodermone 2

A possible route to trichodermone **2** might be developed using preliminary results of the oxidation of tetracyclic compound **273**. The development of the oxidative cleavage of epoxide **303** using ruthenium tetroxide might allow the formation of carboxylic acid **304** through prolonged reaction time. The deprotonation of the α position of carboxylic acid **304** might selectively open the epoxide to generate alkoxide **323** which might cyclized to form protected trichodermone **324**. The removal of the benzoyl protecting group on the γ-lactam might allow the formation of trichodermone **2** (Figure 2.76).

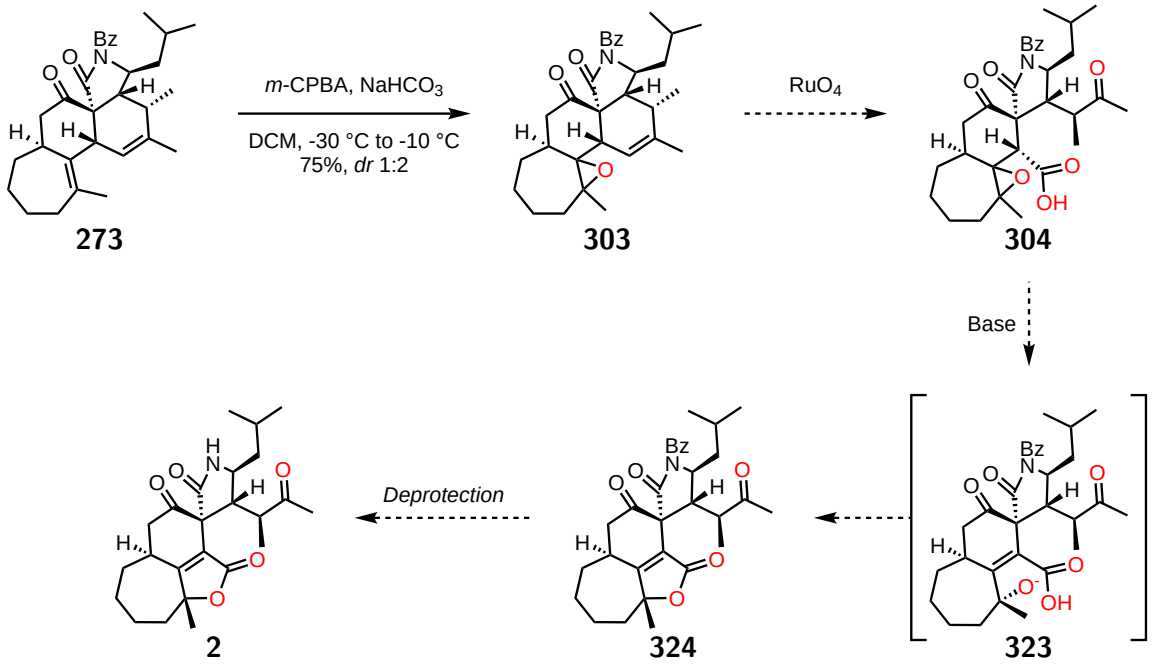

Figure 2.76: Possible route to trichodermone **2**

Possible pathway to trichoderone A 3

Concerning trichoderone A **3**, a different approach might be envisaged using an oxidation of the γ-lactam of tetracyclic intermediate **273**. This strategy might use catalyst developed by White and co-workers to perform late stage oxidative C-H methylation.[95] During the development of the reaction, they observed hydroxylation and acetylation of γ-lactam **325** using manganese catalyst **328**, H_2O_2 and AcOH in MeCN. This approach will reduce the number of possible diastereoisomer during the IMDA reaction. Then allylic oxidation and deprotection of hydroxylated compound **319** might allow the formation of trichoderone A **3** (Figure 2.77).

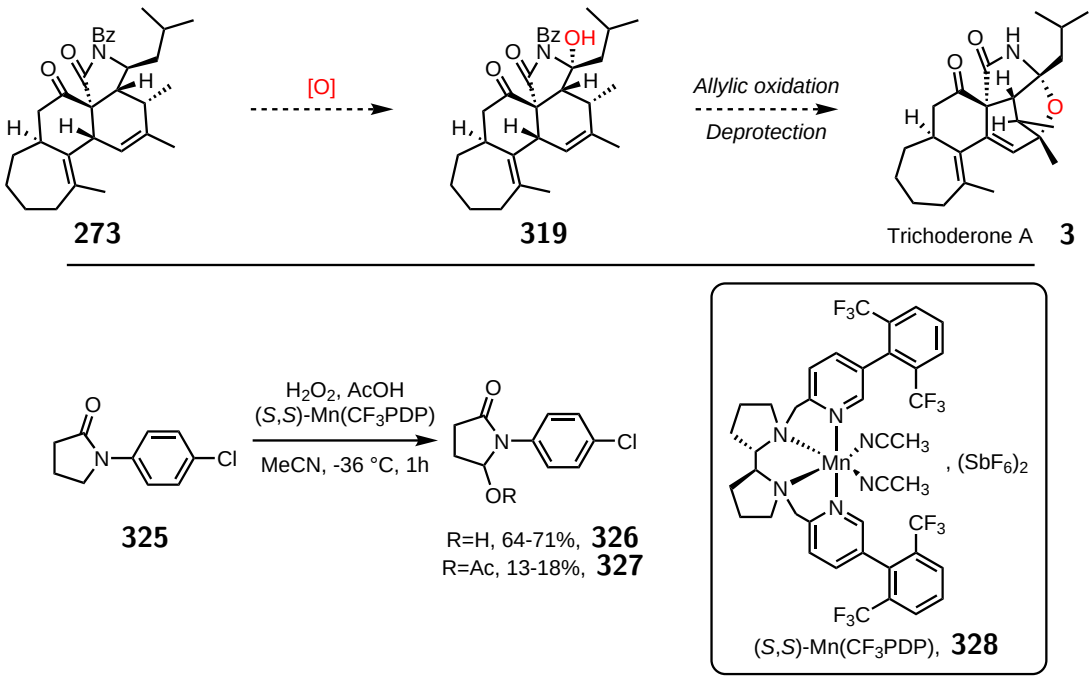

Figure 2.77: Possible route to trichoderone A **3**

[95] K. Feng, R. E. Quevedo, J. T. Kohrt, M. S. Oderinde, U. Reilly, M. C. White, *Nature*, **2020**, *580*, 621-627.

Chapter

3

Interrupted organic peroxide rearrangements: a new path to cyclic ethers

3.1 Introduction

3.1.1 *Brief overview of peroxide rearrangements*[1]

Rearrangements of peroxides are powerful reactions to access oxygenated compounds, for example ketones or carboxylic acids. They can be divided into three major families. The first involves radical rearrangements. The Schenck rearrangement was discovered in 1958 by letting allylic hydroperoxide **329** evolves in chloroform for 3 days, causing the hydroperoxide to migrate (Figure 3.1).[2] Three possible pathways have been proposed. The first involves a five membered ring intermediate **330** but to date no proof of this intermediate has been observed.[3] The second, a five membered ring transition state **331**, is most likely suggested by the observed stereoselective rearrangement of optically pure hydroperoxides.[4] The last pathway involves a dissociation of hydroperoxide **329** into the hydroperoxyl radical and the allylic radical. Experiments using labelled oxygen showed low incorporation during the rearrangement, depending on the viscosity of the solvent.[5] The mechanism might be a mix between transition state **331** and dissociation intermediate **332** leading to hydroperoxide **333**.

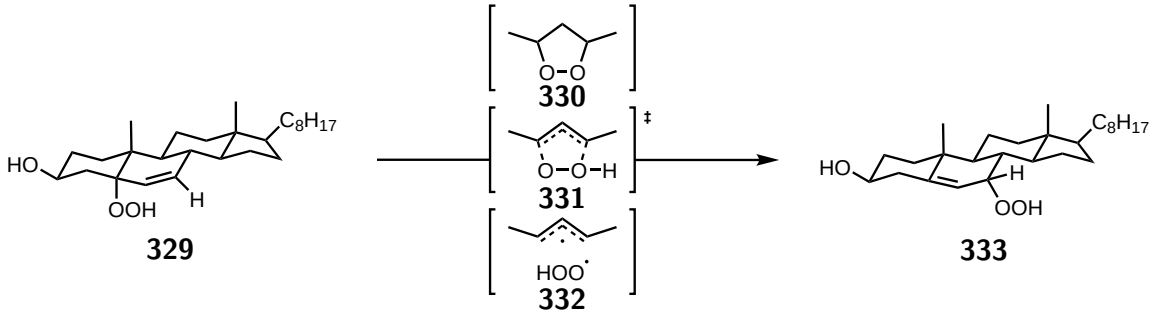

Figure 3.1: Schenck rearrangement.

[1] I. A. Yaremenko, V. A. Vil', D. V. Demchuk, A. O. Terent'ev, *Beilstein J. Org. Chem.* **2016**, *12*, 1647-1748.
[2] (a) G. O. Schenck, O.-A. Neumüller, W. Eisfeld, *Justus Liebigs Ann. Chem.* **1958**, *618*, 202-210. (b) G. O. Schenck, O.-A Neumüller, W. Eisfeld, *Angew. Chem.* **1958**, *70*, 595.
[3] W. F. Brill, *J. Chem. Soc., Perkin Trans. 2*, **1984**, 621-627
[4] N. A. Porter, J. K. Kaplan, P. H. Dussault, *J. Am. Chem. Soc.* **1990**, *112*, 1266-1267.
[5] (a) N. A. Porter, K. A. Mills, S. E. Caldwell, G. R. Dubay, *J. Am. Chem. Soc.* **1994**, *116*, 6697-6705. (b) K. A. Mills, S. E. Caldwell, G. R. Dubay, N. A. Porter, *J. Am. Chem. Soc.* **1992**, *114*, 9689-9691.

In 1973, Smith and co-workers discovered that by leaving hydroperoxide **333** at 40 °C for 2 days in ethyl acetate, partial epimerization occurred (Figure 3.2).[6] This rearrangement might occur through a dissociation mechanism involving the hydroperoxyl radical pair **333**.

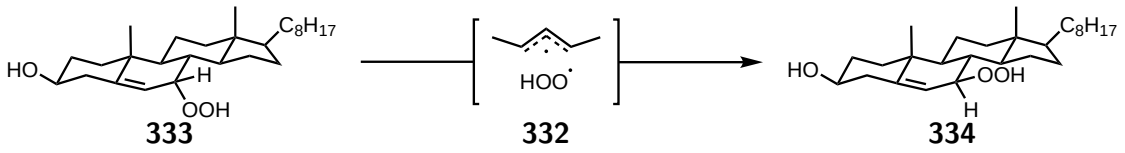

Figure 3.2: Smith rearrangement.

The second family of peroxide rearrangements are base-catalyzed. The Kornblum-DeLaMare rearrangement, first reported in 1951, is able to form a ketone and an alcohol from a peroxide.[7] The first step starts with a deprotonation at the α position of peroxide **335**. Anion **336** fragments to give ketone **337** and alcohol **339** after regeneration of the base (Figure 3.3, top). This rearrangement is a key step in the biosynthesis of prostaglandins D_2 **341** and E_2 **342** from prostaglandin H_2 **340** (Figure 3.3, bottom).[8]

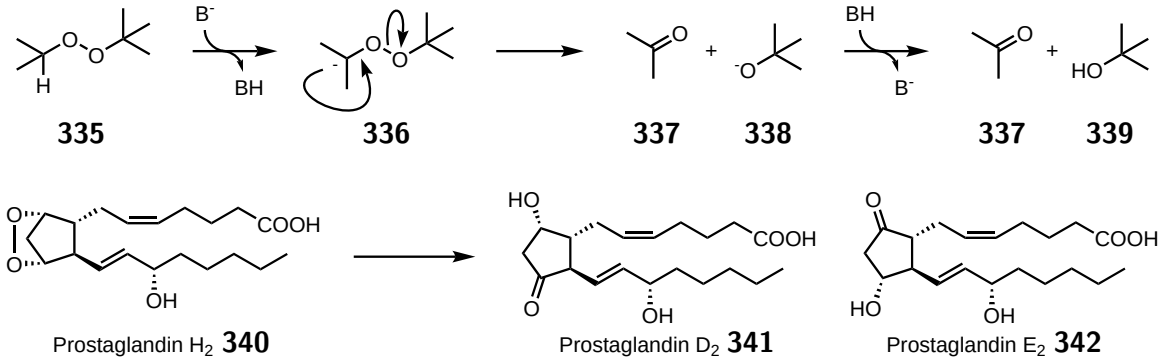

Figure 3.3: top, Kornblum-DeLaMare rearrangement mechanism; bottom, biosynthesis of prostaglandin D_2 **341** and E_2 **342** from prostaglandin H_2 **340**.

The last family is composed of the acid mediated rearrangements. The Baeyer-Villiger

[6] J. I. Teng, M. J. Kulig, L. L. Smith, G. Kan, J. E. van Lier, *J. Org. Chem.* **1973**, *38*, 119-123.
[7] N. Kornblum, H. E. DeLaMare, *J. Am. Chem. Soc.* **1951**, *73*, 880-881.
[8] (a) M. G. Zagorski, R. G. Salomon, *J. Am. Chem. Soc.* **1980**, *102*, 2501-2503. (b) M. G. Zagorski, R. G. Salomon, *J. Am. Chem. Soc.* **1984**, *106*, 1750-1759.

oxidation, discovered in 1899, transforms acyclic and cyclic ketones into esters or lactones.[9] The reaction between a ketone (**343**) and a peracid (**344**) generates a perester (**345**) which can rearrange to form an ester (**346**) and a carboxylic acid (**347**). Some examples of the Baeyer-Villiger reaction have been reported also in basic media.[10]

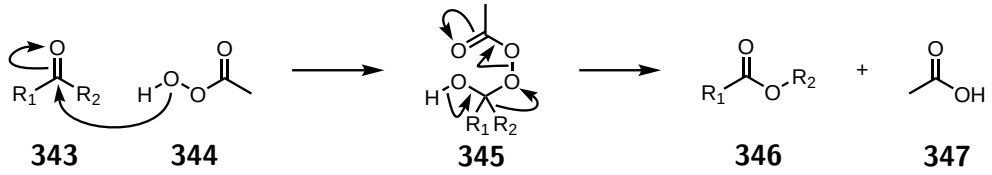

Figure 3.4: The Baeyer-Villiger reaction.

Two other acid-catalysed rearrangements, the Hock cleavage and the Criegee rearrangement, will be discussed in more details in the following subsections.

3.1.2 *Hock cleavage*

The Hock cleavage or rearrangement is a reaction that transforms a hydroperoxide into a ketone and an alcohol or a ketone or an aldehyde.[11] The reaction begins with the protonation of the hydroperoxide **348**. The protonated hydroperoxide **349** can then undergo a rearrangement involving the 1,2 C→O migration of a R group onto the peroxide oxygen and eliminate a molecule of water to form a carbenium ion **350**. This ion is in equilibrium with the oxonium species **351**. The previously released water molecule can then attack the oxocarbenium ion to form acetal **352**. After prototropy, the newly formed acetal **353** can be cleaved into an alcohol **354** and a ketone **355** (Figure 3.5, top). This reaction is a key step in the cumene process used in the industry to convert benzene **356**, propylene **357** and oxygen into phenol **360** and acetone **361** by generating *in-situ* hydroperoxide **358** that

[9] (a) A. Baeyer, V. Villiger, *Ber. Dtsch. Chem. Ges.* **1899**, *32*, 3625-3633. (b) A. Baeyer, V. Villiger, *Ber. Dtsch. Chem. Ges.* **1900**, *33*, 858-864.

[10] (a) T. D. Bradley, A. Dragan, N. C. O. Tomkinson, *Tetrahedron*, **2015**, *71*, 8155-8161. (b) H. O. House, R. L. Wasson, *J. Org. Chem.* **1957**, *22*, 1157-1160.

[11] (a) (c) H. Hock, S. Lang, *Ber. Dtsch. Chem. Ges. A*, **1944**, *77*, 257-264. (b) Z. Wang, *Comprehensive Organic Name Reactions and Reagents*, John Wiley & Sons, New York, NY, USA, **2010**, p. 1438-1442.

rearranges into oxocarbenium **359** (Figure 3.5, bottom).[12]

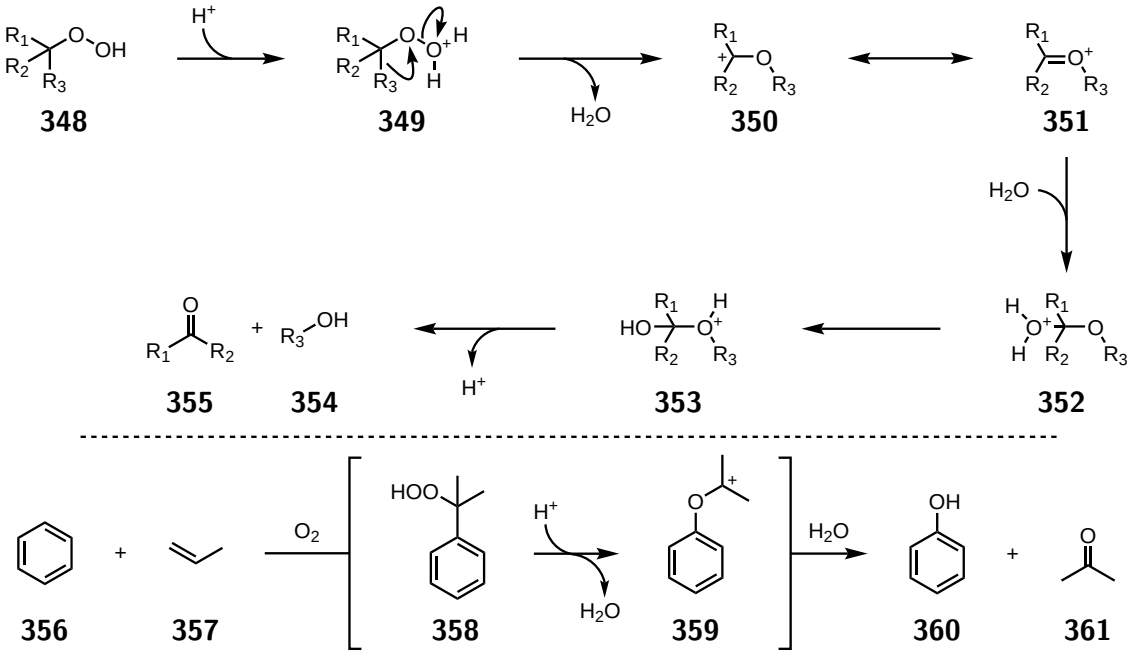

Figure 3.5: top, Hock cleavage mechanism; bottom, Cumene process.

Generally the migration of the most electron rich group is favoured.[13] In the case of 1-phenylcyclohexyl hydroperoxide **362**, using sulfuric acid as a catalyst in acetic acid, cyclohexanone **364** and phenol **360** are formed. These products can only come from the *in-situ* formation of oxocarbenium **363** and the migration of the phenyl group. Applying the same set of conditions to 1-phenylcyclopentyl hydroperoxide **365**. The formation of cyclopentanone **368** and phenol **360** coming from oxocarbenium **366** have been observed with a yield of 65%. In addition, the formation of linear ketone **369** derived from oxocarbenium **367** have been isolated with a yield of 12%. This time, not only the phenyl ring migrates, but also a ring expansion is alternatively observed. This effect can be due to the reduction of hydrogen steric interactions while increasing the size of the ring. This trend

[12](a) R. J. Udris, P. G. Sergeyev, B. D. Kruzhalov, USSR Patent 106, 666, **1947**. (b) P. G. Sergeyev, R. J. Udris, B. D. Kruzhalov, B. D. Nyemtsov, USSR Patent 106, 992, **1947**. (c) H. Hock, H. Kropf, *Angew. Chem.* **1957**, *69*, 313-321.

[13]R. Hiatt, *Organic Peroxides*, ed. Swern, D., Wiley-Interscience, New York, **1971**, *2*, p. 67.

was confirmed during the synthesis of 1-phenylcyclobutyl hydroperoxide **371**. Starting from 1-phenylcyclobutanol **370**, the same conditions used to synthesized hydroperoxides **362** and **365** were applied but the major product was 2-phenyl-2-tetrahydrofuryl hydroperoxide **373**. This can only be obtained by the trapping of oxocarbenium **372** by hydrogen peroxide. The authors found that this hydroperoxide is able to rearrange with and without the presence of a mineral acid. No yield was given for these transformations (Figure 3.6).[14]

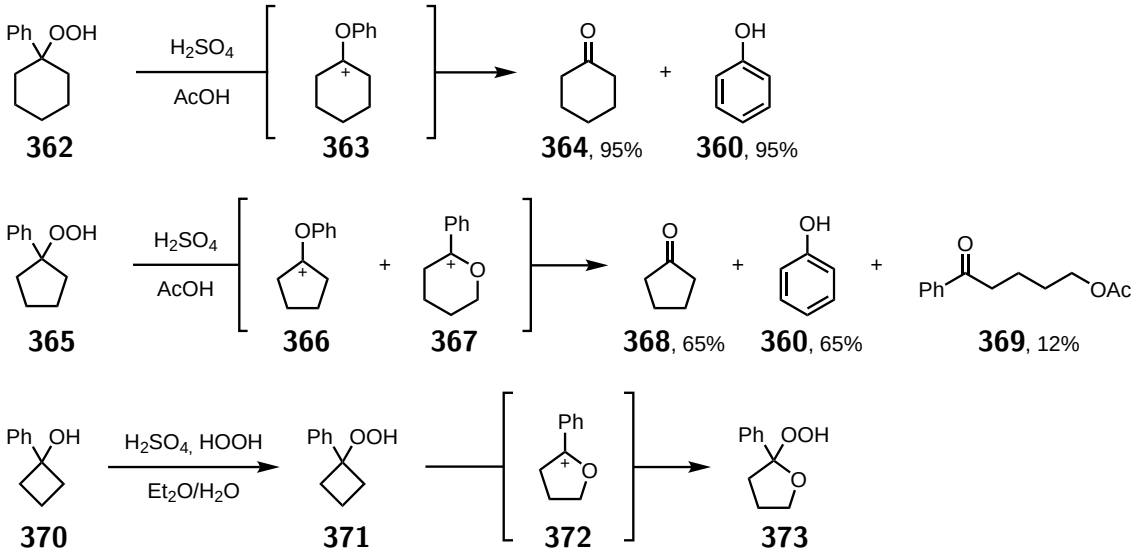

Figure 3.6: Selectivity during the Hock rearrangement depending of the size of the cyclic substrate.

3.1.3 *Criegee rearrangement*

The Criegee rearrangement, first reported in 1944, is a reaction that transforms a perester (**374**) into an alcohol (**354**), a ketone (**343**) and generates a carboxylic acid (**375**) as a byproduct (Figure 3.7).[15] The mechanism is similar to that of the Hock rearrangement, but the migration occurs thanks to the activation of the O-O bond by the ester function.

[14] G. H. Anderson, J. G. Smith, *Can. J. Chem.* **1968**, *46*, 1561-1570.

[15] (a) R. Criegee, Ber.,1944,77, 722-726. (b) Z. Wang, *Comprehensive Organic Name Reactions and Reagents*, John Wiley & Sons, New York, NY, USA, **2010**, p. 770-774.

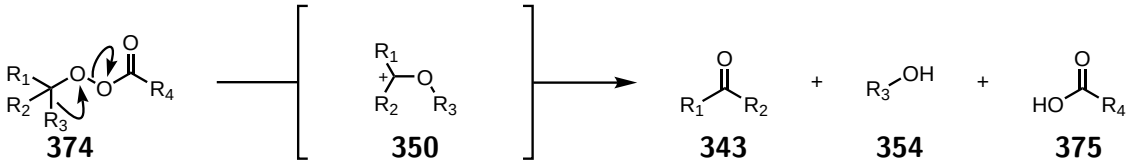

Figure 3.7: Criegee rearrangement.

In 1994, Kishi and Goodman reported a method to synthesize acetals starting from hydroperoxides using the Criegee rearrangement.[16] They found that mixing hydroperoxides with a slight excess of trifluoroacetic anhydride in deuterated chloroform at 0 °C led to the *in-situ* formation of peresters that rearrange spontaneously to trifluoroacetyl acetals with no observed traces of ketones or alcohols. They applied this method to different types of hydroperoxides; cyclic **376**, bicyclic **377** and linear **377**. They did not isolated these compounds but recorded NMR of the crude mixture seeing only cleaned rearranged acetals.

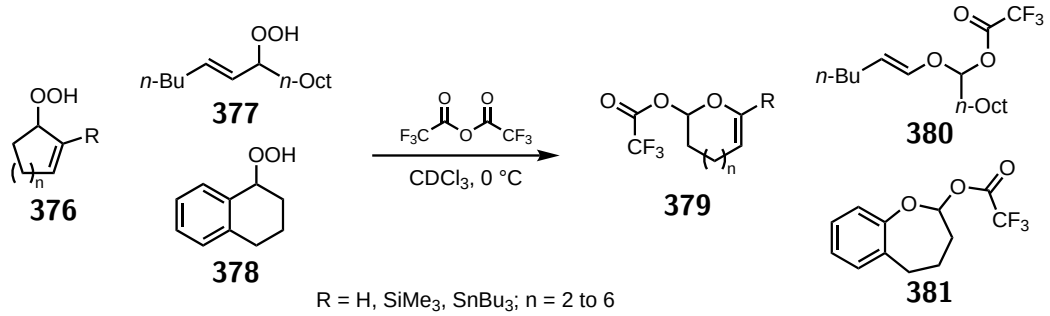

Figure 3.8: Acetal synthesis using Criegee rearrangement.

3.1.4 *Goal of this study: interrupted peroxide rearrangements*

These two rearrangements could lead to valuable cyclic and acyclic ethers **382** if a method is found to trap *in-situ* oxocarbenium ion **350** and **351** by a nucleophile, especially before the hydrolysis occurs (Figure 3.9). This method might facilitate access to natural products such as (+)-neoisoprelaurefucin **383**,[17] or valuable pharmaceutical compounds such as

[16] R. M. Goodman, Y. Kishi, *J. Org. Chem.* **1994**, *59*, 5125-5127.
[17] M. Suzuki, Y. Mizuno, Y. Matsuo, M. Masuda, *Phytochemistry*, **1996**, *43*, 121-124.

sarizotan.[18]

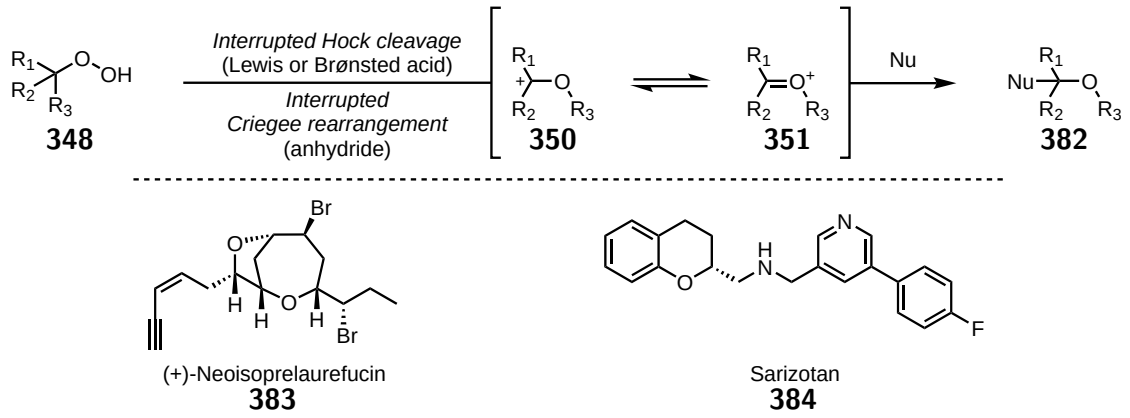

Figure 3.9: Interrupted peroxide rearrangements and molecules of interests.

[18](a) E. V. Kuzhikandathil, G. D. Bartoszyk, *Neuropharmacology*, **2006**, *51*, 873-884. (b) A. P. Abdala, D. T. Lioy, S. K. Garg, S. J. Knopp, J. F. Paton, J. M. Bissonnette, *Am. J. Respir. Cell. Mol. Biol.* **2014**, *50*, 1031-1039. (c) `https://clinicaltrials.gov/ct2/show/NCT02790034`.

3.2 Tandem Schenck-ene/Hock cleavage reaction

3.2.1 *Schenck-ene reaction*

First reported in 1943, the Schenck-ene reaction forms allylic hydroperoxides from singlet oxygen, the first excited state of oxygen, and alkenes.[19] Singlet oxygen can be generated from a photocatalytic process. A photosensitiser ^{1}S, in its ground state, is irradiated with light generating the singlet excited state ^{1}S*. After intersystem crossing, the triplet excited state ^{3}S* is formed and can undergo an energy transfer with triplet oxygen to form reactive singlet oxygen (Figure 3.10, left). The singlet oxygen is then able to react with an alkene through a two-step mechanism without intermediate.[20] During the first transition state **386**, no selectivity is made for the hydrogen abstraction. This species evolves to a second transition state **387** which can lead to different products **388** and **389** if the alkene is not C_s-symmetric (Figure 3.10, right).

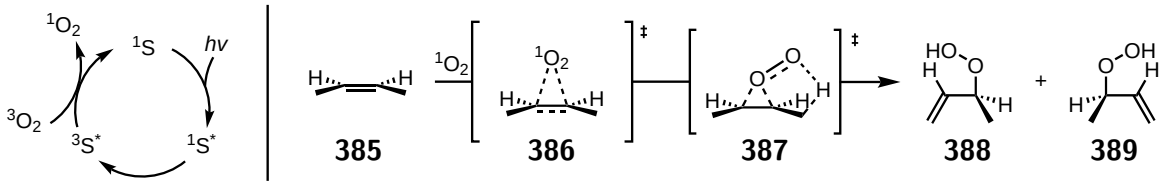

Figure 3.10: right, Generation of singlet oxygen through photochemistry; left, Schenck-ene mechanism.

The regioselectivity for the hydrogen abstraction is controlled by different factors (Figure 3.11).[21]

- the *cis*-effect,[22] when the hydrogen on the most crowed side of the alkene is preferred for abstraction.

- the *gem*-effect,[23] when the hydrogen on the geminal position is favoured for abstrac-

[19] G. O. Schenck. DE-B 933925, **1943**.
[20] D. A. Singleton, C. Hang, M. J. Szymanski, M. P. Meyer, A. G. Leach, K. T. Kuwata, J. S. Chen, A. Greer, C. S. Foote, K. N. Houk, *J. Am. Chem. Soc.* **2003**, *125*, 1319-1328.
[21] M. Prein, W. Adam, *Angew. Chem. Int. Ed. Engl.* **1996**, *35*, 477-494.
[22] M. Orfanopoulos, M. J. Grdina, L. M. Stephenson, *J. Am. Chem. Soc.* **1979**, *101*, 275-276.
[23] M. Orfanopoulos, C. S. Foote, *Tetrahedron Lett.* **1985**, *26*, 5991-5994.

tion.

- the large group nonbonding effect,[24] the least predictable rule.

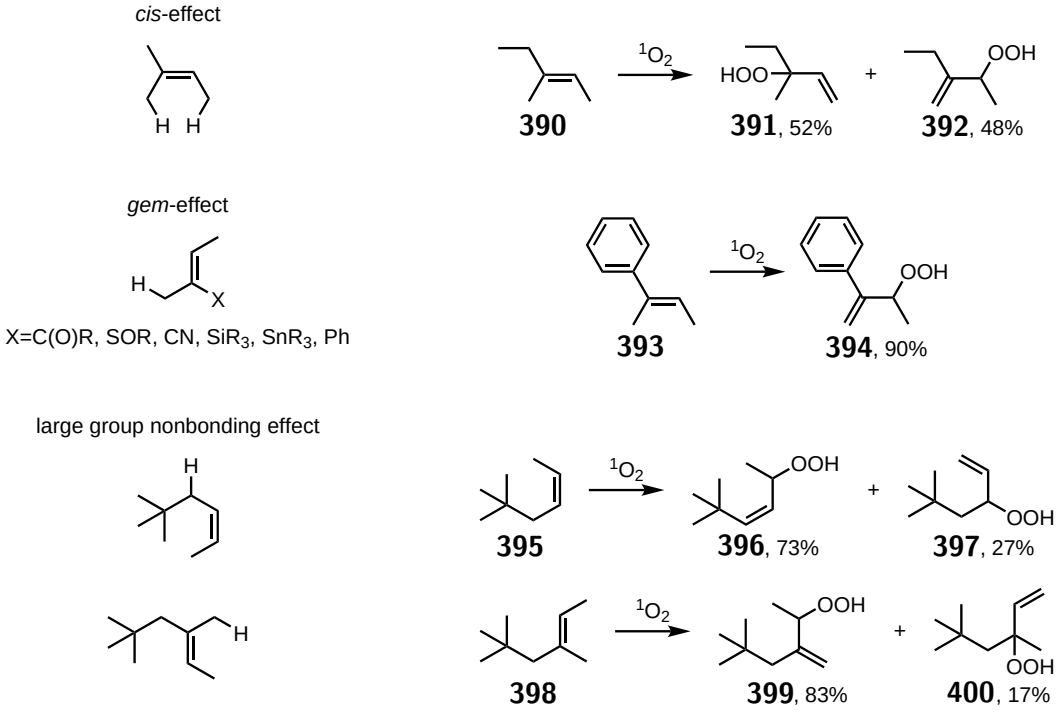

Figure 3.11: Regioselectivity in the Schenck-ene reaction, H shown are the most abstracted proton.

3.2.2 *Choice and reactivity of first generation of substrates*

A first generation of substrates was composed of two parts: a platform for the Schenk-ene/Hock cleavage reaction, the isoprenyl fragment, and an internal nucleophile, the aromatic ring, linked by an oxygen atom in order to perform a Friedel-Crafts reaction. Starting ether **403** was synthesised by heating 3-methoxyphenol **401**, prenyl bromide **402** and potassium carbonate in DMF at 60 °C (Figure 3.12).[25]

[24] (a) M. Orfanopoulos, M. Stratakis, Y. Elemes, *Tetrahedron Lett.* **1989**, *30*, 4875-4878. (b) M. Orfanopoulos, M. Stratakis, Y. Elemes, *J. Am. Chem. Soc.* **1990**, *112*, 6417-6419.
[25] M. Klaper, W. Fudickar, T. Linker, *J. Am. Chem. Soc.*, **2016**, *138*, 7024-7029.

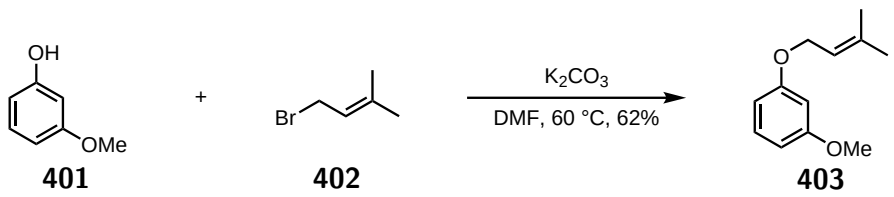

Figure 3.12: Synthesis of starting material **403**.

The use of oxygen combined with tetraphenylporphyrin, TPP, under white LED light allowed a smooth formation of two allylic hydroperoxides **404** and **405** from starting ether **403**. These hydroperoxides were then subjected to different acids to generate *in-situ* oxocarbenium ions **406** and **407**. Only oxocarbenium ion **407** might be able to allow the formation of desired ether **408** (Figure 3.13).

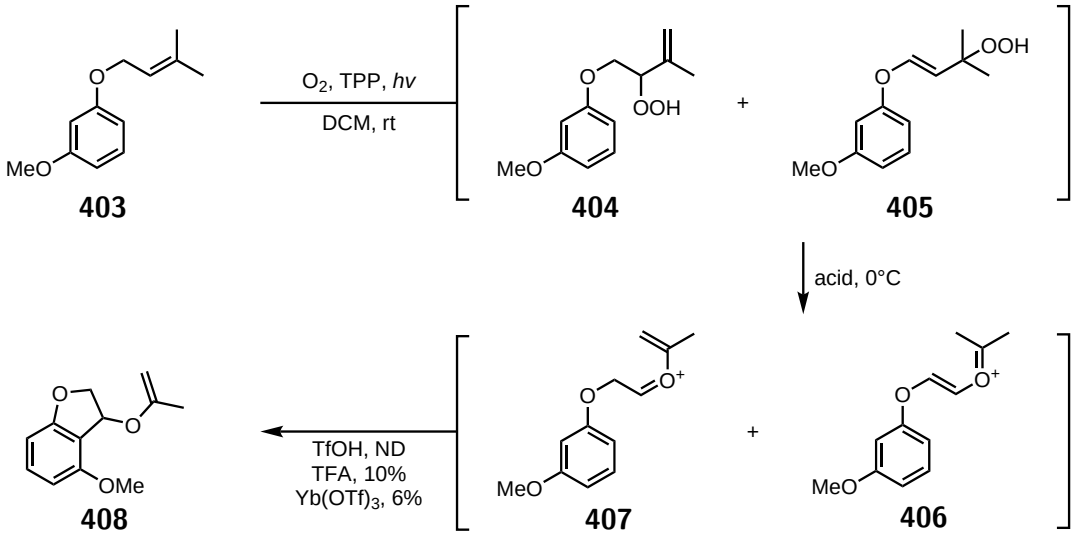

Figure 3.13: First generation of substrate for the Schenck-ene/Hock cleavage reaction tandem.

Unfortunately, the yield of the reaction was low, with less than 10% of product **408**, and many different products were formed during the reaction. Running the reaction at lower temperature, -78 °C, did not afford any traces of desired product **408**. Benzofuran NMR signals were observed in the crude mixture. This might be due to a complete Hock cleavage reaction generating aldehyde **409**, which can react through a Friedel-Crafts reaction leading

to benzotetrahydrofuran **410**. This can generated benzofuran **411** through dehydration. Alternatively, a possible elimination of the isopropenyl ether fragment of compound **408** could produce benzofuran **411** (Figure 3.14).

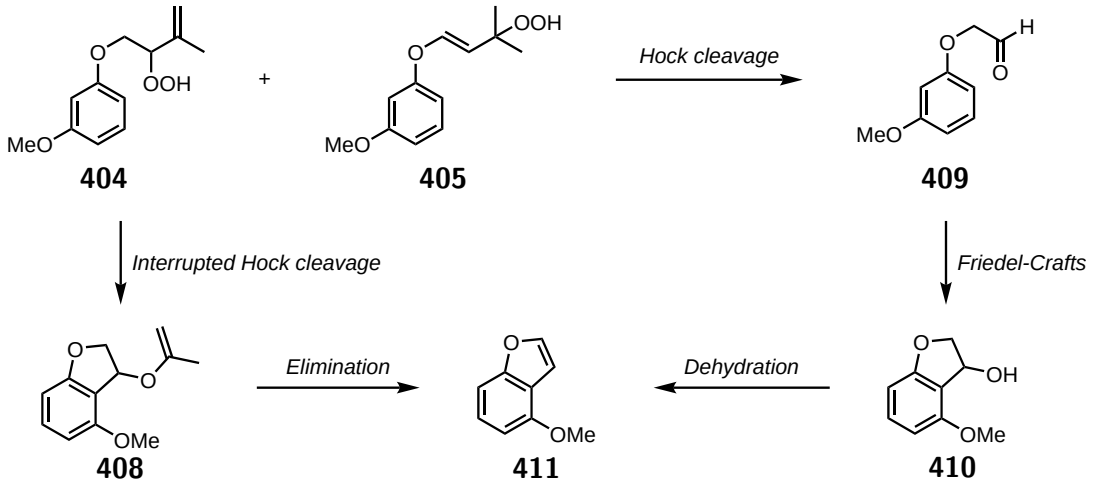

Figure 3.14: Two possible pathway to benzofuran **411**.

In conclusion, the isolation of benzotetrahydrofuran **408**, despite its a low yield, constituted a promising result validating the feasibility of interrupted Hock cleavage.

3.2.3 *Second generation of substrates*

This new generation of substrates was developed using the same type of intramolecular activation, with a nucleophile and electrophile fragment, both linked by a diethyl malonate part. Starting ether **413** was synthesised by mixing at room temperature diethyl benzylmalonate **412**, prenyl bromide **402** and sodium hydride in THF (Figure 3.15).[26]

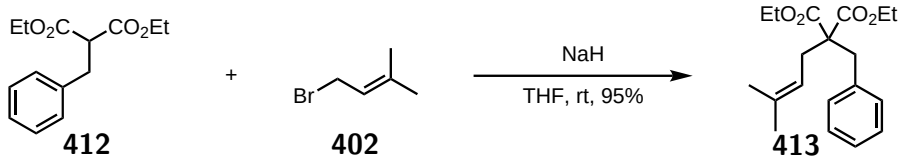

Figure 3.15: Synthesis of starting material **413**.

[26] B. Cacciuttolo, S. Poulain-Martini, E. Dunach, *Eur. J. Org. Chem.*, **2011**, *20-21*, 3710-3714.

Using the same set of conditions, TFA or $BF_3.Et_2O$ as acids, used for the previous substrate did not afford any trace of the product. TPP was replaced by methylene blue **415**, MB, only for the ease of purification. To overcome the problem of a complete Hock cleavage reaction that could lead to the aldehyde product, additives such as 4Å molecular sieves (MS), Na_2SO_4 or $MgSO_4$ were evaluated to trap water. A clean reaction was observed with $MgSO_4$ leading to bicyclic product **414** with a good yield of 83%. A control reaction involving $MgSO_4$ only, without $BF_3.Et_2O$, did not allow the formation of desired product **414** (Figure 3.16).

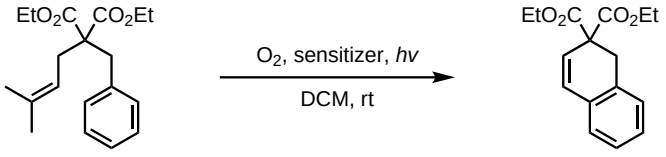

413 **414**

sensitizer	acid (eq)	additive (eq)	yield (%)
TPP	TFA (1) or $BF_3.Et_2O$ (1)	-	-
MB	$BF_3.Et_2O$ (1)	4A MS or Na_2SO_4 (2)	-
MB	$BF_3.Et_2O$ (1)	$MgSO_4$ (2)	83
MB	-	$MgSO_4$ (2)	-

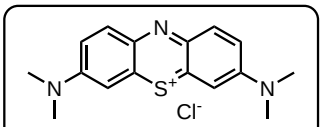

Methylene Blue (MB) **415**

Figure 3.16: Second generation of substrate for the Schenck-ene/Hock cleavage reaction tandem.

In this reaction, hydroperoxides **416** and **417** were formed in a 1:2 ratio which might lead to the same ratio of oxocarbenium **418**/**419**. Based on this hyptothesis, the maximum yield of bicyclic product **414** should be 33% in case of interrupted Hock cleavage. As a higher yield was obtained, an equilibrium though a [1,5]-sigmatropic hydrogen shift rearrangement between oxocarbenium **418** and **419** was hypothesized, with the hope of performing an efficient interruption of the Hock cleavage by the Friedel-Crafts reaction (Figure 3.17). Thus, compound **414** would be formed after an interrupted Hock cleavage, a Friedel-Crafts reaction and an elimination of the isopropenyl ether fragment. Alternatively,

a complete Hock cleavage might also occur as seen previously (Figure 3.14).

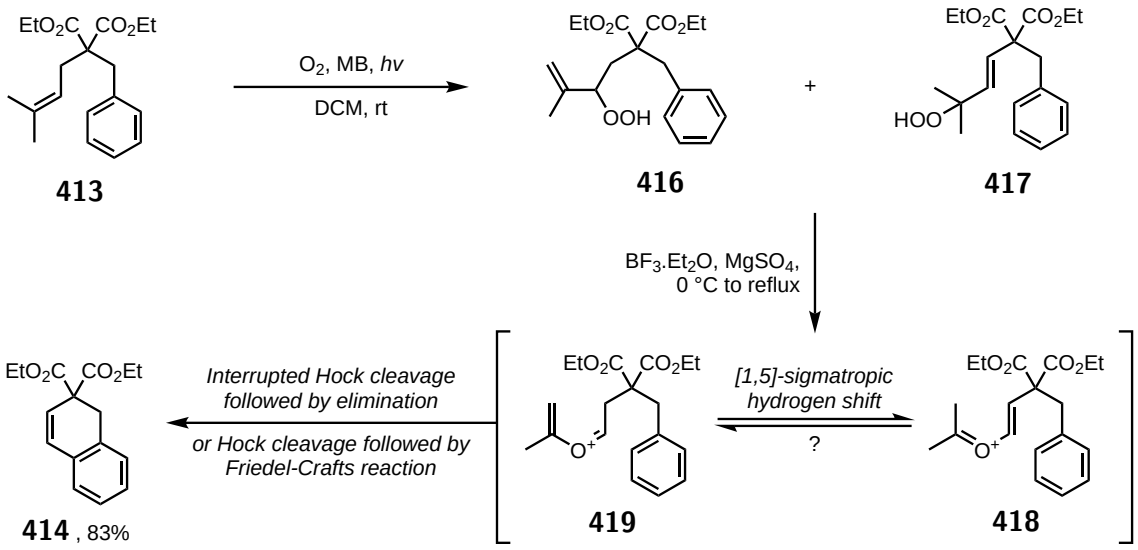

Figure 3.17: Possible pathways for the formation of bicyclic product **414**.

To determine the pathway of this reaction, an external nucleophile, 1,3,5-trimethoxybenzene **420**, was used to trap oxocarbenium species **418** and **419**. New bicyclic product **421** was formed in good yield, 86% (Figure 3.18).

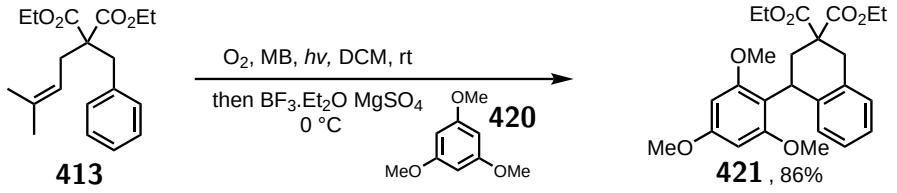

Figure 3.18: Tentative of trapping oxocarbenium species **418** and **419**.

This product could come from the interrupted Hock cleavage by elimination of the isopropenyl ether fragment of compound **423**. This might lead to oxocarbenium **424** which would react in an intramolecular way to form bicyclic product **421**. Alternatively, it could come from the Hock cleavage/Friedel-Crafts reaction sequence through aldehyde **425**. Aldehyde **425** was isolated and seen on TLC, while linear product **422**, or any hydrolyzed products, was never isolated. These observations are in good agreement with a Hock cleavage

leading to aldehyde **425** and followed by a double Friedel-Crafts sequence (Figure 3.19).

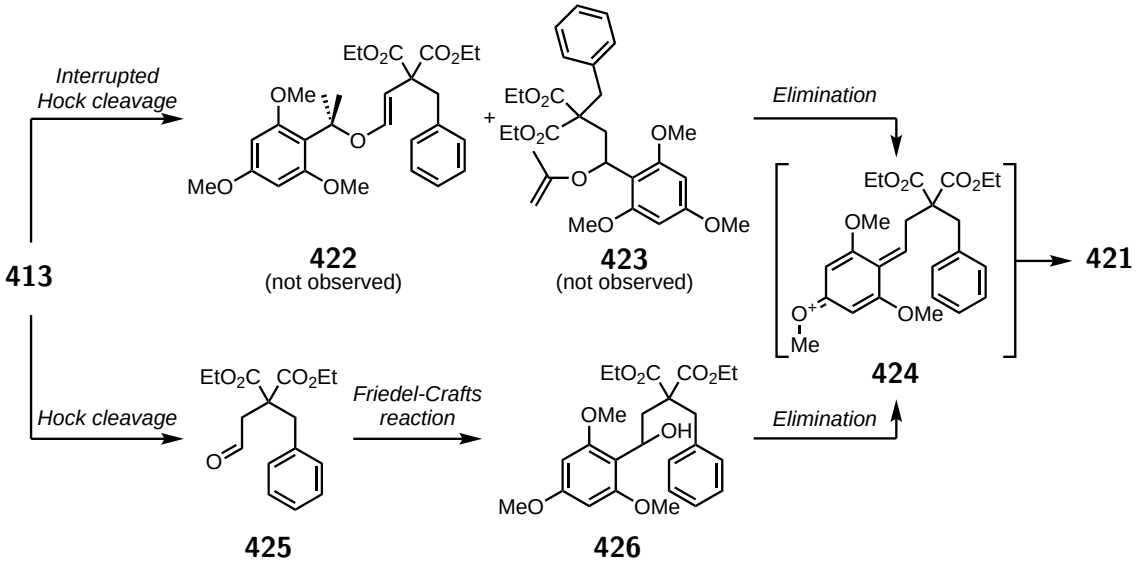

Figure 3.19: Tandem Schenck-ene/Hock cleavage/double Friedel-Crafts reaction.

This pathway was confirmed by the modelling of the previously hypothesized [1,5]-sigmatropic hydrogen shift rearrangement between oxocarbenium species **418** and **419** using M06/6-31G(d,p) level of theory.[27] Cyclic transition state **427** found for the [1,5]-sigmatropic hydrogen shift rearrangement appeared to have a too high difference of enthalpy and Gibbs free energies with both oxocarbenium species to be plausible during the reaction (Figure 3.20).

[27] V. Srinivasadesikan, J.-K. Daib, S.-L. Lee, *Org. Biomol. Chem.* **2014**, *12*, 4163-4171.

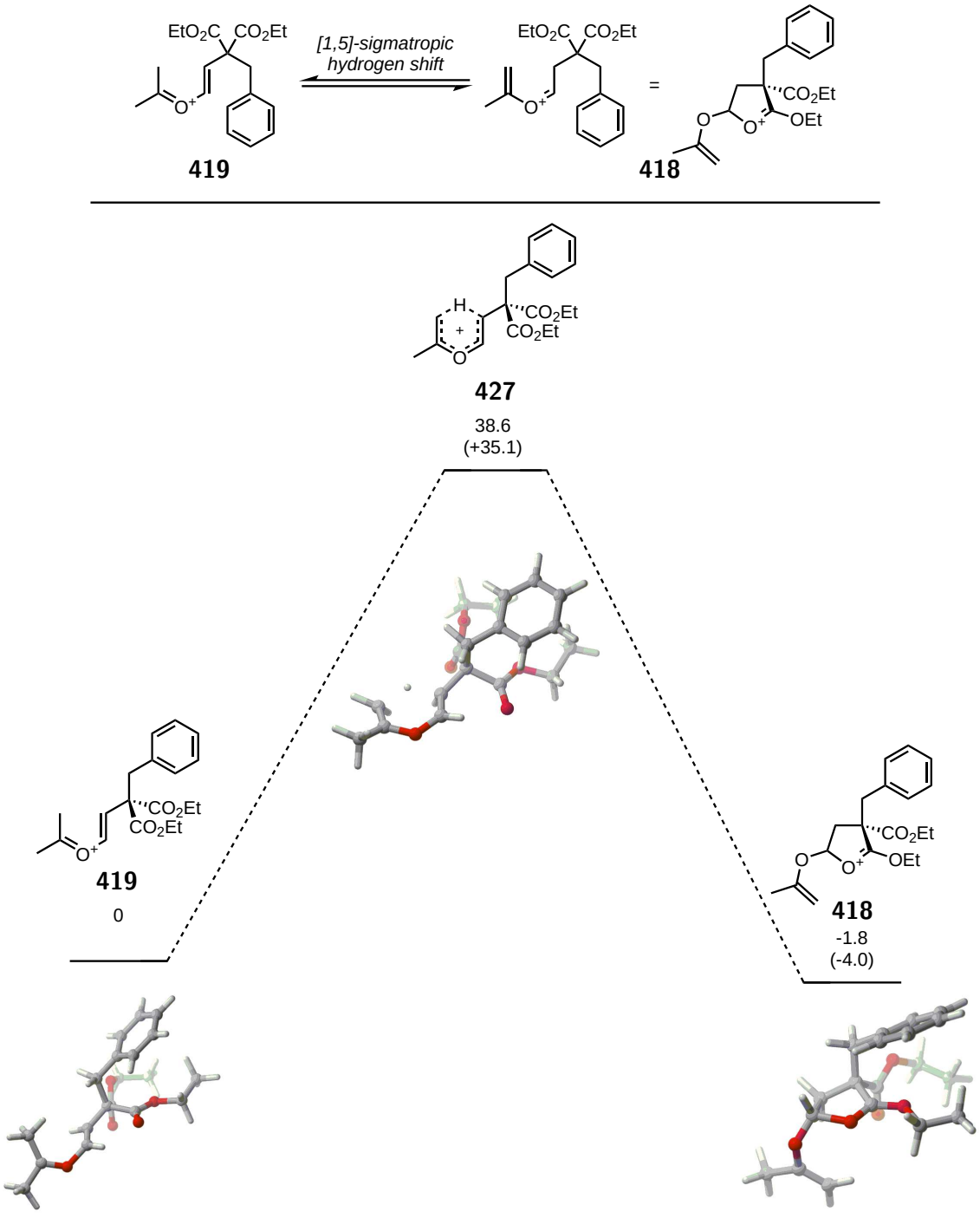

Figure 3.20: Computed enthalpies and Gibbs free energies, in parentheses, for the [1,5]-sigmatropic hydrogen shift rearrangement between oxocarbenium species **418** and **419**. Energies relative to the starting materials are given in kcal.mol^{-1}.

This method leads to the carbocyclic core of lignan natural products (Figure 3.21), such as cagayanin **428**,[28] (-)-podophyllotoxin **429**,[29] or sacidumlignan A **430**.[30] Some of them are important drug compounds, such as podophyllotoxin **429** which is used in dermatology, or its derivative etoposide which is an anticancer medicine.[31]

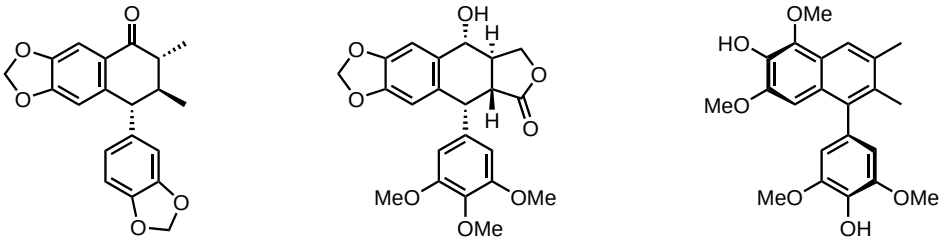

Figure 3.21: Example of lignan natural products.

Thus this strategy, involving a Hock cleavage associated to a double Friedel-Crafts reaction, might be useful to gain quick access to certain lignan natural products or medicinally relevant analogues; the method is currently investigated in the laboratory.

[28] Y.-H. Kuo, R.-E. Wu, *J. Chin. Chem. Soc.* **1985**, *32*, 177-178.
[29] V. Podwyssotzki, *Arch. Exp. Pathol. Pharmakol.* **1880**, *13*, 28.
[30] L.-S. Gan, S.-P. Yang, C.-Q. Fan, J.-M. Yue, *J. Nat. Prod.* **2005**, *68*, 221-225.
[31] (a) M. Gordaliza, P. A. Garcia, J. M. Miguel del Corral, M. A. Castro, M. A. Gómez-Zurita, *Toxicon*, **2004**, *44*, 441-459. (b) C. Canela, R. M. Moraes, F. E. Dayan, D. Ferreira, *Phytochemistry*, **2000**, *54*, 115-120.

3.3 Interrupted Hock rearrangements

3.3.1 *Introduction*

A new generation of substrates using hydroperoxide or peroxide **431** as starting materials was finally evaluated to generate cyclic ether **432** (Figure 3.22, top). These benzocycloether compounds are widely represented in the natural product world (Figure 3.22, bottom); such as psiguadial A **433**,[32] α-tocopherol **434** a member of the vitamin E family,[33], heliannuol A **435**,[34] or radulanine A **24**.[12]

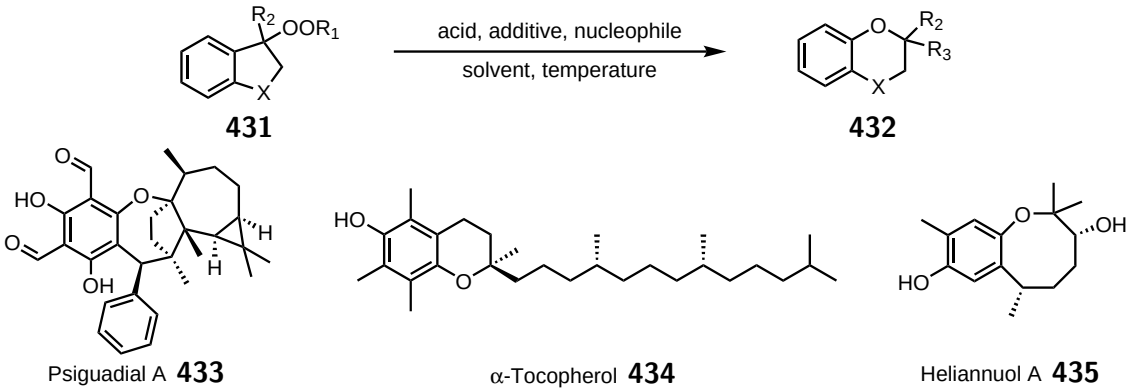

Figure 3.22: top, Envisaged method to synthesize cyclic ethers **432** from peroxides **431** using interrupted Hock cleavage; bottom, Natural products containing cyclic ether.

3.3.2 *Methodology*

Promising results using 1-indanyl hydroperoxide 437

1-Indanyl hydroperoxide **437** was synthesised by mixing indanol **436**, a solution of hydrogen peroxide in water and a catalytic amount of sulfuric acid in a diethyl ether (Figure 3.23).[35]

[32] M. Shao, Y. Wang, Z. Liu, D.-M. Zhang, H.-H. Cao, R.-W. Jiang, C.-L. Fan, X.-Q. Zhang, H.-R. Chen, X.-S. Yao, W.-C. Ye, *Org. Lett.* **2010**, *12*, 5040-5043.
[33] H. M. Evans, O. H. Emerson and G. A. Emerson, *J. Biol. Chem.* **1936**, *113*, 319-332.
[34] F. A. Macías, R. M. Varela, A. Torres, J. M. G. Molinillo, F. R. Fronczek, *Tetrahedron Lett.* **1993**, *34*, 1999-2002.
[35] L. Hamann, *Synlett*, **2001**, *1*, 96-98.

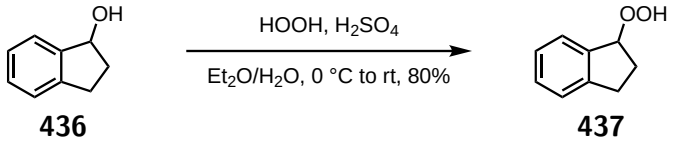

Figure 3.23: Synthesis of starting material **437**.

A first approach for the interrupted Hock cleavage was evaluated starting from hydroperoxide **437** and using allyltrimethylsilane as a nucleophile. Different Lewis and Brønsted acids were then tested for the interrupted Hock cleavage. Metals, Yb^{III}, Sn^{II}, Cu^{II}, Ag^{I}, Y^{III} and Sc^{III}, bearing a perchlorate, triflate or fluorate counter-anion did not furnish any desired product, except for $Sc(OTf)_3$ which allowed the formation of cycloether **438** with a low yield of 14%. With the idea of developing a chiral version of the reaction, diphenyl phosphoric acid was also evaluated, as a model for the reactivity of chiral phosphoric acids. Sadly no conversion was observed even after stirring the reaction at reflux for several days. Interestingly, In^{III} Lewis acids were the most effective catalysts for this transformation. $InCl_3$ and InI_3 were able to deliver cycloether **438** with a NMR yield of 40% (Figure 3.24). This might be explain by the softer acidic character of In^{III} compared to the other Lewis acids evaluated. Other soft Lewis acids, such as $FeCl_3$ or CuCl, have been assessed by Dr. Alexandra Bosnidou, a postdoctoral researcher of the group, without any formation of cyclic ether **438**. $InCl_3$ was picked for the rest of the optimisation due to its lower cost compared to InI_3, 0.47,[36] versus 6.57,[37] euros per mmol.

[36] http://www.fluorochem.co.uk/Products/Search?searchType=C&searchText=10025-82-8
[37] https://www.alfa.com/en/search/?q=+13510-35-5+

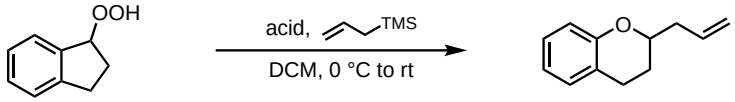

437 **438**

acid (eq) NMR Yield %				
$TMSOTf$ (2) -	TFA (2) -	$Yb(OTf)_3$ (0.1) -	$Sn(OTf)_2$ (0.1) -	$BF_3.Et_2O$ (0.1) traces
$Cu(ClO_4)_2$ (0.1) traces	$AgOTf$ (0.1) -	$Y(OTf)_3$ (0.1) -	$Sc(OTf)_3$ (0.1) 14	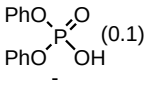 (0.1) -
$InCl_3$ (0.1) 40	$InBr_3$ (0.1) 22	InI_3 (0.1) 40	InF_3 (0.1) -	$In(OTf)_3$ (0.1) -

Figure 3.24: Screening of Lewis and Brønsted acids for the interrupted Hock cleavage (0.1 mmol of **437**, 0.2 mmol of allyltrimethylsilane at 0.1 M in DCM using DCE as internal standard).

Different solvents were evaluated for this transformation. Ethyl acetate, DCE, chloroform and acetonitrile did not allow the formation of desired product **438**. In the case of toluene and HFIP, some product **438** was formed but the yield, 30% and 35% respectively, was lower than the one previously obtained with DCM, 40%. The best conditions for hydroperoxide **437** were found by heating the reaction mixture to reflux after the addition of $InCl_3$. Under these conditions, ether **438** was formed with a yield of 53% (Figure 3.25).

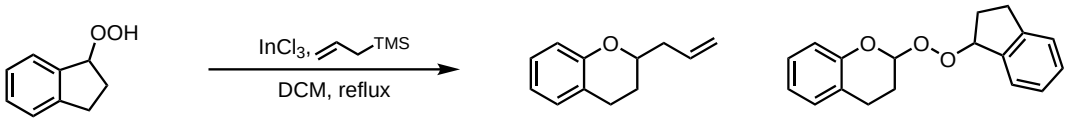

437 **438**, 53% **439**

Figure 3.25: Optimized conditions for the Hock cleavage reaction with hydroperoxide **437**

The yield of the interrupted Hock cleavage was however unsatisfactory. This might be due to a competition of both nucleophilic allyltrimethylsilane and hydroperoxide **437** leading to peroxide **439** which might degrade under acidic condition.

Tert-butyl peroxides: a method to promote the slow release of hydroperoxides

To prevent this competing reaction, the substrate can be modified by switching the hydroperoxide for a *tert*-butyl peroxide fragment, which will slowly decompose to a hydroperoxide in presence of Lewis acid, releasing isobutylene **442**.[38] Peroxide **440** was synthesized by mixing indanol **436**, a 5.0-6.0 M solution of *tert*-butyl hydroperoxide in decane and a catalytic amount of *p*-toluenesulfonic acid in DCM at rt.[39] Peroxide **440** was subjected to the best conditions previously found, except for the temperature to have a better control on the release of hydroperoxide complex **443** (Figure 3.26). The NMR yield was slightly better than the one obtained with hydroperoxide **437** and the same set of conditions at room temperature, 45% versus 40%.

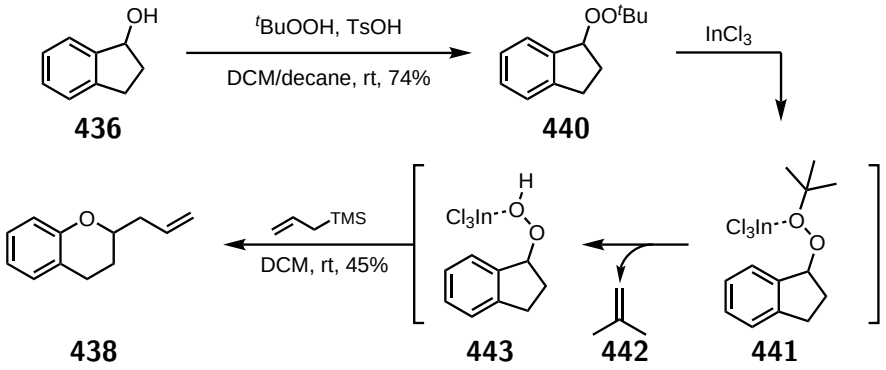

Figure 3.26: Interrupted Hock cleavage with a possible slow release of hydroperoxide **437**.

Another problem might arise from the nature of the oxocarbenium ion impacting its stability. Using hydroperoxide **437**, a secondary cation is generated, which is not the most stable ion possible. One solution might be to introduce a new substituent on the carbon bearing the hydroperoxide. One solution might be to introduce a new substituent on the carbon bearing the hydroperoxide.

[38] M. B. Chaudhari, A. Chaudhary, V. Kumar, B. Gnanaprakasam, *Org. Lett.* **2019**, *21*, 1617-1621.
[39] M. Bietti, O. Lanzalunga, M. Salamone, Michela, *J. Org. Chem.* **2005**, *70*, 1417-1422.

Tertiary cation: key to higher yield

1-Methyl-1-indanol **445** was synthesized by adding methylmagnesium iodide onto indanone **444** in diethyl ether at 0 °C.[40] Tertiary peroxide **446** was synthesized by mixing 1-methyl-1-indanol **445**, a 5.0-6.0 M solution of *tert*-butyl hydroperoxide in decane and a catalytic amount of *p*-toluenesulfonic acid in DCM at rt.[38] The yield was low, probably due to a too long reaction time which might favour degradation of the peroxide. This reaction was only tried once and further optimisations are currently investigated. Tertiary peroxide **446** was subjected to the same conditions used as for compound **440** and desired cycloether **448** was formed with a good yield of 80% (Figure 3.27). Interestingly this chromane system is found in α-tocopherol **434**.

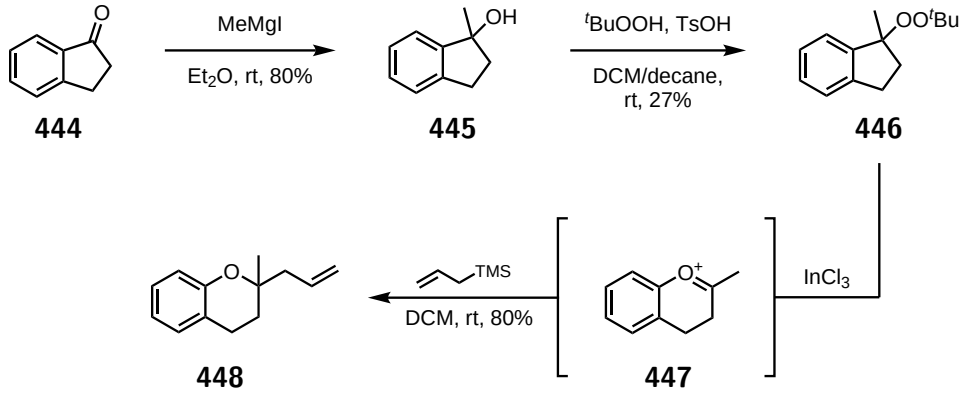

Figure 3.27: Interrupted Hock cleavage with more stable oxocarbenium ion **447**.

Scope and limitations

Different nucleophiles were evaluated with this promising peroxide **446**. Unfortunately, trimethylsilyl cyanide **450** and silyl enol ether derivative **451** did not allow the formation of desired products **453** and **454**. A possible explanation for the silyl enol ether might be due to steric hindrance. Other silyl enol ethers will have to be tested. In the case of product

[40] D. Özdemirhan, *Synth. Commun.*, **2017**, *47*, 629-645.

455, the yield was low, 30%, but this is due to the low quality of the nucleophile used. This reaction should be reproduced and the use of homemade 2-bromoallyltrimethylsilane **452** might significantly increase the yield of the reaction (Figure 3.28).

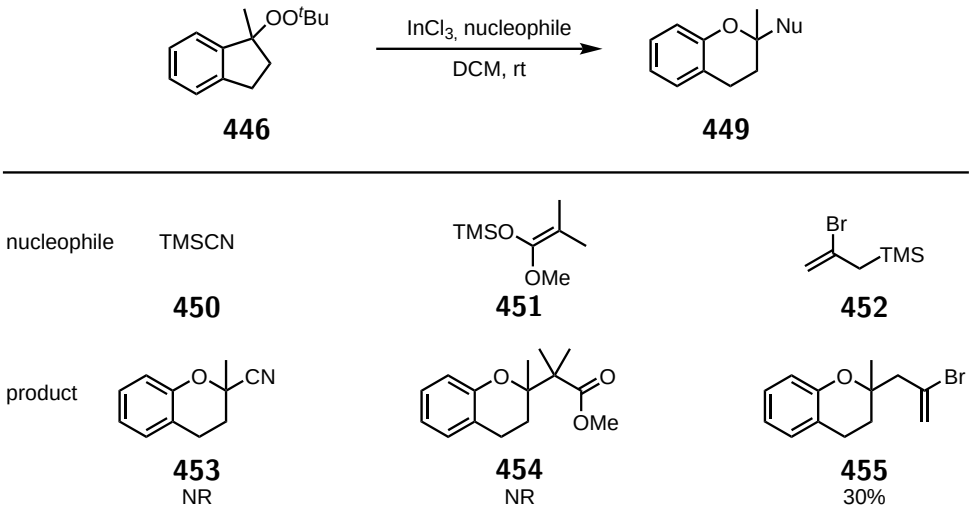

Figure 3.28: Scope of the interrupted Hock cleavage.

The conditions required for the interrupted Hock cleavage have been developed, the scope and limitations of this new transformation must now be found. This is currently investigated.

3.4 Approach to the total synthesis of isolaurepan **456**

3.4.1 *Introduction*

(+)-Isolaurepan **456** is a molecule resulting from the complete hydrogenation of the natural product (+)-isolaurepinnacin **457** isolated in 1981 from the marine red algae genus *Laurencia* (Figure 3.29).[41] Several formal and total syntheses of isolaurepan have been reported.[42]

(+)-Isolaurepan **456** (+)-Isolaurepinnacin **457**

Figure 3.29: (+)-Isolaurepan **456** and (+)-isolaurepinnacin **457**.

The shortest total synthesis of (+)-isolaurepan **456** was made in only four steps.[43] Padrón and co-workers began by opening epoxide **459**, which can be obtained from commercialy available 1-octene **458**,[44] with allyl magnesium bromide combined with CuI in THF at -40 °C, to generate alcohol **460** in excellent yield of 90%. This alcohol can be subjected to the method they developed in the publication, an intramolecular Prins reaction using $Fe(acac)_3$ and butyraldehyde in DCM at rt to generate *in-situ* oxocarbenium **461**, which can be cyclized to allow the formation of seven membered ring **462** with an excellent yield, 95%. Finally, a radical dehalogenation using tributyltin hydride and AIBN in toluene at reflux delivered (+)-isolaurepan **456** in a very good yield of 90% (Figure 3.30).

[41] A. Fukuzawa, T. Masamune, *Tetrahedron Lett.* **1981**, *41*, 4081-4084.
[42] (a) H. Kotsuki, Y. Ushio, I. Kadota, M. Ochi, *J. Org. Chem.* **1989**, *54*, 5153-5161. (b) R. W. Carling, J. S. Clark, A. B. Holmes, *J. Chem. Soc., Perkin Trans. 1*, **1992**, 83-94. (c) D. Berger, L. E. Overman, P. A. Renhowe, *J. Am. Chem. Soc.* **1997**, *119*, 2446-2452. (d) M. C. Carreño, R. Des Mazery, A. Urbano, F. Colobert, G. Solladié, *Org. Lett.* **2004**, *6*, 297-299. (e) D. Tripathi, P. Kumar, *Tetrahedron Lett.* **2008**, 49, 7012-7014. (f) G. Pazos, M. Pérez, Z. Gándara, G. Gómez, Y. Fall, *Tetrahedron Lett.* **2009**, 50, 5285-5287. (g) M. Ebine, Y. Suga, H. Fuwa, M. Sasaki, *Org. Biomol. Chem.* **2010**, *8*, 39-42. (h) G. Pazos, M. Pérez, Z. Gándara, G. Gómez, Y. Fall, *Tetrahedron Lett.* **2012**, 68, 8994-9003.
[43] M. A. Purino, M. A. Ramírez, A. H. Daranas, V. S. Martín, J. I. Padrón, *Org. Lett.* **2012**, *14*, 5904-5907.
[44] M. Lansing, H. Engler, T. M. Leuther, J.-M. Neudörfl, A. Berkessel, *ChemCatChem*, **2016**, *8*, 3706-3709.

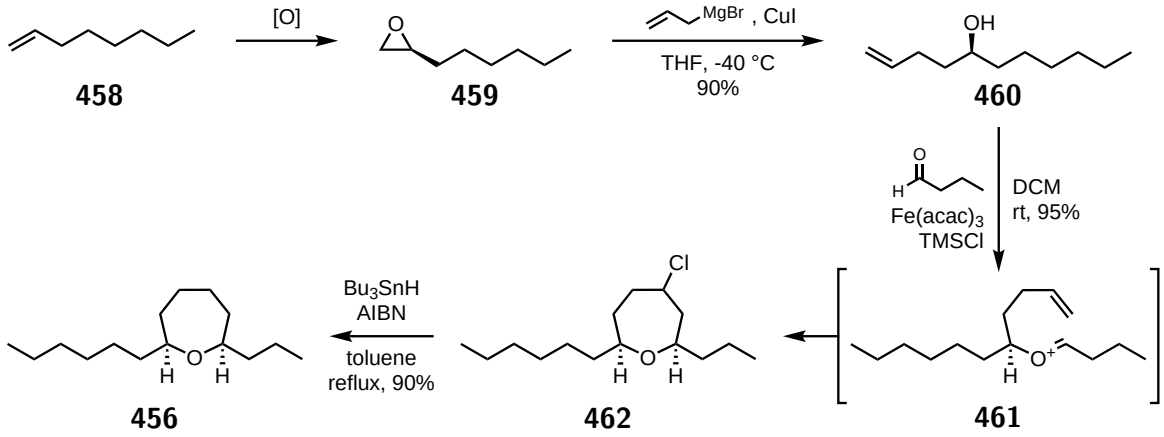

Figure 3.30: Padrón's group total synthesis of (+)-isolaurepan **456**.

In the following part, we will describe an approach based on the interrupted rearrangement of peroxides to develop a short total synthesis of (+)-isolaurepan **456** and other related natural products.

3.4.2 *Approach to the total synthesis of (+)-isolaurepan* **456**

Retrosynthesis

(+)-Isolaurepan **456** might arise from the complete reduction of tetrahydrooxepine **463**. This cyclic ether might be generated using a chiral version of an interrupted Hock or Criegee rearrangement using hydroperoxide **464** and allyltrimethylsilane. Key hydroperoxide **464** might be obtained through a reduction-substitution sequence from substituted cyclohexenone **465**. The *n*-hexyl chain might be introduced by Negishi coupling from a partner derived of the cyclohexenone **364** (Figure 3.31). This strategy might be modified using different coupling partners during the Negishi coupling and different nucleophiles during the interrupted peroxide rearrangement to access multiple oxepane natural products. Starting from cyclopentenone or cycloheptenone, tetrahydropyran or oxocane natural products might be generated using this approach.

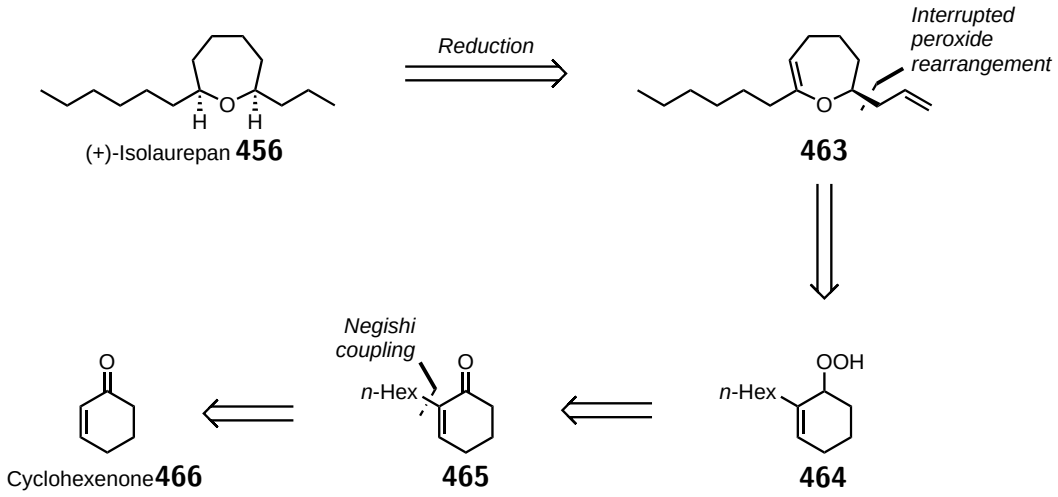

Figure 3.31: Retrosynthesis of (+)-isolaurepan **456**.

Approach to key hydroperoxide 464

The α-iodination of cyclic enones was already described in the literature.[45] Using the reported conditions, a scalable and reproducible reaction allowed the formation of coupling partner **467** from commercially available cyclohexenone **466**. The cross coupling reaction was inspired from a reported Negishi coupling between α-iodoenones and alkylzinc derivatives.[46] The desired hexylzinc bromide was generated *in-situ* using hexylmagnesium bromide and $ZnBr_2$. It was then allowed to react with α-iodocyclohexenone **467** in DMF to form desired coupling product **465** in a moderate yield of 44% (Figure 3.32).

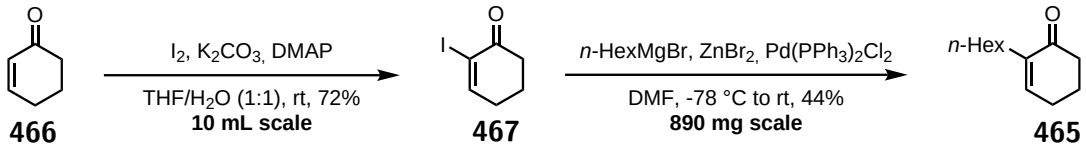

Figure 3.32: Fist steps of the (+)-isolaurepan **456** total synthesis.

Selective reduction of the carbonyl function of enone **465** under Luche conditions us-

[45] M. E. Krafft, J. W. Cran, *Synlett* **2005**, *8*, 1263-1266.
[46] E.-I. Negishi, Z. Tan, S.-Y. Liou, B. Liao, *Tetrahedron*, **2000**, *56*, 10197-10207.

ing $CeCl_3$ and sodium borohydride in methanol allowed the formation of alcohol **468**.[47] At this stage of the synthesis, a model substrate was used to develop the oxidation to the hydroperoxide and the interrupted peroxide rearrangement to build the oxepane core (Figure 3.33).

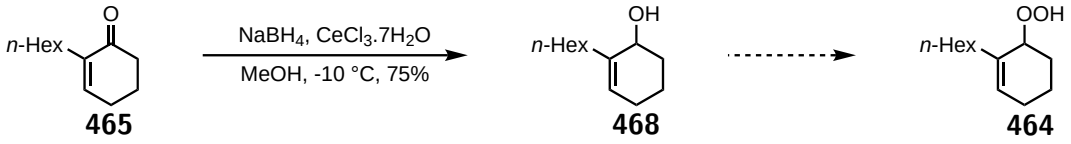

Figure 3.33: Approach to the key hydroperoxide **464**.

Carveol 469 as a model substrate for the interrupted Criegee rearrangement

Carveol **469** was chosen as the model substrate because of the same size of ring combined with a methyl substitution in α of the enone. The first approach to access hydroperoxide **472** was to transform carveol **469** into halide **470**, and then to use a Ag^I salt as a Lewis acid capable of eliminating the chloride.[48] Carveol **469** was subjected to methanesulfonyl chloride combined with triethylamine in DCM to afford corresponding chloride **470**. Different silver salts were evaluated to generate carbocation **471** which could then be trapped by hydrogen peroxide to generate desired hydroperoxide **472**. Unfortunately, none of the conditions tested were able to allow the formation of this product. The solution found was to use sulfuric acid and a solution of hydrogen peroxide in diethyl ether in the presence of carveol. The yield of the reaction was low, 22%, probably due to side reactions involving the isopropenyl fragment (Figure 3.34).

The interrupted Hock cleavage was tried; despite different reaction conditions evaluated, no desired product was ever observed. Alternatively, the interrupted Criegee rearrangement was attempted and, surprisingly, acetal **473** was stable enough to be isolated. Different

[47] (a) J.-L. Luche, *J. Am. Chem. Soc.* **1978**, *100*, 2226-2227. (b) J.-L. Luche, L. Rodriguez-Hahn, P. Crabbé, *J. Chem. Soc., Chem. Commun.* **1978**, 601-602.
[48] A. A. Frimer, *J. Org. Chem.* **1977**, *42*, 3194-3196.

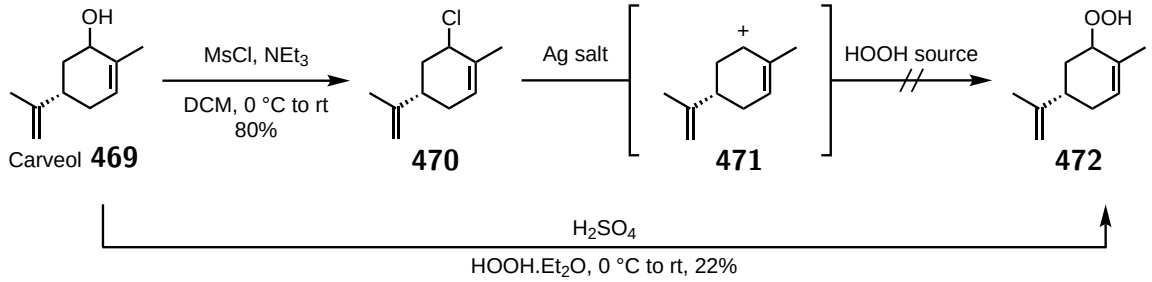

Figure 3.34: Synthesis of the hydroperoxide **472** derived from carveol **469**.

anhydrides were evaluated, but only acetic anhydride was able to form acetal **473** using DMAP in DCM at 0 °C. Under conventional conditions, allyltrimethylsilane and boron trifluoride etherate in DCM, a double allylation was observed and the only product isolated was oxepane **474** in a moderate yield of 51% (Figure 3.35). Although the amount of allyltrimethylsilane was reduced, the mono allylated product was never observed.

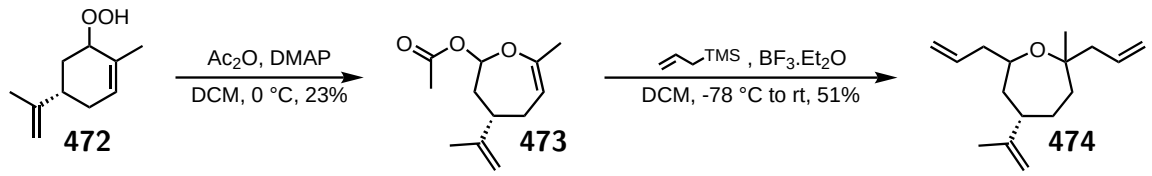

Figure 3.35: Interrupted Criegee rearrangement on the hydroperoxide **472**.

A similar reactivity might be observed with hydroperoxide **464**. A new strategy was thus needed to access the oxepane core of isolaurepan **456**.

A more direct approach starting from cyclohexene

Based on the reactivity of hydroperoxide **472**, a possible pathway to reach isolaurepan **477** might be to use different nucleophiles to introduce the two alkyl chains during the interrupted Criegee rearrangement. Hydroperoxide **476** can be synthetized using a Schenck-ene reaction on cyclohexene **475** (Figure 3.36).[49]

Cyclohex-2-enyl hydroperoxide **476** was synthesized using singlet oxygen generated *in-*

[49]H.-S. Dang, A. G. Davies, *Tetrahedron Lett.* **1991**, *32*, 1745-1748.

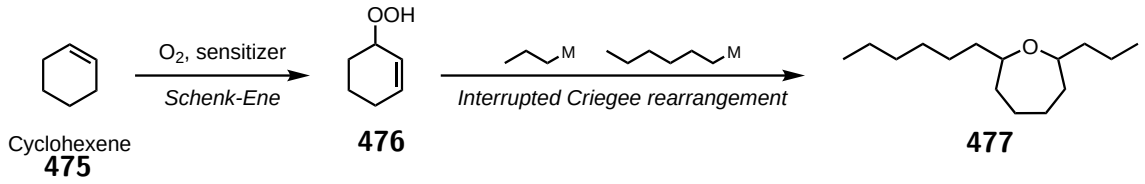

Figure 3.36: Possible pathway to isolaurepan from cyclohexene **475**.

situ using TPP and white LED light under an oxygen atmosphere in $CDCl_3$, which is used to increase the lifetime of singlet oxygen.[50] The reaction was tested on hydroperoxide **476** with trifluoroacetic anhydride to promote a Criegee rearrangement. Acetal **478** formed *in-situ* was directly subjected to allylation conditions using allyltrimethylsilane and boron trifluoride etherate. This allowed the formation of bis-allylated oxepane **479** with a low yield of 27%, which is likely due to the volatility of the compound (Figure 3.37).

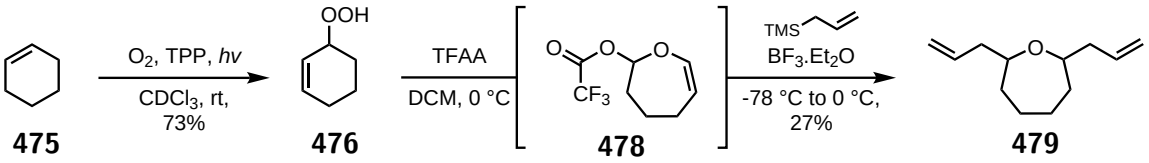

Figure 3.37: Interrupted Criegee rearrangement on the hydroperoxide **476**.

[50]K. I. Salokhiddinov, I. M. Byteva, and G. P. Gurinovich, *J. Appl. Spectrosc.* **1981**, *8*, 561-564.

3.5 Conclusion and perspectives

In this chapter, the work focused on the development of an interrupted Hock and Criegee rearrangement. Different starting materials were evaluated leading to the discovery of three methodologies (Figure 3.38). A first one is composed of a Hock cleavage followed by a mono or double Friedel-Crafts reaction. This sequence made it possible to form bicyclic product **414** and **421**, core structure of lignan natural products. A second one was the interrupted Criegee rearragement where a double allylation was observed using cyclic allylic hydroperoxide **476**. The last one was the interrupted Hock cleavage where tertiary peroxide **446** was mandatory to achieve good yield.

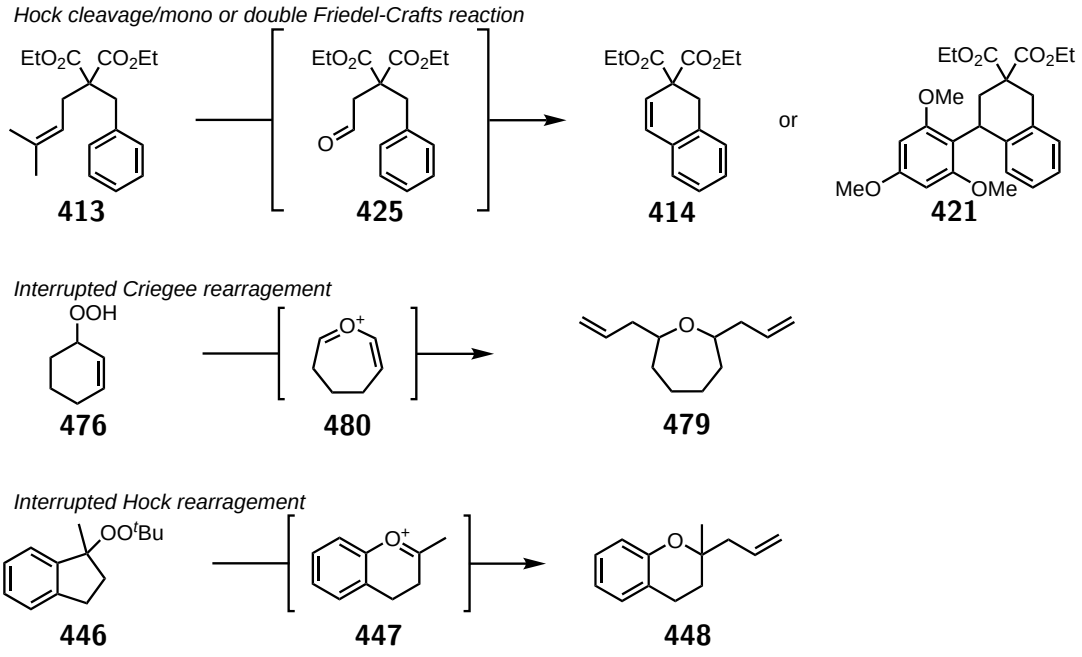

Figure 3.38: Different methodologies discovered.

Further work needs to be done to develop the scope and to find the limitation of these transformations. These are currently under investigation.

Chapter 4

General conclusion

The Nature's two phases synthesis of terpenoids is a great source of inspiration to develop efficient total synthesis of natural products. Total syntheses of the aspochalasines trichodermone **2** and trichoderone A **3** was envisaged using this strategy. In a first time, a common intermediate **273** was synthesized starting from cycloheptanone **169**. Using a Sharpless asymmetric dihydroxylation for installing chirality and a Suzuki cross coupling, triene **165** was formed. An unprecedented Ireland-Claisen rearrangement was developed to access carboxylic acid **164** which was coupled with γ-lactam **163** to allow the formation of triene **246**. γ-Lactam **246** was oxidized to release the dienophile fragment of triene **162** which reacted through an IMDA reaction to form tetracyclic intermediate **273** (Figure 4.1). DFT calculations was used to have a better understanding of this key reaction in cytochalasins total syntheses.

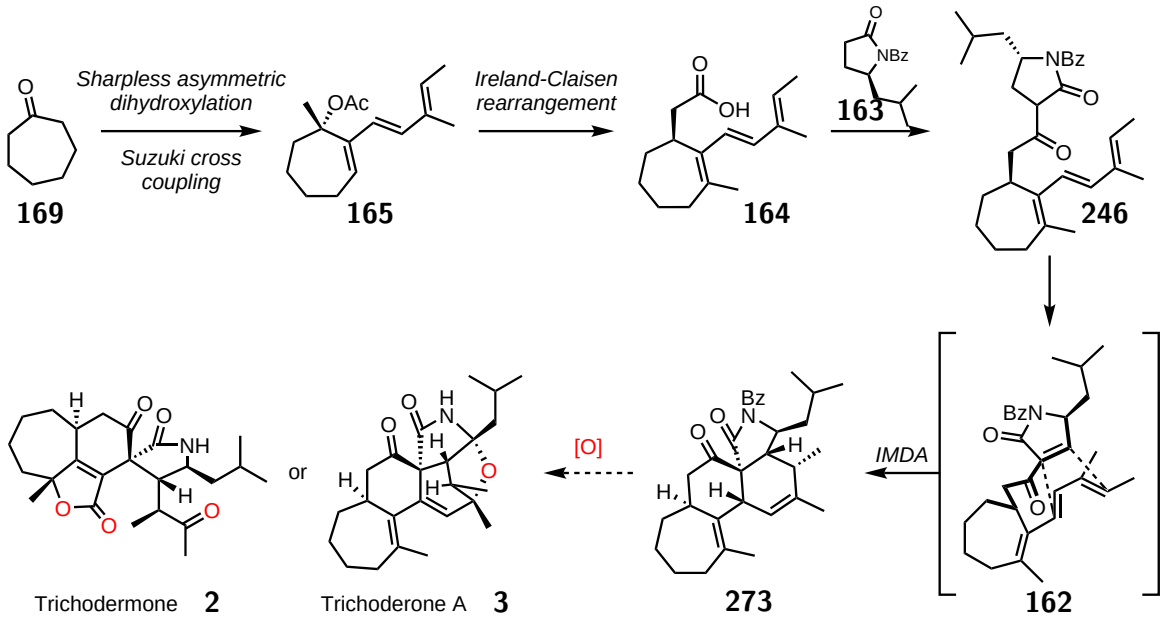

Figure 4.1: Synthesis of tetracyclic intermediate **273**

Once the main carbon core was obtained, diverse oxidation conditions were evaluated to selectively oxidized the different sites of tetracyclic compound **273**. Unfortunately, trichoderone A **3** and trichodermone **2** have not been accessed but others aspochalasines

analogues have been synthesized providing a better understanding on the reactivity of tetracyclic intermediate **273**.

At the same time, organic peroxide rearrangements were investigated to find methods to interrupt them with diverse nucleophiles. Set of conditions were found to interrupt the Hock cleavage and the Criegee rearrangement leading to new methods to access cyclic ethers (Figure 4.2). The work is now focus on the scope and limitations of these reactions.

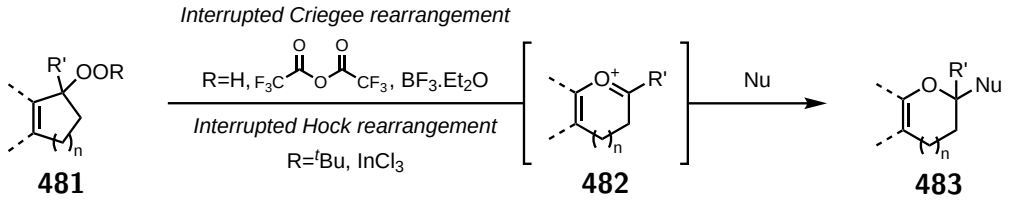

Figure 4.2: Interrupted organic peroxide rearrangements

During this thesis, we took advantage of the synergy between natural product total synthesis, methodology and DFT calculation to investigate total synthesis of aspochalasines and natural products containing cyclic ether. Even if targeted natural products, trichoderone A **3** and trichodermone **2**, have not been reached and the scope of different interrupted organic peroxide rearrangement have not been completed, the work done provided encouraging results and shown the power of interdisciplinary approach.

Chapter

5

Experimental Part

5.1 Experimental section

All reactions were carried out in oven-dried vessels under an atmosphere of argon and in anhydrous solvents unless stated otherwise. Solvents (methylene chloride, diethyl ether and tetrahydrofuran) were purified using a MB-SPS 800 Solvent purification system (MBraun). Analytical thin-layer chromatography (TLC) was carried out using aluminium TLC plates coated with F254 silica gel 60 (Merck), which were visualized by exposure to ultraviolet light and/or exposure to a basic solution of potassium permanganate or p-anisaldehyde stain followed by heating. Flash chromatography was carried out on silica gel 60 (40-63 μm). Infrared spectra were recorded on a PerkinElmer spectrum two FTIR equipped with a Jasco ATR. Absorption maxima (νmax) are reported in wavenumbers (cm^{-1}). High-resolution mass spectra (HRMS) were obtained on JEOL JMS-GCmate II spectrometer or on Tims-TOF (Bruker) and reported as m/z (relative intensity). Nuclear magnetic resonance spectra (^{1}H-NMR and ^{13}C-NMR) were recorded at ambient temperature with a Brucker Avance 400 spectrometer (400 MHz, 1H at 400 MHz, 13C at 100 MHz). For $CDCl_3$, DMSO-d_6 and benzene-d_6 solutions, chemical shifts are reported as parts per million (ppm) referenced to residual protium or carbon of the solvent ($CDCl_3$: δH= 7.26 and δC= 77.1; DMSO-d_6: δH= 2.50 and δC= 39.5; benzene-d_6, δH= 7.16 and δC= 128.1). Coupling constants are reported in Hertz (Hz). Data for ^{1}H-NMR spectra are reported as follows: chemical shift ppm, referenced to protium (br = broad, s = singlet, d = doublet, t = triplet, q = quartet, p = pentet, dd = doublet of doublets, dq = doublet of quartets, dp = doublet of pentets, td = triplet of doublets, qq = quartets of quartets, ddd = doublet of doublet of doublets, m = multiplet, integration, and coupling constants (Hz)).

1-Methylcycloheptene 171[1]

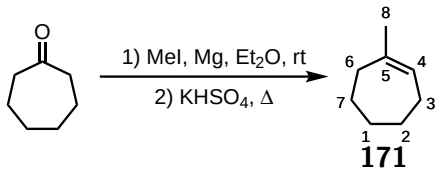

171

Experimental: To a mixture of Mg (8.8 g, 360 mmol, 1.06 equiv.) and a small crystal of iodine in 160 mL of dry diethyl ether in a round bottom flask equiped with a condenser, was added dropwise a solution of MeI (23 mL, 368 mmol, 1.08 equiv.) in 80 mL of dry diethyl ether over 30 min at rt. After the reaction has ceased, a solution of cycloheptanone (40 mL , 340 mmol, 1 equiv.) in 40 mL of dry diethyl ether was added over 20 min at rt and stirred for 30 min at rt. The reaction mixture was then acidified with a 2 M solution of HCl. The organic phase was separated, washed with a solution of $NaHCO_3$, dried over Na_2SO_4 and concentrated in vacuo. The crude product was then heated neat at 150 °C with grinded $KHSO_4$ (85 g, 624 mmol, 1.83 equiv.) for 1 h. The crude material was filtered on a plug of silica using pentane as eluent, concentrated and distilled to yield 26.2 g (70% yield over 2 steps) of 1-methylcycloheptene **171**.

Physical state: colorless liquid.

^{1}**H NMR** (400 MHz, $CDCl_3$) δ ppm: 5.54 (t, J = 6.4 Hz, 1H, H_4), 2.11-2.00 (m, 4H, H_{cycle}), 1.75-1.68 (m, 5H, H_8 and H_{cycle}), 1.52-1.46 (m, 4H, H_{cycle}).

^{13}**C NMR** (100 MHz, $CDCl_3$) δ ppm: 141.0 (C_5), 126.0 (C_4), 34.4, 32.6, 28.4, 27.6, 26.6, 26.4.

[1]M. Barbier, M. F. Hugel, *Bull. Soc. Chem. Fr.* **1961**, 951.

HRMS(EI+) m/z: calculated for C_8H_{14} [M]: 110.1096 found: 110.1093.

IR (ATR) ν (cm^{-1}): 2964, 2916, 2848, 1439, 1375, 1274, 1221, 1096, 964, 883, 841, 799, 790.

***rac-syn*-1,2-Dihydroxy-1-methylcycloheptane 184**

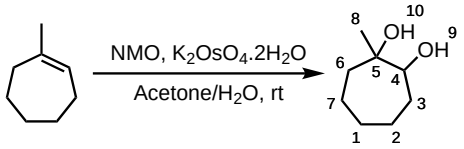

171 **184**

Experimental: To a stirred solution of 1-methylcycloheptene **171** (11 g, 100 mmol, 1 equiv.) and NMO (16.2 g, 120 mmol, 1.2 equiv.) in 200 mL of an acetone/H_2O (7:3) solution was added $K_2OsO_4.2H_2O$ (386 mg, 1 mmol, 0.01 equiv.). The reaction mixture was stirred at rt for 6 days. The reaction was quenched with a saturated solution of $Na_2S_2O_3$ (150 mL), stirred for 1 h at rt and then a saturated solution of $NaHCO_3$ (150 mL) was added. The aqueous layer was extracted with DCM (3 x 150 mL). The organic layers were combined, washed with brine, dried over Na_2SO_4, filtered and concentrated in vacuo. The crude product was purified via silica gel chromatography (PE/EA 6:1 to 2:1) to yield 13.3 g (92% yield) of diol **184**.

Physical state: colorless oil.

^{1}H NMR (400 MHz, $CDCl_3$) δ ppm: 3.44 (br d, 1H, H_4), 2.32 (brs, 1H, $H_{9\ or\ 10}$), 2.17 (brs, 1H, $H_{9\ or\ 10}$), 1.89-1.76 (m, 2H, $H_{2\ and\ 3}$), 1.76-1.66 (m, 3H, $H_{6\ and\ 7}$), 1.65-1.56 (m, 2H, $H_{1\ and\ 3}$), 1.50-1.30 (m, 3H, $H_{1,\ 2\ and\ 7}$), 1.28 (s, 3H, H_8).

^{13}C NMR (100 MHz, $CDCl_3$) δ ppm: 78.1 (C_4), 74.1 (C_5), 38.6 (C_6), 31.6 (C_3), 28.1 (C_1), 27.8 (C_8), 23.6 (C_2), 20.9 (C_7).

HRMS(EI+) m/z: calculated for $C_8H_{16}O_2$ [M]: 144.1150 found: 144.1144.

IR (ATR) ν (cm^{-1}): 3400, 2926, 2859, 1460, 1371, 1261, 1194, 1139, 1096, 1030, 970, 951, 930.

(1*S*,2*R*)-1,2-Dihydroxy-1-methylcycloheptane 168

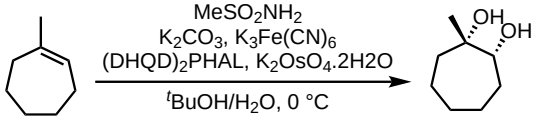

171 **168**

Experimental: To a stirred solution of $MeSO_2NH_2$ (4.75 g, 50 mmol, 1 equiv.), K_2CO_3 (20.7 g, 150 mmol, 3 equiv.), $K_3Fe(CN)_6$ (49.3 g, 150 mmol, 3 equiv.), $(DHQD)_2PHAL$ (681 mg, 0.875 mmol, 0.0175 equiv.), $K_2OsO_4.2H_2O$ (129 mg, 0.350 mmol, 0.007 equiv.) in 500 mL ^{t}BuOH/H_2O (1:1) was added 1-methylcycloheptene **171** (5.5 g, 50 mmol, 1 equiv.) at 0 ° C. The reaction mixture was stirred for 4 days at 0 °C. The reaction was quenched with $Na_2S_2O_3$ (75 g), stirred for 1 h at rt. The aqueous layer was extracted with EtOAc (3 x 300 mL). The organic layers were combined, washed with a 1 M solution of NaOH (500 mL), brine, dried over Na_2SO_4, filtered and concentrated in vacuo. The crude product was purified via silica gel chromatography (PE/EA 6:1 to 2:1) to yield 5.92 g (82% yield) of diol **168**.

$[\alpha]_D^{25}$ -4.6 (c 0.8 in $CHCl_3$).

***rac-syn*-1,2-dihydroxy-2-methylcycloheptane 1-*O*-benzoyl ester 484**

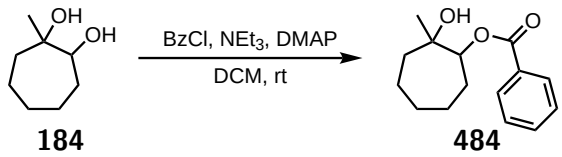

184 **484**

Experimental: To a stirred solution of diol **184** (144 mg, 1 mmol, 1 equiv.) and DMAP (5.5 mg, 0.05 mmol, 0.05 equiv.) in 5 mL of a 1:1 DCM/pyridine mixture was added BzCl (0.29 mL, 2.5 mmol, 2.5 equiv.). After stirring at rt overnight, the reaction was quenched with a saturated solution of NH_4Cl (5 mL). The aqueous layer was extracted with DCM (3 x 5 mL). The organic layers were combined, washed with brine, dried over Na_2SO_4, filtered and concentrated in vacuo. The crude product was purified via silica gel chromatography (PE/EA 9:1) to yield 108 mg (44% yield) of alcohol **484**.

Physical state: colorless oil.

^{1}H NMR (400 MHz, $CDCl_3$) δ ppm: 8.07-8.03 (m, 2H, H_{13}), 7.57-7.52 (m, 1H, H_{14}), 7.45-7.40 (m, 2H, H_{12}), 4.92 (dd, J = 9.6, 2.0 Hz, 1H, H_4), 2.39 (brs, 1H, H_9), 2.15-2.03 (m, 1H, H_3), 1.87-1.71 (m, 4H, $H_{2,\ 6\ and\ 7}$), 1.71-1.62 (m, 2H, $H_{1\ and\ 3}$), 1.62-1.50 (m, 2H, $H_{1\ and\ 2}$), 1.46-1.35 (m, 1H, H_7), 1.26 (s, 3H, H_8).

^{13}C NMR (100 MHz, $CDCl_3$) δ ppm: 165.9 (C_{10}), 133.1 (C_{14}), 130.5 (C_{11}), 129.6 (C_{13}), 128.5 (C_{12}), 81.5 (C_4), 73.9 (C_5), 39.0 (C_6), 28.3 (C_3), 28.1 (C_8), 27.6 (C_1), 23.5 (C_2), 21.1 (C_7).

HRMS(EI+) m/z: calculated for $C_{15}H_{20}O_3$ [M]: 248.1412 found: 248.1395.

IR (ATR) ν (cm^{-1}): 3500, 2929, 2859, 1713, 1602, 1584, 1451, 1315, 1274, 1177, 1114, 1070, 1026, 974, 919, 711, 688.

(1*R*,2*S*)-1,2-dihydroxy-2-methylcycloheptane 1-*O*-benzoyl ester 485

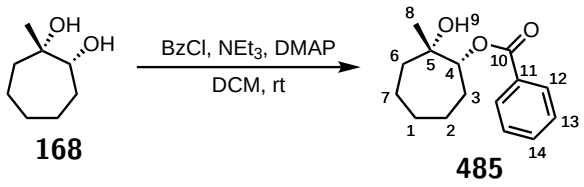

168 **485**

Experimental: To a stirred solution of diol **168** (8 mg, 50 μmol, 1 equiv.), DMAP (cat amount) and NEt_3 (10 μL, 75 μmol, 1.5 equiv.) in 500 μL of dry DCM was added BzCl (9 μL, 75 μmol, 1.5 equiv.). After stirring at rt overnight, the reaction was quenched with a saturated solution of NH_4Cl (1 mL). The aqueous layer was extracted with DCM (3 x 1 mL). The organic layers were combined, washed with brine, dried over Na_2SO_4, filtered and concentrated in vacuo. Alcohol **485** was analyzed without additional purification.

HPLC Cosmosil chiral 3B, $MeCN/H_2O$ = 40/60, 1 mL/min, 40 °C, 230 nm, t_R (minor enantiomer) = 14.5 min, t_R (major enantiomer) = 15.4 min, er = 89.5:10.5.

(2*S*)-hydroxy-2-methylcycloheptan-1-one 189

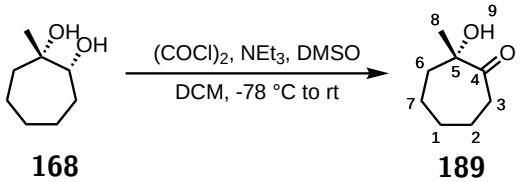

168 **189**

Experimental: To a stirred solution of $(COCl)_2$ (10 mL, 120 mmol, 1.5 equiv.) in 100

mL of dry DCM was added a solution of DMSO (17 mL, 240 mmol, 3 equiv.) in 100 mL of dry DCM at -78 °C over 1 h. After 10 min, a solution of diol **168** (11.5 g, 80 mmol, 1 equiv.) in 200 mL of dry DCM was added dropwise over 1 h. The reaction mixture was stirred for 10 min then Et_3N (67 mL, 480 mmol, 6 equiv.) was added over 30 min and the solution was allowed to warm up slowly to rt. The reaction was quenched with a saturated solution of NH_4Cl (300 mL). The aqueous layer was extracted with DCM (3 x 400 mL). The organic layers were combined, washed with brine, dried over Na_2SO_4, filtered and concentrated in vacuo. Hydroxy ketone **189** was engaged in next step without additional purification.

Physical state: colorless oil.

^{1}**H NMR** (400 MHz, $CDCl_3$) δ ppm: 3.85 (s, 1H, H_9), 2.75-2.67 (m, 1H, H_3), 2.51-2.44 (m, 1H, H_3), 2.06-1.98 (m, 1H, H_6), 1.98-1.93 (m, 1H, H_1), 1.86-1.78 (m, 1H, H_2), 1.78-1.70 (m, 1H, H_7), 1.68-1.62 (m, 1H, H_6), 1.50-1.33 (m, 2H, $H_{1\ and\ 2}$), 1.31 (s, 3H, H_8), 1.28-1.17 (m, 1H, H_7).

^{13}**C NMR** (100 MHz, $CDCl_3$) δ ppm: 216.5 (C_4), 78.8 (C_5), 38.6 (C_3), 38.0 (C_6), 30.5 (C_2), 27.3 (C_1), 27.3 (C_8), 24.0 (C_7).

HRMS(EI+) m/z: calculated for $C_8H_{14}O_2$ [M]: 142.0994 found: 142.0979.

IR (ATR) ν (cm^{-1}): 3491, 2929, 2858, 1706, 1453, 1370, 1263, 1184, 1049.

***rac*-2-hydroxy-2-methylcycloheptan-1-one *p*-tosylhydrazone 185**

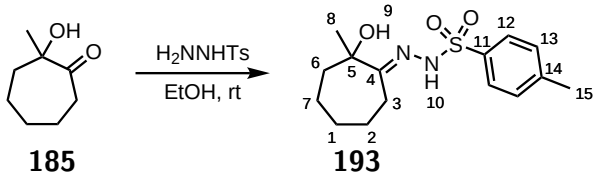

Experimental: To a mixture of hydrocy ketone **185** (142 mg, 1 mmol, 1 equiv.) and *p*-tosylhydrazine (186 mg, 1 mmol, 1 equiv.) was added 1 mL of EtOH at rt. After completion, the reaction mixture was concentrated to yield 310 mg (quantitative) of tosylhydrazone **193**.

Physical state: white solid.

^{1}**H NMR** (400 MHz, DMSO-d_6) δ ppm: 10.13 (s, 1H, H_{10}), 7.72 (d, J = 8.1 Hz, 2H, H_{12}), 7.38 (d, J = 8.1 Hz, 2H, H_{13}), 4.52 (s, 1H, H_9), 2.48-2.40 (m, 1H, H_3), 2.37 (s, 3H, H_{15}), 2.32-2.25 (m, 1H, H_3), 1.68-1.60 (m, 1H, H_6), 1.52-1.40 (m, 4H, $H_{2,\ 6\ and\ 7}$), 1.37-1.27 (m, 1H, H_1), 1.26-1.13 (m, 2H, $H_{1\ and\ 7}$), 1.11 (s, 3H, H_8).

^{13}**C NMR** (100 MHz, DMSO-d_6) δ ppm: 164.6 (C_4), 143.1 (C_{11}), 136.1 (C_{14}), 129.3 (C_{13}), 127.4 (C_{12}), 74.5 (C_5), 41.2 (C_6), 29.0 (C_7), 27.9 (C_8), 25.0 (C_3), 24.1 (C_2), 23.0 (C_1).

HRMS(EI+) m/z: calculated for $C_{15}H_{22}N_2O_3S$ [M]: 310.1351 found: 310.1348.

IR (ATR) ν (cm^{-1}): 3402, 3113, 2925, 1634, 1597, 1492, 1471, 1446, 1376, 1335, 1326, 1292, 1283, 1209, 1183, 1157, 1083, 1050, 1022.

1-Methyl-2-oxocycloheptyl acetate 186

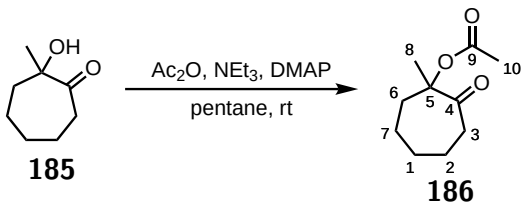

185 186

Experimental: To a stirred solution of hydroxy ketone **185** (883 mg, 6.2 mmol, 1 equiv.), Et_3N (2.1 mL, 14.9 mmol, 2.4 equiv.) and DMAP (72 mg, 0.62 mmol, 0.1 equiv.) in 18 mL of pentane was added Ac_2O (2.4 mL, 24.8 mmol, 4 equiv.) at 0 °C. After stirring at rt overnight, the reaction mixture was quenched with H_2O (18 mL) and stirred for 1 h at rt. The reaction mixture was diluted with H_2O (50 mL) and extracted with pentane (50 mL). The organic layer was dried over Na_2SO_4, filtered and concentrated in vacuo to yield 945 mg (83%) of acetoxy ketone **186** which was used without further purification.

Physical state: orange oil.

^{1}**H NMR** (400 MHz, $CDCl_3$) δ ppm: 2.73 (ddd, J = 14.8, 7.5, 5.5 Hz, 1H, H_3), 2.43 (ddd, J = 14.8, 7.5, 5.5 Hz, 1H, H_3), 2.17 (ddd, J = 14.4, 7.2, 2.9 Hz, 1H, H_6), 2.09 (s, 3H, H_{10}), 1.81-1.65 (m, 3H, $H_{1,\ 2\ and\ 7}$), 1.65-1.52 (m, 2H, $H_{6\ and\ 7}$), 1.53-1.49 (m, 1H, H_2), 1.51 (s, 3H, H_8), 1.46-1.35 (m, 1H, H_1).

^{13}**C NMR** (100 MHz, $CDCl_3$) δ ppm: 209.9 (C_4), 170.5 (C_9), 86.6 (C_5), 40.2 (C_3), 38.0 (C_6), 28.3 (C_1), 24.2 (C_7), 23.3 (C_2), 23.1 (C_8), 21.4 (C_{10}).

HRMS(EI+) m/z: calculated for $C_8H_{13}O_2^+$ [M-Ac]$^+$: 141.0921 found: 141.0905.

IR (ATR) ν (cm^{-1}): 2936, 2862, 1733, 1708, 1447, 1371, 1250, 1153, 1111, 1069, 1015.

8a-Methyl-4,5,6,7,8,8a-hexahydro-2H-cyclohepta[b]furan-2-one 188

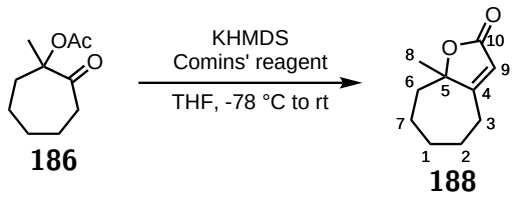

186 **188**

Experimental: To a stirred solution of acetoxy ketone **186** (37 mg, 0.2 mmol, 1 equiv.) in 1.6 mL of dry THF was added a 0.5 M KHMDS solution in toluene (420 μL, 0.42 mmol, 2.1 equiv.) dropwise at -78 °C. After 30 min, a solution of Comins reagent (86 mg, 0.22 mmol, 1.1 equiv.) in 0.4 mL of dry THF was added dropwise. After stirring at -78 °C for 1 h, the reaction mixture was warmed up to rt and stirred overnight. The reaction was quenched with H_2O (2 mL) and extracted with EtOAc (3 x 5 mL). The organic layers were combined, washed with a 1 M solution of NaOH, brine, dried over Na_2SO_4, filtered and concentrated in vacuo. The crude product was purified via silica gel chromatography (PE/EA 80:20) to yield 31 mg (93% yield) of α,β unsaturated lactone **188**.

Physical state: colorless oil.

^{1}**H NMR** (400 MHz, $CDCl_3$) δ ppm: 5.70 (s, 1H, H_9), 2.85-2.77 (m, 1H, H_3), 2.34-2.24 (m, 1H, H_3), 2.09 (s, 3H, H_{10}), 2.04-1.96 (m, 1H, H_6), 1.95-1.87 (m, 1H, H_2), 1.87-1.79 (m, 1H, H_6), 1.73-1.60 (m, 1H, H_1), 1.58-1.47 (m, 3H, $H_{1,\ 2\ and\ 7}$), 1.50 (s, 3H, H_8), 1.46-1.33 (m, 1H, H_7).

^{13}**C NMR** (100 MHz, $CDCl_3$) δ ppm: 178.0 (C_4), 173.0 (C_{10}), 115.8 (C_9), 90.7 (C_5),

37.9 (C_6), 29.7 (C_1), 28.7 (C_2), 27.8 (C_3), 25.0 (C_8), 23.7 (C_7).

(2*S*)-Methyl-2-((trimethylsilyl)oxy)cycloheptan-1-one 190

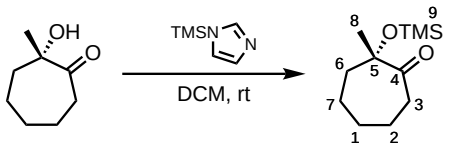

189 **190**

Experimental: To a stirred solution of hydroxy ketone **189** (80 mmol expected, 1 equiv.) in 150 mL of DCM was added *N*-trimethylsilylimidazole (17.5 mL, 120 mmol, 1.5 equiv.). After stirring at rt overnight, the reaction was quenched with a saturated solution of NH_4Cl (200 mL). The aqueous layer was extracted with DCM (3 x 100 mL). The organic layers were combined, washed with brine, dried over Na_2SO_4, filtered and concentrated in vacuo. The crude product was purified via silica gel chromatography (PE/Et_2O 98:2 to 95:5) to yield 14.4 g (84% yield over 2 steps) of ketone **190**.

Physical state: colorless oil.

^{1}**H NMR** (400 MHz, $CDCl_3$) δ ppm: 2.78-2.68 (m, 1H, H_3), 2.40-2.31 (m, 1H, H_3), 1.84-1.77 (m, 1H, H_6), 1.76-1.68 (m, 3H, $H_{1\ and\ 2}$), 1.58-1.48 (m, 3H, $H_{6\ and\ 7}$), 1.33 (s, 3H, H_8), 1.30-1.22 (m, 1H, H_1), 0.12 (s, 9H, H_9).

^{13}**C NMR** (100 MHz, $CDCl_3$) δ ppm: 214.9 (C_4), 82.3 (C_5), 40.9 (C_6), 39.9 (C_3), 28.9 (C_1), 26.3 (C_8), 24.8 (C_5), 24.7 (C_7), 2.4 (C_9).

HRMS(EI+) m/z: calculated for $C_{11}H_{22}O_2Si$ [M]: 214.1389 found: 214.1392.

IR (ATR) ν (cm^{-1}): 2931, 2858, 1719, 1453, 1371, 1251, 1203, 1172, 1081.

$[\alpha]_D^{25}$ +2.8 (c 1.5 in $CHCl_3$).

7-Methyl-7-((trimethylsilyl)oxy)cyclohept-1-en-1-yl trifluoromethanesulfonate 487

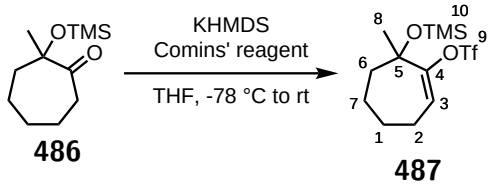

486 **487**

Experimental: To a stirred solution of ketone **486** (42 mg, 0.2 mmol, 1 equiv.) in 1 mL of dry THF was added a 0.5 M KHMDS solution in toluene (600 μL, 0.3 mmol, 1.5 equiv.) dropwise at -78 °C. After 30 min, a solution of Comins reagent (118 mg, 0.3 mmol, 1.5 equiv.) in 0.5 mL of dry THF was added dropwise. After stirring at -78 °C for 1 h, the reaction mixture was warmed up to rt and stirred overnight. The reaction was quenched with H_2O (2 mL) and extracted with EtOAc (3 x 5 mL). The organic layers were combined, washed with a 1 M solution of NaOH, brine, dried over Na_2SO_4, filtered and concentrated in vacuo. The crude product was purified via silica gel chromatography (PE/EA 90:10) to yield 35 mg (50% yield) of enol triflate **487**.

Physical state: yellowish oil.

^{1}**H NMR** (400 MHz, $CDCl_3$) δ ppm: 5.76 (t, J = 6.7 Hz, 1H, H_3), 2.27-2.06 (m, 2H, H_1), 2.01-1.80 (m, 3H, $H_{6\ and\ 7}$), 1.75-1.54 (m, 3H, $H_{2\ and\ 7}$), 1.45 (s, 3H, H_8), 0.17 (s, 9H,

H_{10}).

^{13}C NMR (100 MHz, $CDCl_3$) δ ppm: 155.5 (C_4), 121.1 (C_3), 118.6 (q, J = 318.8 Hz, C_9), 76.7 (C_5), 38.9 (C_6), 27.1 (C_8), 25.6 (C_2), 23.3 (C_1), 22.5 (C_7), 2.4 (C_{10}).

IR (ATR) ν (cm^{-1}): 2943, 1414, 1248, 1199, 1143, 1113, 1045, 1015, 979.

(7*S*)-Hydroxy-7-methylcyclohept-1-en-1-yl trifluoromethanesulfonate 167

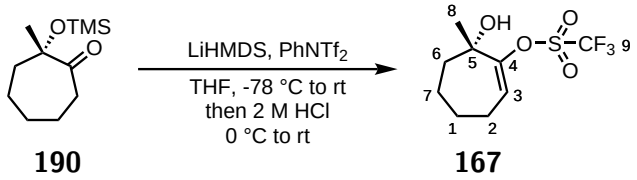

190 **167**

Experimental: To a stirred solution of ketone **190** (5.2 g, 24 mmol, 1 equiv.) and $PhNTf_2$ (12.8 g, 36 mmol, 1.5 equiv.) in 200 mL of dry THF was added a 1 M LiHMDS solution in THF (48 mL, 48 mmol, 2 equiv.) dropwise over 2 h at -78 °C. After stirring at -78 °C for 1 h, the reaction mixture was warmed up to rt and stirred overnight. The reaction was quenched with a solution of 2 M HCl (200 mL) at 0 °C and then stirred at rt for 1 h. The aqueous layer was extracted with EtOAc (3 x 200 mL). The organic layers were combined, washed with a saturated solution of $NaHCO_3$, brine, dried over Na_2SO_4, filtered and concentrated in vacuo. The crude product was purified via silica gel chromatography (PE/EA 98:2 to 95:5) to yield 5.7 g (86% yield) of enol triflate **167**.

Physical state: yellowish oil.

^{1}H NMR (400 MHz, $CDCl_3$) δ ppm: 5.86 (t, J = 6.5 Hz, 1H, H_3), 2.29-2.11 (m, 2H,

H_1), 1.94-1.90 (m, 2H, H_6), 1.90-1.81 (m, 1H, H_7), 1.73-1.62 (m, 3H, $H_{2\ and\ 7}$), 1.42 (s, 3H, H_8).

^{13}C NMR (100 MHz, $CDCl_3$) δ ppm: 154.8 (C_4), 122.7 (C_3), 120.0 (q, J = 319.5 Hz, C_9), 73.7 (C_5), 39.7 (C_6), 26.2 (C_8), 25.6 (C_2), 23.4 (C_1), 22.3 (C_7).

HRMS(EI+) m/z: calculated for $C_8H_{10}F_3O_4S^+$ $[M\text{-}CH_3]^+$: 259.0246 found: 259.0241.

IR (ATR) ν (cm^{-1}): 2941, 1411, 1247, 1204, 1143, 1003, 980.

$[\boldsymbol{\alpha}]_{\boldsymbol{D}}^{\mathbf{25}}$ +0.9 (c 0.9 in $CHCl_3$).

(1*S*)-Methyl-2-(((trifluoromethyl)sulfonyl)oxy)cyclohept-2-en-1-yl acetate 191

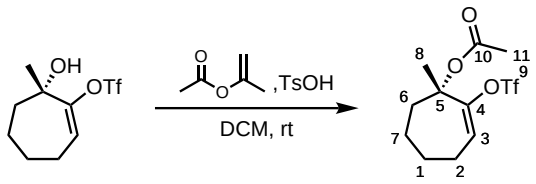

167 **191**

Experimental: To a stirred solution of enol triflate **167** (1.4 g, 5 mmol, 1 equiv.) and isopropenyl acetate (2.8 mL, 25 mmol, 5 equiv.) in 50 mL of DCM was added TsOH (125 mg, 0.25 mmol, 0.05 equiv.) at rt. After stirring at rt overnight, the reaction was quenched with a saturated solution of $NaHCO_3$ (50 mL). The aqueous layer was extracted with DCM (3 x 25 mL). The organic layers were combined, washed with brine, dried over Na_2SO_4, filtered and concentrated in vacuo. The crude product was purified via silica gel chromatography (PE/EA 98:2 to 95:5) to yield 1.5 g (95% yield) of acetoxy enol triflate **191**.

Physical state: colorless oil.

^{1}H NMR (400 MHz, $CDCl_3$) δ ppm: 5.97 (dd, J = 7.6, 6.2 Hz, 1H, H_3), 2.49-2.41 (m, 1H, H_6), 2.34-2.24 (m, 1H, H_2), 2.21-2.09 (m, 1H, H_2), 2.04 (s, 3H, H_{11}), 1.79-1.64 (m, 3H, $H_{1\ and\ 7}$), 1.62 (s, 3H, H_8).

^{13}C NMR (100 MHz, $CDCl_3$) δ ppm: 169.8 (C_{10}), 151.2 (C_4), 124.4 (C_3), 118.5 (q, J = 319.5 Hz, C_9), 82.5 (C_5), 35.0 (C_6), 25.4 (C_1), 24.2 (C_8), 23.5 (C_2), 23.0 (C_7), 21.9 (C_{11}).

HRMS(EI+) m/z: calculated for $C_{10}H_{15}O_2^+$ $[M\text{-}OTf]^+$: 167.1067 found: 167.1067.

IR (ATR) ν (cm^{-1}): 2941, 2865, 1744, 1669, 1413, 1369, 1245, 1209, 1142, 1099, 1050, 1009, 985.

$[\boldsymbol{\alpha}]_{\boldsymbol{D}}^{\mathbf{25}}$ -10.5 (c 1.1 in $CHCl_3$).

(1*S*)-methyl-2-((1*E*,3*E*)-3-methylpenta-1,3-dien-1-yl)cyclohept-2-en-1-yl acetate 165

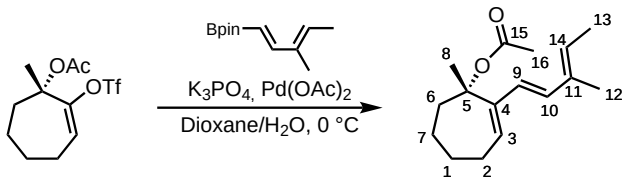

191 **165**

Experimental: $Pd(OAc)_2$ (113 mg, 0.5 mmol, 0.1 equiv.) was dissolved in 35 mL of dioxane then 15 mL of a 2 M solution of K_3PO_4 (9.5 g, 45 mmmol, 9 equiv.) in water was added. The solution was cooled down to 4 °C. After 5 min at 4 °C, acetoxy enol triflate **191**

(1.58 g, 5 mmol, 1 equiv.) followed by pinacol boronate **202** (1.15 g, 5.5 mmol, 1.1 equiv.) were added in that order. After stirring at 4 °C for 1 h, the reaction was quenched with a saturated solution of NH_4Cl (50 mL). The aqueous layer was extracted with pentane (3 x 50 mL). The organic layers were combined, washed with brine, dried over Na_2SO_4, filtered and concentrated in vacuo. The crude product was purified via silica gel chromatography (pentane/Et_2O 98:2) to yield 880 mg (71% yield) of triene **165**.

Physical state: colorless oil.

^{1}H NMR (400 MHz, $CDCl_3$) δ ppm: 6.35 (d, J = 15.9 Hz, 1H, H_{10}), 6.08 (d, J = 15.9 Hz, 1H, H_9), 5.93 (ddd, J = 7.9, 5.3, 1.0 Hz, 1H, H_3), 5.58-5.50 (m, 1H, H_{14}), 2.75-2.65 (m, 1H, H_6), 2.39-2.29 (m, 1H, H_2), 2.18-2.10 (m, 1H, H_2), 1.97 (s, 3H, H_{16}), 1.88-1.80 (m, 1H, H_1), 1.79-1.75 (m, 1H, H_6), 1.74 (s, 3H, H_{13}), 1.72 (s, 3H, H_{12}), 1.71-1.65 (m, 2H, $H_{1\ and\ 7}$), 1.62-1.57 (m, 1H, H_7), 1.53 (s, 3H, H_8).

^{13}C NMR (100 MHz, $CDCl_3$) δ ppm: 169.9 (C_{15}), 144.4 (C_4), 135.0 (C_{11}), 133.6 (C_{10}), 128.3 (C_3), 126.5 (C_9), 126.5 (C_{14}), 85.5 (C_5), 36.6 (C_6), 27.0 (C_2), 26.0 (C_7), 25.9 (C_8), 23.6 (C_1), 22.2 (C_{16}), 14.1 (C_{13}), 12.1 (C_{12}).

HRMS(EI+) m/z: calculated for $C_{16}H_{24}O_2$ [M]: 248.1776 found: 248.1777.

IR (ATR) ν (cm^{-1}): 2928, 2858, 1737, 1445, 1367, 1244, 1166, 1144, 1081, 1014, 959.

$[\boldsymbol{\alpha}]_{\boldsymbol{D}}^{\mathbf{25}}$ +29.1 (c 0.8 in $CHCl_3$).

HPLC , MeCN/H_2O = 90/10, 0.6 mL/min, 40 °C, 230 nm, t_R (minor enantiomer) = 19.6 min, t_R (major enantiomer) = 20.4 min, er = 89.5:10.5.

(*E*)-Trimethyl(3-methylpent-3-en-1-yn-1-yl)silane 199

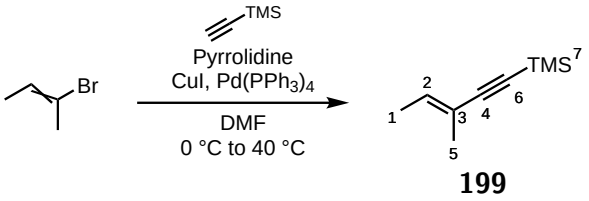

199

Experimental: To a stirred solution of 2-bromo-2-butene (8.6 mL, 84 mmol, 1.4 equiv.) in 34 mL of dry DMF was added $Pd(PPh_3)_4$ (680 mg, 0.6 mmol, 0.01 equiv.), pyrrolidine (8.5 mL, 60 mmol, 1 equiv.), ethynyltrimethylsilane (8.3 mL, 60 mmol, 1 equiv.) and CuI (220 mg, 1.2 mmol, 0.02 equiv.), in that order at 0 °C and in the dark. The reaction mixture was then heated up to 50 °C for 3 h without light proctection. The reaction was cooled down and quenched with a saturated solution of NH_4Cl (50 mL). The aqueous layer was extracted with pentane (3 x 50 mL). The organic layers were combined, washed with a saturated solution of $CuSO_4$ then with brine, dried over Na_2SO_4, filtered and concentrated in vacuo. TMS alkyne **199** was engaged in next step without additional purification. The product can be purified by distillation.

Physical state: colorless oil.

^{1}H NMR (400 MHz, $CDCl_3$) δ ppm: 5.99 (qq, J = 7.1, 1.6 Hz, 1H, H_2), 1.77 (p, J = 1.2 Hz, 3H, H_5), 1.67 (dq, J = 7.1, 1.2 Hz, 3H, H_1), 0.17 (s, 9H, H_7).

^{13}C NMR (100 MHz, $CDCl_3$) δ ppm: 134.0 (C_2), 118.7 (C_3), 108.7 (C_6), 89.8 (C_4), 16.9 (C_5), 14.2 (C_1), 0.2 (C_7).

HRMS(EI+) m/z: calculated for $C_9H_{16}Si$ [M]: 152.1021 found: 152.1014.

IR (ATR) ν (cm^{-1}): 2959, 2142, 1248, 1219, 1094, 1019.

(3*E*)-Methylpent-3-en-1-yne 200

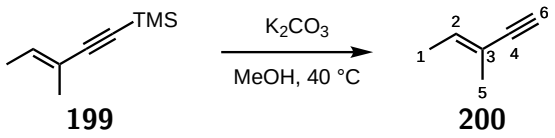

199 **200**

Experimental: To a stirred solution of TMS alkyne **199** (8.4 g, 55 mmol supposed, 1 equiv. supposed) in 20 mL of MeOH was added K_2CO_3 (115 mg, 0.83 mmol, 0.015 equiv.). The reaction mixture was stirred at 40 °C overnight. After completion, the reaction mixture was cooled down to 0 °C and extracted with 50 mL of pentane. The pentane layer was washed with cold H_2O (7 x 40 mL), dried over Na_2SO_4, filtered and directly engaged in the next step without evaporation or additional purification.

^{1}H NMR (400 MHz, $CDCl_3$) δ ppm: 6.02 (m, 1H, H_2), 2.72 (s, 1H, H_6), 1.79 (p, J = 1.3 Hz, 3H, H_5), 1.69 (dp, J = 7.1, 1.1 Hz, 3H, H_1).

^{13}C NMR (100 MHz, $CDCl_3$) δ ppm: 134.2 (C_2), 117.8 (C_3), 87.0 (C_4), 73.3 (C_6), 16.8 (C_5), 14.1 (C_1).

4,4,5,5-Tetramethyl-2-((1*E*,3*E*)-3-methylpenta-1,3-dien-1-yl)-1,3,2-dioxaborolane 202

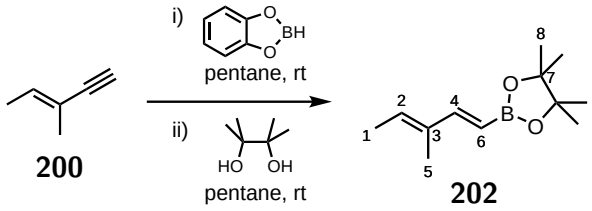

Experimental: To half of the solution coming from the previous solution in pentane was added catecholborane (3.3 g, 27.5 mmol, 1 equiv.) at 0 °C. The reaction mixture was then stirred at rt for 15 min, at reflux for 2.5 h and then at rt overnight. The reaction mixture was quenched with H_2O (25 mL). The organic layer was washed with H_2O (2 x 25 mL) and dried over Na_2SO_4. To the organic layer was added pinacol (3.25 g, 27.5 mmol, 1 equiv.). The reaction mixture was stirred at rt overnight. After completion, the reaction mixture was washed with H_2O (2 x 25 mL), dried over Na_2SO_4, filtered and concentrated. The crude product was purified via silica gel chromatography (PE/Et_2O 98:2) to yield 3.2 g (51% yield over 4 steps) of pinacol boronate **202**.

Physical state: colorless oil.

^{1}H NMR (400 MHz, $CDCl_3$) δ ppm: 7.04 (d, J = 18.1 Hz, 1H, H_4), 5.78 (q, J = 7.1 Hz, 1H, H_2), 5.43 (d, J = 18.1 Hz, 1H, H_6), 1.75 (d, J = 7.1 Hz, 3H, H_1), 1.73 (s, 3H, H_5), 1.27 (s, 12H, H_8).

^{13}C NMR (100 MHz, $CDCl_3$) δ ppm: 154.6 (C_4), 136.2 (C_3), 131.8 (C_2), 83.2 (C_7), 24.9 (C_8), 14.4 (C_1), 11.4 (C_5).

HRMS(EI+) m/z: calculated for $C_{12}H_{21}BO_2$ [M]: 208.1635 found: 208.1626.

IR (ATR) ν (cm^{-1}): 2978, 2929, 1635, 1608, 1459, 1398, 1379, 1341, 1319, 1272, 1230, 1199, 1145, 1110.

2-((1*E*,3*E*)-3-Methylpenta-1,3-dien-1-yl)benzo[d][1,3,2]dioxaborole 201

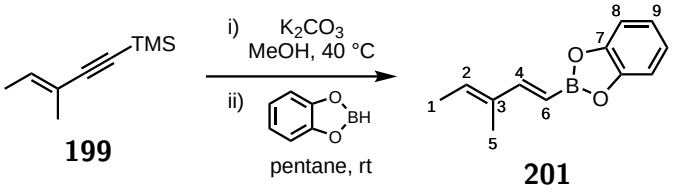

Experimental: To a stirred solution of distilled TMS alkyne **199** (3.04 g, 20 mmol, 1 equiv.) in 8 mL of MeOH was added K_2CO_3 (42 mg, 0.3 mmol, 0.015 equiv.). The reaction mixture was stirred at 40 °C overnight. After completion, the reaction mixture was cooled down to 0 °C and extracted with 20 mL of pentane. The pentane layer was washed with cold H_2O (7 x 16 mL) and dried over Na_2SO_4. To the organic layer was added catecholborane (2.14 mL, 20 mmol, 1 equiv.) 0 °C. The reaction mixture was then stirred at rt for 15 min, at reflux for 2.5 h and then at rt overnight. The reaction mixture was quenched with H_2O (20 mL). The organic layer was washed with H_2O (2 x 20 mL), dried over Na_2SO_4, filtered and concentrated to yield 2.38 g (60% yield over 2 steps) of catechol boronate **201**.

Physical state: white solid.

^{1}H NMR (400 MHz, $CDCl_3$) δ ppm: 7.41 (d, J = 18.2 Hz, 1H, H_4), 7.22 (m, 2H, H_9), 7.07 (m, 2H, H_8), 5.94 (q, J = 6.5 Hz, 1H, H_2), 5.75 (d, J = 18.2 Hz, 1H, H_6), 1.84 (s, 3H, H_5), 1.83 (d, J = 6.5 Hz, 3H, H_1).

^{13}C NMR (100 MHz, $CDCl_3$) δ ppm: 157.2 (C_4), 148.5 (C_7), 136.3 (C_3), 134 (C_2), 122.6 (C_9), 112.4 (C_8), 14.6 (C_1), 11.5 (C_5).

HRMS(EI+) m/z: calculated for $C_{12}H_{13}BO_2$ [M]: 200.1009 found: 200.0994.

IR (ATR) ν (cm^{-1}): 3060, 2921, 2853, 1632, 1605, 1473, 1399, 1367, 1330, 1286, 1264, 1239, 1191, 1127, 1032, 986.

Trifluoro((1*E*,3*E*)-3-methylpenta-1,3-dien-1-yl)-λ^4-borane, potassium salt 203

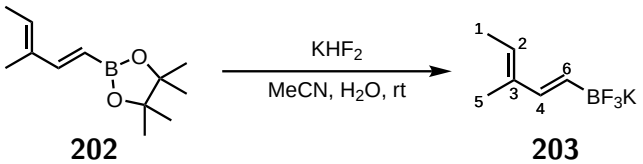

202 **203**

Experimental: To a stirred solution of pinacol boronate **202** (208 mg, 1 mmol, 1 equiv.) in 3 mL of MeCN was added KHF_2 (234 mg, 3 mmol, 3 equiv.) and 1 mL of H_2O at rt. After stirring at rt overnight, the solution was concentrated in vacuo. The crude solid was dissolved in acetone then filtered and concentrated in vacuo. The resulting white solid was purified by dissolving in hot acetone and precipating with Et_2O. After filtration, the solid was washed with Et_2O and dried under vaccum to yield to 120 mg (64% yield) of potassium trifluoroborate **203**.

Physical state: white solid.

^{1}H NMR (400 MHz, $CDCl_3$) δ ppm: 6.12 (d, J = 18.1 Hz, 1H, H_4), 5.44-5.35 (m, 1H, H_6), 5.31-5.25 (m, 1H, H_2), 1.64 (d, J = 7.1 Hz, 3H, H_1), 1.59-1.61 (m, 3H, H_5).

^{13}**C NMR** (100 MHz, $CDCl_3$) δ ppm: 138.1 (C_4), 136.7 (C_3), 121.1 (C_2), 13.6 (C_1), 11.9 (C_5).

HRMS(EI+) m/z: calculated for $C_6H_9BOF_3K$ [M]: 188.0386 found:.

IR (ATR) ν (cm^{-1}): 2986, 2913, 2855, 1641, 1609, 1439, 1392, 1377, 1349, 1250, 1230, 1130, 1095, 1072, 1041, 1003, 969, 951, 922, 852, 800, 741, 610.

Bis(4,4,5,5-tetramethyl-1,3,2-dioxaborolan-2-yl)methane 206[2]

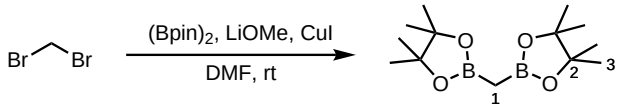

206

Experimental: $(Bpin)_2$ (114 g, 0.45 mol, 0.5 equiv.), LiOMe (25.5 g, 0.68 mol, 1.5 equiv.) and CuI (4.26 g, 22.5 mmol, 0.05 equiv.) were added in a flask. The flask was then purged 3 times by a vaccuum/argon cycle and 450 mL of DMF were added. After solubilisation, dibromomethane (31.5 mL, 0.45 mol, 1 equiv.) was added at rt. After stirring overnight at rt, 600 mL of Et_2O were added. The slurry was filtered through a silica gel plug, rinsed with Et_2O, and concentrated in vacuo. The crude reaction mixture in DMF was diluted with hexane (900 mL), washed with H_2O (4 x 250 mL), dried over Na_2SO_4, filtered and concentrated in vacuo to yield to 42.7 g (71% yield) of bis[(pinacolato)boryl]methane **206**.

Physical state: white solid.

[2]K. Hong, X. Liu, J. P. Morken, *J. Am. Chem. Soc.* **2014**, *136*, 10581-10584.

^{1}**H NMR** (400 MHz, $CDCl_3$) δ ppm: 1.23 (s, 24H, H_3), 0.34 (s, 2H, H_1).

^{13}**C NMR** (100 MHz, $CDCl_3$) δ ppm: 83.1 (C_2), 24.9 (C_3).

HRMS(EI+) m/z: calculated for $C_{13}H_{26}B_2O_4$ [M]: 268.2017 found: 268.2015.

IR (ATR) ν (cm^{-1}): 2976, 2934, 1479, 1468, 1403, 1379, 1354, 1309, 1267, 1214, 1164, 1139, 1091, 966, 896, 844, 674.

4,4,5,5-Tetramethyl-2-((1*E*,3*E*)-3-methylpenta-1,3-dien-1-yl)-1,3,2-dioxaborolane 202[3]

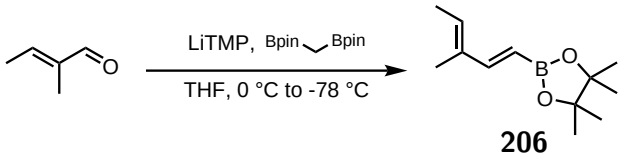

206

Experimental: To a stirred solution of TMP (30 mL, 175 mmol, 1.4 equiv.) in 60 mL of dry THF was added a 2.13 M solution of *n*-BuLi (70 mL, 150 mmol, 1.2 equiv.) in hexanes over 30 min at 0 °C. After 30 min, a solution of bis[(pinacolato)boryl]methane **206** (40.3 g, 150 mmol, 1.2 equiv.) in 110 mL of dry THF was added dropwise over 30 min at 0 °C. After 5 min, the reaction mixture was cooled down to -78 °C and a solution of tiglic aldehyde (12 mL, 125 mmol, 1 equiv.) in 230 mL of THF was added dropwise over 30 min. The reaction was stirred 4 h at this temperature and was quenched with H_2O before being allowed to warm up to rt. The mixture was extracted with Et_2O (3 x 300 mL). The organic layers were combined, washed with brine, dried over Na_2SO_4, filtered and concentrated in vacuo. The crude product was purified via silica gel chromatography (PE/Et_2O 98:2) to

[3]J. R. Coombs, L. Zhang, J. P. Morken, *Org. Lett.* **2015**, *17*, 1708-1711.

yield 21.3 g (82% yield) of pinacol boronate **202**. All data were consistent with those above reported.

2-((3*S*)-methyl-2-((1*E*,3*E*)-3-methylpenta-1,3-dien-1-yl)cyclohept-2-en-1-yl)acetic acid 164

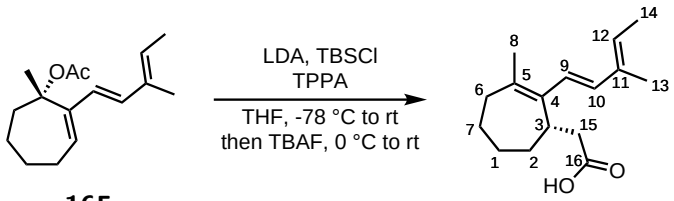

165 **164**

Experimental: To a stirred solution of triene **165** (860 mg, 3.5 mmol, 1 equiv.) and TPPA (1.6 mL, 7 mmol, 2 equiv.) in 20 mL of dry THF was added a 1 M LDA solution in THF/hexane (7 mL, 7 mmol, 2 equiv.) dropwise over 20 min at -78 °C. After 1 h, a solution of TBSCl (1.05 g, 7 mmol, 2 equiv.) in 7 mL of dry THF was added dropwise over 20 min. After stirring at -78 °C for 1 h, the reaction mixture was warmed up to rt and stirred overnight. The reaction mixture was cooled down to 0 °C and a 1 M solution of TBAF in THF (10.5 mL, 10.5 mmol, 3 equiv.) was added. The reaction mixture was warmed up to rt, stirred for 1 h and 150 mL of pentane were added. The slurry was filtered and washed with pentane. The precipate was dissolved with a saturated solution NH_4Cl and extracted with Et_2O (3 x 50 mL). The organic layers were combined, washed with brine, dried over Na_2SO_4, filtered and concentrated in vacuo to yield 617 mg (71% yield) of crude carboxylic acid **164** which was engaged in the next step without additional purification.

Physical state: yellowish oil.

^{1}**H NMR** (400 MHz, $CDCl_3$) δ ppm: 6.33 (d, J = 16.0 Hz, 1H, H_{10}), 6.27 (d, J = 16.0 Hz,

1H, H_9), 5.58 (q, J = 14.0, 7.0, 1H, H_{12}), 3.35-3.24 (m, 1H, H_3), 2.62 (dd, J = 15.2, 10.4, 1H, H_{15}), 2.51 (dd, J = 15.2, 5.0 Hz, 1H, H_{15}), 2.43-2.31 (m, 1H, H_6), 2.16-2.06 (m, 1H, H_6), 1.85 (s, 3H, H_8), 1.78 (s, 3H, H_{13}), 1.74 (d, J = 7.0 Hz, 3H, H_{14}), 1.72-1.58 (m, 5H, $H_{1,\ 2\ and\ 7}$), 1.51-1.38 (m, 1H, H_1).

^{13}C NMR (100 MHz, $CDCl_3$) δ ppm: 179.7 (C_{16}), 137.1 (C_4), 135.1 (C_{11}), 134.7 (C_5), 131.8 (C_{10}), 126.4 (C_{12}), 125.2 (C_9), 36.7 (C_{15}), 35.8 (C_3), 35.2 (C_6), 29.3 (C_2), 25.8 (C_1), 24.9 (C_7), 22.9 (C_8), 14.0 (C_{14}), 12.1 (C_{13}).

HRMS(EI+) m/z: calculated for $C_{16}H_{24}O_2$ [M]: 248.1776 found: 248.1772.

IR (ATR) ν (cm^{-1}): 3053, 2986, 2924, 2857, 1705, 1441, 1410, 1288, 1265, 741, 704.

1-(1*H*-Imidazol-1-yl)-2-((3*S*)-methyl-2-((1*E*,3*E*)-3-methylpenta-1,3-dien-1-yl) cyclohept-2-en-1-yl)ethan-1-one 245

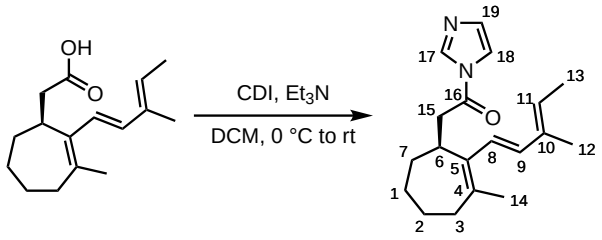

164 **245**

Experimental: To a stirred solution of carboxylic acid **164** (87 mg, 0.35 mmol, 1 equiv.) in 3.5 mL of dry DCM was added Et_3N (56 μL, 0.35 mmol, 1 equiv.), followed by CDI (113 mg, 0.7 mmol, 2 equiv.) portionwise over 15 min at 0 °C. The reaction mixture was then warmed up to rt and stirred in the dark for 5 h before being quenched with cold water (4 mL). The organic layer was washed with cold water (5 x 4 mL), dried over Na_2SO_4,

filtered and concentrated in vacuo. Carbonylimidazole **245** was directly engaged in the next step without additional purification.

Physical state: yellowish oil.

^{1}H NMR (400 MHz, $CDCl_3$) δ ppm: 8.10 (s, 1H, H_{17}), 7.43 (brs, 1H, H_{18}), 7.06 (brs, 1H, H_{19}), 6.25 (d, J = 16.1 Hz, 1H, H_9), 6.13 (d, J = 16.1 Hz, 1H, H_8), 5.51 (q, J = 13.1, 6.7 Hz, 1H, H_{11}), 3.52-3.42 (m, 1H, H_6), 3.06 (dd, J = 15.8, 8.7 Hz, 1H, H_{15}), 2.99 (dd, J = 15.8, 5.9 Hz, 1H, H_{15}), 2.44-2.32 (m, 1H, H_3), 2.21-2.10 (m, 1H, H_3), 1.85 (s, 3H, H_{14}), 1.74 (s, 3H, H_{12}), 1.69 (brs, 3H, H_{13}), 1.78-1.60 (m, 5H, $H_{1,\ 2\ and\ 7}$), 1.55-1.42 (m, 1H, H_1).

2-((3*S*)-methyl-2-((1*E*,3*E*)-3-methylpenta-1,3-dien-1-yl)cyclohept-2-en-1-yl)acetic pivalic anhydride 247

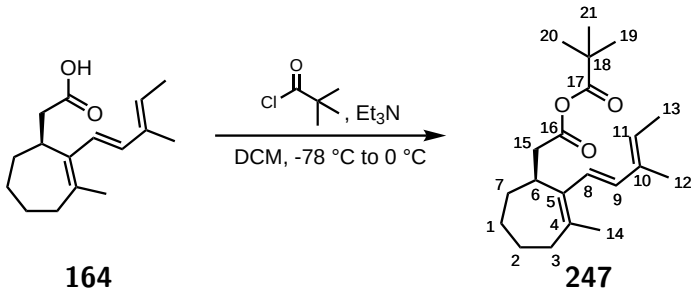

164 **247**

Experimental: To a stirred solution of carboxylic acid **164** (62 mg, 0.25 mmol, 1 equiv.) in 2 mL of dry DCM was added Et_3N (70 μL, 0.25 mmol, 1 equiv.), followed by a solution of pivaloyl chloride (60 μL, 0.5 mmol, 2 equiv.) in 0.5 mL of DCM dropwise at -78 °C. The reaction mixture was then warmed up to 0 °C and stirred in the dark for 30 min before being quenched with 4 mL of cold water. The aqueous layer was extracted with Et_2O (3 x 5 mL). The organic layers were combined, washed with cold water, cold brine, dried over Na_2SO_4, filtered and concentrated in vacuo. Anhydride **247** was directly engaged in

the next step without additional purification.

Physical state: yellowish oil.

^{1}**H NMR** (400 MHz, $CDCl_3$) δ ppm: 6.33 (d, J = 16.1 Hz, 1H, H_9), 6.24 (d, J = 16.1 Hz, 1H, H_8), 5.56 (q, J = 13.1, 6.7 Hz, 1H, H_{11}), 3.38-3.29 (m, 1H, H_6), 3.17 (td, J = 6.7, 3.4 Hz, 1H, H_{15}), 2.75-2.59 (m, 1H, H_{15}), 2.42-2.33 (m, 1H, H_3), 2.16-2.08 (m, 1H, H_3), 1.85 (s, 3H, H_{14}), 1.79 (t, J = 1.1 Hz, 3H, H_{12}), 1.74 (brs, 3H, H_{13}), 1.78-1.60 (m, 5H, $H_{1,\ 2\ and\ 7}$), 1.50-1.39 (m, 1H, H_1), 1.26 (s, 9H, $H_{19,\ 20\ and\ 21}$).

(5*S*)-1-Benzoyl-5-isobutyl-3-(2-((3*S*)-methyl-2-((1*E*,3*E*)-3-methylpenta-1,3-dien-1-yl)cyclohept-2-en-1-yl)acetyl)pyrrolidin-2-one 246

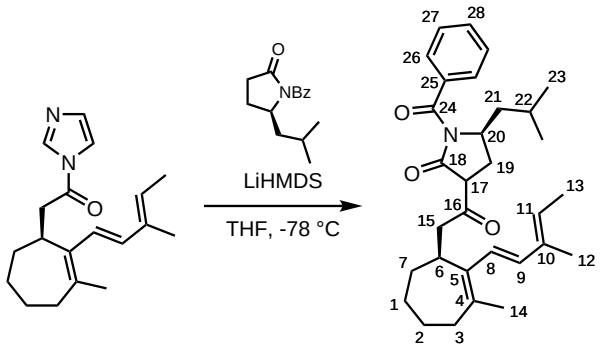

245 **246**

To a stirred solution of γ-lactam **163** (171 mg, 0.7 mmol, 2 equiv. supposed) in 1.5 mL of dry THF was added a 1 M solution of LiHMDS in THF (0.77 mL, 0.77 mmol, 2.2 equiv. supposed) dropwise at -78 °C. The reaction mixture was stirred 1 h at this temperature before adding a cold solution of carbonylimidazole **245** (0.35 mmol supposed, 1 equiv. supposed) in 1.5 mL of dry THF dropwise. After 2 h at -78 °C, the reaction mixture was quenched with a saturated solution of NH_4Cl (4 mL) and then allowed to warmed up

to rt. The aqueous layer was extracted with Et_2O (3 x 5 mL). The organic layers were combined, washed with brine, dried over Na_2SO_4, filtered and concentrated in vacuo. The crude product was purified via silica gel chromatography (PE/Et_2O 9:1) to yield 67 mg (40% yield over 2 steps) of triene **246**.

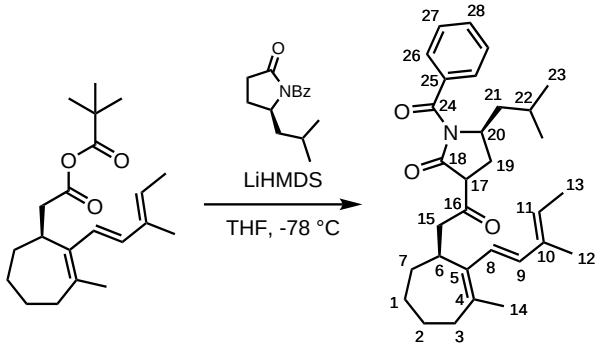

247 **246**

To a stirred solution of γ-lactam **163** (120 mg, 0.5 mmol, 2 equiv. supposed) in 1 mL of dry THF was added a 1 M solution of LiHMDS in THF (0.5 mL, 0.5 mmol, 2 equiv. supposed) dropwise at -78 °C. The reaction mixture was stirred 1 h at this temperature before adding a cold solution of anhydride **247** (0.25 mmol supposed, 1 equiv. supposed) in 1 mL of dry THF dropwise. After 5 h at -78 °C, the reaction mixture was quenched with a saturated solution of NH_4Cl (4 mL) and then allowed to warmed up to rt. The aqueous layer was extracted with Et_2O (3 x 5 mL). The organic layers were combined, washed with brine, dried over Na_2SO_4, filtered and concentrated in vacuo. The crude product was purified via silica gel chromatography (PE/Et_2O 9:1) to yield 69 mg (58% yield over 2 steps) of triene **246**.

Physical state: yellowish oil.

^{1}H NMR (400 MHz, $CDCl_3$) δ ppm: 7.65-7.48 (m, 3H, $H_{26\ and\ 28}$), 7.45-7.35 (m, 2H, H_{27}), 6.46-6.06 (m, 2H, $H_{8\ and\ 9}$), 5.65-5.46 (m, 1H, H_{11}), 4.62-4.31 (m, 1H, H_{20}), 3.50-3.22 (m,

1H, H_{17}), 2.60-1.98 (m, 5H, $H_{8,\ 15\ and\ 19}$), 1.92-1.52 (m, 17H, $H_{2,\ 3,\ 7,\ 12,\ 13,\ 14,\ 21\ and\ 22}$), 1.51-1.27 (m, 3H, $H_{1\ and\ 7}$), 1.04-0.93 (m, 6H, H_{23}).

^{13}C NMR (100 MHz, $CDCl_3$) δ ppm: 204.1 (C_{16}), 172.6 (C_{18}), 170.6 (C_{24}), 136.8 (C_5), 135.4 (C_{10}), 135.1 (C_4), 134.4 (C_{16}), 134.4 (C_{25}), 132.1 (C_9), 131.9 (C_{28}), 129.1 (C_{26}), 127.9 (C_{27}), 126.4 (C_{11}), 125.6 (C_8), 56.0 (C_{17}), 54.5 (C_{20}), 45.5 (C_{21}), 43.3 (C_{15}), 34.8 (C_6), 30.1 (C_3), 29.9 (C_{19}), 27.0 (C_7), 25.8 (C_1), 25.4 (C_2), 23.8 ($C_{22\ and\ 23}$), 22.8 (C_{22}), 21.6 (C_{14}), 14.0 (C_{13}), 12.6 (C_{12}).

HRMS(ESI+) m/z: calculated for $C_{31}H_{42}NO_3^+$ $[MH]^+$: 475.3086 found: 476.3159.

IR (ATR) ν (cm^{-1}): 3059, 3030, 2957, 2926, 2868, 2855, 1713, 1665, 1632, 1449, 1290, 1281, 1236.

$[\boldsymbol{\alpha}]_{\boldsymbol{D}}^{\mathbf{25}}$ +56.2 (c 0.8 in $CHCl_3$).

(*S*)-*tert*-Butyl,(1-(2,2-dimethyl-4,6-dioxo-1,3-dioxan-5-yl)-4-methyl-1-oxopentan-2-yl)carbamate 240

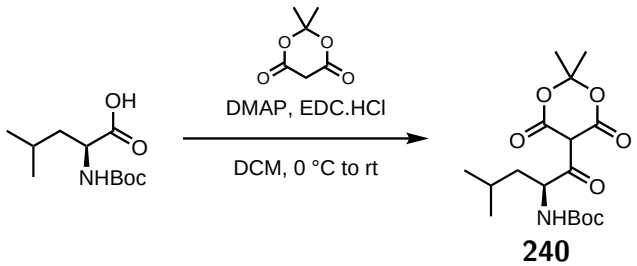

240

Experimental: To a stirred solution of N-Boc-L-leucine (23.1 g, 0.1 mol, 1 equiv.), Meldrum's acid (14.4 g, 0.1 mol, 1 equiv.) and DMAP (7.4 g, 0.2 mol, 2 equiv.) in 1 L

of dry dichloromethane was added EDC.HCl (38.3 g, 0.2 mol, 2 equiv.) portionwise over 50 minutes at 0 °C. The mixture was allowed to slowly warm up to rt and was stirred overnight. The reaction mixture was quenched with a 5 % solution of $KHSO_4$ (500 mL) then washed with brine, dried with $MgSO_4$, filtered and concentrated in vacuo. Meldrum's acid derivative **240** was engaged in the next step without additional purification.

(*S*)-*tert*-Butyl,(1-(2,2-dimethyl-4,6-dioxo-1,3-dioxan-5-yl)-4-methylpentan-2-yl)carbamate 241

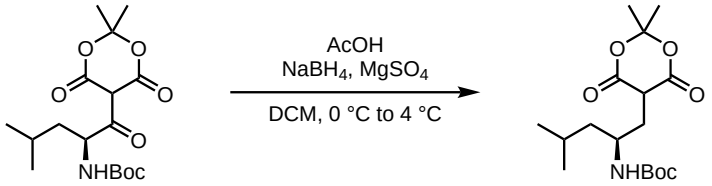

240 **241**

To a stirred solution of Meldrum's acid derivative **240** in 1 L of dry DCM was added 5 spatulas of $MgSO_4$ and AcOH (86 mL, 1.5 mol, 15 equiv.) at 0 °C. Then $NaBH_4$ (18.9 g, 0.5 mol, 5 equiv.) was added portionwise while stirring. After the gaz evolution ceased, the reaction mixture was left in the refrigerator (4°C) for 2 days. The reaction mixture was quenched with brine and stirred in air for 10 minutes. When no further hydrogen release was observed, the mixture was filtered and then washed with brine. The organic phase was dried with $MgSO_4$, filtered and concentrated in vacuo. The crude product was purified via silica gel chromatography (DCM/MeOH 98:2) to yield 28.0 g (83% yield over 2 steps) of alkyl Meldrum's acid derivative **241**.

All spectra and physical data matched published value.[4]

[4]M. Smrcina, P. Majer, E. Majerová, T. A. Guerassina, M. A. Eissenstat, *Tetrahedron* **1997**, *53*, 12867-12874.

(*R*)-*tert*-Butyl 2-isobutyl-5-oxopyrrolidine-1-carboxylate 243

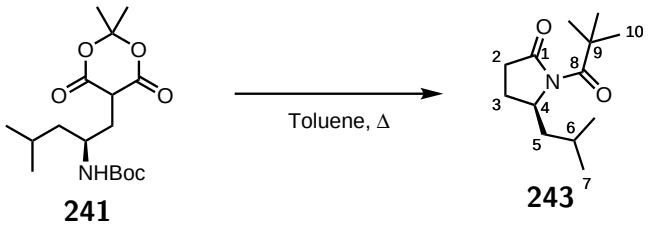

Experimental: Alkyl Meldrum's acid derivative **241** (27.5 g, 80 mmol) was refluxed in 500 mL of toluene overnight. Toluene was evaporated and *N*-Boc protected γ-lactam **243** was engaged in the next step without any additional purification.

All spectra and physical data matched published value.[4]

^{1}H NMR (400 MHz, $CDCl_3$) δ ppm: 4.20-4.09 (m, 1H, H_4), 2.58 (ddd, J = 17.7, 11.4, 9.1 Hz, 1H, H_2), 2.40 (ddd, J = 17.7, 9.3, 2.3 Hz, 1H, H_2), 2.16-2.00 (m, 1H, H_3), 1.81-1.70 (m, 1H, H_3), 1.65-1.61 (m, 1H, H_6), 1.61-1.56 (m, 1H, H_5), 1.52 (s, 9H, H_{10}), 1.40 (td, J = 12.3, 3.3 Hz, 1H, H_5), 0.96 (d, J = 1.7 Hz, 3H, H_7), 0.94 (d, J = 1.5 Hz, 3H, H_7).

^{13}C NMR (100 MHz, $CDCl_3$) δ ppm: 174.6 (C_1), 150.0 (C_8), 82.8 (C_9), 56.8 (C_4), 42.6 (C_5), 31.3 (C_2), 28.2 (C_{10}), 25.4 (C_6), 24.0 (C_7), 22.8 (C_3), 21.6 (C_7).

(5*R*)-Isobutylpyrrolidin-2-one 244

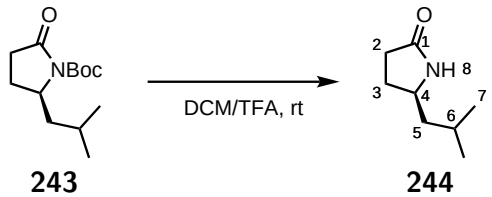

Experimental: To a stirred solution of N-Boc protected γ-lactam **243** in 80 mL of dry DCM was added 80 mL of TFA at rt. The reaction mixture was stirred for 4 h before being

carefully quenched with a saturated solution of $NaHCO_3$ until pH reached neutrality. The reaction mixture was extracted with DCM (3 x 50 mL), dried over Na_2SO_4, filtered and concentrated in vacuo to yield to 10.6 g (94% over 2 steps) of γ-lactam **244**. γ-Lactam **244** was engaged in the next step without any additional purification.

All spectra and physical data matched published value.[4]

^{1}**H NMR** (400 MHz, $CDCl_3$) δ ppm: 7.53 (brs, H_8), 3.71 (p, J = 7.1 Hz, 1H, H_4), 2.28-2.20 (m, 2H, H_5), 2.20-2.09 (m, 1H, H_6), 1.64-1.53 (m, 2H, H_2), 1.31 (m, 2H, H_3), 0.85 (d, J = 3.4 Hz, 3H, H_7), 0.84 (d, J = 3.4 Hz, 3H, H_7).

^{13}**C NMR** (100 MHz, $CDCl_3$) δ ppm: 178.8 (C_1), 52.9 (C_4), 46.0 (C_5), 30.5 (C_2), 27.7 (C_3), 25.1 (C_6), 22.9 (C_7), 22.4 (C_7).

(1*R*)-Benzoyl-5-isobutylpyrrolidin-2-one 163

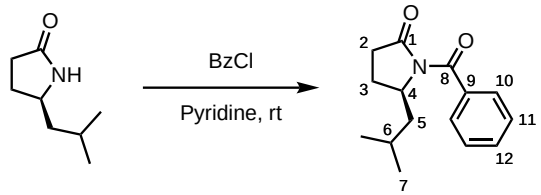

244 **163**

Experimental: To a stirred solution of γ-lactam **244** (2.68 g, 19 mmol, 1 equiv.) in 47 mL of dry pyridine was added benzoyl chloride (4.4 mL, 38 mmol, 2 equiv.) at rt. The reaction mixture was stirred for 5 h and Et_2O was added. The slurry was filtered through celite and the solution was concentrated in vacuo. The crude product was purified via silica gel chromatography (DCM) to yield 3.05 g (65% yield) *N*-benzoylated γ-lactam **163**.

All spectra and physical data matched published value.[4]

^{1}**H NMR** (400 MHz, $CDCl_3$) δ ppm: 7.64-7.55 (m, 2H, H_{10}), 7.51 (t, J = 7.4 Hz, 1H, H_{12}), 7.40 (t, J = 7.6 Hz, 2H, H_{11}), 4.54 (ddt, J = 10.0, 8.0, 4.1 Hz, 1H, H_4), 2.74-2.60 (m, 1H,

H_2), 2.49 (ddd, J = 17.8, 9.3, 5.4 Hz, 1H, H_2), 2.27 (ddd, J = 17.3, 12.8, 8.2 Hz, 1H, H_3), 1.91-1.79 (m, 1H, H_3), 1.84-1.78 (m, 1H, H_5), 1.76-1.65 (m, 1H, H_6), 1.42 (ddd, J = 13.0, 9.9, 4.5 Hz, 1H, H_5), 1.00 (d, J = 6.5 Hz, 3H, H_7), 0.97 (d, J = 6.6 Hz, 3H, H_6).

^{13}C NMR (100 MHz, $CDCl_3$) δ ppm: 175.1 (C_1), 171.0 (C_8), 135.1 (C_9), 132.1 (C_{12}), 129.0 (C_{10}), 128.0 (C_{11}), 56.5 (C_4), 42.8 (C_5), 32.0 (C_2), 25.3 (C_6), 23.9 (C_7), 23.7 (C_3), 21.7 (C_7).

(5*S*)-1-Benzoyl-5-isobutyl-3-(2-((3*S*)-methyl-2-((1*E*,3*E*)-3-methylpenta-1,3-dien-1-yl)cyclohept-2-en-1-yl)acetyl)-3-(phenylselanyl)pyrrolidin-2-one 248

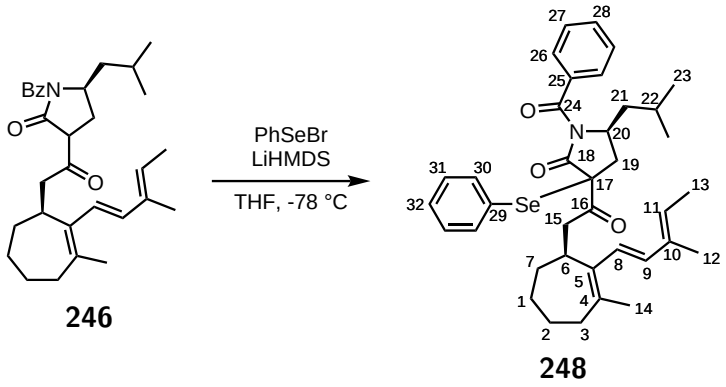

Experimental: To a stirred solution of triene **246** (48 mg, 109 μmol, 1 equiv.) in 0.5 mL of dry THF was added a 1 M solution of LiHMDS in THF (120 μL, 120 μmol, 1.1 equiv.) dropwise at -78 °C. The reaction mixture was stirred 1 h at this temperature before adding a cold solution of PhSeBr (36 mg, 150 μmol, 1.4 equiv.) in 0.5 mL of dry THF dropwise. After 2 h at -78 °C, the reaction mixture was quenched with a saturated solution of NH_4Cl (2 mL) and then allowed to warmed up to rt. The aqueous layer was extracted with Et_2O (3 x 5 mL). The organic layers were combined, washed with brine, dried over Na_2SO_4, filtered and concentrated in vacuo. The crude product was purified via silica gel

chromatography (PE/Et_2O 20:1) to yield 65 mg (95% yield) of selenium derivative **248**.

Physical state: yellowish oil.

^{1}H NMR (400 MHz, $CDCl_3$) δ ppm: 7.27-7.68 (m, 10H, $H_{26,\ 27,\ 28,\ 30,\ 31\ and\ 32}$), 6.42-6.06 (m, 2H, $H_{8\ and\ 9}$), 5.63-5.36 (m, 1H, H_{11}), 4.38-4.06 (m, 1H, H_{20}), 2.55-1.93 (m, 3H, $H_{8\ and\ 15}$), 1.90-1.46 (m, 19H, $H_{2,\ 3,\ 7,\ 12,\ 13,\ 14,\ 19,\ 21\ and\ 22}$), 1.38-1.08 (m, 3H, $H_{1\ and\ 7}$), 0.96-0.76 (m, 6H, H_{23}).

^{13}C NMR (100 MHz, $CDCl_3$) δ ppm: 201.3, 200.3, 170.9, 137.6, 137.2, 135.3, 134.5, 132.7, 131.4, 130.2, 129.4, 129.3, 128.1, 125.9, 60.7, 54.2, 53.1, 40.5, 35.4, 32.6, 29.7, 25.9, 25.2, 24.8, 23.9, 22.8, 21.2, 14.1, 12.3.

HRMS(ESI+) m/z: calculated for $C_{37}H_{46}NO_3Se^+$ $[MH]^+$: 632.2637 found: 632.2628.

IR (ATR) ν (cm^{-1}): 2957, 2924, 2866, 2857, 1724, 1690, 1288, 1273, 1231.

$[\boldsymbol{\alpha}]_{\boldsymbol{D}}^{\mathbf{25}}$ +109.1 (c 1.0 in $CHCl_3$).

(3*S*,3a*R*,4*S*,6a*S*,8a*S*,13b*R*)-5-benzoyl-4-isobutyl-2,3,13-trimethyl-3,4,5,8,8a,9,10, 11,12,13b-decahydro-6H-cyclohepta[3,4]benzo[1,2-d]isoindole-6,7(3aH)-dione 273

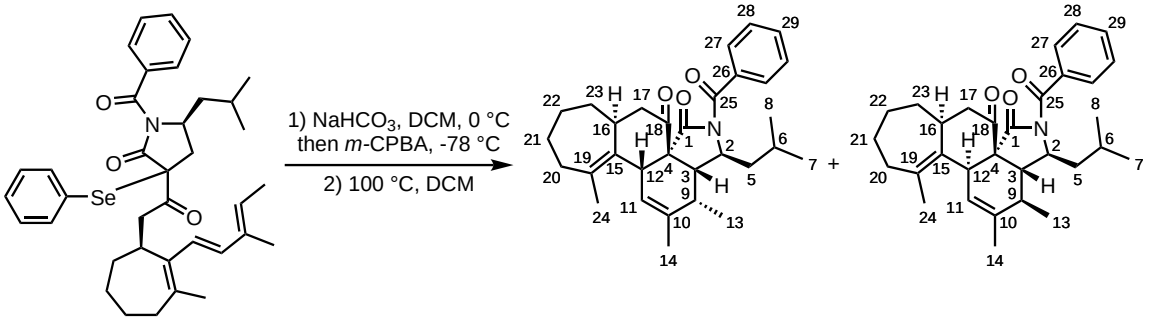

Experimental: To a stirred solution of triene **246** (70 mg, 110 μmol, 1 equiv.) in 10 mL of dry DCM was added $NaHCO_3$ (20 mg, 236 μmol, 2.1 equiv.) at 0 °C. The reaction mixture was cooled down to -78 °C and a cold solution of *m*-CPBA (50 mg, 220 μmol, 2 equiv.) in 1 mL of dry DCM dropwise at -78 °C. After 1 h at -78 °C, the reaction mixture was quenched with a saturated solution of $Na_2S_2O_3$ (5 mL) and then allowed to warmed up to rt. The organic layer was washed with cold $NaHCO_3$ (5 mL), cold water (5 mL) and cold brine (5 mL), dried over Na_2SO_4, filtered and transferred into a flame-dry sealed tube with a catalytic amount of BHT. The resulting solution was heated at 100 °C overnight before being cold down to rt and concentrated in vacuo. The crude product was purified via silica gel chromatography (PE/Et_2O 20:1 to 9:1) to yield 17.7 mg (38% yield) of *endo*-tetracyclic product **273** and 12.5 mg (27% yield over 2 steps) of *exo*-tetracyclic product **285**.

Physical state: yellowish oil.

^{1}**H NMR** (400 MHz, $CDCl_3$) δ ppm: *endo*-product **273**: 7.50-7.45 (m, 3H, $H_{27\ and\ 29}$), 7.40-7.34 (m, 2H, H_{28}), 5.78 (brs, 1H, H_{11}), 4.33-4.30 (m, 1H, H_2), 3.56-3.48 (m, 1H, H_{16}), 3.35 (brs, 1H, H_{12}), 2.75 (dd, J = 6.3, 1.8 Hz, 1H, H_3), 2.69 (dd, J = 16.5, 5.5 Hz, 1H, H_{17}),

2.56-2.44 (m, 1H, H_9), 2.30 (dd, J = 16.6, 11.3 Hz, H_{17}), 2.20-2.09 (m, 2H, H_{20}), 1.85-1.79 (m, 1H, H_5), 1.79 (s, 3H, H_{14}), 1.72-1.67 (m, 2H, $H_{21\ and\ 22}$), 1.65 (s, 3H, H_{24}), 1.64-1.56 (m, 3H, $H_{5\ and\ 23}$), 1.54-1.47 (m, 3H, $H_{6,\ 21 and\ 22}$), 1.31 (d, J = 7.3 Hz, 3H, H_{13}), 0.99 (d, J = 4.5 Hz, 3H, $H_{7\ or\ 8}$), 0.98 (d, J = 4.5 Hz, 3H, $H_{7\ or\ 8}$).

exo-product **285**: 7.77-7.73 (m, 2H, H_{27}), 7.52-7.48 (m, 1H, H_{29}), 7.41-7.37 (m, 2H, H_{28}), 5.48-5.45 (m, 1H, H_{11}), 4.24-4.20 (m, 1H, H_2), 3.51-3.47 (m, 1H, H_{12}), 2.92-2.84 (m, 1H, H_{16}), 2.69 (t, J = 13.2 Hz, 1H, H_{17}), 2.32 (d, J = 4.3 Hz, 1H, H_3), 2.31-2.24 (m, 2H, $H_{17\ and\ 20}$), 2.17-2.09 (m, 1H, H_9), 2.00-1.84 (m, 2H, $H_{20\ and\ 22}$), 1.80 (s, 3H, H_{14}), 1.78-1.71 (m, 1H, $H_{5\ and\ 6}$), 1.71-1.66 (m, 2H, $H_{5\ and\ 21}$), 1.63 (d, J = 1.6 Hz, 3H, H_{24}), 1.62-1.54 (m, 1H, H_{22}), 1.60-1.46 (m, 1H, H_{23}), 1.36-1.28 (m, 1H, H_{23}), 1.20-1.16 (m, 1H, H_{21}), 1.13 (d, J = 7.4 Hz, 3H, H_{13}), 0.97 (d, J = 6.4 Hz, 3H, $H_{7\ or\ 8}$), 0.92 (d, J = 6.4 Hz, 3H, $H_{7\ or\ 8}$).

^{13}C NMR (100 MHz, $CDCl_3$) δ ppm: *endo*-product **273**: 208.4 (C_{18}), 171.7 (C_1), 170.5 (C_{25}), 137.1 (C_{10}), 135.1 (C_{19}), 134.8 (C_{26}), 133.4 (C_{15}), 132.1 (C_{29}), 129.8 (C_{11}), 128.7 (C_{27}), 128.0 (C_{28}), 69.6 (C_4), 54.4 (C_2), 47.7 (C_{17}), 46.0 (C_3), 44.7 (C_5), 43.2 (C_{12}), 37.3 (C_{16}), 35.0 (C_{20}), 34.5 (C_9), 33.7 (C_{22}), 27.3 (C_{23}), 24.7 (C_6), 24.4 (C_{21}), 24.2 (C_{24}), 24.1 ($C_{7\ or\ 8}$), 21.9 ($C_{7\ or\ 8}$), 19.4 (C_{14}), ($C_{13.5}$).

exo-product **285**: 211.6 (C_{18}), 173.4 (C_1), 171.7 (C_{25}), 137.1 (C_{19}), 136.6 (C_{10}), 134.3 (C_{26}), 135.9 (C_{15}), 132.8 (C_{29}), 129.8 (C_{27}), 128.0 (C_{28}), 125.3 (C_{11}), 60.4 (C_4), 57.9 (C_2), 49.5 (C_3), 45.2 (C_{17}), 42.6 (C_5), 39.4 (C_{12}), 38.9 (C_{16}), 36.1 (C_{20}), 33.1 (C_9), 31.7 (C_{22}), 26.9 (C_{23}), 25.1 (C_{21}), 24.8 (C_6), 23.5 ($C_{7\ or\ 8}$), 23.0 ($C_{7\ or\ 8}$), 21.6 (C_{14}), 21.3 (C_{24}), 18.5 (C_{13}).

HRMS(ESI+) m/z: calculated for $C_{31}H_{40}NO_3^+$ $[MH]^+$: 474.3003 found: 474.3005.

IR (ATR) ν (cm^{-1}): 2957, 2922, 2851, 1740, 1736, 1701, 1684, 1653, 1448, 1283, 1244, 1201, 1163, 721, 694, 660.

((3*S*,3a*R*,4*S*,6a*S*,8a*S*,13b*R*)-4-isobutyl-2,3,13-trimethyl-3,4,5,8,8a,9,10,11,12,13b-decahydro-6H-cyclohepta[3,4]benzo[1,2-d]isoindole-6,7(3aH)-dione 1

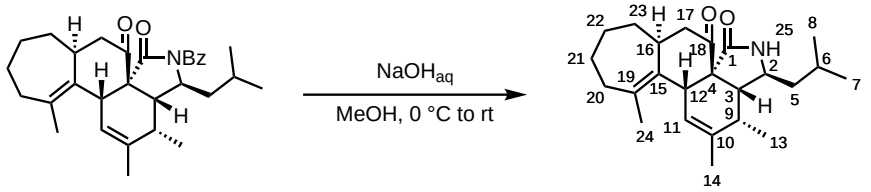

273 **1**

Experimental: To a stirred solution of tetracyclic product **273** (17.7 mg, 37 μmol, 1 equiv.) in 0.8 mL of MeOH was added a 14.8 M solution of NaOH in water (10 μL, 150 μmol, 4 equiv.) at 0 °C. The reaction mixture was allowed to warm up to rt over 2 h. The reaction mixture was quenched with a water (0.5 mL). The aqueous layer was extracted with Et_2O (3 x 0.5 mL). The organic layers were combined, washed with brine, dried over Na_2SO_4, filtered and concentrated in vacuo. The crude product was purified via silica gel chromatography (DCM/Et_2O 95:5) to yield 11.8 mg (87% yield) of deprotected tetracyclic product **1**.

Physical state: colorless oil.

^{1}**H NMR** (400 MHz, $CDCl_3$) δ ppm: 5.94 (s, 1H, H_{11}), 5.58 (s, 1H, H_{25}), 3.64-3.53 (m, 1H, H_{16}), 3.28 (s, brs, H_{12}), 3.16 (td, J = 10.1, 3.5 Hz, 1H, H_2), 2.69 (dd, J = 5.3, 3.5 Hz, 1H, H_3), 2.56 (dd, J = 17.3, 5.5 Hz, 1H, H_{17}), 2.42-2.28 (m, 2H, $H_{9\ and\ 20}$), 2.28 (dd, 1H, J = 17.3, 12.2 Hz, 1H, H_{17}), 2.19-2.08 (m, 1H, H_{20}), 1.88-1.79 (m, 1H, H_5), 1.76 (s, 3H, H_{14}), 1.73 (s, 3H, H_{24}), 1.71-1.41 (m, 6H, $H_{5,\ 21,\ 22\ and\ 23}$), 1.36-1.28 (m, 1H, H_{21}), 1.17 (d, J = 7.2 Hz, 3H, H_{13}), 0.97 (d, J = 6.8 Hz, 3H, $H_{7\ or\ 8}$), 0.92 (d, J = 6.8 Hz, 3H, $H_{7\ or\ 8}$).

^{13}**C NMR** (100 MHz, $CDCl_3$) δ ppm: 210.5 (C_{18}), 173.3 (C_1), 136.9 (C_{10}), 134.9 (C_{19}),

133.6 (C_{15}), 128.5 (C_{11}), 65.8 (C_4), 51.2 (C_2), 51.1 (C_3), 47.8 (C_{17}), 47.2 (C_5), 41.6 (C_{12}), 36.6 (C_{16}), 35.7 (C_{22}), 34.7 (C_9), 33.5 ($C_{20\ and\ 23}$), 28.2 (C_{21}), 24.2 (C_6), 23.7 (C_{24}), 21.5 ($C_{7\ and\ 8}$), 20.2 (C_{14}), 13.6 (C_{13}).

HRMS(ESI+) m/z: calculated for $C_{24}H_{36}NO_2^+$ $[MH]^+$: 370.2741 found: 370.2730.

IR (ATR) ν (cm^{-1}): 2957, 2922, 2851, 1688, 1653, 1554, 1273, 1264, 745, 696, 664.

(3*S*,3a*R*,4*S*,6a*R*,8a*S*,14b*S*)-5-benzoyl-13-hydroxy-4-isobutyl-2,3,13-trimethyl -3,3a,4,5,8a,9,10,11,12,13,14a,14b-dodecahydro-6H-oxocino[2',3':3,4]benzo[1,2-d] isoindole-6,7(8H)-dione 296

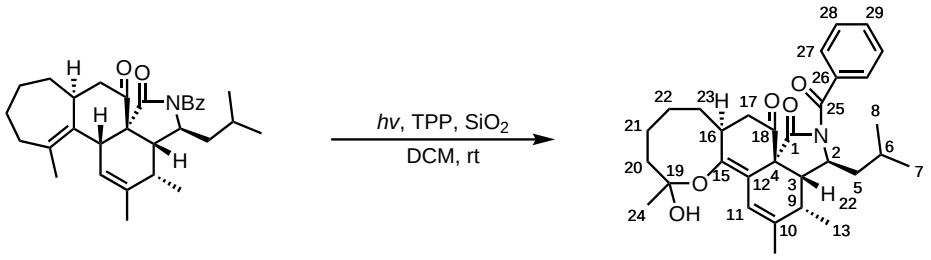

273 **296**

Experimental: To a stirred solution of tetracyclic product **273** (6 mg, 14 μmol, 1 equiv.) in 1 mL of DCM was added a catalytic amount of TPP and SiO_2 at rt. The reaction mixture was purged with O_2 and irradiated with white LED light at rt. After 3 h, the reaction mixture was filtered and concentrated in vacuo. The crude product was purified via silica gel chromatography (PE/EA 9:1 to 4:1) to yield 2 mg (31% yield) of acetal **296**.

Physical state: colorless oil.

^{1}H NMR (400 MHz, $CDCl_3$) δ ppm: 7.57-7.48 (m, 2H, H_{27}), 7.48-7.46 (m, 1H, H_{29}), 7.39-7.36 (m, 2H, H_{28}), 6.58 (brs, 1H, H_{11}), 4.37-4.34 (m, 1H, H_2), 3.45-3.41 (m, 2H, H_{17}), 3.00-2.98 (m, 1H, H_3), 2.62-2.57 (m, 1H, H_{16}), 2.35-2.32 (m, 3H, $H_{9\ and\ 23}$), 2.29-2.27 (m, 2H, H_{20}), 1.90 (t, J = 1.5 Hz, 3H, H_{14}), 1.87-1.83 (m, 2H, H_5), 1.75-1.70 (m, 2H, H_{21}), 1.65-1.58 (m, 1H, H_6), 1.33 (s, 3H, H_{24}), 1.32-1.30 (m, 5H, $H_{13\ and\ 22}$), 1.02-1.00 (dd, J = 6.5, 1.8 Hz, $H_{7\ and\ 8}$).

^{13}C NMR (100 MHz, $CDCl_3$) δ ppm: 204.1 (C_{18}), 171.5 (C_1), 170.5 (C_{25}), 143.3 (C_{15}), 141.3 (C_{10}), 134.5 (C_6), 132.6 (C_{29}), 128.8 (C_{27}), 128.1 (C_{12}), 128.2 (C_{28}), 125.9 (C_{11}), 88.5 (C_{19}), 70.8 (C_4), 55.3 (C_2), 46.8 (C_{17}), 45.3 (C_5), 43.6 (C_3), 40.7 (C_{20}), 39.3 (C_{16}), 35.2 (C_9), 35.1 (C_{23}), 30.1 (C_{21}), 29.9 (C_{22}), 25.7 (C_{24}), 24.6 (C_6), 23.7 ($C_{7\ or\ 8}$), 22.2 ($C_{7\ or\ 8}$), 20.1 (C_{14}), 13.7 (C_{13}).

HRMS(ESI+) m/z: calculated for $C_{31}H_{40}NO_5^+$ $[MH]^+$: 506.2901 found: 506.2904.

IR (ATR) ν (cm^{-1}): 3368, 2930, 2847, 1714, 1691, 1450, 1365, 1277, 1152, 800.

(2a*R*,5*S*,5a*R*,6*S*,8a*S*,13a*S*)-4-benzoyl-5-isobutyl-6,7,9a-trimethyl-5,5a,6,8a,9a,10,11,12,13,13a-decahydrooxireno[2",3":1',7']cyclohepta[1',2':3,4]benzo[1,2-d]isoindole-2,3(1H,4H)-dione 303

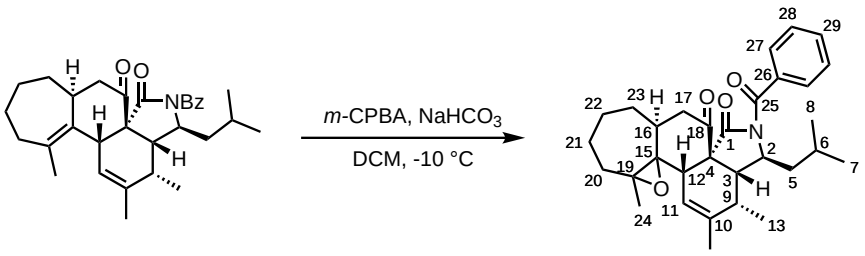

273 **303**

Experimental: To a stirred solution of tetracyclic product **273** (6 mg, 12 μmol, 1 equiv.) and $NaHCO_3$ (1 mg, 12 μmol, 1 equiv.) in 0.3 mL of DCM was added a solution of *m*-CPBA (2.8 mg, 12 μmol, 1 equiv.) in 0.1 mL of DCM. The reaction mixture was allowed to warm up to -10 °C over 2 h before being quenched with a saturated solution of $Na_2S_2O_3$ (1 mL). The reaction was allowed to warm up to rt and the organic layer was washed with a saturated solution of $NaHCO_3$ (1 mL), brine (1 mL), dried with Na_2SO_4, filtered and concentrated in vacuo. The crude product was purified via silica gel chromatography (PE/EA 9:1) to yield 4.4 mg (75% yield) of a mixture of diastereoisomers **303**.

Physical state: colorless oil.

^{1}H NMR (400 MHz, C_6D_6) δ ppm: Data for major diastereoisomer: 7.63-7.58 (m, 2H, H_{27}), 7.09-7.02 (m, 3H, $H_{28\ and\ 29}$), 5.84-5.89 (m, 1H, H_{11}), 4.55-4.50 (m, 1H, H_2), 3.96 (dd, J = 12.1, 6.8 Hz, 1H, H_{17}), 3.14 (d, J = 6.6 Hz, 1H, H_{12}), 2.81-2.76 (m, 1H, H_3), 2.31-2.23 (m, 1H, H_{16}), 2.03 (t, J = 7.2 Hz 1H, H_9), 1.96 (dd, J = 12.1, 2.4 Hz, 1H, H), 1.81-1.59 (m, 4H, $H_{5,\ 6\ and\ 20}$), 1.58-1.55 (m, 3H, H_{14}), 1.54-1.25 (m, 8H, $H_{20,\ 21,\ 22\ and\ 23}$), 1.14 (d, J = 0.8 Hz, 3H, H_{24}), 1.04 (d, J = 6.4 Hz, 9H, $H_{7\,8\ and\ 13}$).

Data for minor diastereoisomer: 7.78-7.81 (m, 2H, H_{27}), 7.04-6.96 (m, 3H, $H_{28\ and\ 29}$), 5.94 (brs, 1H, H_{11}), 4.40-4.36 (m, 1H, H_2), 3.15-3.11 (m, 1H, H_{12}), 2.79 (t, J = 4.9 Hz, 1H, H_3), 2.52-2.44 (m, 2H, $H_{16\ and\ 17}$), 2.36-2.30 (m, 1H, H_{17}), 1.85-1.71 (m, 4H, $H_{5,\ 6,\ and\ 9}$), 1.68-1.51 (m, 5H, $H_{20,\ 21,\ and\ 23}$), 1.57 (brs, 3H, H_{14}), 1.51-1.47 (m, 2H, H_{22}), 1.27-1.21 (m, 1H, H_{21}), 1.24 (s, 3H, H_{24}), 1.00 (d, J = 5.9 Hz, 3H, $H_{7\ and\ 8}$), 0.93 (d, J = 7.4 Hz, 3H, H_{13}), 0.89 (d, J = 5.9 Hz, 3H, $H_{7\ and\ 8}$).

^{13}C NMR (100 MHz, C_6D_6) δ ppm: Data for major diastereoisomer: 204.1 (C_{18}), 171.4 (C_1), 170.0 (C_{25}), 137.5 (C_{10}), 135.5 (C_{26}), 131.9 ($C_{28\ or\ 29}$), 129.1 (C_{27}), 128.4 ($C_{28\ or\ 29}$), 124.9 (C_{11}), 71.4 (C_4), 64.0 (C_{15}), 61.2 (C_{19}), 54.7 (C_2), 45.8 (C_{16}), 45.0 (C_5), 44.2 (C_3), 43.6 (C_{17}), 41.4 (C_{12}), 38.4 (C_{20}), 34.3 (C_9), 34.0 (C_{23}), 29.1 (C_{22}), 25.1 (C_6), 24.1 (C_{21}), 23.9 ($C_{7\ or\ 8}$), 21.9 ($C_{7\ or\ 8}$), 19.4 (C_{14}), 18.0 (C_{24}), 13.4 (C_{13}).
Data for minor diastereoisomer: 208.4 (C_{18}), 172.4 (C_1), 170.8 (C_{25}), 138.0 (C_{10}), 135.1 (C_{26}), 132.6 (C_{29}), 130.0 (C_{27}), 128.3 (C_{28}), 122.9 (C_{11}), 66.1 (C_4), 66.0 (C_{19}), 65.2 (C_{15}), 56.0 (C_2), 48.5 (C_3), 47.5 (C_5), 46.6 (C_{17}), 42.2 (C_{12}), 35.8 (C_{20}), 35.1 (C_9), 34.8 (C_{16}), 29.7 (C_{22}), 29.6 (C_{23}), 25.0 (C_6), 24.0 ($C_{7\ or\ 8}$), 23.6 (C_{21}), 22.7 ($C_{7\ or\ 8}$), 21.3 (C_{24}), 20.5 (C_{14}), 14.7 (C_{13}).

HRMS(ESI+) m/z: calculated for $C_{31}H_{40}NO_4^+$ $[MH]^+$: 490.2952 found: 490.2953.

IR (ATR) ν (cm^{-1}): 2926, 2854, 1714, 1690, 1452, 1366, 1280, 1212, 1155.

(2a*R*,5*S*,5a*R*,6*R*,8a*R*,13a*S*)-4-benzoyl-5-isobutyl-6,7,9a-trimethyl-5,5a,6,8a,9a,10,11,12,13,13a-decahydrooxireno[2",3":1',7']cyclohepta[1',2':3,4]benzo[1,2-d]isoindole-2,3(1H,4H)-dione 309

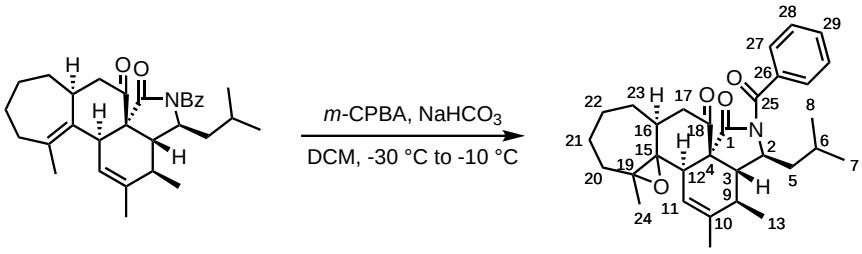

273 **309**

Experimental: To a stirred solution of tetracyclic product **273** (7.3 mg, 15.4 μmol, 1 equiv.) and $NaHCO_3$ (1.3 mg, 15.4 μmol, 1 equiv.) in 0.4 mL of DCM was added a solution of *m*-CPBA (3.5 mg, 15.4 μmol, 1 equiv.) in 0.1 mL of DCM. The reaction mixture was allowed to warm up to -10 °C over 2 h before being quenched with a saturated solution of $Na_2S_2O_3$ (1 mL). The reaction was allowed to warm up to rt and the organic layer was washed with a saturated solution of $NaHCO_3$ (1 mL), brine (1 mL), dried with Na_2SO_4, filtered and concentrated in vacuo. The crude product was purified via silica gel chromatography (PE/EA 9:1) to yield 3 mg (40% yield) of epoxide **309**.

Physical state: colorless oil.

^{1}H NMR (400 MHz, benzene-d_6) δ ppm: 7.81-7.77 (m, 2H, H_{27}), 7.12-7.00 (m, 3H, $H_{28\ and\ 29}$), 5.36 (brs, 1H, H_{11}), 4.31-4.25 (m, 1H, H_2), 3.87-3.78 (m, 1H, H_{12}), 2.94 (dd, J = 7.0, 5.4 Hz, 1H, H_3), 2.78-2.73 (m, 1H, H_{17}), 2.23-2.14 (m, 1H, H_{16}), 2.18-2.03 (m, 1H, H_{17}), 1.90-1.57 (m, 8H, $H_{5,\ 6,\ 9,\ 20,\ 21\ and\ 22}$), 1.55-1.52 (m, 3H, H_{14}), 1.50-1.35 (m, 3H, $H_{20\ and\ 23}$), 1.17-1.07 (m, 1H, H_{21}), 1.15 (d, J = 7.2 Hz, 3H, H_{13}), 1.11 (brs, 3H, H_{24}), 0.95 (d, J = 6.5 Hz, $H_{7\ or\ 8}$), 0.91 (d, J = 6.5 Hz, $H_{7\ or\ 8}$).

^{13}**C NMR** (100 MHz, benzene-d_6) δ ppm: 205.4 (C_{18}), 172.0 (C_1), 171.4 (C_{25}), 139.3 (C_{10}), 135.2 (C_{26}), 132.4 (C_{29}), 130.2 (C_{27}), 127.9 (C_{28}), 122.9 (C_{11}), 65.3 (C_{15}), 63.3 (C_{19}), 61.6 (C_4), 57.4 (C_2), 45.1 (C_{12}), 45.1 (C_{16}), 44.8 (C_{17}), 43.9 (C_3), 42.8 (C_5), 37.0 (C_{20}), 33.4 (C_9), 33.1 (C_{22}), 30.7 (C_{23}), 25.0 (C_6), 25.0 (C_{21}), 23.7 ($C_{7\ or\ 8}$), 23.2 ($C_{7\ or\ 8}$), 21.5 (C_{14}), 20.1 (C_{24}), 18.4 (C_{13}).

HRMS(ESI+) m/z: calculated for $C_{31}H_{40}NO_4^+$ $[MH]^+$: 490.2952 found: 490.2953.

IR (ATR) ν (cm^{-1}): 2937, 1739, 1710, 1680, 1451, 1413, 1366, 1283, 1245, 1212, 1191, 1143, 1081, 1019, 911, 894, 799.

(5a*S*,7a*R*,10*S*,10a*R*,11*S*,12b*R*)-9-benzoyl-10-isobutyl-1,11,11a-trimethyl-2,4,5,5a,6,9,10,10a,11,11a,12a,12b-dodecahydro-7H-cyclohepta[3,4]benzo[1,2-d]oxireno[2,3-f]isoindole-7,8(3H)-dione 301

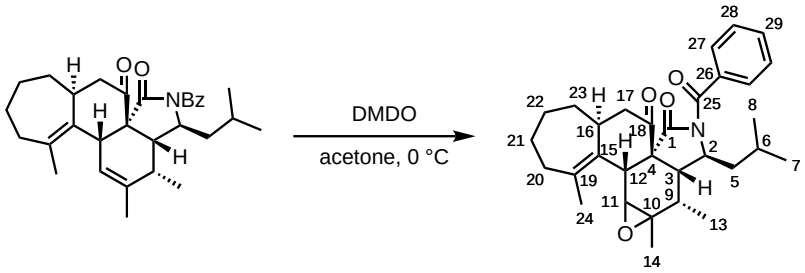

273 **301**

Experimental: To a stirred solution of tetracyclic product **273** (15.6 mg, 33 μmol, 1 equiv.) in 140 μL of acetone was added a freshly prepared solution of DMDO (260 μL, 36 μmol, 1.1 equiv.) at 0 °C.[5] The reaction mixture was stirred at 0 °C until completion. The reaction mixture was quenched with a saturated solution of $Na_2S_2O_3$ (1 mL), washed with brine (1 mL), dried with Na_2SO_4, filtered and concentrated in vacuo. The crude product

[5]D. F. Taber, P. W. DeMatteo, R. A. Hassan, *Org. Synth.* **2013**, *90*, 350-357.

was purified via silica gel chromatography (PE/Et_2O 9:1) to yield 6.5 mg (40% yield) of epoxide **301**.

Physical state: colorless oil.

^{1}H NMR (400 MHz, $CDCl_3$) δ ppm: 7.58-7.54 (m, 2H, H_{27}), 7.54-7.51 (m, 1H, H_{29}), 7.44-7.39 (m, 2H, H_{28}), 4.60-4.54 (m, 1H, H_2), 3.42-3.31 (m, 1H, H_{16}), 3.13 (d, J = 5.9 Hz, 1H, H_{11}), 2.84-2.76 (m, 3H, $H_{3,\ 12\ and\ 17}$), 2.36-2.26 (m, 2H, $H_{17\ and\ 20}$), 2.08-1.99 (m, 1H, H_{20}), 1.86 (t, J = 1.9 Hz, 3H, H_{24}), 1.90-1.79 (m, 2H, $H_{5\ and\ 9}$), 1.72-1.36 (m, 8H, $H_{5,\ 6,\ 21,\ 22\ and\ 23}$), 1.28-1.24 (m, 6H, $H_{13\ and\ 14}$), 0.99 (dd, J = 8.0, 6.2 Hz, 6H, $H_{7\ and\ 8}$).

^{13}C NMR (100 MHz, $CDCl_3$) δ ppm: 207.4 (C_{18}), 171.4 (C_1), 170.8 (C_{25}), 136.8 (C_{19}), 134.4 (C_{26}), 132.9 (C), 131.4 (C_{15}), 129.1 (C_{27}), 128.4 (C_{29}), 66.9 (C_4), 64.5 (C_{11}), 60.9 (C_{10}), 53.6 (C_2), 46.8 (C_{17}), 45.5 (C_{12}), 44.8 (C_3), 44.5 (C_5), 38.3 (C_{16}), 36.6 (C_9), 36.4 (C_{20}), 34.6 (C_{22}), 28.2 (C_{23}), 24.8 (C_6), 23.7 ($C_{7\ or\ 8}$), 23.5 (C_{21}), 23.0 (C_{24}), 21.9 ($C_{7\ or\ 8}$), 18.9 (C_{14}), 12.8 (C_{13}).

HRMS(ESI+) m/z: calculated for $C_{31}H_{40}NO_4^+$ $[MH]^+$: 490.2952 found: 490.2959.

IR (ATR) ν (cm^{-1}): 2925, 1695, 1452, 1281, 1205, 1158.

1-Methoxy-3-((3-methylbut-2-en-1-yl)oxy)benzene 403

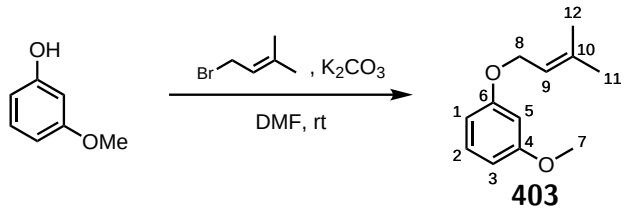

403

Experimental: To a stirred solution of 3-methoxyphenol (621 mg, 5 mmol, 1 equiv.) and allyl bromide (1.12 g, 7.5 mmol, 1.5 equiv.) in 25 mL of dry DMF was added K_2CO_3 (2.08 g, 15 mmol, 3 equiv.) under light protection at rt. After stirring overnight at rt in the dark, the reaction mixture was quenched with 125 mL of H_2O. The aqueous layer was extracted with pentane (3 x 125 mL). The organic layers were combined, washed with H_2O, brine, dried over Na_2SO_4, filtered and concentrated in vacuo. The crude product was purified via silica gel chromatography (PE/EA 99:1 to 98:2) to yield 816 mg (85% yield) of alkene **403**.

Physical state: yellowish oil.

^{1}**H NMR** (400 MHz, $CDCl_3$) δ ppm: 7.23-7.18 (m, 1H, H_2), 6.58-6.52 (m, 3H, $H_{1,\ 3\ and\ 5}$), 5.57-5.50 (m, 1H, H_9), 4.52 (m, 2H, H_8), 3.80 (s, 3H, H_7), 1.84-1.82 (m, 3H, H_{11}), 1.78-1.76 (m, 3H, H_{12}).

^{13}**C NMR** (100 MHz, $CDCl_3$) δ ppm: 160.8 (C_4), 160.2 (C_6), 138.1 (C_{10}), 129.8 (C_2), 119.7 (C_9), 106.8 (C_1), 106.2 (C_3), 101.1 (C_5), 64.7 (C_8), 55.2 (C_7), 25.8 (C_{11}), 18.2 (C_{12}).

HRMS(EI+) m/z: calculated for $C_{12}H_{16}O_2$ [M]: 192.1150 found: 192.1153.

IR (ATR) ν (cm^{-1}): 2915, 2835, 1589, 1490, 1466, 1451, 1382, 1334, 1282, 1262, 1198, 1146, 1081, 1041, 1010, 990, 833, 759, 686.

4-Methoxy-3-(prop-1-en-2-yloxy)-2,3-dihydrobenzofuran 408

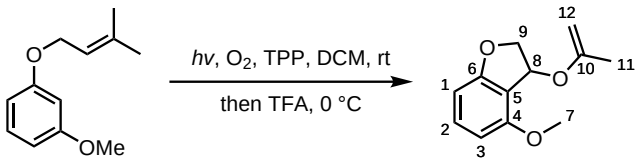

403 **408**

Experimental: To a vigorously stirred solution of alkene **403** (48 mg, 0.25 mmol, 1 equiv.) in 5 mL of dry DCM was added TPP (3 mg, 5 μmol, 0.02 equiv.) at rt under O_2 atmosphere. The reaction mixture was then irradiated with white LED light for 2 h. The reaction mixture was cooled down to 0 °C and TFA (60 μL, 0.75 mmol, 3 equiv.) was added. After 6 h at 0 °C, the reaction mixture was quenched with a 5 mL of a saturated solution of $NaHCO_3$. The aqueous layer was extracted with DCM (3 x 5 mL). The organic layers were combined, washed with brine, dried over Na_2SO_4, filtered and concentrated in vacuo. The crude product was purified via silica gel chromatography (PE/EA 95:5 to 90:10) to yield 5 mg (10% yield) of bicyclic compound **408**.

Physical state: yellowish oil.

^{1}**H NMR** (400 MHz, $CDCl_3$) δ ppm: 6.86-6.82 (dd, J = 8.7, 0.5 Hz, 1H, H_2), 6.48-6.42 (m, 2H, $H_{1\ and\ 3}$), 5.18-5.15 (m, 1H, H_{12}), 5.10-5.07 (m, 1H, H_{12}), 4.49-4.45 (m, 1H, H_8), 4.30-4.25 (m, 1H, H_9), 3.98-3.90 (m, 1H, H_9), 3.74 (s, 3H, H_7), 1.85-1.83 (m, 3H, H_{11})).

^{13}**C NMR** (100 MHz, $CDCl_3$) δ ppm: 154.2 (C_4), 143.3 (C_6), 140.1 (C_{10}), 137.5 (C_5),

117.6 (C_2), 114.3 (C_{12}), 107.3 (C_1), 102.4 (C_3), 75.9 (C_8), 67.7 (C_9), 55.8 (C_7), 19.0 (C_{11}).

HRMS(EI+) m/z: calculated for $C_{12}H_{14}O_3$ [M]: 206.0943 found: 206.0933.

IR (ATR) ν (cm^{-1}): 2921, 2851, 1598, 1503, 1464, 1443, 1318, 1266, 1206, 1157, 1088, 1035, 912, 831, 798.

Diethyl 2-benzyl-2-(3-methylbut-2-en-1-yl)malonate 413

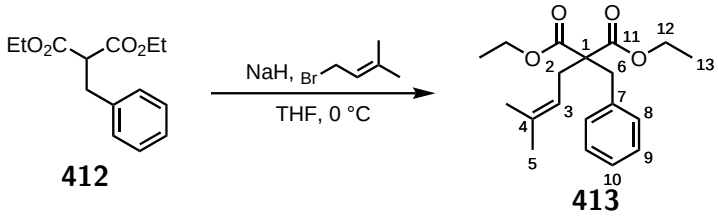

412 413

Experimental: To a stirred solution of NaH 60 % dispersion in mineral oil (3.08 g, 77 mmol, 3.85 equiv.) in 40 mL of dry THF was added diethyl benzylmalonate **412** (4.7 mL, 20 mmol, 1 equiv.) at 0 °C. The reaction mixture was then stirred at rt until gaz evolution ceased. The reaction mixture was then cooled down to 0 °C, allyl bromide (3.0 mL, 24 mmol, 1.2 equiv.) was added dropwise. After 1 h at rt, the reaction mixture was quenched with a 40 mL of a saturated solution of NH_4Cl. The aqueous layer was extracted with EtOAc (3 x 20 mL). The organic layers were combined, washed with brine, dried over Na_2SO_4, filtered and concentrated in vacuo. The crude product was purified via silica gel chromatography (PE/EA 99:1 to 95:5) to yield 6.04 g (95% yield) of alkene **413**.

Physical state: yellowish oil.

^{1}H NMR (400 MHz, $CDCl_3$) δ ppm: 7.26-7.17 (m, 3H, $H_{8,\ and\ 10}$), 7.09-7.05 (m, 2H,

H_9), 5.15-5.07 (m, 1H, H_3), 4.22-4.11 (m, 4H, H_{12}), 3.23 (s, 2H, H_6), 2.52-2.47 (m, 2H, H_2), 1.75-1.72 (m, 3H, H_5), 1.59-1.56 (m, 3H, H_5), 1.23 (t, J = 7.1 Hz, 6H, H_{13}).

^{13}C NMR (100 MHz, $CDCl_3$) δ ppm: 171.3 (C_{11}), 136.4 (C_7), 135.5 (C_4), 130.2 (C_9), 128.3 (C_8), 126.9 (C_{10}), 118.0 (C_3), 61.3 (C_{12}), 59.0 (C_1), 38.0 (C_6), 30.6 (C_2), 26.3 (C_5), 18.3 (C_5), 14.2 (C_{13}).

HRMS(EI+) m/z: calculated for $C_{12}H_{19}O_4^+$ $[M\text{-}Bz]^+$: 227.1278 found: 227.1282

IR (ATR) ν (cm^{-1}): 2925, 2855, 1733, 1496, 1446, 1367, 1280, 1244, 1216, 1191, 1082, 1061, 1024, 862, 744, 702.

Diethyl naphthalene-2,2(*1H*)-dicarboxylate 414

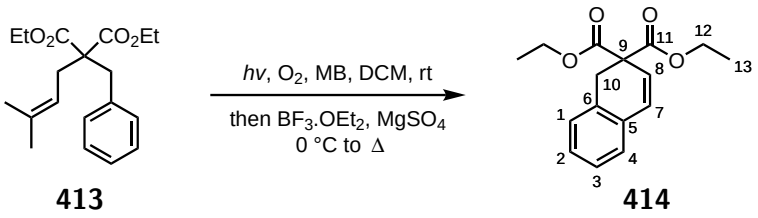

413 **414**

Experimental: To a stirred solution of alkene **413** (64 mg, 0.2 mmol, 1 equiv.) in 2 mL of dry DCM was added MB (3.2 mg, 10 μmol, 0.05 equiv.) at rt under O_2 atmosphere. The reaction mixture was then irradiated with white LED light for 5 h. The reaction mixture was cooled down to 0 °C and $BF_3.OEt_2$ (25 μL, 0.2 mmol, 1 equiv.) was added followed by $MgSO_4$ (48 mg, 0.4 mmol, 2 equiv.) and 2 mL of dry DCM. The reaction mixture was stirred 30 min at 0 °C then under reflux overnight. After completion, the reaction mixture was concentrated in vacuo. The crude product was purified via silica gel chromatography (PE/Et_2O 95:5) to yield 45 mg (82% yield) of bicyclic product **414**.

Physical state: yellowish oil.

^{1}H NMR (400 MHz, $CDCl_3$) δ ppm: 7.21-7.14 (m, 3H, $H_{2,\ 3\ and\ 4}$), 7.09-7.05 (m, 1H, H_1), 6.64 (d, J = 9.6 Hz, 1H, H_8), 6.15 (d, J = 9.6 Hz, 1H, H_7), 4.26-4.13 (m, 4H, H_{12}), 3.41 (s, 2H, H_{10}), 1.26-1.21 (m, 6H, H_{13}).

^{13}C NMR (100 MHz, $CDCl_3$) δ ppm: 170.3 (C_{11}), 132.3 (C_5), 131.8 (C_6), 129.9 (C_7), 128.2 (C_4), 127.9 (C_2), 127.1 (C_3), 126.7 (C_1), 124.7 (C_8), 61.9 (C_{12}), 55.0 (C_9), 34.1 (C_{10}), 14.2 (C_{13}).

HRMS(EI+) m/z: calculated for $C_{16}H_{18}O_4$ [M]: 274.1205 found: 274.1207.

IR (ATR) ν (cm^{-1}): 2957, 2923, 2853, 1731, 1490, 1454, 1388, 1366, 1260, 1237, 1224, 1200, 1185, 1104, 1048.

Diethyl 4-(2,4,6-trimethoxyphenyl)-3,4-dihydronaphthalene-2,2(1H)-dicarboxylate 421

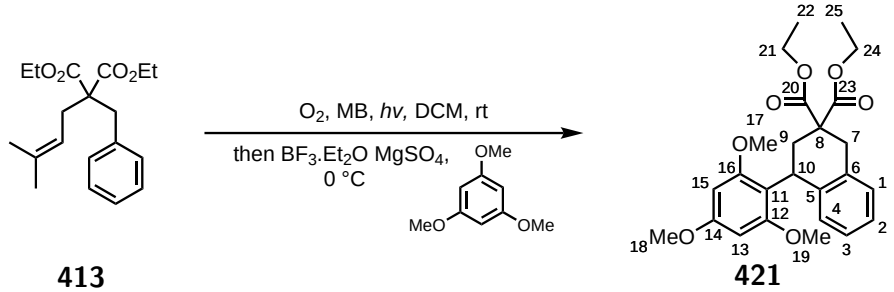

413 **421**

Experimental: To a stirred solution of alkene **413** (32 mg, 0.1 mmol, 1 equiv.) in 1 mL of dry DCM was added MB (1.6 mg, 5 μmol, 0.05 equiv.) at rt under O_2 atmosphere. The

reaction mixture was then irradiated with white LED light for 5 h. The reaction mixture was cooled down to 0 °C and $BF_3.OEt_2$ (13 μL, 0.1 mmol, 1 equiv.) was added followed by $MgSO_4$ (24 mg, 0.2 mmol, 2 equiv.), 1,3,5-trimethoxybenzene (20 mg, 0.12 mmol, 1.2 equiv.) and 1 mL of dry DCM. The reaction mixture was stirred 2 h at 0 °C. After completion, the reaction mixture was concentrated in vacuo. The crude product was purified via silica gel chromatography (PE/Et_2O 98:2 to 90:10) to yield 38 mg (86% yield) of bicyclic product **421**.

Physical state: yellowish solid.

^{1}**H NMR** (400 MHz, $CDCl_3$) δ ppm: 7.08-6.91 (m, 3H, $H_{2,\ 3\ and\ 4}$), 6.72-6.70 (m, 1H, H_1), 6.14 (s, 2H, $H_{13\ and\ 15}$), 4.84-4.79 (m, 1H, H_{10}), 4.24-4.06 (m, 4H, $H_{21\ and\ 24}$), 3.80-2.25 (m, 11H, $H_{7,\ 17,\ 18\ and\ 19}$), 2.56-2.43 (m, 2H, H 9), 1.27-1.16 (m, 6H, $H_{25\ and\ 25}$).

^{13}**C NMR** (100 MHz, $CDCl_3$) δ ppm: 172.2 ($C_{20\ or\ 23}$), 170.9 ($C_{20\ or\ 23}$), 159.9 ($C_{12\ and\ 16}$), 159.3 (C_{14}), 139.8 (C_5), 133.4 (C_6), 128.2 (C_4), 127.0 (C_1), 126.0 (C_3), 124.8 (C_2), 114.7 (C_{11}), 91.1 ($C_{13\ and\ 15}$), 61.5 ($C_{21\ or\ 24}$), 61.2 ($C_{21\ or\ 24}$), 55.9 ($C_{8\ and\ 18}$), 55.4 (C_{17}), 54.8 (C_{19}), 35.4 (C_7), 33.4 (C_9), 31.7 (C_{10}), 14.2 ($C_{22\ or\ 25}$), 14.1 ($C_{22\ or\ 25}$).

HRMS(EI+) m/z: calculated for $C_{25}H_{30}O_7$ [M]: 442.1992 found: 442.1999.

IR (ATR) ν (cm^{-1}): 2936, 2839, 1730, 1606, 1590, 1453, 1204, 1151, 745.

(((1-Methylcyclohex-2-en-1-yl)oxy)methyl)benzene 488

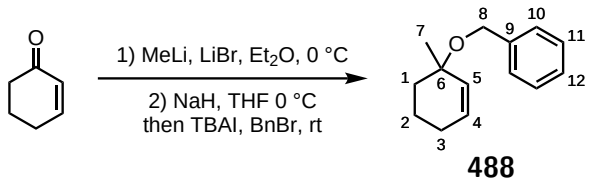

488

Experimental: To a stirred solution of cyclohexenone (193 μL, 2 mmol, 1 equiv.) and LiBr (260 mg, 3 mmol, 1.5 equiv.) in 5 mL of dry Et_2O was added a 1.2 M solution of MeLi in Et_2O (2.5 mL, 3 mmol, 1.5 equiv.) at 0 °C. After 7 h at 0 °C, the reaction mixture was quenched with a 10 mL of a saturated solution of NH_4Cl. The aqueous layer was extracted with DCM (3 x 10 mL). The organic layers were combined, washed with brine, dried over Na_2SO_4, filtered and concentrated in vacuo.

The crude mixture was solubilized in 4 mL of dry THF and NaH 60 % dispersion in mineral oil (385 mg, 3 mmol, 1.5 equiv. supposed) was added at 0 °C. After gaz evolution has ceased, the reaction mixture was allowed to warm up to rt and BnBr (357 μL, 3 mmol, 1.5 equiv.) followed by TBAI (7.2 mg, 0.02 mmol, 0.01 equiv.) were added. After 1 d at rt, the reaction mixture was quenched with a 10 mL of a saturated solution of NH_4Cl. The aqueous layer was extracted with EtOAc (3 x 10 mL). The organic layers were combined, washed with brine, dried over Na_2SO_4, filtered and concentrated in vacuo. The crude product was purified via silica gel chromatography (PE/Et_2O 99:1 to 95:5) to yield 293 mg (73% yield over 2 steps) of benzyl derivative **488**.

Physical state: yellowish oil.

^{1}H NMR (400 MHz, $CDCl_3$) δ ppm: 7.38-7.28 (m, 4H, $H_{10\ and\ 11}$), 7.26-7.21 (m, 1H, H_{12}), 5.88 (dt, J = 10.2, 3.7 Hz, 1H, H_4), 5.71-5.66 (m, 1H, H_5), 4.51-4.43 (m, 2H, H_8), 2.13-1.92 (m, 3H, $H_{1\ and\ 3}$), 1.90-1.79 (m, 1H, H_2), 1.68-1.54 (m, 2H, $H_{1\ and\ 2}$), 1.35 (s, 3H,

H_7).

^{13}**C NMR** (100 MHz, $CDCl_3$) δ ppm: 140.1 (C_9), 132.4 (C_5), 130.6 (C_4), 128.4 (C_{11}), 127.6 (C_{10}), 127.2 (C_{12}), 73.6 (C_6), 64.6 (C_8), 34.2 (C_1), 27.0 (C_7), 25.3 (C_3), 20.1 (C_2).

HRMS(EI+) m/z: calculated for $C_{14}H_{18}O$ [M]: 202.1358 found: 202.1358.

IR (ATR) ν (cm^{-1}): 3063, 3025, 2966, 2934, 2863, 1496, 1453, 1378, 1366, 1331, 1274, 1200, 1181, 1126, 1101, 1086, 1058, 1028, 914, 889, 732, 696.

1-indanyl hydroperoxide 437

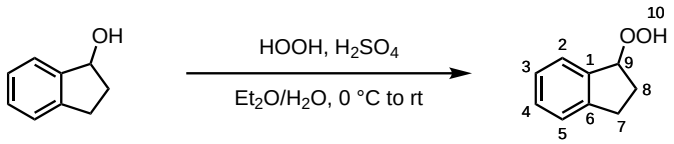

436 **437**

Experimental: To a stirred solution of indanol **436** (537 mg, 4 mmol, 1 equiv.) in 3 mL of Et_2O was added a 35% solution of HOOH (3.1 mL, 32 mmol, 8 equiv.) in H_2O followed by H_2SO_4 (45 μL, 0.8 mmol, 0.2 equiv.) at 0 °C. The reaction mixture was stirred at rt for 6 h. The organic layers was washed with water, dried over Na_2SO_4, filtered and concentrated in vacuo. The crude product was purified via silica gel chromatography (PE/EA 9:1) to yield 482 mg (80% yield) of hydroperoxide **437**.
All spectra and physical data matched published value.[6]

Physical state: colorless oil.

[6]K. Sugamoto, Y. Matsushita, T. Matsui, *J. Chem. Soc., Perkin Trans. 1*, **1998**, 3989-3998.

^{1}H NMR (400 MHz, $CDCl_3$) δ ppm: 7.75 (s, 1H, H_{10}), 7.51-7.49 (m, 1H, H_5), 7.35-7.20 (m, 3H, $H_{2,\ 3\ and\ 4}$), 5.54-5.51 (dd, J= 6.3, 3.1 Hz, 1H, H_9), 3.16-3.09 (m, 1H, H_7), 2.90-2.83 (m, 1H, H_7), 2.40-2.26 (m, 2H, H_8).

^{13}C NMR (100 MHz, $CDCl_3$) δ ppm: 145.7 (C_1), 139.9 (C_6), 129.5 (C_5), 126.6 (C_3), 126.2 (C_4), 125.2 (C_2), 89.4 (C_9), 30.5 (C_7), 30.2 (C_8).

2-allylchromane 438

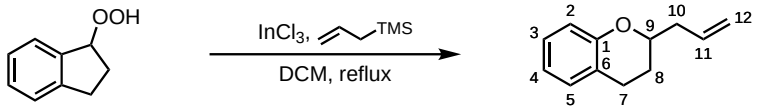

437 **438**

Experimental: To a stirred solution of hydroperoxide **437** (30 mg, 0.2 mmol, 1 equiv.) in 2 mL of DCM was added allyltrimethylsilane (64 μL, 0.4 mmol, 2 equiv.) followed by $InCl_3$ (4.4 mg, 0.02 mmol, 0.1 equiv.) at rt. The reaction mixture was stirred at reflux until completion. The reaction was quenched with $NaHCO_3$ and the aqueous layer was washed with Et_2O (3 x 5 mL). The organic layers were combined, washed with brine, dried over Na_2SO_4, filtered and concentrated in vacuo. The crude product was purified via silica gel chromatography (PE/EA 9:1) to yield 19 mg (53% yield) of chromane **438**.

Physical state: colorless oil.

^{1}H NMR (400 MHz, $CDCl_3$) δ ppm: 7.12-7.04 (m, 2H, $H_{3\ and\ 5}$), 6.86-6.81 (m, 2H, $H_{2\ and\ 4}$), 6.00-5.89 (m, 1H, H_{11}), 5.21-5.13 (m, 2H, H_{12}), 4.10-4.03 (m, 1H, H_9), 2.90-2.74 (m, 2H, H_7), 2.60-2.53 (m, 1H, H_{10}), 2.45-2.38 (m, 1H, H_{10}), 2.06-2.00 (m, 1H, H_8), 1.80-1.70 (m, 1H, H_8).

^{13}C NMR (100 MHz, $CDCl_3$) δ ppm: 155.0 (C_1), 134.2 (C_{11}), 129.6 (C_5), 127.3 (C_3), 122.1 (C_6), 120.2 (C_4), 117.6 (C_{12}), 116.9 (C_2), 75.4 (C_9), 39.9 (C_{10}), 26.9 (C_8), 24.8 (C_7).

HRMS(EI+) m/z: calculated for $C_{12}H_{14}O$ [M]: 174.1045 found: 174.1043.

IR (ATR) ν (cm^{-1}): 2930, 1582, 1488, 1457, 1230, 1052, 752.

1-(tert-butylperoxy)-2,3-dihydro-1H-indene 440

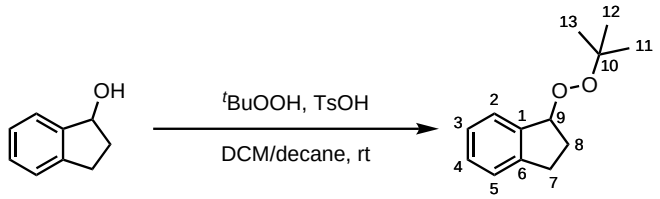

436 **440**

Experimental: To a stirred solution of indanol **436** (1.34 g, 10 mmol, 1 equiv.) in 5 mL of DCM was added a 5.5 M solution of ^{t}BuOOH (2.2 mL, 12 mmol, 1.2 equiv.) in decane followed by TsOH (190 mg, 1 mmol, 0.1 equiv.) at rt. The reaction mixture was stirred at rt until completion. The reaction was quenched with $NaHCO_3$ and the aqueous layer was washed with Et_2O (3 x 10 mL). The organic layers were combined, washed with brine, dried over Na_2SO_4, filtered and concentrated in vacuo. The crude product was purified via silica gel chromatography (PE/Et_2O 98:2) to yield 1.5 g (74% yield) of peroxide **440**.

Physical state: colorless oil.

^{1}H NMR (400 MHz, $CDCl_3$) δ ppm: 7.52-7.48 (m, 1H, H_2), 7.32-7.18 (m, 3H, $H_{3,\ 4\ and\ 5}$), 5.48-5.44 (m, 1H, H_9), 3.16-3.05 (m, 1H, H_7), 2.88-2.77 (m, 1H, H_7), 2.33-2.22 (m, 2H, H_8), 1.25 (s, 9H, $H_{11,\ 12\ and\ 13}$).

^{13}C NMR (100 MHz, $CDCl_3$) δ ppm: 145.4 (C_1), 140.7 (C_6), 129.1 (C_3), 126.5 (C_2), 126.3 (C_4), 125.0 (C_5), 87.5 (C_9), 80.3 (C_{10}), 30.8 (C_8), 30.4 (C_7), 26.6 ($C_{11,\ 12\ and\ 13}$).

HRMS(ESI+) m/z: calculated for $C_{13}H_{19}O_2^+$ $[MH]^+$: 207.1380 found: 207.1375.

IR (ATR) ν (cm^{-1}): 2979, 2935, 1584, 1489, 1457, 1378, 1363, 1304, 1277, 1250, 1240, 1218, 1194, 1178, 1139, 1096, 946, 873, 847, 752.

1-methyl-1-indanol 445

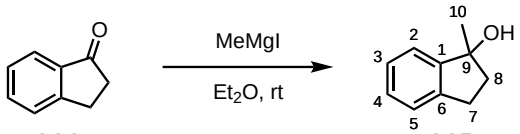

444 **445**

Experimental: To a stirred solution of indanone **109** (904 mg, 7 mmol, 1 equiv.) in 20 mL of Et_2O was added a 3.0 M solution of MeMgI (14 mL, 14 mmol, 2 equiv.) in Et_2O at rt. The reaction mixture was stirred 30 min at rt before being quenched with cold water (40 mL). The acqueous layer was washed with EtOAc (100 mL). The organic layers were combined, washed with brine, dried over Na_2SO_4, filtered and concentrated in vacuo. The crude product was purified via silica gel chromatography (PE/EA 8:1 to 5:1) to yield 830 mg (80% yield) of methyl indanol **445**.
All spectra and physical data matched published value.[7]

Physical state: yellowish oil.

^{1}H NMR (400 MHz, $CDCl_3$) δ ppm: 7.37-7.35 (m, 1H, H_5), 7.26-7.23 (m, 3H, $H_{2,\ 3\ and\ 4}$),

[7]H. Kurouchi, H. Sugimoto, Y. Otani, T. Ohwada, *J. Am. Chem. Soc.* **2010**, *132*, 807–815.

3.07-3.00 (m, 1H, H_7), 2.88-2.80 (m, 1H, H_7), 2.28-2.15 (m, 2H, H_8), 1.75 (brs, 1H, H_{10}), 1.58 (s, 3H, H_{11}).

^{13}C NMR (100 MHz, $CDCl_3$) δ ppm: 148.3 (C_1), 142.5 (C_6), 128.0 (C_4), 126.8 (C_2), 124.8 (C_3), 122.2 (C_5), 81.0 (C_9), 42.1 (C_8), 29.3 (C_7), 27.2 (C_{10}).

1-(tert-butylperoxy)-1-methyl-2,3-dihydro-1H-indene 446

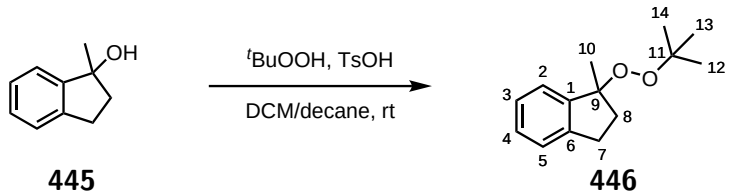

445 **446**

Experimental: To a stirred solution of methyl indanol **445** (293 mg, 2 mmol, 1 equiv.) in 4 mL of DCM was added a 5.5 M solution of ^{t}BuOOH (440 μL, 2.4 mmol, 1.2 equiv.) in decane followed by TsOH (38 mg, 0.2 mmol, 0.1 equiv.) at rt. The reaction mixture was stirred at rt until completion. The reaction was quenched with $NaHCO_3$ and the aqueous layer was washed with Et_2O (3 x 5 mL). The organic layers were combined, washed with brine, dried over Na_2SO_4, filtered and concentrated in vacuo. The crude product was purified via silica gel chromatography (PE/Et_2O 98:2) to yield 120 mg (27% yield) of peroxide **446**.

Physical state: colorless oil.

^{1}H NMR (400 MHz, $CDCl_3$) δ ppm: 7.39-7.36 (m, 1H, H_5), 7.28–7.18 (m, 3H, $H_{2,\ 3\ and\ 4}$), 3.11–3.01 (m, 1H, H_7), 2.85–2.74 (m, 1H, H_7), 2.48 (ddd, J = 13.7, 8.2, 3.1 Hz, 1H, H_8), 2.00 (ddd, J = 13.7, 8.7, 7.9 Hz, 1H, H_8), 1.64 (s, 3H, H_{10}), 1.05 (s, 9H, $H_{12,\ 13\ and\ 14}$).

^{13}C NMR (100 MHz, $CDCl_3$) δ ppm: 144.9 (C_1), 144.8 (C_6), 128.3 (C_3), 125.8 (C_2), 124.6 (C_4), 124.5 (C_5), 90.1 (C_9), 78.9 (C_{12}), 37.3 (C_8), 30.1 (C_7), 26.4 ($C_{12,\ 13\ and\ 14}$), 25.7 (C_{11}), 23.1 (C_{10}).

HRMS(ESI+) m/z: calculated for $C_{14}H_{21}O_2^+$ $[MH]^+$: 221.1536 found: 221.1530.

IR (ATR) ν (cm^{-1}): 2979, 2935, 1584, 1489, 1457, 1378, 1363, 1304, 1277, 1250, 1240, 1218, 1194, 1178, 1139, 1096, 946, 873, 847, 752.

2-allyl-2-methylchromane 448

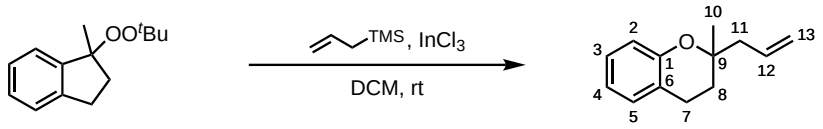

446 **448**

Experimental: To a stirred solution of peroxide **446** (21 mg, 0.1 mmol, 1 equiv.) in 1 mL of DCM was added allyltrimethylsilane (32 μL, 0.2 mmol, 2 equiv.) followed by $InCl_3$ (2.2 mg, 0.01 mmol, 0.1 equiv.) at rt. The reaction mixture was stirred at rt until completion. The reaction was quenched with $NaHCO_3$ and the aqueous layer was washed with Et_2O (3 x 5 mL). The organic layers were combined, washed with brine, dried over Na_2SO_4, filtered and concentrated in vacuo. The crude product was purified via silica gel chromatography (PE/Et_2O 98:2) to yield 15 mg (80% yield) of chromane **448**.

Physical state: colorless oil.

^{1}H NMR (400 MHz, $CDCl_3$) δ ppm: 7.12-7.02 (m, 2H, $H_{3\ and\ 5}$), 6.86-6.76 (m, 2H, $H_{2\ and\ 4}$), 5.95-5.81 (m, 1H, H_{12}), 5.14-5.04 (m, 2H, H_{13}), 2.80-2.73 (t, J = 6.8 Hz, 2H,

H_7), 2.44-2.33 (m, 2H, H_{11}), 1.90-1.71 (m, 2H, H_8), 1.29 (s, 3H, H_{10}).

^{13}C NMR (100 MHz, $CDCl_3$) δ ppm: 153.9 (C_1), 133.7 (C_{12}), 129.6 (C_5), 127.4 (C_3), 121.2 (C_6), 119.8 (C_4), 118.3 (C_{13}), 117.4 (C_2), 75.9 (C_9), 44.3 (C_{11}), 30.8 (C_8), 24.6 (C_{10}), 22.2 (C_7).

HRMS(ESI+) m/z: calculated for $C_{13}H_{17}O^+$ $[MH]^+$: 189.1274 found: 189.1274.

IR (ATR) ν (cm^{-1}): 3074, 2976, 2930, 2852, 1640, 1610, 1582, 1487, 1455, 1377, 1304, 1244, 1230, 1149, 1109, 999, 942, 915, 752.

2-(2-bromoallyl)-2-methylchromane 455

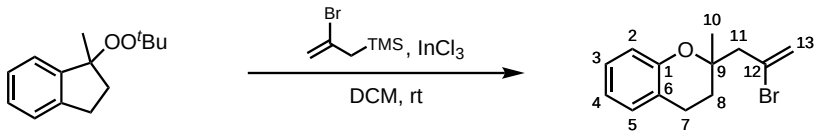

446 **455**

Experimental: To a stirred solution of peroxide **446** (21 mg, 0.1 mmol, 1 equiv.) in 1 mL of DCM was added 2-bromoallyltrimethylsilane (34 μL, 0.2 mmol, 2 equiv.) followed by $InCl_3$ (2.2 mg, 0.01 mmol, 0.1 equiv.) at rt. The reaction mixture was stirred at rt until completion. The reaction was quenched with $NaHCO_3$ and the aqueous layer was washed with Et_2O (3 x 5 mL). The organic layers were combined, washed with brine, dried over Na_2SO_4, filtered and concentrated in vacuo. The crude product was purified via silica gel chromatography (PE/Et_2O 98:2) to yield 8 mg (30% yield) of chromane **448**.

Physical state: colorless oil.

^{1}H NMR (400 MHz, $CDCl_3$) δ ppm: 7.12-7.02 (m, 2H, $H_{3\ and\ 5}$), 6.86-6.76 (m, 2H,

$H_{2\ and\ 4}$), 5.71-5.69 (m, 1H, H_{13}), 5.63-5.62 (m, 1H, H_{13}), 2.91-2.73 (m, 4H, $H_{7\ and\ 11}$), 2.05-1.84 (m, 2H, H_8), 1.42 (s, 3H, H_{10}).

^{13}C NMR (100 MHz, $CDCl_3$) δ ppm: 153.5 (C_1), 129.6 (C_5), 127.6 (C_{12}), 127.5 (C_3), 121.8 (C_{13}), 120.9 (C_6), 120.1 (C_4), 117.5 (C_2), 75.8 (C_9), 50.2 (C_{11}), 31.2 (C_8), 24.8 (C_{10}), 22.1 (C_7).

HRMS(ESI+) m/z: calculated for $C_{13}H_{16}O^+$ $[MH]^+$: 267.0379 found: 267.1210.

IR (ATR) ν (cm^{-1}): 2976, 2929, 1624, 1582, 1487, 1455, 1379, 1306, 1243, 1232, 1145, 1108, 943, 892, 752.

2-Iodocyclohex-2-en-1-one 467

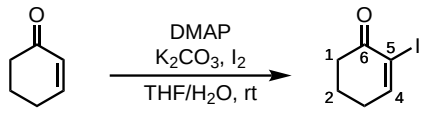

467

Experimental: To a stirred solution of cyclohexenone (10 mL, 100 mmol, 1 equiv.) in a 500 mL of a 1:1 mixture THF/H_2O was added K_2CO_3 (16.6 g, 120 mmol, 1.2 equiv.), I_2 (38.1 g, 150 mmol, 1.5 equiv.) and DMAP (2.4 g, 20 mmol, 0.2 equiv.) at rt. The reaction was quenched with a saturated solution of Na_2SO_3 (500 mL) and extracted with EtOAc (3 x 200 mL). The organic layers were combined, washed with 0.1 M HCl, brine, dried over Na_2SO_4, filtered and concentrated in vacuo. The crude product was purified via silica gel chromatography (PE/EA 9:1) to yield 16.1 g (72% yield) of 2-iodo-2-cyclohexenone **467**.

Physical state: yellowish solid.

^{1}H NMR (400 MHz, $CDCl_3$) δ ppm: 7.76 (t, J = 4.5 Hz, 1H, H_4), 2.69-2.62 (m, 2H, H_1), 2.47-2.40 (m, 2H, H_3), 2.12-2.03 (m, 2H, H_2).

^{13}C NMR (100 MHz, $CDCl_3$) δ ppm: 192.3 (C_6), 159.6 (C_4), 104.0 (C_5), 37.4 (C_1), 30.0 (C_3), 22.9 ppm (C_2).

HRMS(EI+) m/z: calculated for C_6H_7IO [M]: 221.9542 found: 221.9532.

IR (ATR) ν (cm^{-1}): 3033, 2928, 2866, 2817, 1677, 1583, 1453, 1422, 1328, 1313, 1228, 1153, 1118, 1068, 983, 964, 901, 872, 798, 701, 634.

2-Hexylcyclo-2-en-1-one 465

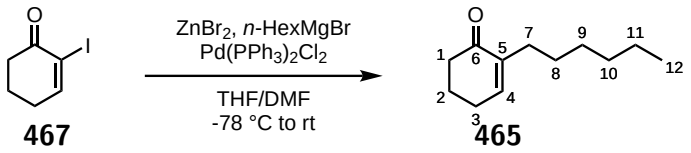

467 **465**

Experimental: $ZnBr_2$ (1.53 g, 6.8 mmol, 1.7 equiv.) was melted under high vacuum and then allowed to cooled down to rt under argon. The white solid was then dissolved with 5 mL of dry THF, cooled down to -78 °C and a 2 M solution of *n*-HexMgBr in THF (3 mL, 6 mmol, 1.5 equiv.) was added dropwise. The reaction mixture was warmed up to -60 °C and a solution of 2-iodo-2-cyclohexenone **467** (890 mg, 4 mmol, 1 equiv.) and $Pd(PPh_3)_2Cl_2$ (130 mg, 0.2 mmol, 0.05 equiv.) in 24 mL of dry DMF was added dropwise over 30 min. The reaction mixture was then allowed to warm up to rt. After 1 h, the reaction mixture was quenched with a saturated solution of NH_4Cl (50 mL) and extracted with Et_2O (3 x 30 mL). The organic layers were combined, washed with water, brine, dried over Na_2SO_4, filtered and concentrated in vacuo. The crude product was purified via silica gel

chromatography (PE/EA 98:2 to 95:5) to yield 320 mg (44% yield) of 2-hexylcyclo-2-enone **465**.

Physical state: colorless oil.

^{1}H NMR (400 MHz, $CDCl_3$) δ ppm: 6.69 (t, J = 8.5 Hz, 1H, H_4), 2.44-2.38 (m, 2H, H_1), 2.36-2.31 (m, 2H, H_3), 2.18-2.12 (m, 2H, H_7), 1.92-2.01 (m, 2H, H_2), 1.31-1.23 (m, 8H, $H_{7,\ 8,\ 9\ and\ 10}$) 0.90-0.83 (m, 3H, H_{12}).

^{13}C NMR (100 MHz, $CDCl_3$) δ ppm: 199.7 (C_6), 144.9 (C_4), 140.1 (C_5), 38.8 (C_1), 31.8 (C_{10}), 29.7 (C_7), 29.2 (C_9), 28.7 (C_8), 26.2 (C_3), 23.3 (C_2), 22.8 (C_{11}), 14.2 (C_{12}).

HRMS(EI+) m/z: calculated for $C_{12}H_{20}O$ [M]: 180.1514 found: 180.1503.

IR (ATR) ν (cm^{-1}): 2924, 2856, 1746, 1672, 1456, 1432, 1376, 1320, 1250, 1172, 1138, 1119, 1094.

2-Hexylcyclo-2-en-1-ol 468

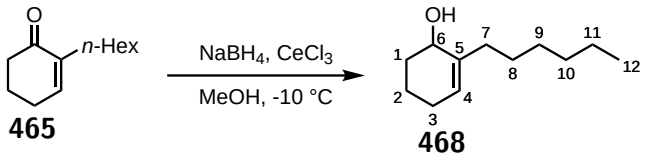

465 468

Experimental: To a stirred solution of 2-hexylcyclo-2-enone **465** (90 mg, 0.5 mmol, 1 equiv.) and $CeCl_3$ (203 mg, 0.55 mmol, 1.1 equiv.) in 15 mL of MeOH was added $NaBH_4$ (28 mg, 0.75 mmol, 1.5 equiv.) at -10 °C. After 5 min, the reaction mixture was quenched with a saturated solution of NH_4Cl (10 mL) and extracted with Et_2O (3 x 10 mL).

The organic layers were combined, washed with water, brine, dried over Na_2SO_4, filtered and concentrated in vacuo. The crude product was purified via silica gel chromatography (PE/Et_2O 95:5 to 90:10) to yield 68 mg (75% yield) of 2-hexylcyclo-2-enol **468**.

Physical state: colorless oil.

^{1}H NMR (400 MHz, $CDCl_3$) δ ppm: 5.53 (t, J = 3.8 Hz, 1H, H_5), 4.05 (t, J = 4.5 Hz, 1H, H_1), 2.20-2.09 (m, 1H, H_1), 2.09-1.99 (m, 2H, $H_{1\ and\ 2}$), 1.98-1.89 (m, 1H, H_2), 1.78-1.69 (m, 2H, H_7), 1.66-1.51 (m, 2H, H_3), 1.47-1.34 (m, 2H, H_8), 1.33-1.23 (m, 6H, $H_{9,\ 10\ and\ 11}$), 0.92-0.85 (m, 3H, H_{12}).

^{13}C NMR (100 MHz, $CDCl_3$) δ ppm: 139.6 (C_5), 124.9 (C_4), 66.9 (C_6), 34.3 (C_1), 32.4 (C_7), 31.9 (C_{10}), 29.3 (C_9), 28.3 (C_8), 25.6 (C_2), 22.8 (C_{11}), 18.2 (C_3), 14.2 (C_{12}).

HRMS(EI+) m/z: calculated for $C_{12}H_{22}O$ [M]: 182.1671 found: 182.1674.

IR (ATR) ν (cm^{-1}): 3335, 2926, 2857, 1456, 1154, 1054, 984, 913.

(4*S*)-6-Chloro-1-methyl-4-(prop-1-en-2-yl)cyclohex-1-ene 470

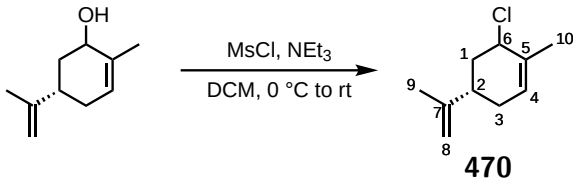

470

Experimental: To a stirred solution of carveol (0.64 mL, 4 mmol, 1 equiv.) and NEt_3 (0.62 mL, 8 mmol, 2 equiv.) in 10 mL of dry DCM was added MsCl (0.62 mL, 8 mmol, 2

equiv.) at 0 °C. The reaction mixture was allowed to warm up to rt. After 1 h, the reaction mixture was quenched with a saturated solution of $NaHCO_3$ (10 mL) and extracted with DCM (3 x 10 mL). The organic layers were combined, washed with water, brine, dried over Na_2SO_4, filtered and concentrated in vacuo. The crude product was purified via silica gel chromatography (PE/Et_2O 98:2) to yield 537 mg (80% yield) of carveol derivative **470**.

Physical state: colorless oil.

^{1}**H NMR** (400 MHz, $CDCl_3$) δ ppm: Data for major diastereoisomer: 5.65-5.60 (m, 1H, H_4), 4.79-4.70 (m, 2H, H_8), 4.61-4.47 (m, 1H, H_6), 2.65-2.54 (m, 1H, H_2), 2.28-2.17 (m, 2H, $H_{1\ and\ 3}$), 2.09-1.87 (m, 1H, H_3), 1.95-1.83 (m, 1H, H_1), 1.84-1.80 (m, 3H, H_{10}), 1.77-1.75 (m, 3H, H_9).
Data for minor diastereoisomer: 5.65-5.60 (m, 1H, H_4), 4.79-4.70 (m, 2H, H_8), 4.65-4.56 (m, 1H, H_6), 2.45-2.38 (m, 1H, H_1), 2.28-2.17 (m, 3H, $H_{2\ and\ 3}$), 2.09-1.87 (m, 1H, H_3), 1.95-1.83 (m, 1H, H_1), 1.84-1.80 (m, 3H, H_{10}), 1.74-1.72 (m, 3H, H_9).

^{13}**C NMR** (100 MHz, $CDCl_3$) δ ppm: Data for major diastereoisomer: 148.6 (C_7), 133.3 (C_5), 126.9 (C_4), 109.4 (C_8), 60.8 (C_6), 37.3 (C_1), 35.2 (C_2), 30.9 (C_3), 21.2 (C_{10}), 21.1 (C_9).
Data for major diastereoisomer: 148.1 (C_7), 133.6 (C_5), 126.7 (C_4), 109.8 (C_8), 61.8 (C_6), 42.1 (C_2), 40.1 (C_1), 30.9 (C_3), 21.1 (C_{10}), 20.6 (C_9).

HRMS(EI+) m/z: calculated for $C_{10}H_{15}Cl$ [M]: 170.0862 found: 170.0859.

IR (ATR) ν (cm^{-1}): 3082, 2968, 2939, 2916, 2839, 1645, 1439, 1378, 1282, 1244, 1228, 1203, 1152, 1045, 1013.

(4*S*)-6-Hydroperoxy-1-methyl-4-(prop-1-en-2-yl)cyclohex-1-ene 472

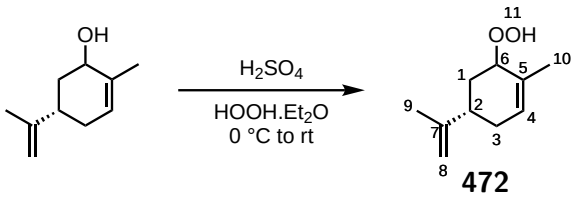

472

Experimental: A 30% solution of H_2O_2 in H_2O was extracted two times with 40 mL of Et_2O and then dried over Na_2SO_4.

To a stirred solution of carveol (3.84 mL, 24 mmol, 1 equiv.) in 60 mL of the solution previously made was added H_2SO_4 (0.82 mL, 24 mmol, 1 equiv.) dropwise at 0 °C. The reaction mixture was allowed to warm up to rt. After 2 h, the reaction mixture was quenched with a saturated solution of $NaHCO_3$ (50 mL) and extracted with Et_2O (3 x 20 mL). The organic layers were combined, washed with water, brine, dried over Na_2SO_4, filtered and concentrated in vacuo. The crude product was purified via silica gel chromatography ($PE/Et_2O/NEt_3$ 90:9:1) to yield 888 mg (22% yield) of hydroperoxide **472**.

Physical state: colorless oil.

^{1}H NMR (400 MHz, $CDCl_3$) δ ppm: Data for major diastereoisomer: 7.98 (s, 1H, H_{11}), 5.77-5.73 (m, 1H, H_4), 4.78-4.72 (m, 2H, H_8), 4.38-4.34 (m, 1H, H_6), 2.42-2.30 (m, 3H, $H_{1,\ 2\ and\ 3}$), 2.21-2.11 (m, 1H, H_1), 1.89-1.79 (m, 1H, H_3), 1.81-1.79 (m, 3H, H_{10}), 1.77-1.74 (m, 3H, H_9).

Data for minor diastereoisomer: 7.63 (s, 1H, H_{11}), 5.67-5.62 (m, 1H, H_4), 4.78-4.72 (m, 2H, H_8), 4.57-4.50 (m, 1H, H_6), 2.33-2.24 (m, 2H, H_2), 2.25-2.18 (m, 2H, H_1), 2.01-1.94 (m, 2H, H_3), 1.78-1.76 (m, 3H, H_{10}), 1.75-1.73 (m, 3H, H_9).

^{13}C NMR (100 MHz, $CDCl_3$) δ ppm: Data for major diastereoisomer: 149.3 (C_7), 129.9

(C_4), 129.4 (C_5), 109.2 (C_8), 82.7 (C_6), 35.3 (C_1), 31.2 (C_1), 31.1 (C_3), 21.4 (C_{10}), 21.1 (C_9).

Data for minor diastereoisomer: 148.9 (C_7), 132.9 (C_5), 127.3 (C_4), 109.4 (C_8), 84.4 (C_6), 40.7 (C_2), 32.5 (C_1), 30.9 (C_3), 20.6 (C_{10}), 19.3 (C_9).

HRMS(EI+) m/z: calculated for $C_{10}H_{15}O^+$ [M-OH]$^+$: 151.1128 found: 151.1114.

IR (ATR) ν (cm^{-1}): 3394, 3082, 2916, 2854, 1644, 1438, 1374, 1319, 1299, 1269, 1214, 1157, 1089, 1058, 1046, 1027, 965.

(4*S*)-7-Methyl-4-(prop-1-en-2-yl)-2,3,4,5-tetrahydrooxepin-2-yl acetate 473

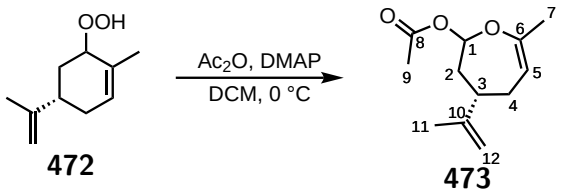

472 473

Experimental: To a stirred solution of hydroperoxide **472** (504 mg, 3 mmol, 1 equiv.) in 27 mL of dry DCM was added Ac_2O (3 mL, 30 mmol, 10 equiv.) followed by DMAP (18 mg, 0.15 mmol, 0.05) at 0 °C. After 30 min at 0 °C, the reaction mixture was quenched with a saturated solution of $NaHCO_3$ (30 mL) and extracted with Et_2O (3 x 20 mL). The organic layers were combined, washed with water, brine, dried over Na_2SO_4, filtered and concentrated in vacuo. The crude product was purified via silica gel chromatography (PE/EA 99:1) to yield 148 mg (23% yield) of acetate **473**.

Physical state: colorless oil.

^{1}H NMR (400 MHz, $CDCl_3$) δ ppm: 6.20-6.15 (m, 1H, H_5), 4.75-4.70 (m, 3H, $H_{1\ and\ 12}$), 2.73-2.63 (m, 1H, H_3), 2.33-2.23 (m, 1H, H_2), 2.23-2.15 (m, 1H, H_4), 2.10 (s, 3H, H_9), 2.06-1.97 (m, 1H, H_2), 1.96-1.88 (m, 1H, H_4), 1.75-1.73 (m, 3H, H_7), 1.73-1.71 (m, 3H, H_{11}).

^{13}C NMR (100 MHz, $CDCl_3$) δ ppm: 169.6 (C_8), 152.6 (C_6), 148.7 (C_{10}), 109.8 (C_{12}), 105.4 (C_1), 94.9 (C_5), 40.2 (C_3), 38.5 (C_4), 30.6 (C_2), 21.3 (C_9), 21.1 (C_7), 20.5 (C_{11}).

HRMS(EI+) m/z: calculated for $C_{12}H_{18}O_3$ [M]: 210.1256 found: 210.1258.

IR (ATR) ν (cm^{-1}): 3075, 3041, 2921, 2846, 1756, 1680, 1645, 1440, 1373, 1319, 1220, 1192, 1173, 1127, 1090, 1026, 1006, 944.

(5*S*)-2,7-Diallyl-2-methyl-5-(prop-1-en-2-yl)oxepane 474

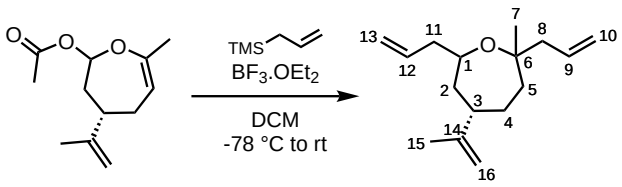

473 **474**

Experimental: To a stirred solution of acetate **473** (11 mg, 0.05 mmol, 1 equiv.) in 0.5 mL of dry DCM was added allyltrimethylsilane (16 μL, 0.1 mmol, 2 equiv.) followed by $BF_3.OEt_2$ (12 μL, 0.1 mmol, 2 equiv.) at -78 °C. The reaction mixture was allowed to slowly warmed up to rt. After completion, the reaction mixture was quenched with a saturated solution of $NaHCO_3$ (30 mL) and extracted with Et_2O (3 x 20 mL). The organic layers were combined, washed with water, brine, dried over Na_2SO_4, filtered and concentrated in vacuo. The crude product was purified via silica gel chromatography (pentane/Et_2O 100:0 to 99:1) to yield 6 mg (51% yield) of oxepane **474**.

Physical state: colorless oil.

^{1}H NMR (400 MHz, $CDCl_3$) δ ppm: 5.92-5.75 (m, 2H, $H_{9\ and\ 12}$), 5.12-4.96 (m, 4H, $H_{10\ and\ 13}$), 4.72-4.62 (m, 2H, H_{16}), 3.63-3.55 (m, 1H, H_1), 2.33-2.06 (m, 4H, $H_{7\ and\ 11}$), 2.05-1.95 (m, 1H, H_3), 1.76-1.69 (m, 1H, H_4), 1.69-1.60 (m, 3H, $H_{2\ and\ 5}$), 1.58-1.50 (m, 1H, H_2), 1.46-1.36 (m, 1H, H_4), 1.12 (s, 3H, H_7).

^{13}C NMR (100 MHz, $CDCl_3$) δ ppm: 151.3 (C_{14}), 136.1 (C_{12}), 135.2 (C_9), 117.3 (C_{10}), 116.7 (C_{13}), 108.9 (C_{16}), 76.8 (C_6), 70.9 (C_1), 49.5 (C_3), 45.4 (C_8), 42.5 (C_{11}), 41.9 (C_2), 38.9 (C_5), 27.8 (C_4), 26.1 (C_7), 20.6 (C_{15}).

HRMS(EI+) m/z: calculated for $C_{13}H_{21}O^+$ [M-allyl]$^+$: 193.1587 found: 193.1584.

IR (ATR) ν (cm^{-1}): 3075, 2976, 2934, 1641, 1435, 1376, 1288, 1233, 1124, 1083, 1025, 997.

3-Hydroperoxycyclohex-1-ene 476

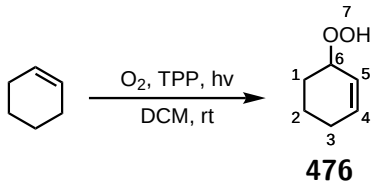

476

Experimental: To a stirred solution of cyclohexene (200 μL, 2 mmol, 1 equiv.) in 10 mL of dry DCM was added TPP (3.2 mg, 0.02 mmol, 0.01 equiv.) at rt under O_2 atmosphere. The reaction mixture was irradiated with white LED light. After 4 days, the

reaction mixture was concentrated in vacuo. The crude product was purified via silica gel chromatography (PE/Et_2O 80:20) to yield 103 mg (45% yield) of hydroperoxide **476**.
All spectra and physical data matched published value.[8]

Physical state: colorless oil.

^{1}H NMR (400 MHz, $CDCl_3$) δ ppm: 7.96-7.87 (m, 1H, H_7), 6.04-5.99 (m, 2H, H_5), 5.78-5.72 (m, 2H, H_4), 4.56-4.52 (m, 2H, H_6), 2.13-1.89 (m, 3H, $H_{1\ and\ 3}$), 1.80-1.53 (m, 3H, $H_{2\ and\ 3}$).

^{13}C NMR (100 MHz, $CDCl_3$) δ ppm: 134.5 (C_5), 124.0 (C_4), 78.6 (C_6), 26.4 (C_3), 25.3 (C_1), 18.3.

2,7-Diallyloxepane 479

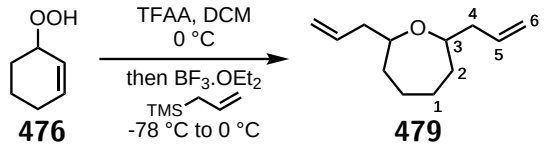

476 479

Experimental: To a stirred solution of hydroperoxide **476** (23 mg, 0.2 mmol, 1 equiv.) in 2 mL of dry DCM was added TFAA (28 μL, 0.2 mmol, 1 equiv.) at 0 °C. After 5 min, the reaction mixture was cooled down to -78 °C and allyltrimethylsilane (127 μL, 0.8 mmol, 4 equiv.) followed by $BF_3.OEt_2$ (40 μL, 0.32 mmol, 1.6 equiv.) were added. The reaction mixture was allowed to slowly warmed up over 2 h to 0 °C. After completion, the reaction mixture was cooled down to -78 °C, quenched with 3 mL of a 1:1:1 solution of DCM/MeOH/Et_3N and extracted with DCM (3 x 5 mL). The organic layers were combined, washed with brine, dried over Na_2SO_4, filtered and concentrated in vacuo. The crude

[8]T. Kuga, Y. Sasanoa, Y. Iwabuchi, *Chem. Commun.* **2018**, *54*, 798-801.

product was purified via silica gel chromatography (pentane/Et_2O 100:0 to 99:1) to yield 10 mg (27% yield) of oxepane **479**.

Physical state: colorless oil.

^{1}**H NMR** (400 MHz, $CDCl_3$) δ ppm: 5.92-5.79 (m, 2H, H_5), 5.09-4.98 (m, 4H, H_6), 3.72-3.63 (m, 2H, H_1), 2.33-2.24 (m, 2H, H_4), 2.16-2.07 (m, 2H, H_4), 1.85-1.75 (m, 2H, $H_{2\ and\ 4}$), 1.40-1.33 (m, 2H, $H_{2\ and\ 4}$).

^{13}**C NMR** (100 MHz, $CDCl_3$) δ ppm: 136.2 (C_5), 116.4 (C_6), 74.5 (C_1), 41.5 (C_4), 35.8 (C_2), 27.4 (C_3).

HRMS(EI+) m/z: calculated for $C_9H_{15}O^+$ [M-allyl]$^+$: 139.1117 found: 139.1120.

IR (ATR) ν (cm^{-1}): 3075, 2977, 2924, 2854, 1640, 1443, 1354, 1249, 1200, 1098, 1041, 991, 956, 909, 866, 839, 805.

5.2 Computation

Calculations were carried out with the Gaussian09 package,[9] and all structures were fully optimized without any symmetry constraints at the DFT level by means of the M06 and M06-2X functionals, which is known to perform well for main group compounds and non-covalent bonds and to include partly dispersion forces.[10] The 6-31G(d,p) basis set was applied for all atoms. Each stationary point has been characterized with frequency analysis and shows the correct number of negative eigenvalues (zero for a local minimum and one for a transition state). All transition states were verified by stepping along the reaction coordinate (intrinsic reaction coordinate calculations) and confirming that they transformed into the corresponding reactants/products. Final energy calculations at the M06 and M06-2X levels associated with the 6-311+G(2d,2p) basis set, including solvation effect, have been achieved on the M06/6-31G(d,p) and M06-2X/6-31G(d,p) geometries. Solvent effects are accounted for by means of single point calculations with the integral equation formalism version of the polarizable continuum model (IEFPCM) for chloroform and dichloromethane. To get accurate geometries and energies, the SCF convergence criterion was systematically tightened to 10^{-8}au, and the force minimizations were carried out until the rms force became smaller that (at least) 1 x 10^{-5}au ("tight" optimization keyword in Gaussian 09). The "UltraFine" grid (99 radial shells and 590 angular points per shell) was used throughout the calculations, as recommended when using Gaussian 09. The enthalpies and Gibbs free energies presented in this ex-

[9] M. J. Frisch, G. W. Trucks, H. B. Schlegel, G. E. Scuseria, M. A. Robb, J. R. Cheeseman, G. Scalmani, V. Barone, B. Mennucci, G. A. Petersson, H. Nakatsuji, M. Caricato, X. Li, H. P. Hratchian, A. F. Izmaylov, J. Bloino, G. Zheng, J. L. Sonnenberg, M.Hada, M. Ehara, K. Toyota, R. Fukuda, J. Hasegawa, M. Ishida, T. Nakajima, Y. Honda, O. Kitao, H. Nakai,T. Vreven, J. A. Montgomery Jr., J. E. Peralta, F. Ogliaro, M. Bearpark, J. J. Heyd, E. Brothers, K. N. Kudin, V. N. Staroverov, R. Kobayashi,J. Normand, K. Raghavachari, A. Rendell, J. C. Burant, S. S. Iyengar, J. Tomasi, M. Cossi, N. Rega, J. M. Millam, M. Klene, J. E. Knox, J. B. Cross, V. Bakken, C. Adamo, J. Jaramillo, R. Gomperts, R. E. Stratmann, O. Yazyev, A. J. Austin, R. Cammi, C. Pomelli, J. W. Ochterski, R. L. Martin, K. Morokuma, V. G. Zakrzewski, G. A. Voth, P. Salvador, J. J. Dannenberg, S.Dapprich, A. D. Daniels, Ö. Farkas, J. B. Foresman, J. V. Ortiz, J. Cioslowski, D. J. Fox, Gaussian, Inc., Wallingford CT, Gaussian 09, Revision D.01, **2013**.

[10] Y. Zhao, D. G. Truhlar, *Theor. Chem. Acc.* **2008**, *120*, 215-241.

perimental secion are IEFPCM(chloroform)-M06/6-311+G(2d,2p)//M06/6-31G(d,p) and IEFPCM(dichloromethane)-M06/6-311+G(2d,2p)//M06/6-31G(d,p) electronic energies (which include solvation-energy corrections from the IEFPCM method) modified with thermal and entropy corrections from gas phase M06/6-31G(d,p) calculations. Due to the well-known errors associated with entropy calculations, we apply a scaling factor of 0.5 to the entropic contributions as recommended in the literature.[11] Therefore, the calculated Gibbs free energy values reported in this study include the ZPE, enthalpic temperature correction, solvation energy, and half the gas phase entropy.

Cartesian coordinates of the optimized geometries and associated energies and free energy corrections obtained.

[11] (a) J. Cooper, T. A. Ziegler, *Inorg. Chem.* **2002**, *41*, 6614-6622. (b) J. K. C. Lau, D. V. Deudel, *J. Chem. Theory Comput.* **2006**, *2*, 103-106. (c) H. Li, G. Lu, J. Jiang, F. Huang, Z. X. Wang, *Organometallics*, **2011**, *30*, 2349-2363. (d) J. Hua, H. E. Krizner, D. O. De Haan, *J. Phys. Chem. A* **2011**, *115*, 1667-1675.

Cartesian coordinates of the optimized geometries and associated energies and free energy corrections obtained at the M06/6-31G(d,p) level of theory

419

C	2.052719000	0.345516000	0.039207000
C	2.825784000	-0.433868000	0.779800000
H	2.523960000	1.106862000	-0.584323000
O	4.241142000	-0.213289000	0.788764000
C	4.557928000	-0.962329000	-1.487054000
H	4.360692000	-0.118631000	-2.164465000
H	5.355184000	-1.551716000	-1.948706000
C	5.016048000	-0.430511000	-0.193371000
H	3.631717000	-1.536626000	-1.399610000
C	6.434727000	-0.129965000	0.041780000
H	6.986173000	-1.080973000	0.070840000
H	6.847560000	0.428981000	-0.806180000
H	6.586749000	0.407441000	0.978547000
H	2.534525000	-1.161015000	1.528619000
C	0.548678000	0.281583000	-0.041186000
C	0.130556000	-0.735344000	-1.163839000
H	0.341935000	-0.266653000	-2.133047000
H	0.808435000	-1.593454000	-1.057186000
C	-0.074189000	-0.233162000	1.260697000
O	0.411826000	-1.119147000	1.926567000
O	-1.239273000	0.345420000	1.476901000
C	0.086440000	1.725875000	-0.254588000
O	0.584640000	2.634069000	0.367007000
O	-0.868658000	1.832291000	-1.161641000
C	-1.560406000	3.101760000	-1.244030000
H	-1.952998000	3.131675000	-2.264276000
H	-0.834088000	3.909355000	-1.111428000
C	-2.653886000	3.132169000	-0.207990000
H	-2.227242000	3.116429000	0.800815000
H	-3.253753000	4.041094000	-0.312557000
H	-3.311625000	2.262809000	-0.324980000
C	-2.079033000	-0.217049000	2.518897000
H	-1.949926000	-1.304916000	2.505995000
H	-1.715021000	0.160195000	3.480880000
C	-3.491677000	0.195929000	2.215464000
H	-3.794432000	-0.187070000	1.233518000
H	-4.169708000	-0.214211000	2.969583000
H	-3.598550000	1.285589000	2.217068000
C	-1.289488000	-1.246601000	-1.111748000
C	-2.320151000	-0.648050000	-1.838924000
C	-1.585936000	-2.362771000	-0.324431000
C	-3.618927000	-1.137269000	-1.759695000
H	-2.101605000	0.206801000	-2.473869000
C	-2.885832000	-2.849348000	-0.237540000
H	-0.788918000	-2.855000000	0.232232000
C	-3.908034000	-2.233287000	-0.952071000
H	-4.408375000	-0.664702000	-2.338839000
H	-3.096495000	-3.720378000	0.378021000
H	-4.923530000	-2.616322000	-0.893696000

There are no imaginary frequencies.

SCF energy=-1114.24412618 hartree

Zero-point correction=+0.408147 hartree

Energy correction=+0.434066 hartree

Enthalpy correction=+0.435011 hartree

Gibbs Free Energy correction=+0.350117 hartree

427

C	2.088309000	0.208200000	0.336641000
C	2.742642000	-0.981244000	0.601335000
H	2.366265000	1.097981000	0.911721000
O	4.064443000	-1.117573000	0.531282000
C	4.463148000	0.976179000	-0.513679000
H	4.156726000	1.680197000	0.256087000
H	5.019119000	1.446208000	-1.323452000
C	4.864977000	-0.307417000	-0.185493000
H	3.049111000	0.646098000	-0.602616000
C	6.055898000	-1.018794000	-0.692955000
H	6.588184000	-0.409442000	-1.425270000
H	6.741524000	-1.207690000	0.143823000
H	5.794181000	-1.991104000	-1.121783000
H	2.249708000	-1.940197000	0.746541000
C	0.602752000	0.218587000	0.049222000
C	0.216282000	-0.685996000	-1.162555000
H	0.454579000	-0.133859000	-2.080012000
H	0.882312000	-1.559931000	-1.138501000
C	-0.132202000	-0.331853000	1.290612000
O	0.306222000	-1.244716000	1.950888000
O	-1.292647000	0.266287000	1.453455000
C	0.231414000	1.700559000	-0.095397000
O	0.742569000	2.543014000	0.608934000
O	-0.666889000	1.912321000	-1.033713000
C	-1.287272000	3.223375000	-1.079534000
H	-1.603165000	3.336521000	-2.119971000
H	-0.531297000	3.978680000	-0.845359000
C	-2.447697000	3.245469000	-0.119863000
H	-2.096222000	3.131694000	0.911419000
H	-2.986377000	4.194538000	-0.195957000
H	-3.143413000	2.429334000	-0.346752000
C	-2.214285000	-0.321619000	2.413347000
H	-2.118247000	-1.410833000	2.345474000
H	-1.896489000	-0.009458000	3.414089000
C	-3.589974000	0.158222000	2.047597000
H	-3.839900000	-0.153652000	1.026357000
H	-4.327878000	-0.272614000	2.730497000
H	-3.662084000	1.248578000	2.111696000
C	-1.207267000	-1.187494000	-1.193152000
C	-2.213177000	-0.513903000	-1.888226000
C	-1.535074000	-2.360984000	-0.508875000
C	-3.519026000	-0.991146000	-1.880680000
H	-1.969454000	0.389762000	-2.441549000
C	-2.842127000	-2.835671000	-0.492183000
H	-0.757323000	-2.910288000	0.022076000
C	-3.839405000	-2.147865000	-1.175901000
H	-4.289326000	-0.461164000	-2.435355000
H	-3.077498000	-3.752467000	0.042427000
H	-4.860112000	-2.521206000	-1.173951000

There is one imaginary frequency=-1216.21 cm^{-1}.

SCF energy=-1114.18906188 hartree

Zero-point correction=+0.405340 hartree

Energy correction=+0.429687 hartree

Enthalpy correction=+0.430632 hartree

Gibbs Free Energy correction=+0.350973 hartree

418

C	1.929476000	0.183753000	-1.283072000
C	2.267604000	-1.206146000	-0.767627000
H	2.567893000	0.920023000	-0.782348000
O	3.498596000	-1.464577000	-0.329674000
C	3.864917000	-0.020484000	1.530114000
H	2.972668000	-0.381212000	2.030492000
H	4.471562000	0.717170000	2.043916000
C	4.250232000	-0.474524000	0.344991000
H	2.085400000	0.239912000	-2.364575000
C	5.470646000	-0.120984000	-0.418973000
H	6.086006000	0.589690000	0.136822000
H	6.065759000	-1.018395000	-0.622413000
H	5.212138000	0.320233000	-1.390563000
H	1.953076000	-2.032015000	-1.414199000
C	0.466089000	0.421429000	-0.891312000
C	-0.536358000	-0.132637000	-1.954901000
H	-0.753225000	0.691643000	-2.642673000
H	-0.005764000	-0.899387000	-2.535155000
C	0.381531000	-0.433345000	0.337094000
O	1.252067000	-1.353288000	0.431655000
O	-0.528784000	-0.245422000	1.199499000
C	0.233160000	1.858261000	-0.404972000
O	0.998040000	2.365479000	0.379559000
O	-0.881123000	2.383265000	-0.873553000
C	-1.332484000	3.612677000	-0.238294000
H	-2.021982000	4.049187000	-0.964378000
H	-0.471605000	4.275287000	-0.111083000
C	-2.002221000	3.277525000	1.070268000
H	-1.278069000	2.874100000	1.785853000
H	-2.445735000	4.176549000	1.507819000
H	-2.797438000	2.537955000	0.920088000
C	-0.726670000	-1.207923000	2.304980000
H	-0.771318000	-2.200864000	1.844054000
H	0.158514000	-1.140140000	2.945799000
C	-2.004260000	-0.809108000	2.977376000
H	-2.836373000	-0.850436000	2.265998000
H	-2.214905000	-1.502197000	3.796601000
H	-1.935417000	0.200666000	3.392139000
C	-1.798627000	-0.733121000	-1.393556000
C	-2.933720000	0.038394000	-1.143564000
C	-1.816544000	-2.089763000	-1.056518000
C	-4.057136000	-0.532102000	-0.554390000
H	-2.934974000	1.091015000	-1.417573000
C	-2.936983000	-2.661854000	-0.461997000
H	-0.948022000	-2.713118000	-1.278837000
C	-4.059403000	-1.879899000	-0.204870000
H	-4.940380000	0.076464000	-0.377111000
H	-2.941696000	-3.721782000	-0.220273000
H	-4.941957000	-2.324902000	0.247062000

There are no imaginary frequencies.

SCF energy=-1114.25893752 hartree

Zero-point correction=+0.412434 hartree

Energy correction=+0.436497 hartree

Enthalpy correction=+0.437441 hartree

Gibbs Free Energy correction=+0.358485 hartree

250 258

C	-1.336802000	-1.335424000	0.456406000
C	-1.551698000	-0.690172000	-1.752485000
H	-1.938766000	-0.392354000	-2.722491000
O	-1.593464000	-1.636720000	1.589595000
C	-2.267274000	-0.991608000	-0.662697000
C	-3.747374000	-0.962921000	-0.531424000
O	-4.314862000	-1.466450000	0.412959000
N	-0.031466000	-1.157974000	-0.086433000
C	1.143014000	-1.599066000	0.553677000
C	2.422673000	-1.000474000	0.067718000
C	2.535928000	0.345173000	-0.288543000
C	3.560842000	-1.808580000	0.080684000
C	3.771718000	0.871609000	-0.643365000
H	1.658756000	0.989236000	-0.246168000
C	4.789919000	-1.287161000	-0.298690000
H	3.460848000	-2.843159000	0.399740000
C	4.896705000	0.053256000	-0.661424000
H	3.855136000	1.925365000	-0.901272000
H	5.671269000	-1.923581000	-0.301378000
H	5.862331000	0.462690000	-0.948449000
O	1.125537000	-2.417982000	1.442565000
C	-0.092188000	-0.758238000	-1.483209000
H	0.360310000	0.228312000	-1.658400000
H	0.428191000	-1.474891000	-2.135148000
C	-4.500187000	-0.253809000	-1.630181000
H	-4.330301000	-0.735041000	-2.600977000
H	-5.567137000	-0.277231000	-1.401625000
H	-4.162265000	0.786582000	-1.715674000
C	-0.352052000	2.326379000	0.873538000
C	-2.758873000	1.756469000	1.243023000
H	-3.109150000	2.518562000	0.547298000
H	-3.510336000	1.142785000	1.733984000
C	-1.460120000	1.589736000	1.501661000
H	-1.171457000	0.849999000	2.253292000
C	0.605780000	3.436937000	-1.213764000
H	0.154258000	4.335702000	-1.653542000
H	1.459007000	3.764133000	-0.611203000
H	0.999725000	2.849829000	-2.056835000
C	0.799774000	2.601251000	1.795244000
H	1.644422000	3.098907000	1.310305000
H	0.480500000	3.220487000	2.642796000
H	1.169154000	1.657678000	2.222282000
C	-0.400802000	2.665090000	-0.427664000
H	-1.285828000	2.340339000	-0.983482000
H	-0.788918000	-2.855000000	0.232232000
C	-3.908034000	-2.233287000	-0.952071000
H	-4.408375000	-0.664702000	-2.338839000
H	-3.096495000	-3.720378000	0.378021000
H	-4.923530000	-2.616322000	-0.893696000

There are no imaginary frequencies.

SCF energy=-1016.38207024 hartree

Zero-point correction=+0.356525 hartree

Energy correction=+0.380630 hartree

Enthalpy correction=+0.381574 hartree

Gibbs Free Energy correction=+0.300714 hartree

TS1 non catalysed

C	-0.951565000	-1.528090000	0.347948000
C	-1.427132000	0.240561000	-1.138327000
H	-1.904929000	0.572681000	-2.058844000
O	-1.040385000	-2.410314000	1.160332000
C	-2.009039000	-0.738903000	-0.329906000
C	-3.419220000	-1.167357000	-0.383928000
O	-3.870936000	-2.055079000	0.313045000
N	0.281329000	-0.987909000	-0.130932000
C	1.516383000	-1.650790000	0.016804000
C	2.721012000	-0.773687000	-0.066361000
C	2.735878000	0.495085000	0.512861000
C	3.880032000	-1.278030000	-0.655308000
C	3.890077000	1.266749000	0.481575000
H	1.841309000	0.854539000	1.017552000
C	5.029119000	-0.499536000	-0.703574000
H	3.860696000	-2.284815000	-1.065830000
C	5.034418000	0.773413000	-0.138832000
H	3.898384000	2.250036000	0.947776000
H	5.928047000	-0.888169000	-1.175583000
H	5.937659000	1.377967000	-0.172369000
O	1.608867000	-2.841660000	0.199462000
C	0.063249000	0.010443000	-1.173660000
H	0.655448000	0.918142000	-1.008532000
H	0.357578000	-0.388736000	-2.156866000
C	-4.305913000	-0.445910000	-1.380551000
H	-4.000976000	-0.681489000	-2.407643000
H	-5.336107000	-0.775614000	-1.232810000
H	-4.255578000	0.646416000	-1.274662000
C	-1.031870000	2.156213000	0.831326000
C	-2.485040000	0.469765000	1.863068000
H	-3.366774000	0.729025000	1.284767000
H	-2.607811000	-0.355375000	2.558922000
C	-1.375899000	1.260395000	1.873177000
H	-0.620920000	1.083420000	2.641786000
C	-1.435196000	3.079186000	-1.488079000
H	-1.583239000	4.126104000	-1.192160000
H	-0.392632000	2.986708000	-1.819504000
H	-2.076021000	2.892070000	-2.356610000
C	0.210677000	2.985375000	0.951433000
H	0.925715000	2.805803000	0.135740000
H	-0.032961000	4.055846000	0.909867000
H	0.728088000	2.800929000	1.899069000
C	-1.755460000	2.138920000	-0.363179000
H	-2.811729000	1.883496000	-0.279199000
H	-0.788918000	-2.855000000	0.232232000
C	-3.908034000	-2.233287000	-0.952071000
H	-4.408375000	-0.664702000	-2.338839000
H	-3.096495000	-3.720378000	0.378021000
H	-4.923530000	-2.616322000	-0.893696000

There is one imaginary frequency=-462.53 cm^{-1}.

SCF energy=-1016.35251594 hartree

Zero-point correction=+0.356982 hartree

Energy correction=+0.379364 hartree

Enthalpy correction=+0.380308 hartree

Gibbs Free Energy correction=+0.305605 hartree

259

C	0.881463000	-1.397671000	-0.432174000
C	1.465679000	0.501477000	0.986174000
H	1.941944000	0.242538000	1.939297000
O	0.938006000	-2.319799000	-1.212158000
C	2.026928000	-0.441015000	-0.084559000
C	3.271749000	-1.198913000	0.415279000
O	3.755292000	-0.941047000	1.497053000
N	-0.256918000	-0.957169000	0.222148000
C	-1.495753000	-1.649276000	0.158117000
C	-2.706098000	-0.787624000	0.073923000
C	-2.706634000	0.418977000	-0.631560000
C	-3.890418000	-1.260559000	0.640520000
C	-3.879626000	1.153001000	-0.749382000
H	-1.791939000	0.762139000	-1.114602000
C	-5.056381000	-0.514892000	0.539044000
H	-3.874895000	-2.218543000	1.154532000
C	-5.050720000	0.692652000	-0.154107000
H	-3.881933000	2.084285000	-1.310502000
H	-5.974703000	-0.877844000	0.993524000
H	-5.966008000	1.273628000	-0.238945000
O	-1.552929000	-2.854658000	0.166878000
C	-0.043782000	0.219326000	1.061151000
H	-0.628843000	1.070040000	0.691078000
H	-0.379385000	0.013626000	2.085436000
C	3.891738000	-2.205850000	-0.508832000
H	4.654874000	-2.765422000	0.035343000
H	3.131118000	-2.868248000	-0.933363000
H	4.366875000	-1.691315000	-1.353184000
C	1.207246000	2.311694000	-0.686547000
C	2.420537000	0.295835000	-1.398660000
H	3.459074000	0.654532000	-1.294094000
H	2.418400000	-0.426518000	-2.222660000
C	1.522138000	1.461595000	-1.671604000
H	1.165689000	1.626776000	-2.688085000
C	1.273240000	2.877894000	1.822024000
H	1.527821000	3.928710000	1.647535000
H	0.186313000	2.823884000	1.964628000
H	1.743268000	2.575973000	2.764716000
C	0.345389000	3.512581000	-0.907947000
H	-0.563709000	3.487527000	-0.290058000
H	0.867677000	4.442940000	-0.648207000
H	0.037241000	3.583151000	-1.956432000
C	1.753597000	1.982760000	0.689001000
H	2.854832000	2.070395000	0.645668000
H	-0.788918000	-2.855000000	0.232232000
C	-3.908034000	-2.233287000	-0.952071000
H	-4.408375000	-0.664702000	-2.338839000
H	-3.096495000	-3.720378000	0.378021000
H	-4.923530000	-2.616322000	-0.893696000

There are no imaginary frequencies.

SCF energy=-1016.44648671 hartree

Zero-point correction=+0.363869 hartree

Energy correction=+0.384987 hartree

Enthalpy correction=+0.385931 hartree

Gibbs Free Energy correction=+0.313231 hartree

250 258 256

C	0.490412000	1.889452000	-1.166866000
C	-0.098118000	3.717737000	-2.432922000
H	-0.577146000	4.400912000	-3.127493000
O	0.476158000	0.784730000	-0.674451000
C	-0.449181000	2.452131000	-2.172551000
C	-1.544811000	1.643174000	-2.750433000
O	-1.456357000	0.426828000	-2.762611000
N	1.375683000	2.927429000	-0.841443000
C	2.542688000	2.725005000	-0.063811000
C	3.213455000	3.933407000	0.481359000
C	2.513838000	5.042088000	0.964040000
C	4.604074000	3.876699000	0.607504000
C	3.203806000	6.097630000	1.545763000
H	1.425295000	5.051468000	0.935262000
C	5.290875000	4.944896000	1.165931000
H	5.120866000	2.979638000	0.272396000
C	4.592141000	6.056001000	1.632337000
H	2.654699000	6.950462000	1.938925000
H	6.373598000	4.907477000	1.251042000
H	5.132310000	6.887093000	2.079058000
O	2.979352000	1.615341000	0.132516000
F	4.643812000	-6.115055000	0.761449000
C	4.014281000	-5.744703000	-0.361808000
C	3.611540000	-4.302192000	-0.304911000
F	2.975625000	-6.562786000	-0.532398000
F	4.872033000	-5.964283000	-1.369407000
C	2.281432000	-3.931774000	-0.435704000
C	4.622429000	-3.359005000	-0.134986000
C	1.945297000	-2.575449000	-0.383324000
H	1.511328000	-4.681071000	-0.573695000
C	4.277299000	-2.017099000	-0.099144000
H	5.657807000	-3.672694000	-0.037930000
N	0.647120000	-2.077071000	-0.559703000
C	2.949877000	-1.621486000	-0.217947000
C	5.312107000	-0.949847000	0.094965000
C	-0.568072000	-2.601308000	-0.209493000
H	0.636799000	-1.077478000	-0.756059000
H	2.696133000	-0.561777000	-0.174676000
F	5.254888000	-0.026796000	-0.876859000
F	6.554290000	-1.447247000	0.098007000
F	5.138774000	-0.300214000	1.251247000
S	-0.811471000	-4.066168000	0.544617000
N	-1.565310000	-1.728888000	-0.590532000
H	-1.283637000	-0.997602000	-1.243389000
C	-2.911745000	-1.656853000	-0.228878000
C	-3.718795000	-0.831135000	-1.021524000
C	-3.477292000	-2.261119000	0.896876000
C	-5.033805000	-0.574635000	-0.668587000
H	-3.298608000	-0.379959000	-1.918331000
C	-4.811723000	-2.019962000	1.208775000
H	-2.878753000	-2.913123000	1.524327000
C	-5.604755000	-1.169663000	0.450152000
C	-5.779786000	0.449984000	-1.461037000
C	-5.368167000	-2.703850000	2.423040000
H	-6.636091000	-0.976281000	0.724392000
F	-5.522948000	0.362608000	-2.773195000
F	-7.098790000	0.372741000	-1.295439000
F	-5.408940000	1.697533000	-1.092908000
F	-5.341342000	-4.032838000	2.286210000
F	-6.634324000	-2.348374000	2.665334000
F	-4.651509000	-2.409853000	3.514597000
C	1.074778000	4.124829000	-1.615429000
H	0.797811000	4.973106000	-0.975422000
H	1.933322000	4.437326000	-2.225905000
C	-2.767974000	2.342353000	-3.258075000
H	-2.567022000	3.338621000	-3.662514000
H	-3.261689000	1.718079000	-4.006754000
H	-3.466229000	2.459079000	-2.416419000

C	-0.989519000	3.992303000	1.626965000
C	-2.473744000	2.291413000	0.538365000
H	-3.247810000	3.018265000	0.293904000
H	-2.659492000	1.255267000	0.255818000
C	-1.365276000	2.634854000	1.198953000
H	-0.663336000	1.843591000	1.477940000
C	-1.021511000	6.501043000	1.164655000
H	-1.959025000	7.069914000	1.212457000
H	-0.500501000	6.652562000	2.115154000
H	-0.418495000	6.975007000	0.375957000
C	-0.242953000	4.037020000	2.927799000
H	0.086895000	5.039893000	3.212663000
H	-0.861191000	3.639762000	3.742343000
H	0.647824000	3.394695000	2.874744000
C	-1.286664000	5.062773000	0.867428000
H	-1.800530000	4.863780000	-0.078167000

There are no imaginary frequencies.

SCF energy=-3374.02148235 hartree

Zero-point correction=+0.604847 hartree

Energy correction=+0.657397 hartree

Enthalpy correction=+0.658341 hartree

Gibbs Free Energy correction=+0.512408 hartree

TS catalysed

C	-0.189677000	1.846836000	-0.926628000
C	-1.853501000	3.313573000	-1.683910000
H	-2.373446000	3.762249000	-2.529269000
O	0.443023000	0.849837000	-0.647827000
C	-1.412032000	1.984389000	-1.726449000
C	-1.910401000	0.921359000	-2.586158000
O	-1.346168000	-0.166634000	-2.683393000
N	0.131137000	3.139073000	-0.461261000
C	1.406779000	3.461976000	0.067038000
C	1.459446000	4.693588000	0.898280000
C	0.426253000	5.026440000	1.775370000
C	2.616130000	5.472627000	0.860244000
C	0.532934000	6.146826000	2.587996000
H	-0.442720000	4.374830000	1.843712000
C	2.713893000	6.603819000	1.659276000
H	3.428450000	5.170958000	0.203420000
C	1.672555000	6.943619000	2.519217000
H	-0.268219000	6.393154000	3.281661000
H	3.609229000	7.218659000	1.620409000
H	1.755966000	7.825936000	3.148944000
O	2.385453000	2.785455000	-0.144354000
F	6.600479000	-4.073168000	0.828211000
C	5.928444000	-3.988935000	-0.328164000
C	5.051665000	-2.774419000	-0.356862000
F	5.242946000	-5.122531000	-0.480839000
F	6.850589000	-3.940439000	-1.301172000
C	3.679200000	-2.892387000	-0.512993000
C	5.668128000	-1.531291000	-0.235379000
C	2.893632000	-1.735904000	-0.536380000
H	3.218051000	-3.867403000	-0.614743000
C	4.880219000	-0.392206000	-0.277663000
H	6.745450000	-1.459926000	-0.117198000
N	1.506086000	-1.745142000	-0.739711000
C	3.500022000	-0.484262000	-0.424087000

C	5.480544000	0.974220000	-0.140903000	C	-3.173429000	3.306924000	0.713417000
C	0.557447000	-2.609872000	-0.267445000	C	-2.760311000	0.888503000	0.458388000
H	1.140579000	-0.828448000	-1.000059000	H	-3.436879000	0.748731000	-0.380328000
H	2.893574000	0.423303000	-0.443119000	H	-2.239246000	-0.004454000	0.798446000
F	5.129373000	1.765839000	-1.161299000	C	-2.687529000	2.045585000	1.161082000
F	6.818607000	0.935293000	-0.106658000	H	-2.129665000	2.042679000	2.099232000
F	5.070756000	1.578725000	0.979646000	C	-4.191537000	4.773336000	-1.073900000
S	0.849258000	-3.977249000	0.640424000	H	-5.137817000	4.971476000	-0.554823000
N	-0.688296000	-2.183057000	-0.674199000	H	-3.537424000	5.635286000	-0.890234000
H	-0.700361000	-1.451472000	-1.389709000	H	-4.410513000	4.745535000	-2.146876000
C	-1.960479000	-2.516791000	-0.215248000	C	-3.117827000	4.475791000	1.645512000
C	-3.033746000	-2.143828000	-1.036487000	H	-2.544992000	5.321587000	1.238642000
C	-2.238548000	-3.077544000	1.035164000	H	-4.129382000	4.861926000	1.831306000
C	-4.340406000	-2.274174000	-0.592241000	H	-2.683373000	4.204532000	2.613019000
H	-2.825505000	-1.719664000	-2.017518000	C	-3.577456000	3.482370000	-0.612577000
C	-3.559815000	-3.228428000	1.444331000	H	-3.973373000	2.596137000	-1.109964000
H	-1.425145000	-3.385501000	1.684501000				
C	-4.625915000	-2.819974000	0.654414000				
C	-5.430843000	-1.701356000	-1.438261000				
C	-3.796032000	-3.829018000	2.798930000				
H	-5.648716000	-2.926217000	0.999176000				
F	-5.229661000	-1.910360000	-2.742369000				
F	-6.634719000	-2.173630000	-1.123552000				
F	-5.491640000	-0.352160000	-1.284121000				
F	-3.322916000	-5.075683000	2.868028000				
F	-5.095407000	-3.870654000	3.112957000				
F	-3.175475000	-3.122422000	3.752827000				
C	-0.761942000	4.139512000	-1.046154000				
H	-1.117862000	4.861022000	-0.303722000				
H	-0.234231000	4.712584000	-1.823555000				
C	-3.173853000	1.151440000	-3.377115000				
H	-3.441108000	2.202544000	-3.523749000				
H	-3.070369000	0.661651000	-4.348911000				
H	-4.008511000	0.655540000	-2.861553000				

There is one imaginary frequency=-380.80 cm^{-1}.

SCF energy=-3373.99950528 hartree

Zero-point correction=+0.603694 hartree

Energy correction=+0.655228 hartree

Enthalpy correction=+0.656172 hartree

Gibbs Free Energy correction=+0.512128 hartree

259 256

C	-0.202373000	1.989472000	-0.515827000
C	-1.470626000	3.927585000	-1.288619000
H	-1.618680000	4.093597000	-2.365149000
O	0.095698000	0.879175000	-0.124027000
C	-1.590251000	2.419707000	-0.969797000
C	-2.044065000	1.577616000	-2.161739000
O	-1.494793000	0.535953000	-2.461568000
N	0.628616000	3.079582000	-0.526082000
C	2.031574000	2.950118000	-0.275367000
C	2.634478000	3.932784000	0.647883000
C	1.886072000	4.580490000	1.635784000
C	4.017082000	4.126211000	0.577672000
C	2.513730000	5.441620000	2.525004000
H	0.821659000	4.370935000	1.733833000
C	4.636822000	4.999315000	1.458802000
H	4.584138000	3.568629000	-0.163890000
C	3.885123000	5.660905000	2.426956000
H	1.935607000	5.935108000	3.302095000
H	5.710232000	5.157776000	1.400338000
H	4.374363000	6.340585000	3.120410000
O	2.655711000	2.059130000	-0.800811000
F	5.727258000	-5.164895000	0.481888000
C	5.097421000	-4.803489000	-0.644282000
C	4.445403000	-3.462292000	-0.490566000
F	4.227240000	-5.766960000	-0.947245000
F	6.027091000	-4.778981000	-1.610275000
C	3.064454000	-3.337758000	-0.550947000
C	5.275470000	-2.364278000	-0.280564000
C	2.488384000	-2.074272000	-0.384622000
H	2.439699000	-4.206372000	-0.719658000
C	4.692655000	-1.115143000	-0.129086000
H	6.353909000	-2.487201000	-0.238751000
N	1.118422000	-1.798143000	-0.473968000
C	3.313156000	-0.968854000	-0.175625000
C	5.527625000	0.117201000	0.042051000
C	0.023681000	-2.580115000	-0.222480000
H	0.922734000	-0.798829000	-0.534658000
H	2.872071000	0.018683000	-0.056804000
F	5.543470000	0.859400000	-1.073877000
F	6.798382000	-0.174025000	0.340970000
F	5.055366000	0.904934000	1.017645000
S	0.053265000	-4.152948000	0.327158000
N	-1.122775000	-1.872601000	-0.510047000
H	-0.993628000	-1.009038000	-1.037454000
C	-2.449494000	-2.116371000	-0.153686000
C	-3.431570000	-1.478714000	-0.920589000
C	-2.847503000	-2.871698000	0.952442000
C	-4.770878000	-1.570933000	-0.571197000
H	-3.133577000	-0.924080000	-1.808285000
C	-4.198124000	-2.972754000	1.267074000
H	-2.106033000	-3.377710000	1.562061000
C	-5.175516000	-2.323285000	0.524862000
C	-5.762953000	-0.772302000	-1.353512000
C	-4.567039000	-3.798119000	2.464586000
H	-6.223562000	-2.404466000	0.792137000
F	-5.478209000	-0.757253000	-2.663696000
F	-7.010306000	-1.214105000	-1.210903000
F	-5.755534000	0.521411000	-0.960362000
F	-4.189364000	-5.070180000	2.313619000
F	-5.884096000	-3.790918000	2.695304000
F	-3.962778000	-3.340507000	3.568559000
C	-0.020879000	4.321092000	-0.931520000
H	0.003230000	5.052369000	-0.114609000
H	0.511170000	4.763606000	-1.782357000
C	-3.273254000	2.021431000	-2.909033000
H	-3.577371000	3.053205000	-2.715969000
H	-3.110116000	1.871191000	-3.979812000
H	-4.103051000	1.363410000	-2.619542000

C	-2.405921000	4.450383000	0.952331000
C	-2.572745000	2.117148000	0.196331000
H	-3.603920000	2.096054000	-0.192346000
H	-2.359290000	1.104283000	0.560251000
C	-2.437426000	3.150090000	1.272102000
H	-2.379921000	2.826569000	2.310428000
C	-2.378972000	6.257116000	-0.886699000
H	-3.161704000	6.853855000	-0.407646000
H	-1.414622000	6.689141000	-0.592852000
H	-2.481631000	6.391124000	-1.969991000
C	-2.290962000	5.531475000	1.977947000
H	-1.406890000	6.164468000	1.815852000
H	-3.158441000	6.204241000	1.958639000
H	-2.220476000	5.106553000	2.984300000
C	-2.499655000	4.783930000	-0.524174000
H	-3.495126000	4.450394000	-0.869172000

There are no imaginary frequencies.

SCF energy=-3374.07545409 hartree

Zero-point correction=+0.610427 hartree

Energy correction=+0.660746 hartree

Enthalpy correction=+0.661690 hartree

Gibbs Free Energy correction=+0.520521 hartree

Cartesian coordinates of the optimized geometries and associated energies and free energy corrections obtained at the M06-2X/6-31G(d,p) level of theory

268

C	5.519956000	-0.599876000	-0.196274000
C	5.205461000	-1.618968000	-1.286872000
C	3.967059000	-2.481663000	-1.045287000
C	4.363929000	0.383580000	0.036299000
C	2.617852000	-1.725544000	-0.966088000
H	5.754137000	-1.111473000	0.746242000
H	5.069443000	-1.079852000	-2.234466000
H	4.090057000	-3.081818000	-0.134038000
H	2.654230000	-0.882333000	-1.662363000
H	6.416877000	-0.040800000	-0.483893000
H	6.070090000	-2.277311000	-1.427846000
H	3.906399000	-3.193285000	-1.876963000
H	4.753101000	1.281152000	0.529122000
C	2.380153000	-1.101249000	0.420981000
C	3.247602000	-0.174675000	0.893113000
C	1.167566000	-1.498338000	1.146608000
H	0.873908000	-2.542156000	1.078449000
C	3.263762000	0.355348000	2.304575000
H	2.884249000	1.386054000	2.348233000
H	2.689921000	-0.254432000	3.002023000
H	4.302082000	0.392565000	2.653422000
H	3.962274000	0.708253000	-0.933321000
C	1.536307000	-2.704764000	-1.504286000
H	1.847419000	-3.736844000	-1.316180000
H	1.513224000	-2.583426000	-2.594561000
C	-0.641882000	-1.456801000	-0.777362000
C	0.095822000	-2.690117000	-1.023531000
O	-0.443238000	-3.759549000	-0.749778000

C	0.408462000	-0.664877000	1.931510000	O	-2.460606000	2.556923000	0.066226000
H	0.769149000	0.343064000	2.122218000	C	-0.161059000	2.953803000	-0.290337000
C	-1.888044000	-1.488296000	-0.147680000	C	-0.382462000	4.300861000	-0.586771000
H	-2.525307000	-2.358469000	-0.274329000	C	1.118840000	2.526152000	0.069219000
C	-0.925781000	-0.923173000	2.333426000	C	0.670533000	5.207424000	-0.560937000
C	-1.644630000	-1.999942000	1.804818000	C	2.165526000	3.440673000	0.115520000
H	-1.085370000	-2.873670000	1.469663000	C	1.947097000	4.778016000	-0.206801000
C	-0.265177000	-0.072985000	-1.069024000	H	-1.390722000	4.619682000	-0.827638000
C	-2.481343000	-0.099700000	-0.199171000	H	1.310261000	1.484382000	0.297846000
H	-2.907862000	0.224125000	0.750847000	H	0.493846000	6.249053000	-0.807731000
C	-1.616972000	0.114442000	3.181769000	H	3.158029000	3.102884000	0.398366000
H	-2.212365000	-0.350567000	3.972719000	H	2.770287000	5.484945000	-0.178627000
H	-0.887495000	0.779258000	3.648006000				
H	-2.297720000	0.743867000	2.593138000				
O	0.679805000	0.361109000	-1.694485000				
N	-1.294817000	0.717146000	-0.480592000				
C	-3.050163000	-2.289533000	2.271252000				
H	-3.491279000	-3.105948000	1.695026000				
H	-3.059313000	-2.583630000	3.326493000				
H	-3.700143000	-1.412596000	2.170936000				
C	-3.555623000	0.023202000	-1.289651000				
H	-3.676568000	1.083675000	-1.534321000				
H	-3.197195000	-0.490851000	-2.190323000				
C	-4.909849000	-0.546748000	-0.848868000				
H	-4.742042000	-1.529215000	-0.380783000				
C	-5.817811000	-0.749587000	-2.061738000				
H	-6.795214000	-1.139613000	-1.763418000				
H	-5.980236000	0.204147000	-2.576152000				
H	-5.375387000	-1.447334000	-2.778416000				
C	-5.590128000	0.366479000	0.174317000				
H	-6.537187000	-0.064793000	0.511659000				
H	-4.970428000	0.546550000	1.058016000				
H	-5.801130000	1.342500000	-0.275449000				
C	-1.378339000	2.082919000	-0.244924000				

There is one imaginary frequency=-397.69 cm^{-1}.

SCF energy=-1484.56982288 hartree

Zero-point correction=+0.644371 hartree

Energy correction=+0.677641 hartree

Enthalpy correction=+0.678585 hartree

Gibbs Free Energy correction=+0.581072 hartree

269

C	5.324506000	-0.835695000	-0.260689000
C	4.994068000	-2.181095000	-0.904299000
C	3.747315000	-2.887948000	-0.368982000
C	4.179736000	0.181898000	-0.385164000
C	2.421600000	-2.113153000	-0.558832000
H	5.569179000	-0.973612000	0.800531000
H	4.858019000	-2.021386000	-1.982911000
H	3.869953000	-3.131156000	0.694541000
H	2.487240000	-1.556770000	-1.497189000
H	6.222494000	-0.431181000	-0.740556000
H	5.854105000	-2.852086000	-0.798501000
H	3.665580000	-3.845386000	-0.897785000
H	4.572614000	1.196322000	-0.259191000
C	2.211457000	-1.055395000	0.536436000
C	3.082839000	-0.024530000	0.635427000
C	1.009466000	-1.175830000	1.363088000
H	0.673329000	-2.182632000	1.599170000
C	3.137857000	0.960230000	1.772575000
H	2.735878000	1.935007000	1.465826000
H	2.604661000	0.623241000	2.661732000
H	4.187093000	1.125456000	2.043579000
H	3.757604000	0.137123000	-1.397961000
C	1.299293000	-3.165715000	-0.740335000
H	1.527908000	-4.059693000	-0.150506000
H	1.324473000	-3.486775000	-1.789419000
C	-0.793810000	-1.584415000	-0.532089000
C	-0.157759000	-2.893534000	-0.395323000
O	-0.807942000	-3.800652000	0.117150000
C	0.283806000	-0.125443000	1.870438000
H	0.679829000	0.881391000	1.755584000
C	-2.047515000	-1.351301000	0.038366000
H	-2.755689000	-2.169835000	0.125185000
C	-1.060156000	-0.205727000	2.313688000
C	-1.841085000	-1.341873000	2.067813000
H	-1.334705000	-2.303449000	1.983567000
C	-0.290613000	-0.354292000	-1.132732000
C	-2.513962000	0.026347000	-0.374652000
H	-2.911145000	0.601572000	0.460290000
C	-1.686585000	1.054239000	2.857086000
H	-2.371739000	0.837936000	3.681037000
H	-0.913236000	1.732277000	3.225134000
H	-2.253282000	1.600541000	2.089867000
O	0.696925000	-0.174644000	-1.815579000
N	-1.254879000	0.650782000	-0.809769000
C	-3.263991000	-1.419613000	2.565064000
H	-3.747285000	-2.335398000	2.217294000
H	-3.299497000	-1.419605000	3.660019000
H	-3.860955000	-0.567640000	2.218940000
C	-3.563582000	0.002995000	-1.490979000
H	-3.589709000	0.998603000	-1.950438000
H	-3.243181000	-0.708648000	-2.262189000
C	-4.965129000	-0.350252000	-0.976692000
H	-4.880923000	-1.215048000	-0.300755000
C	-5.874678000	-0.745500000	-2.139798000
H	-6.884314000	-0.979740000	-1.790255000
H	-5.951532000	0.079059000	-2.857371000
H	-5.485604000	-1.618762000	-2.671015000
C	-5.578753000	0.815390000	-0.196580000
H	-6.547594000	0.534476000	0.226435000
H	-4.939775000	1.157977000	0.623141000
H	-5.735284000	1.670692000	-0.862779000
C	-1.101631000	2.005350000	-0.542922000
O	-2.077150000	2.638389000	-0.165112000
C	0.246187000	2.674444000	-0.554182000
C	0.446123000	3.572135000	0.504324000
C	1.229833000	2.543958000	-1.536708000
C	1.628773000	4.293849000	0.606649000
C	2.410035000	3.278444000	-1.433941000

C	2.618209000	4.143551000	-0.363981000
H	-0.348720000	3.700844000	1.231848000
H	1.077043000	1.876295000	-2.371565000
H	1.775360000	4.976940000	1.436954000
H	3.167599000	3.175609000	-2.204318000
H	3.542576000	4.708114000	-0.291699000

There is one imaginary frequency=-398.40 cm^{-1}.

SCF energy=-1484.56795575 hartree

Zero-point correction=+0.644472 hartree

Energy correction=+0.677522 hartree

Enthalpy correction=+0.678466 hartree

Gibbs Free Energy correction=+0.582286 hartree

270

C	-5.893156000	-1.772762000	-0.094690000
C	-6.094854000	-0.575319000	-1.019649000
C	-5.244922000	0.657341000	-0.706969000
C	-4.435840000	-2.257491000	-0.073589000
C	-3.712686000	0.458321000	-0.806563000
H	-6.206137000	-1.520410000	0.926960000
H	-5.869523000	-0.893181000	-2.046917000
H	-5.489010000	1.049797000	0.289206000
H	-3.511116000	-0.249798000	-1.614340000
H	-6.541979000	-2.588890000	-0.430784000
H	-7.151675000	-0.285132000	-1.011432000
H	-5.534267000	1.434546000	-1.424218000
H	-4.401331000	-3.293931000	0.277296000
C	-3.131355000	-0.189366000	0.462234000
C	-3.542117000	-1.427651000	0.821157000
C	-2.123892000	0.566701000	1.209194000
H	-2.273052000	1.641211000	1.274278000
C	-3.268727000	-2.082012000	2.151029000
H	-2.536681000	-2.894081000	2.055726000
H	-2.921010000	-1.385304000	2.913505000
H	-4.196402000	-2.544364000	2.508018000
H	-4.039115000	-2.261326000	-1.096547000
C	-3.108642000	1.821293000	-1.250518000
H	-3.763714000	2.639453000	-0.936093000
H	-3.108567000	1.828892000	-2.347733000
C	-0.591538000	1.386489000	-0.721391000
C	-1.735218000	2.288339000	-0.803901000
O	-1.597980000	3.447640000	-0.420112000
C	-1.063074000	0.032660000	1.905716000
H	-0.983955000	-1.048603000	1.989547000
C	0.600923000	1.801895000	-0.130814000
H	0.887304000	2.849006000	-0.174591000
C	0.054573000	0.782721000	2.340857000
C	0.274418000	2.080949000	1.870332000

H	-0.587455000	2.683628000	1.585469000	C	4.909985000	-2.889894000	0.787150000
C	-0.449730000	0.024662000	-1.257603000	H	1.775071000	-1.679340000	1.306685000
C	1.656196000	0.737350000	-0.358819000	H	3.751881000	-2.504139000	-2.392276000
H	2.120291000	0.431958000	0.580859000	H	3.773566000	-2.467350000	2.569110000
C	1.106138000	0.108150000	3.184927000	H	5.780115000	-3.260016000	-1.146645000
H	1.195818000	0.614887000	4.152648000	H	5.786736000	-3.226120000	1.331156000
H	0.851933000	-0.936943000	3.377514000				
H	2.102349000	0.141429000	2.726116000				
O	-1.250690000	-0.656244000	-1.856026000				
N	0.868010000	-0.378313000	-0.914446000				
C	1.465052000	2.876086000	2.344070000				
H	1.522204000	3.836837000	1.827119000				
H	1.400679000	3.078968000	3.418990000				
H	2.406773000	2.341193000	2.170783000				
C	2.748418000	1.218327000	-1.326197000				
H	3.237204000	0.348785000	-1.783669000				
H	2.271052000	1.779088000	-2.139253000				
C	3.828179000	2.063967000	-0.641713000				
H	3.336256000	2.849295000	-0.047785000				
C	4.706007000	2.743433000	-1.692827000				
H	5.483926000	3.352457000	-1.223817000				
H	5.200486000	1.991423000	-2.317942000				
H	4.114927000	3.389361000	-2.348102000				
C	4.688429000	1.208854000	0.294239000				
H	5.480631000	1.809299000	0.750889000				
H	4.111470000	0.751291000	1.104697000				
H	5.159912000	0.391369000	-0.264804000				
C	1.467850000	-1.553615000	-1.390497000				
O	1.067945000	-2.169479000	-2.349174000				
C	2.671068000	-2.007400000	-0.611755000				
C	2.666776000	-2.011681000	0.782926000				
C	3.783526000	-2.480190000	-1.307285000				
C	3.783136000	-2.456596000	1.483518000				
C	4.907432000	-2.907295000	-0.606900000				

There is one imaginary frequency=-425.10 cm^{-1}.

SCF energy=-1484.55740145 hartree

Zero-point correction=+0.643882 hartree

Energy correction=+0.677157 hartree

Enthalpy correction=+0.678101 hartree

Gibbs Free Energy correction=+0.580533 hartree

271

C	5.664047000	1.474578000	-0.648503000
C	5.970264000	-0.009188000	-0.844708000
C	5.109950000	-0.978232000	-0.031667000
C	4.205074000	1.834631000	-0.971822000
C	3.594354000	-0.912422000	-0.334455000
H	5.888768000	1.773851000	0.383553000
H	5.838656000	-0.248689000	-1.908881000
H	5.266509000	-0.822276000	1.043747000
H	3.471826000	-0.673196000	-1.393761000
H	6.330558000	2.054936000	-1.296009000
H	7.026071000	-0.193602000	-0.615330000
H	5.464651000	-1.992597000	-0.252402000
H	4.132748000	2.906259000	-1.180104000
C	2.903366000	0.228089000	0.430767000
C	3.244569000	1.506973000	0.149250000
C	1.835424000	-0.145657000	1.357472000
H	1.942636000	-1.110415000	1.848851000
C	2.781686000	2.716103000	0.915494000
H	1.961183000	3.207899000	0.375949000
H	2.449632000	2.482588000	1.927769000
H	3.603813000	3.436558000	0.982370000
H	3.891039000	1.320571000	-1.888896000
C	3.024759000	-2.337300000	-0.134053000
H	3.542199000	-2.838150000	0.691655000
H	3.275722000	-2.914805000	-1.032900000
C	0.473294000	-1.721233000	-0.275764000
C	1.557081000	-2.601977000	0.165333000
O	1.277412000	-3.536478000	0.910719000
C	0.723477000	0.594683000	1.678267000
H	0.648925000	1.613551000	1.311052000
C	-0.792905000	-1.846864000	0.283292000
H	-1.142770000	-2.818090000	0.618639000
C	-0.465015000	0.056333000	2.240584000
C	-0.685242000	-1.318520000	2.300284000
H	0.172940000	-1.987161000	2.352487000
C	0.480636000	-0.626796000	-1.249130000
C	-1.738859000	-0.903981000	-0.438600000
H	-2.377660000	-0.351352000	0.252612000
C	-1.580918000	1.004666000	2.604633000
H	-1.882416000	0.853943000	3.647218000
H	-1.270810000	2.043955000	2.485192000
H	-2.481486000	0.858689000	1.993544000
O	1.317169000	-0.295915000	-2.051276000
N	-0.809824000	0.019835000	-1.113371000
C	-1.959719000	-1.873287000	2.883618000
H	-1.993392000	-2.960478000	2.782402000
H	-2.044904000	-1.634650000	3.949786000
H	-2.846215000	-1.457364000	2.388581000
C	-2.595980000	-1.716964000	-1.427508000
H	-2.989319000	-1.065431000	-2.216405000
H	-1.937036000	-2.434539000	-1.931517000
C	-3.757735000	-2.456686000	-0.750826000
H	-3.369485000	-2.967598000	0.142712000
C	-4.328151000	-3.517351000	-1.692456000
H	-5.163363000	-4.049392000	-1.228309000
H	-4.698144000	-3.050208000	-2.612148000
H	-3.567650000	-4.251949000	-1.971131000
C	-4.863658000	-1.496020000	-0.305507000
H	-5.661510000	-2.037301000	0.210857000
H	-4.501523000	-0.713676000	0.370001000
H	-5.308414000	-1.001018000	-1.177760000
C	-0.829016000	1.412088000	-1.023837000
O	0.178460000	2.078134000	-1.162651000
C	-2.124342000	2.096253000	-0.676374000
C	-2.009489000	3.300252000	0.025393000
C	-3.390755000	1.632779000	-1.031920000
C	-3.145055000	4.002595000	0.408684000
C	-4.529397000	2.341498000	-0.657604000

C	-4.409127000	3.519864000	0.073426000
H	-1.014840000	3.666993000	0.258505000
H	-3.495030000	0.727775000	-1.617389000
H	-3.046264000	4.928992000	0.964897000
H	-5.509421000	1.971763000	-0.942154000
H	-5.297461000	4.067393000	0.371385000

There is one imaginary frequency=-365.76 cm^{-1}.

SCF energy=-1484.55785042 hartree

Zero-point correction=+0.643972 hartree

Energy correction=+0.676957 hartree

Enthalpy correction=+0.677901 hartree

Gibbs Free Energy correction=+0.582115 hartree

272

C	5.288523000	-0.915361000	-0.322889000
C	4.922668000	-1.603994000	-1.636077000
C	3.649017000	-2.448885000	-1.606261000
C	4.197470000	0.037342000	0.190264000
C	2.358534000	-1.660352000	-1.281398000
H	5.499240000	-1.665519000	0.450265000
H	4.803919000	-0.832467000	-2.409246000
H	3.752004000	-3.273690000	-0.888835000
H	2.448190000	-0.666496000	-1.728980000
H	6.215157000	-0.350907000	-0.475224000
H	5.759218000	-2.235489000	-1.956160000
H	3.536252000	-2.909928000	-2.595325000
H	4.654466000	0.741794000	0.893380000
C	2.182246000	-1.444450000	0.225389000
C	3.060378000	-0.672858000	0.898851000
C	1.034112000	-2.104973000	0.879860000
H	0.853605000	-3.154509000	0.639325000
C	3.070751000	-0.487795000	2.394927000
H	2.765999000	0.532577000	2.666141000
H	2.417801000	-1.187398000	2.916104000
H	4.093598000	-0.615515000	2.768719000
H	3.811502000	0.638896000	-0.645198000
C	1.200930000	-2.382404000	-2.008316000
H	1.343714000	-3.467047000	-1.956401000
H	1.280011000	-2.118547000	-3.072017000
C	-0.882169000	-0.909025000	-1.250806000
C	-0.265115000	-2.207527000	-1.651645000
O	-0.993168000	-3.184308000	-1.689060000
C	0.163456000	-1.461383000	1.674250000
H	0.365006000	-0.409608000	1.894616000
C	-2.121038000	-0.854511000	-0.747423000
H	-2.795469000	-1.700025000	-0.688350000
C	-1.080477000	-1.995528000	2.256061000
C	-1.770895000	-2.964797000	1.629239000

H	-1.376268000	-3.333099000	0.682403000	C	2.641072000	4.554273000	0.653354000
C	-0.273662000	0.447473000	-1.182305000	H	-0.591680000	5.079906000	-0.248601000
C	-2.471262000	0.518383000	-0.275586000	H	1.402242000	1.391699000	0.675829000
H	-2.717308000	0.514730000	0.793744000	H	1.533846000	6.324292000	0.125251000
C	-1.506927000	-1.324030000	3.537995000	H	3.476706000	2.633831000	1.147659000
H	-2.477693000	-1.664144000	3.897582000	H	3.564801000	5.091201000	0.844330000
H	-0.770228000	-1.502385000	4.328468000				
H	-1.560369000	-0.238349000	3.396502000				
O	0.762054000	0.837888000	-1.669194000				
N	-1.201175000	1.233655000	-0.463824000				
C	-3.045752000	-3.616944000	2.071291000				
H	-2.885291000	-4.687642000	2.239276000				
H	-3.455026000	-3.192161000	2.988562000				
H	-3.809362000	-3.539016000	1.289077000				
C	-3.643150000	1.116769000	-1.075904000				
H	-3.860398000	2.105840000	-0.664796000				
H	-3.307409000	1.252340000	-2.111428000				
C	-4.911362000	0.252466000	-1.051683000				
H	-4.715730000	-0.675324000	-1.606378000				
C	-6.042511000	0.993930000	-1.764281000				
H	-6.943598000	0.376685000	-1.819683000				
H	-6.295317000	1.913027000	-1.224532000				
H	-5.756256000	1.270588000	-2.783204000				
C	-5.327388000	-0.116653000	0.374673000				
H	-6.284054000	-0.646656000	0.372963000				
H	-4.594422000	-0.762810000	0.870351000				
H	-5.444102000	0.786909000	0.984228000				
C	-1.069896000	2.531335000	0.033045000				
O	-2.061780000	3.117067000	0.426341000				
C	0.277410000	3.167533000	0.161868000				
C	0.318062000	4.556440000	0.025133000				
C	1.419544000	2.472184000	0.563916000				
C	1.502686000	5.247071000	0.250169000				
C	2.593757000	3.171880000	0.819562000				

There are no imaginary frequencies.

SCF energy=-1484.58734429 hartree

Zero-point correction=+0.642830 hartree

Energy correction=+0.678041 hartree

Enthalpy correction=+0.678985 hartree

Gibbs Free Energy correction=+0.574781 hartree

273

C	5.470921000	-0.813048000	-0.132782000
C	5.166129000	-1.910114000	-1.147189000
C	3.873452000	-2.682470000	-0.885361000
C	4.316814000	0.189886000	-0.024109000
C	2.556331000	-1.874259000	-0.978044000
H	5.665833000	-1.252705000	0.854326000
H	5.100750000	-1.454655000	-2.144675000
H	3.915244000	-3.162280000	0.101735000
H	2.638914000	-1.137310000	-1.787137000
H	6.386817000	-0.293084000	-0.434043000
H	6.000137000	-2.619861000	-1.185264000
H	3.823446000	-3.493518000	-1.622114000
H	4.687658000	1.124955000	0.410839000
C	2.234443000	-1.129198000	0.330566000
C	3.153903000	-0.282786000	0.831787000
C	0.858216000	-1.433499000	0.918281000
H	0.833228000	-2.491652000	1.229897000
C	3.246219000	0.251950000	2.245367000
H	2.871665000	1.280675000	2.339879000
H	2.744909000	-0.373838000	2.981820000
H	4.306808000	0.284885000	2.518905000
H	3.958383000	0.441602000	-1.030190000
C	1.460636000	-2.875040000	-1.381988000
H	1.477317000	-3.724302000	-0.680868000
H	1.648209000	-3.284182000	-2.376964000
C	-0.235455000	-1.342428000	-0.228693000
C	0.060837000	-2.331331000	-1.352644000
O	-0.792739000	-2.652216000	-2.148383000
C	0.348926000	-0.595751000	2.069354000
H	0.943236000	0.205478000	2.482425000
C	-1.682620000	-1.469122000	0.303540000
H	-2.195985000	-2.250678000	-0.265102000
C	-0.890226000	-0.794970000	2.531869000
C	-1.716119000	-1.835112000	1.805618000
H	-1.200534000	-2.803497000	1.896890000
C	-0.149068000	0.064191000	-0.828449000
C	-2.362746000	-0.107133000	-0.013493000
H	-2.855008000	0.322688000	0.863987000
C	-1.484341000	0.023224000	3.641697000
H	-1.790322000	-0.606905000	4.483857000
H	-0.764963000	0.758126000	4.009076000
H	-2.379310000	0.560414000	3.307246000
O	0.719733000	0.471216000	-1.562229000
N	-1.245251000	0.779797000	-0.363738000
C	-3.136716000	-2.039034000	2.326201000
H	-3.628993000	-2.843722000	1.772749000
H	-3.130513000	-2.317061000	3.383384000
H	-3.752952000	-1.140638000	2.222329000
C	-3.347726000	-0.218826000	-1.181990000
H	-3.532034000	0.781235000	-1.587919000
H	-2.861018000	-0.817077000	-1.964616000
C	-4.689224000	-0.849737000	-0.793215000
H	-4.493891000	-1.759158000	-0.205609000
C	-5.460166000	-1.258344000	-2.048630000
H	-6.429350000	-1.696735000	-1.792908000
H	-5.644910000	-0.382847000	-2.681190000
H	-4.898174000	-1.987477000	-2.639007000
C	-5.528781000	0.107567000	0.055955000
H	-6.467511000	-0.363159000	0.362949000
H	-5.008120000	0.436878000	0.960191000
H	-5.771331000	1.006214000	-0.521381000
C	-1.427964000	2.164936000	-0.359269000
O	-2.551438000	2.620064000	-0.261739000
C	-0.224425000	3.053407000	-0.367248000
C	-0.387474000	4.331246000	-0.903144000
C	0.987319000	2.698511000	0.230479000
C	0.666187000	5.237946000	-0.877764000
C	2.033170000	3.612088000	0.268154000

C	1.877634000	4.878472000	-0.292687000
H	-1.347882000	4.596967000	-1.331888000
H	1.119556000	1.712218000	0.664319000
H	0.540677000	6.225659000	-1.308639000
H	2.973799000	3.333478000	0.733633000
H	2.699998000	5.586443000	-0.268951000

There are no imaginary frequencies.

SCF energy=-1484.63326104 hartree

Zero-point correction=+0.648246 hartree

Energy correction=+0.680733 hartree

Enthalpy correction=+0.681677 hartree

Gibbs Free Energy correction=+0.585982 hartree

274

C	5.633000000	-0.468475000	-0.074200000
C	5.348078000	-0.976769000	-1.484390000
C	4.137416000	-1.900576000	-1.623949000
C	4.443601000	0.302385000	0.514961000
C	2.762254000	-1.282323000	-1.269909000
H	5.886426000	-1.306289000	0.588278000
H	5.194091000	-0.108098000	-2.139263000
H	4.279753000	-2.811058000	-1.026856000
H	2.766647000	-0.232778000	-1.578565000
H	6.510526000	0.186331000	-0.105689000
H	6.232333000	-1.498645000	-1.867377000
H	4.101541000	-2.221652000	-2.671570000
H	4.792081000	0.947198000	1.328799000
C	2.504543000	-1.263893000	0.247295000
C	3.350939000	-0.590347000	1.061140000
C	1.297839000	-1.932206000	0.747403000
H	1.031446000	-2.882774000	0.294825000
C	3.368690000	-0.693915000	2.564772000
H	2.996271000	0.226539000	3.033871000
H	2.793680000	-1.536629000	2.947618000
H	4.408539000	-0.808218000	2.893031000
H	4.029233000	0.967919000	-0.254332000
C	1.711671000	-2.007111000	-2.159798000
H	2.066928000	-3.012399000	-2.405045000
H	1.660628000	-1.454303000	-3.106228000
C	-0.510611000	-1.223646000	-1.037486000
C	0.283671000	-2.248507000	-1.704531000
O	-0.199308000	-3.370184000	-1.839675000
C	0.520708000	-1.460717000	1.777860000
H	0.868606000	-0.589730000	2.325983000
C	-1.754109000	-1.536000000	-0.485224000
H	-2.337490000	-2.343257000	-0.918354000
C	-0.805292000	-1.875347000	2.048641000
C	-1.496356000	-2.705776000	1.161936000

H	-0.913294000	-3.384937000	0.539681000	C	1.088848000	5.271946000	-0.427248000
C	-0.221417000	0.200775000	-0.853422000	H	-1.941391000	4.042119000	-1.321532000
C	-2.443932000	-0.251062000	-0.088791000	H	-0.441284000	5.970887000	-1.773414000
H	-2.834832000	-0.262978000	0.930118000	H	2.411829000	4.350723000	0.995141000
C	-1.526820000	-1.231604000	3.205040000	H	1.748118000	6.116150000	-0.602446000
H	-2.048425000	-1.978632000	3.811256000	C	1.075207000	2.096745000	1.671600000
H	-0.827627000	-0.695392000	3.849534000	H	0.232628000	1.729360000	2.267507000
H	-2.282926000	-0.510070000	2.868860000	H	1.494911000	1.252739000	1.112418000
O	0.743979000	0.850892000	-1.200537000	H	1.838683000	2.471396000	2.358700000
N	-1.347859000	0.722818000	-0.162020000				
C	-2.891540000	-3.180384000	1.483590000				
H	-3.314770000	-3.744275000	0.649103000				
H	-2.887887000	-3.836597000	2.360939000				
H	-3.564554000	-2.343781000	1.704574000				
C	-3.585851000	0.087956000	-1.059694000				
H	-3.806504000	1.157788000	-0.983176000				
H	-3.238055000	-0.110911000	-2.081218000				
C	-4.868060000	-0.700953000	-0.766859000				
H	-4.605293000	-1.760814000	-0.627031000				
C	-5.827825000	-0.604926000	-1.952867000				
H	-6.755681000	-1.149391000	-1.755449000				
H	-6.088179000	0.441841000	-2.145556000				
H	-5.378916000	-1.013218000	-2.862819000				
C	-5.550497000	-0.198200000	0.507777000				
H	-6.446046000	-0.786807000	0.727409000				
H	-4.896605000	-0.244540000	1.384035000				
H	-5.851243000	0.847780000	0.385714000				
C	-1.584157000	2.013520000	0.291744000				
O	-2.640859000	2.260990000	0.846789000				
C	-0.576261000	3.097303000	0.034782000				
C	-0.971596000	4.109064000	-0.837955000				
C	0.645005000	3.173778000	0.714221000				
C	-0.134242000	5.191783000	-1.083884000				
C	1.463866000	4.275161000	0.469122000				

There is one imaginary frequency=-401.01 cm^{-1}.

SCF energy=-1523.86538343 hartree

Zero-point correction=+0.671823 hartree

Energy correction=+0.706798 hartree

Enthalpy correction=+0.707742 hartree

Gibbs Free Energy correction=+0.606991 hartree

275

C	5.646354000	1.317366000	-0.181751000
C	5.655683000	0.551364000	-1.501142000
C	4.891460000	-0.773045000	-1.502413000
C	4.224543000	1.654874000	0.290193000
C	3.368518000	-0.673553000	-1.239943000
H	6.157532000	0.737957000	0.597953000
H	5.224401000	1.197216000	-2.278246000
H	5.332086000	-1.470726000	-0.778001000
H	3.003038000	0.253997000	-1.689635000
H	6.214179000	2.245313000	-0.309205000
H	6.692217000	0.359173000	-1.800188000
H	5.035076000	-1.224141000	-2.491173000
H	4.272948000	2.485707000	1.002817000
C	3.045232000	-0.556746000	0.260702000
C	3.517198000	0.499306000	0.964428000
C	2.176240000	-1.582249000	0.847658000
H	2.308743000	-2.599006000	0.488916000
C	3.484368000	0.621958000	2.467074000
H	2.747929000	1.368934000	2.796337000
H	3.272528000	-0.319232000	2.973719000
H	4.460937000	0.983513000	2.809174000
H	3.630638000	2.008332000	-0.563541000
C	2.708404000	-1.842883000	-2.024744000
H	3.413108000	-2.676115000	-2.106828000
H	2.538567000	-1.482200000	-3.046981000
C	0.303898000	-1.788195000	-1.003972000
C	1.426735000	-2.523228000	-1.573037000
O	1.369800000	-3.749827000	-1.604004000
C	1.241260000	-1.364294000	1.830220000
H	1.197859000	-0.385735000	2.303571000
C	-0.758198000	-2.465316000	-0.393436000
H	-1.041564000	-3.446950000	-0.762686000
C	0.162690000	-2.232927000	2.129579000
C	-0.121806000	-3.332135000	1.310784000
H	0.706537000	-3.777691000	0.759560000
C	0.095710000	-0.344344000	-0.918329000
C	-1.827982000	-1.456864000	-0.035184000
H	-2.192932000	-1.563922000	0.987184000
C	-0.794044000	-1.778301000	3.203823000
H	-1.465063000	-2.573322000	3.531182000
H	-0.236771000	-1.424386000	4.075471000
H	-1.410406000	-0.936837000	2.857317000
O	0.735716000	0.571181000	-1.391647000
N	-1.089779000	-0.193869000	-0.140324000
C	-1.234893000	-4.298786000	1.642398000
H	-1.314647000	-5.067362000	0.870308000
H	-1.049073000	-4.802377000	2.596552000
H	-2.205662000	-3.795825000	1.716863000
C	-3.024001000	-1.490209000	-0.995739000
H	-3.551581000	-0.532212000	-0.917814000
H	-2.643630000	-1.575919000	-2.021367000
C	-4.001270000	-2.631231000	-0.688315000
H	-3.425099000	-3.560853000	-0.559049000
C	-4.963015000	-2.830117000	-1.859774000
H	-5.676941000	-3.632526000	-1.652967000
H	-5.532965000	-1.912163000	-2.041029000
H	-4.425265000	-3.079459000	-2.778931000
C	-4.784868000	-2.362294000	0.599157000
H	-5.459886000	-3.193382000	0.823618000
H	-4.135918000	-2.214891000	1.468129000
H	-5.387079000	-1.454232000	0.489289000
C	-1.623145000	0.927540000	0.456806000
O	-2.665699000	0.845905000	1.083393000
C	-0.877903000	2.230195000	0.384965000
C	-1.542586000	3.395045000	-0.009473000
C	0.436127000	2.314200000	0.841031000
C	-0.894350000	4.625299000	0.057087000
C	1.074287000	3.545452000	0.927114000

C	0.408255000	4.703509000	0.537184000
H	0.968414000	1.405229000	1.102821000
H	-1.412827000	5.516504000	-0.276582000
H	2.096340000	3.597057000	1.289432000
H	0.905270000	5.665979000	0.593438000
C	-2.957281000	3.353097000	-0.536428000
F	-3.168645000	2.275435000	-1.310299000
F	-3.868803000	3.338497000	0.438297000
F	-3.214871000	4.432805000	-1.294468000

There is one imaginary frequency=-409.78 cm^{-1}.

SCF energy=-1821.50375842 hartree

Zero-point correction=+0.649652 hartree

Energy correction=+0.686383 hartree

Enthalpy correction=+0.687327 hartree

Gibbs Free Energy correction=+0.582215 hartree

276

C	5.653950000	0.080120000	-0.172999000
C	5.489927000	-0.746181000	-1.444815000
C	4.417449000	-1.834232000	-1.391100000
C	4.356352000	0.792468000	0.235072000
C	2.964491000	-1.342122000	-1.178941000
H	5.991059000	-0.558214000	0.654026000
H	5.245638000	-0.063788000	-2.270494000
H	4.658875000	-2.572342000	-0.614772000
H	2.847657000	-0.383164000	-1.692053000
H	6.439173000	0.826212000	-0.336436000
H	6.448983000	-1.210259000	-1.701408000
H	4.456776000	-2.368843000	-2.347373000
H	4.602425000	1.628789000	0.898317000
C	2.659484000	-1.052163000	0.302045000
C	3.370191000	-0.102327000	0.954745000
C	1.553756000	-1.789950000	0.923135000
H	1.436714000	-2.829882000	0.632005000
C	3.339043000	0.130576000	2.444292000
H	2.794490000	1.051973000	2.695696000
H	2.898298000	-0.695285000	3.002213000
H	4.366495000	0.273889000	2.797924000
H	3.882427000	1.228999000	-0.654405000
C	2.045031000	-2.358548000	-1.914955000
H	2.526545000	-3.340902000	-1.939192000
H	1.974020000	-2.023643000	-2.957410000
C	-0.284620000	-1.662063000	-0.964492000
C	0.634238000	-2.681640000	-1.453051000
O	0.285822000	-3.859105000	-1.406363000
C	0.689969000	-1.285449000	1.865341000
H	0.883742000	-0.298243000	2.278077000
C	-1.487281000	-2.021165000	-0.347829000
H	-1.990014000	-2.931918000	-0.660897000
C	-0.573571000	-1.839547000	2.185784000
C	-1.109085000	-2.889979000	1.431813000

H	-0.408713000	-3.563599000	0.937544000	C	1.398516000	4.645609000	0.378038000
C	-0.145062000	-0.205118000	-0.986287000	H	1.081423000	1.321780000	0.920929000
C	-2.289731000	-0.763282000	-0.098041000	H	-0.125482000	5.930716000	-0.412034000
H	-2.687805000	-0.702754000	0.915864000	H	2.748563000	3.142051000	1.127918000
C	-1.405613000	-1.089952000	3.196895000	H	2.122159000	5.451760000	0.446405000
H	-2.227346000	-1.690559000	3.589506000	O	-2.078051000	4.074331000	-0.675002000
H	-0.781252000	-0.777002000	4.037916000	C	-2.455189000	5.371791000	-1.078474000
H	-1.833205000	-0.175732000	2.761345000	H	-2.396566000	6.081536000	-0.245077000
O	0.705295000	0.485881000	-1.507349000	H	-1.830537000	5.732005000	-1.904560000
N	-1.272432000	0.280267000	-0.264521000	H	-3.488604000	5.293431000	-1.413378000
C	-2.430988000	-3.526732000	1.792351000				
H	-2.693335000	-4.299383000	1.066008000				
H	-2.385586000	-3.998585000	2.779338000				
H	-3.245886000	-2.794363000	1.812746000				
C	-3.447052000	-0.598534000	-1.092356000				
H	-3.747635000	0.455312000	-1.092852000				
H	-3.079711000	-0.841934000	-2.097318000				
C	-4.661844000	-1.465630000	-0.739765000				
H	-4.312719000	-2.486497000	-0.519935000				
C	-5.620031000	-1.540236000	-1.928549000				
H	-6.501144000	-2.142779000	-1.689578000				
H	-5.964125000	-0.536088000	-2.200440000				
H	-5.133960000	-1.978038000	-2.805097000				
C	-5.390990000	-0.926339000	0.493660000				
H	-6.234700000	-1.570190000	0.759257000				
H	-4.740001000	-0.848074000	1.369838000				
H	-5.779049000	0.077566000	0.290932000				
C	-1.540048000	1.540647000	0.252430000				
O	-2.608546000	1.736592000	0.805209000				
C	-0.478893000	2.595333000	0.199957000				
C	-0.825600000	3.899915000	-0.194274000				
C	0.808668000	2.339038000	0.659260000				
C	0.122580000	4.922232000	-0.106243000				
C	1.750747000	3.357222000	0.760785000				

There is one imaginary frequency=-412.97 cm^{-1}.

SCF energy=-1599.04459466 hartree

Zero-point correction=+0.677601 hartree

Energy correction=+0.713371 hartree

Enthalpy correction=+0.714316 hartree

Gibbs Free Energy correction=+0.611638 hartree

277

C	5.533929000	-1.229359000	-0.096100000
C	5.211698000	-1.630363000	-1.532742000
C	3.929107000	-2.441295000	-1.722900000
C	4.410284000	-0.399922000	0.541235000
C	2.610249000	-1.730835000	-1.330325000
H	5.717591000	-2.122069000	0.515811000
H	5.131651000	-0.715619000	-2.136064000
H	3.993894000	-3.393242000	-1.179419000
H	2.705743000	-0.668718000	-1.573631000
H	6.461859000	-0.647306000	-0.092166000
H	6.051074000	-2.200418000	-1.946860000
H	3.869410000	-2.697612000	-2.787195000
H	4.808688000	0.164673000	1.390992000
C	2.350560000	-1.782567000	0.185530000
C	3.247631000	-1.231609000	1.036557000
C	1.091824000	-2.378074000	0.646070000
H	0.746647000	-3.271659000	0.134420000
C	3.257402000	-1.432673000	2.530458000
H	2.964950000	-0.516354000	3.060183000
H	2.613769000	-2.247065000	2.862012000
H	4.284191000	-1.655704000	2.843801000
H	4.052013000	0.341571000	-0.185393000
C	1.504155000	-2.307140000	-2.260453000
H	1.770612000	-3.323871000	-2.564385000
H	1.507169000	-1.698209000	-3.173231000
C	-0.643350000	-1.403128000	-1.084235000
C	0.057407000	-2.447954000	-1.820560000
O	-0.523473000	-3.510464000	-2.029451000
C	0.355053000	-1.907538000	1.706277000
H	0.774161000	-1.104361000	2.306624000
C	-1.909551000	-1.642221000	-0.541760000
H	-2.566082000	-2.356346000	-1.030667000
C	-1.003454000	-2.217376000	1.952003000
C	-1.758498000	-2.929383000	1.013488000
H	-1.227254000	-3.620247000	0.358386000
C	-0.223219000	-0.029332000	-0.798270000
C	-2.474248000	-0.334747000	-0.034542000
H	-2.844541000	-0.395153000	0.989758000
C	-1.660292000	-1.547236000	3.133110000
H	-2.477318000	-2.144625000	3.543297000
H	-0.929139000	-1.377207000	3.926795000
H	-2.070965000	-0.564065000	2.862019000
O	0.799492000	0.553813000	-1.096133000
N	-1.297717000	0.540273000	-0.062372000
C	-3.191976000	-3.310693000	1.294457000
H	-3.640665000	-3.796246000	0.424658000
H	-3.253184000	-4.010973000	2.134421000
H	-3.804642000	-2.438312000	1.548178000
C	-3.595160000	0.200968000	-0.936382000
H	-3.715232000	1.272833000	-0.738979000
H	-3.279965000	0.087565000	-1.981767000
C	-4.939760000	-0.497370000	-0.699898000
H	-4.770321000	-1.584561000	-0.671515000
C	-5.900150000	-0.198956000	-1.851150000
H	-6.871521000	-0.674826000	-1.688863000
H	-6.066142000	0.880855000	-1.935735000
H	-5.500830000	-0.554058000	-2.805441000
C	-5.560413000	-0.067437000	0.631756000
H	-6.493096000	-0.607486000	0.819168000
H	-4.895546000	-0.239816000	1.483765000
H	-5.786257000	1.004142000	0.611617000
C	-1.370748000	1.772881000	0.568015000
O	-2.339586000	2.023538000	1.266107000
C	-0.297931000	2.794538000	0.315394000
C	-0.592744000	3.821787000	-0.588564000
C	0.906793000	2.772885000	1.020111000
C	0.350948000	4.827802000	-0.782043000
C	1.821368000	3.802137000	0.807379000

C	1.560726000	4.837814000	-0.088232000
H	0.134312000	5.625310000	-1.489419000
H	2.763387000	3.790788000	1.351604000
C	1.235641000	1.629821000	1.940843000
H	0.367587000	1.330247000	2.538475000
H	1.557838000	0.768548000	1.342779000
H	2.044715000	1.897192000	2.625596000
C	-1.900999000	3.828881000	-1.338554000
H	-2.032674000	2.898848000	-1.903261000
H	-2.743800000	3.914385000	-0.646316000
H	-1.943049000	4.661104000	-2.043558000
C	2.549322000	5.958809000	-0.282445000
H	2.321884000	6.798806000	0.382259000
H	3.568136000	5.630633000	-0.063361000
H	2.523874000	6.334934000	-1.308126000

There is one imaginary frequency=-413.80 cm^{-1}.

SCF energy=-1602.46494887 hartree

Zero-point correction=+0.727368 hartree

Energy correction=+0.765900 hartree

Enthalpy correction=+0.766845 hartree

Gibbs Free Energy correction=+0.657822 hartree

278

C	4.730710000	-2.561841000	-0.207668000
C	4.099475000	-3.435907000	-1.286656000
C	2.652080000	-3.856071000	-1.031648000
C	3.951597000	-1.258185000	0.017411000
C	1.614078000	-2.709255000	-0.957092000
H	4.793874000	-3.112663000	0.739660000
H	4.136361000	-2.889598000	-2.239174000
H	2.583316000	-4.455683000	-0.114365000
H	1.910698000	-1.929120000	-1.664747000
H	5.757934000	-2.322647000	-0.503608000
H	4.707609000	-4.337069000	-1.424133000
H	2.362650000	-4.518955000	-1.855345000
H	4.611233000	-0.528505000	0.501258000
C	1.598038000	-2.025730000	0.422455000
C	2.719202000	-1.421349000	0.882267000
C	0.326230000	-2.003601000	1.156408000
H	-0.284200000	-2.900957000	1.108942000
C	2.911547000	-0.909632000	2.287682000
H	2.883480000	0.188775000	2.320275000
H	2.174656000	-1.294751000	2.992067000
H	3.907878000	-1.205805000	2.635616000
H	3.670616000	-0.830417000	-0.954956000
C	0.272413000	-3.299680000	-1.478289000
H	0.243592000	-4.375967000	-1.283223000
H	0.277857000	-3.182773000	-2.569245000
C	-1.394838000	-1.421616000	-0.759337000
C	-1.084942000	-2.827554000	-0.986140000
O	-1.927896000	-3.670090000	-0.687820000
C	-0.119567000	-0.957522000	1.926941000
H	0.545657000	-0.113880000	2.095095000
C	-2.580201000	-1.045747000	-0.123181000
H	-3.462176000	-1.670178000	-0.231595000
C	-1.462293000	-0.768028000	2.338330000
C	-2.491705000	-1.570157000	1.834917000

H	-2.242259000	-2.583463000	1.519146000	C	3.065114000	3.640042000	-0.205862000
C	-0.602353000	-0.232726000	-1.078411000	H	-0.140654000	4.606655000	-0.774474000
C	-2.701237000	0.458660000	-0.200778000	H	1.395309000	0.730422000	0.224203000
H	-2.999122000	0.918289000	0.742183000	H	2.190528000	5.521733000	-0.731688000
C	-1.777309000	0.453766000	3.164195000	H	3.653226000	1.626267000	0.335053000
H	-2.495087000	0.225029000	3.956976000	O	4.286621000	4.225865000	-0.193853000
H	-0.871082000	0.849996000	3.626087000	C	5.398932000	3.411096000	0.108581000
H	-2.209983000	1.261533000	2.558790000	H	5.323092000	2.991590000	1.118859000
O	0.423259000	-0.134839000	-1.720742000	H	5.501118000	2.592412000	-0.613578000
N	-1.317649000	0.850395000	-0.494750000	H	6.273701000	4.057505000	0.050455000
C	-3.911595000	-1.389781000	2.313303000				
H	-4.595214000	-2.033489000	1.755230000				
H	-4.002255000	-1.647881000	3.374084000				
H	-4.250381000	-0.353752000	2.198722000				
C	-3.685439000	0.897625000	-1.294935000				
H	-3.461328000	1.936182000	-1.559674000				
H	-3.514680000	0.279170000	-2.185096000				
C	-5.148705000	0.799440000	-0.845328000				
H	-5.302817000	-0.176905000	-0.359865000				
C	-6.079607000	0.878115000	-2.055220000				
H	-7.129023000	0.826021000	-1.751090000				
H	-5.930933000	1.825291000	-2.585656000				
H	-5.886965000	0.064101000	-2.759844000				
C	-5.495401000	1.900091000	0.160778000				
H	-6.530256000	1.803272000	0.502099000				
H	-4.848805000	1.885167000	1.043402000				
H	-5.380793000	2.884346000	-0.305579000				
C	-0.959691000	2.177676000	-0.274534000				
O	-1.840591000	2.975018000	0.013297000				
C	0.467698000	2.605687000	-0.306417000				
C	0.705795000	3.964364000	-0.557071000				
C	1.543614000	1.783895000	0.021074000				
C	1.988075000	4.477236000	-0.523428000				
C	2.837957000	2.291741000	0.078473000				

There is one imaginary frequency=-399.79 cm^{-1}.

SCF energy=-1599.05153462 hartree

Zero-point correction=+0.677490 hartree

Energy correction=+0.713294 hartree

Enthalpy correction=+0.714238 hartree

Gibbs Free Energy correction=+0.611012 hartree

279

C	4.777763000	-2.933418000	0.103963000
C	4.073788000	-3.913832000	-0.843404000
C	2.539513000	-3.956503000	-0.794564000
C	4.326083000	-1.465565000	-0.031879000
C	1.913687000	-2.580446000	-1.123469000
H	4.628413000	-3.249411000	1.144906000
H	4.365093000	-3.660558000	-1.872278000
H	2.191940000	-4.303106000	0.186735000
H	2.618365000	-2.072896000	-1.789016000
H	5.854742000	-2.995774000	-0.087336000
H	4.465298000	-4.919768000	-0.654576000
H	2.201677000	-4.701131000	-1.523131000
H	5.075628000	-0.807619000	0.417539000
C	1.856466000	-1.752915000	0.168224000
C	3.006459000	-1.256816000	0.680910000
C	0.602027000	-1.791960000	0.920700000
H	0.090740000	-2.749944000	0.884461000
C	3.165557000	-0.672195000	2.059873000
H	3.259642000	0.418580000	2.010604000
H	2.348805000	-0.923921000	2.735384000
H	4.097531000	-1.044937000	2.498856000
H	4.267172000	-1.184943000	-1.088786000
C	0.618862000	-2.686845000	-1.987816000
H	0.691198000	-3.593074000	-2.594132000
H	0.582338000	-1.818736000	-2.646672000
C	-1.311653000	-1.499687000	-0.835220000
C	-0.691992000	-2.763810000	-1.238210000
O	-1.199262000	-3.829513000	-0.908901000
C	0.081900000	-0.827540000	1.744000000
H	0.633358000	0.098789000	1.890089000
C	-2.494531000	-1.421685000	-0.103687000
H	-3.214026000	-2.234195000	-0.143655000
C	-1.237080000	-0.870357000	2.269777000
C	-2.133373000	-1.869752000	1.887953000
H	-1.724623000	-2.821901000	1.553453000
C	-0.806226000	-0.148837000	-1.102872000
C	-2.960514000	0.016464000	-0.100186000
H	-3.295031000	0.359581000	0.878798000
C	-1.698896000	0.297765000	3.104806000
H	-2.307761000	-0.030829000	3.951543000
H	-0.842782000	0.852455000	3.494122000
H	-2.304515000	1.007636000	2.524605000
O	0.160559000	0.217576000	-1.739350000
N	-1.720346000	0.722683000	-0.443560000
C	-3.515066000	-1.953229000	2.486623000
H	-4.112855000	-2.716525000	1.982962000
H	-3.464092000	-2.220322000	3.548075000
H	-4.052722000	-1.001186000	2.416817000
C	-4.082747000	0.268032000	-1.117291000
H	-4.106182000	1.338852000	-1.347798000
H	-3.842471000	-0.269214000	-2.043042000
C	-5.456730000	-0.158657000	-0.584159000
H	-5.354794000	-1.145023000	-0.105445000
C	-6.456139000	-0.290700000	-1.732926000
H	-7.446790000	-0.572474000	-1.364704000
H	-6.554254000	0.664556000	-2.260696000
H	-6.133638000	-1.043831000	-2.457467000
C	-5.975585000	0.834021000	0.459309000
H	-6.922750000	0.491828000	0.886253000
H	-5.270754000	0.988067000	1.281988000
H	-6.145605000	1.810991000	-0.005685000
C	-1.649069000	2.076411000	-0.170997000
O	-2.639847000	2.640772000	0.269663000
C	-0.378718000	2.857382000	-0.357142000
C	-0.551437000	4.214741000	-0.643010000
C	0.906678000	2.355598000	-0.150649000
C	0.544582000	5.059936000	-0.763898000
C	1.995341000	3.215919000	-0.251828000

C	1.827233000	4.561739000	-0.565431000
H	-1.561208000	4.590902000	-0.763884000
H	0.399434000	6.106669000	-1.007001000
H	2.694905000	5.206009000	-0.655537000
C	3.371157000	2.687052000	0.030685000
F	4.324877000	3.425151000	-0.551617000
F	3.636312000	2.682768000	1.352687000
F	3.520795000	1.422014000	-0.390944000
H	1.079500000	1.305691000	0.057033000

There is one imaginary frequency=-371.05 cm^{-1}.

SCF energy=-1821.51176004 hartree

Zero-point correction=+0.650277 hartree

Energy correction=+0.686921 hartree

Enthalpy correction=+0.687865 hartree

Gibbs Free Energy correction=+0.582663 hartree

280

C	-2.790418000	-5.284158000	-0.101880000
C	-3.773548000	-4.740051000	-1.146744000
C	-4.071756000	-3.233977000	-1.111842000
C	-1.409947000	-4.597261000	-0.092869000
C	-2.790677000	-2.388196000	-1.304353000
H	-3.228509000	-5.199698000	0.901412000
H	-3.374965000	-4.975355000	-2.143370000
H	-4.567269000	-2.957935000	-0.172606000
H	-2.110478000	-2.993306000	-1.911200000
H	-2.655838000	-6.354617000	-0.292132000
H	-4.715489000	-5.292642000	-1.056903000
H	-4.784644000	-3.014637000	-1.913679000
H	-0.686661000	-5.234468000	0.424370000
C	-2.117777000	-2.210679000	0.063978000
C	-1.492474000	-3.269246000	0.629969000
C	-2.441646000	-0.990027000	0.802914000
H	-3.461900000	-0.643428000	0.663689000
C	-1.030239000	-3.345174000	2.061581000
H	0.060570000	-3.257096000	2.123138000
H	-1.479887000	-2.589095000	2.704188000
H	-1.284972000	-4.330794000	2.466133000
H	-1.039167000	-4.481924000	-1.116822000
C	-3.019867000	-1.119029000	-2.182516000
H	-3.833793000	-1.333488000	-2.879348000
H	-2.106704000	-0.931931000	-2.748291000
C	-2.295643000	0.969666000	-0.925496000
C	-3.390765000	0.152059000	-1.452698000
O	-4.553643000	0.471190000	-1.236726000
C	-1.669021000	-0.325356000	1.719125000
H	-0.684659000	-0.716742000	1.967433000
C	-2.491209000	2.139611000	-0.194703000
H	-3.403582000	2.714703000	-0.322014000
C	-1.987577000	0.961753000	2.229919000
C	-3.078021000	1.682603000	1.740547000

H	-3.907698000	1.124243000	1.309863000	C	4.140396000	-1.133707000	-0.066635000
C	-0.861186000	0.697015000	-1.047106000	H	3.631948000	2.221544000	-0.247893000
C	-1.159218000	2.838444000	-0.042549000	H	4.935070000	-1.870747000	-0.092962000
H	-0.979312000	3.210202000	0.966211000	C	2.503790000	-2.973630000	0.359949000
C	-1.007715000	1.601910000	3.181258000	F	3.443198000	-3.780547000	-0.146407000
H	-1.520462000	2.144769000	3.979855000	F	2.418900000	-3.246952000	1.675960000
H	-0.368054000	0.844703000	3.639173000	F	1.327617000	-3.322298000	-0.180929000
H	-0.345970000	2.317843000	2.674358000	H	0.765071000	-0.940646000	0.257972000
O	-0.272681000	-0.189865000	-1.631827000	C	5.837621000	0.663744000	-0.470951000
N	-0.225221000	1.736650000	-0.307139000	F	6.726157000	-0.213466000	0.015910000
C	-3.454376000	3.023444000	2.319306000	F	6.083395000	0.788926000	-1.782893000
H	-4.253025000	3.489053000	1.737171000	F	6.085572000	1.853746000	0.090902000
H	-3.814924000	2.915991000	3.348356000				
H	-2.605107000	3.715207000	2.343274000				
C	-0.992248000	4.000818000	-1.031356000				
H	0.077867000	4.206879000	-1.145083000				
H	-1.378853000	3.686695000	-2.008667000				
C	-1.697883000	5.276934000	-0.553980000				
H	-2.700945000	5.006245000	-0.189322000				
C	-1.864248000	6.257615000	-1.714410000				
H	-2.346037000	7.182266000	-1.384115000				
H	-0.885520000	6.520271000	-2.131126000				
H	-2.467493000	5.825948000	-2.518068000				
C	-0.927738000	5.937224000	0.592461000				
H	-1.466600000	6.810050000	0.972110000				
H	-0.754608000	5.257223000	1.432174000				
H	0.054337000	6.270864000	0.240677000				
C	1.084453000	1.883699000	0.101175000				
O	1.437446000	2.940746000	0.601788000				
C	2.080295000	0.761332000	-0.015096000				
C	3.407224000	1.163175000	-0.172459000				
C	1.785808000	-0.593420000	0.144245000				
C	4.424544000	0.218046000	-0.216201000				
C	2.819782000	-1.524172000	0.122958000				

There is one imaginary frequency=-367.87 cm^{-1}.

SCF energy=-2158.44773424 hartree

Zero-point correction=+0.655302 hartree

Energy correction=+0.695681 hartree

Enthalpy correction=+0.696625 hartree

Gibbs Free Energy correction=+0.581540 hartree

ECOLE DOCTORALE

Titre : Une plongée dans la synthèse totale des aspochalasines. D'une stratégie en deux phases aux réarrangements de peroxydes.

Mots clés : synthèse totale, bio-inspiration, aspochalasines, DFT, méthodologie.

Résumé : Pendant près de deux siècles, les chimistes de synthèse se sont intéressé·e·s à la reproduction des molécules présentes dans la nature. Les produits naturels sont une source presque infinie de défis synthétiques grâce à leur diversité structurale et leur complexité. Les chimistes ont utilisé diverses approches pour accéder à un grand nombre d'entre eux. De la synthèse totale ciblée à la synthèse totale diversifiée, les stratégies de synthèse des produits naturels ont évolué pour produire divers composés à partir d'intermédiaires communs en un court nombre d'étapes. De plus, les calculs DFT ont parfois été utilisés pour aider les chimistes à résoudre les problèmes rencontrés lors des synthèses totales. Le but de cette thèse était de réaliser la synthèse totale de substances naturelles de la famille des cytochalasines, tout en développant des méthodes de synthèse appropriées, en s'aidant des calculs DFT. Une approche en deux phases pour produire des produits naturels de la famille des aspochalasines, tels que la trichodermone et la trichodérone A, sera présentée. La construction du noyau principal utilisera une réaction de couplage croisé de Suzuki-Miyaura, une dihydroxylation asymétrique de Sharpless, un réarrangement d'Ireland-Claisen et une réaction de Diels-Alder. La synthèse du noyau isoindolone sera améliorée par des calculs DFT. Ensuite, une deuxième phase utilisant divers procédés d'oxydoréduction sera employée pour oxyder sélectivement un intermédiaire tétracyclique afin d'atteindre diverses aspochalasines. Les réarrangements de peroxydes organiques peuvent produire une grande variété de fonctions oxygénées. Lors des réarrangements de Criegee et de Hock, les peroxydes allyliques et benzyliques se réarrangent pour former des oxocarbéniums qui sont ensuite piégés par de l'eau pour former des dérivés carbonylés. De nouvelles méthodes seront présentées où divers nucléophiles seront utilisés pour piéger les oxocarbeniums et générer des éthers cycliques.

Title : A journey into the total synthesis of Aspochalasins. From a two-phase strategy to peroxide rearrangements.

Keywords : total synthesis, bio-inspiration, aspochalasines, DFT, methodology.

Abstract : Over almost two centuries, synthetic chemists have been interested in reproducing molecules found in Nature. Natural products are an almost infinite source of synthetic challenges by their complex structural diversity. Chemists have employed diverse approaches to access a vast number of them. From target-oriented synthesis to diverted total synthesis, strategies in natural product synthesis have evolved to produce diverse compounds from common intermediates in a short number of steps. Furthermore, DFT calculations have sometimes been used to assist chemists to solve problems encountered during total syntheses. The purpose of this thesis was the total synthesis of natural products of the cytochalasin family and the development of related synthetic methods, by using the strong support of DFT calculation. A two-phase approach to produce aspochalasin natural products, such as trichodermone and trichoderone A, will be presented. The construction of the main core will use Suzuki-Miyaura cross coupling reaction, Sharpless asymmetric dihydroxylation, Ireland-Claisen rearrangement and Diels-Alder cycloaddition. The Diels-Alder reaction towards the isoindolone core will be enhanced by DFT calculations. Then, a second phase using diverse redox processes will be employed to selectively oxidized tetracyclic intermediate to reach diverse aspochalasins. Organic peroxide rearrangements can produce a diverse variety of oxygenated functions. During the Criegee and Hock rearrangements, allylic and benzylic peroxides rearrange to form oxocarbenium species which are then trapped by water to form carbonyl derivatives. In this chapter, new methods will be presented where diverse nucleophiles will be used to trap oxocarbeniums and generate cyclic ethers.

Institut Polytechnique de Paris
91120 Palaiseau, France